ORNL/TM-2007/001

RFQ Designs and Beam-Loss Distributions for IFMIF

R. A. Jameson

IFMIF Accelerator Facility Team Leader

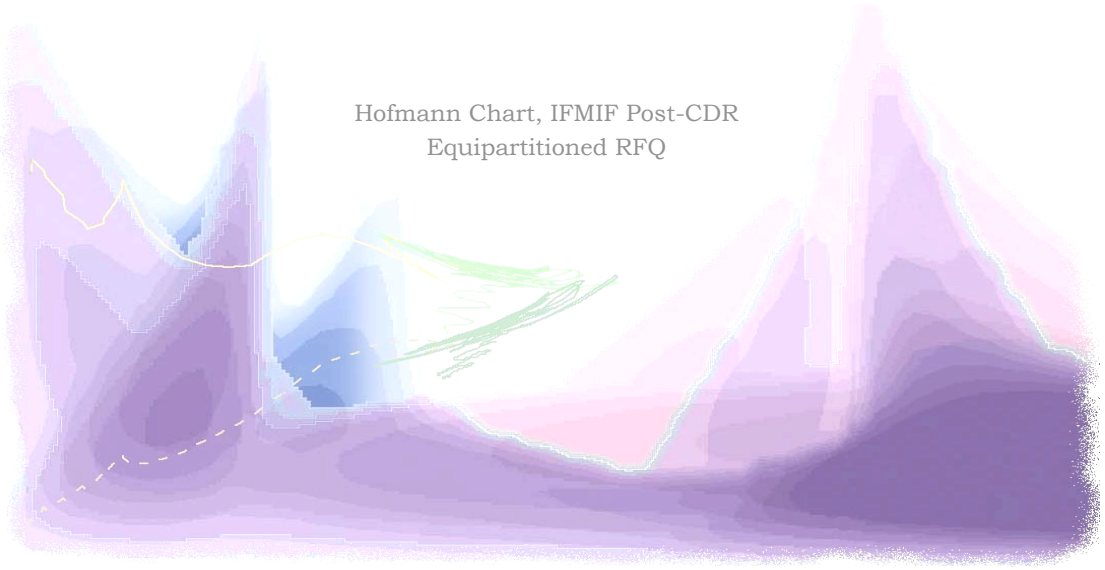

Written for the IFMIF Project,
as a United States contribution to EU Work Package TW5-TTMI-001,
Task Deliverable 3

January 2007

International Fusion Materials Irradiation Facility (IFMIF)
An Activity of the International Energy Agency (IEA) Implementing Agreement for a
Program of Research and Development on Fusion Materials

ORNL/TM-2007/001

RFQ Designs and Beam-Loss Distributions for IFMIF

R. A. Jameson

IFMIF Accelerator Facility Team Leader

Written for the IFMIF Project,
as a United States contribution to EU Work Package TW5-TTMI-001,
Task Deliverable 3

January 2007

International Fusion Materials Irradiation Facility (IFMIF)
An Activity of the International Energy Agency (IEA) Implementing Agreement for a
Program of Research and Development on Fusion Materials

Research sponsored by the Office of Fusion Energy Sciences,
U.S. Department of Energy,
under Contract DE-AC05-00OR22725 with UT-Battelle, LLC.

Table of Contents

RFQ DESIGNS AND BEAM-LOSS DISTRIBUTIONS FOR IFMIF

APPENDIX

List of Figures

List of Tables

List of Acronyms

AltCDR	An alternative CDR design
CDA	Conceptual Design Activity
CDR	Conceptual Reference Design
cw	Continuous-wave (100% duty factor)
ECR	Electron cyclotron resonance
EP	Equipartitioned, a beam equilibrium state
HEBT	High-energy-beam-transport
IAP	Institut für Angewandte Physik, Goethe Uni Frankfurt, Germany
IFMIF	International Fusion Materials Irradiation Facility
IHEP	Inst. High energy Physics, Protvino, Russia
K	Thousand (10^3)
KP	Kilpatrick, developer of a voltage breakdown criterion. Here KP indicates the factor by which Kilpatrick's Criterion can be exceeded.
LEBT	Low-energy-beam-transport
LEDA	Low energy Demonstration Accelerator
LIDOS	RFQ design and simulation code, Moscow Radiotechnical Institute
M	Million (10^6)
m	meter
MeV	Million electron volts
MW	Megawatts
PARMTEQ(M)	RFQ simulation code, Los Alamos Scientific Laboratory
Post-CDR	A new design generated after publication of the CDR
RF	Radiofrequency
RFQ	Radio-Frequency Quadrupole
Rho/r0	Ratio of vane tip radius (Rho) to average aperture (r0)
Rs	Rf shunt impedance ≡ (vane voltage)^2/(rf power)
TOUTATIS	RFQ simulation code, CEA Saclay
α	Alpha ellipse parameter
β	Beta ellipse parameter

Abstract

The IFMIF 125 mA cw 40 MeV accelerators will set an intensity record. Minimization of particle loss along the accelerator is a top-level requirement and requires sophisticated design intimately relating the accelerated beam and the accelerator structure. Such design technique, based on the space-charge physics of linear accelerators (linacs), is used in this report in the development of conceptual designs for the Radio-Frequency-Quadrupole (RFQ) section of the IFMIF accelerators. Design comparisons are given for the IFMIF CDR Equipartitioned RFQ, a CDR Alternative RFQ, and new IFMIF Post-CDR Equipartitioned RFQ designs. Design strategies are illustrated for combining several desirable characteristics, prioritized as minimum beam loss at energies above ~ 1 MeV, low rf power, low peak field, short length, high percentage of accelerated particles. The CDR design has ~0.073% losses above 1 MeV, requires ~1.1 MW rf structure power, has KP factor 1.7,is 12.3 m long, and accelerates ~89.6% of the input beam. A new Post-CDR design has ~0.077% losses above 1 MeV, requires ~1.1 MW rf structure power, has KP factor 1.7 and ~8 m length, and accelerates ~97% of the input beam. A complete background for the designs is given, and comparisons are made. Beam-loss distributions are used as input for nuclear physics simulations of radioactivity effects in the IFMIF accelerator hall, to give information for shielding, radiation safety and maintenance design. Beam-loss distributions resulting from a ~1M particle input distribution representative of the IFMIF ECR ion source are presented.

The simulations reported were performed with a consistent family of codes. Relevant comparison with other codes has not been possible as their source code is not available. Certain differences have been noted but are not consistent over a broad range of designs and parameter range. The exact transmission found by any of these codes should be treated as indicative, as each has various sensitivities in its internal methods. Continued work to compare results between different codes more broadly and deeply than heretofore is highly recommended - this requires comparison at source code level and devising of appropriate tests. It is strongly recommended that the project obtain source code for all important simulation work.

1. Introduction

Progress toward the realization of fusion power requires development of low-activation and neutron-damage resistant materials, with experimental suitability evidence satisfying technical and licensing requirements. Decades of work have established that a high-flux source of neutrons with appropriate spectrum must be built and operated, and that a neutron source based on the D-Li stripping reaction best suits this purpose. Facility design was first developed by the Fusion Materials Irradiation Test (FMIT) Project (1978-84) [1], later by the Energy Selective Neutron Irradiation Test Facility (ESNIT) Program (1988-92) [2], and from 1994-2006 by the International Fusion Materials Irradiation Facility (IFMIF) Project [3]. Major worldwide advances in accelerator technology over the past decade have further added to the credibility of this approach.

This report has been written for the IFMIF Project, as a United States contribution to EU Work Package TW5-TTMI-001, Task Deliverable 3, and complements extensive 2006 work by the Institut Angewandte Physik (IAP), Goethe Uni. Frankfurt on end-to-end simulation, beam loss modeling, and the potential advantages of superconducting technology for the IFMIF linac.

IFMIF uses two continuous-wave (cw) 175 MHz linear accelerators, each providing a 125 mA, 40 MeV deuteron beam. The top-level performance requirements for the IFMIF accelerators are described in Table 1-1. Many aspects of the design are driven by the requirement that hands-on maintenance of the accelerator must be allowed throughout the life of the facility.

Table 1-1. Top-level specification for the IFMIF Accelerator Facility

IFMIF Accelerator Facilities	
Performance requirements	
Particle type	D^+; H_2^+ for testing (to avoid activation)
Accelerator type	RF linac
Number of accelerators	2 , in parallel operation
Beam distribution	Rectangular flat top (20 cm horizontal × 5 cm vertical)
Output energy	40 MeV
Output energy dispersion	± 0.5 MeV FWHM
Duty factor	CW (pulsed tune-up and start-up)
Availability	≥ 88 %
Maintainability	Hands-on (For accelerator components up to final bend in HEBT with local shielding as required; design not to preclude capability for remote maintenance.)
Design lifetime	30 years

A Radio-Frequency Quadrupole (RFQ) accelerates the beam from 95 keV to 5 MeV and bunches the dc beam from the injector as required for injection into the following linac, which continues the acceleration to 40 MeV. The top-level

specification for the RFQ is given in Table 1-2. The maintainability specification is a deceptively simple statement to the non-expert - it involves stringent minimization of stray particle loss along the linac; it is the crux of the design, and has been the subject of many years of research effort. This report strives to explore this aspect in breadth and depth, and therefore assumes, already from this point on, that the reader is familiar with the general description and elementary theory of the RFQ [4,5,6].

Table 1-2. Top-level specification for the IFMIF RFQ.

Radio Frequency Quadrupole	
RFQ type	Resonant longitudinal coupling (3 RF segments), 4-vane integral structure
RF operating frequency	175 MHz
Input / output energy	95 keV / 5 MeV
Input / output current	130-140 mA / 125 mA (nearly all losses below 2 MeV)
RFQ length	~12.5 m
Total input RF power	1.3 MW
Cavity power	685 kW
Transverse emittance	≤ 0.4 π mm mrad (normalized rms)
Longitudinal emittance	≤ 0.8 π mm mrad (normalized rms)
Duty factor	CW (pulsed tune-up and start-up)
Maintainability	Hands-on. May require local shielding. Design not to preclude remote maintainability.

The report compares in some depth three RFQs - the CDR Equipartitioned RFQ, a CDR Alternative RFQ, and a new Post-CDR Equipartitioned RFQ design - concerning the design strategies and trade-offs, the resulting designs and their performance in terms of beam loss:

- The CDR RFQ is an equipartitioned design ~12m long. The design strategy is described in detail in [7].
- An alternative CDR design uses a simpler design technique and had an additional design objective – to reduce peak surface field. It is also ~12m long, and has about the same transmission and loss features as the CDR RFQ although crossing a parametric resonance.
- Refined equipartitioned design and optimization techniques result in a Post-CDR design. The beam loss at energies above ~1 MeV, rf power and peak field are similar to the older designs, while the length is reduced to ~8m (significant cost saving) and the percentage of accelerated beam is significantly higher.

The decision to use the equipartitioned RFQ design for the CDR is recorded in [8]. This report gives background and further development.

Although this report presents three RFQ designs and beam-loss distributions, any one of these should not be considered as a final design. The intent of these designs has been to develop improved design and optimization techniques, and to explore design strategy options. Using these tools and from these examples, a final design

can be decided. Very substantial work is required for the final design. Issues include:

1.1 Caveats

1.1.1 LEBT Design and Simulation Refinement

The low-energy-beam-transport (LEBT) design has a very strong influence on the RFQ design (beam loss and transmission performance, length, rf power consumption). The CDR presents a feasible conceptual case; a fully integrated and optimized LEBT/RFQ combination for IFMIF has not been designed yet.

The choice of injection energy into the RFQ is important. Typically, a lower injection energy results in a shorter RFQ but other aspects of the RFQ performance may suffer. Lower injection energy results in higher space-charge effect in the sections of the LEBT which are not space-charge neutralized. Studies during the IFMIF project led to the choice of 0.095 MeV injection energy presented in the CDR. This choice was re-evaluated; the conclusion is that 0.095 MeV appears optimal.

A much more accurate representation of the ion-source/LEBT is required to fully characterize the beam distribution entering the RFQ. The best beam-loss model produced so far is described in the CDA [9] Issues include:

- ECR ion source performance at the require 130-140 mA deuteron current with the specified emittance has not been demonstrated. Scaling to 125 mA deuterons requires 200 mA H+ from the source; this level has not been demonstrated and the corresponding emittance is not known.
- There is a paucity of emittance data from the ECR ion source; only one 125 mA H+ emittance data set has been available to the Project, and no deuteron beam emittance measurement. This data set has been numerically transformed to the input ellipse matching parameters required by the RFQs. However, this data set is thresholded by an inaccurate (and optimistic) method. The more accurate method developed by M. Stockli at SNS should be used. [10]
- The beam is composed of multiple species of deuteron ions (and may also be contaminated with other ions). The emittance data need to be separated according to species, and all species tracked simultaneously through the LEBT and the RFQ. (The simulation program pteqHI can transport multiple species simultaneously.)

Other LEBT effects include:

- beam neutralization (~98%),
- high-frequency noise on the ion-source beam. This noise may result in an amplified beam current variation in the LEBT if the time constant of the neutralization phenomenon is slower than the noise, and this effect must be included in the simulation. [9,11]
- a short (~3cm) section at the RFQ input where there is neither neutralization nor focusing, resulting in a strong space-charge effect.
- The 2-solenoid low-energy-beam transport (LEBT) between the ion source and the RFQ has not been designed in detail and is not included in the input beam distribution used in this report. The solenoid simulation should include higher-

order field effects both within the solenoid and in the solenoid end fringe field regions, which will produce further aberrations in the input beam. [12]

- Coulomb scattering of beam particles on residual gas [13]
- Effect of auxiliary gasses [14]

These issues are being addressed by IAP, Goethe Uni Frankfurt in the same EU 2006 Work Package; these results and method for presenting beam loss should be used in the final RFQ design work.

These effects will probably produce larger beam-losses in the presented RFQ designs. As the RFQ design is intimately related to the input beam, it may be possible to reduce the RFQ losses again with further optimization work using the more accurate ion-source/LEBT input distribution in the optimization process.

1.1.2 HEBT Design and Simulation

Conceptual design of the IMFIF High-Energy-Beam-Transport, from the end of the linac to the target, is not complete and presents design challenges, which may be influenced by the linac performance, including errors.

1.1.3 RFQ Design Strategy, Trade-offs, Optimization

- The RFQs presented here require detailed design work to add vane gaps between manufactured sections, and the transition and output radial matching cells at the output.
- The final choice of parameters and design strategy has to ultimately be made by the IFMIF program - selecting the desired trade-off between the top-level specifications for low beam loss, cost factors such as RFQ length and rf power requirement, and engineering factors such as peak field. In this report, a prioritization of the top-level specs has been chosen:

1) Minimum beam loss at energies above ~ 1 MeV. This has been chosen as the highest priority because maintenance of the linac without the use of remote manipulators ("hands-on" maintenance) is of primary importance. There is no lower energy threshold for inducement of radioactivity when deuterons strike material, but confinement of beam losses as much as possible to under 1 MeV (~10 times the injection energy) can be achieved with design and optimization techniques.

2) Low rf power requirement for the RFQ structure. The cost of rf power comprises the initial capital cost plus the operating cost over the factory life, and therefore overshadows the capital cost of the RFQ structure.

3) Low peak field. If the peak field were too high, sparking and performance degradation could occur. This requirement is not so difficult to achieve, as the required beam focusing can be achieved without needing the highest practical fields.

4) Short length. Modern RFQs can be built to any length. For IFMIF, considerations of the beam acceleration and efficiency have guided the choice of 5 MeV as the output energy of the RFQ. The RFQ capital cost is then optimized for the shortest RFQ that accelerates from 0.095 - 5 MeV, while meeting the other specs.

5) High percentage of accelerated particles. The IFMIF ECR deuteron ion source should reliably produce at least 140 mA cw beam current, and 125 mA (89.3%) must be accelerated. Better would be ~96.2% acceleration of 130 mA input, and this has been a design goal of the CDR and Post-CDR work. Some sacrifice of

accelerated beam percentage could be made, assuming the ion source should have some excess capacity, in order to minimize >1MeV losses; i.e., transmission is hardly the full story.

- Then the final design must be optimized, including sensitivity checks of various factors (e.g., different input emittance, beam current and matching). Guidance is provided in this report. At present, the optimization procedure is still tedious.

- It is important to recall also that IFMIF decided for multiple linacs for increased reliability of beam on target. Each linac would provide 125 mA cw beam, with the present IFMIF consisting of two such modules. A later upgrade of the module for higher beam current would not be done; if higher current were desired, another module would be installed. This strategy then allows module performance and cost optimization, which guided the choice of main parameters such as the rf frequency.

- New insights into factors influencing optimum transmission and low beam loss have been gained and are the subject of ongoing research; it is hoped they will be useful in the final design work for IFMIF.

1.1.4 Design and Simulation Tools

- The LINACS design tool [15,16] used in this report gives complete control over the space-charge physics, including utilization of an equilibrium beam [17], control of the tune trajectory with respect to resonances, and control of all parameter variations inside the RFQ.

- Simulation results presented in this report were obtained using the pteqHI code [18], a version of PARMTEQ with many improvements, including the ability to simultaneously handle multiple species. Multipole and image effects are represented analytically using the method of Crandall [19,20]. The source code is available. Final design work should use a code with similar improvements and also a field map representation of the vane surfaces. The RFQTRAK [21] or LIDOS [22] codes are recommended. The newest version of PARMTEQM also uses field maps, but continues to use an approximate method for space-charge computation (the independent variable is position instead of time, transformations at the space-charge computation points are inaccurate, resulting in inaccurate beam loss localization (beam-loss pattern) [12]). Despite arduous attempts, reproduction of published results of the TOUTATIS code [23] was not successful, and therefore it has not been used further.

The exact transmission found by any of these codes should be treated as indicative, as each has various sensitivities in its internal methods. Continued work to compare results between different codes more broadly and deeply than heretofore is highly recommended - this requires comparison at source code level and devising of appropriate tests. It is strongly recommended that the project obtain source code for all important simulation work.

1.2. Outline of the Report

The report has two main purposes:

1) (Sections 2-3) To present three designs in the usual format of:
   - their vane parameters vs. cell number
   - their transmission
   - their beam-loss pattern.
2) (Sections 4-9) To go beyond the usual format,to:
   - explain in some depth the development of linac design technique, and how this influences the three designs.
   - explain enhanced design and simulation tools that afford control of the beam space-charge physics and the design strategy and parameters.
   - analyze the designs in these terms.
   - give comments on a varying vane-voltage profile, the rf power estimates, the design and simulation codes, and the LEBT.

Section 2 presents and compares the vane parameter characteristics and basic rms beam behavior of each of the three RFQs.

Section 3 presents, under restricted conditions, beam-loss distributions for each of the RFQs.

Section 4 outlines the process of "conventional" RFQ design technique, exemplified by the Alternative CDR RFQ.

Section 5 discusses Beam-Based Linear Accelerator Design Technique, of which RFQ design is a subset, exemplified by the CDR and Post-CDR RFQs,

Section 6 presents and compares the performance of the three example RFQs against the background of beam-based design. The underlying space-charge physics of the beam as it travels through the RFQs is revealed. This is the key section, with a summary and suggestions for further design work.

Section 7 discusses the use of a variable vane voltage profile, which has been used by experienced RFQ designers in operating RFQs. The characteristics of the Russian IFMIF partner's preliminary proposal for an RFQ are given as an example of support for variable vane voltage.

Section 8 characterizes the computer codes used for design and simulation, upon which the results for all three designs critically depend. Variation of results with the number of particles simulated is presented.

The material in Sections 5-8 goes beyond the commonly used practice, and must be understood by project team members, as well as project leaders, reviewers and other interested parties.

In capsule form: "Conventional" design techniques involve a global characterization of space charge defocusing vs. rf field focusing in terms of a "current limit" and simplified rules for parameter variation. The advanced beam-based technique requires definition of the detailed space-charge defocusing vs. rf field focusing at

each cell, and then finds the appropriate RFQ structure to satisfy this space-charge physics definition. There are more parameters available than needed to satisfy the space-charge physics requirements; the extra ones are specified by rules. All of the many RFQ parameters are under direct control of the designer.

Accurate beam distributions for the ion-source and simulation through the LEBT are crucial for accurate simulation through the RFQ and post-RFQ linacs to the full energy of 40 MeV, as discussed in Section 1.1; a few additional notes are given in Section 9.

Section 10 gives a few concluding remarks.

2. Presentation of Three IFMIF RFQ Designs

The figures are traditional for RFQ experts, and are given here without further elaboration.

2.1 CDR Equipartitioned RFQ

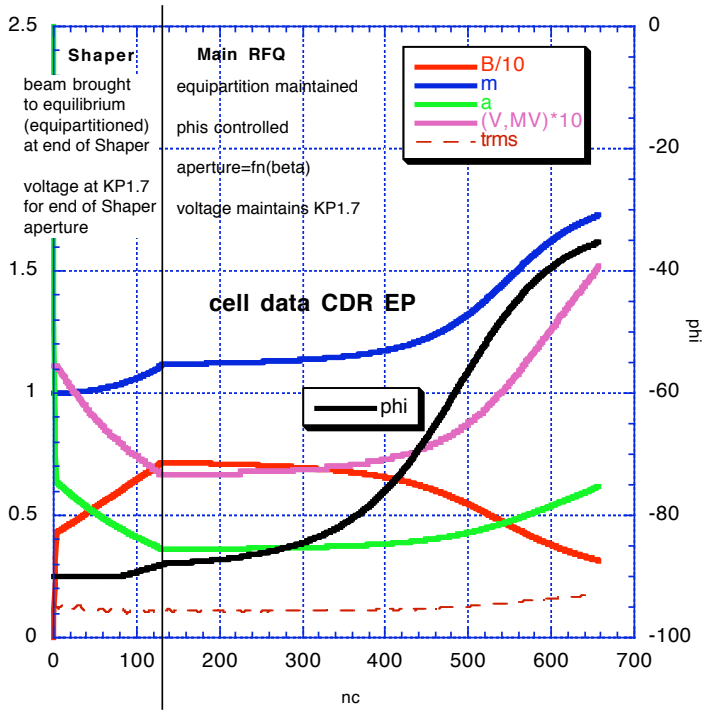

Fig. 2.1-1. Vane parameters for the 140 mA CDR equipartitioned RFQ. Aperture (a) and trms = transverse rms beam radius are in cm. (m) is the vane modulation, V is the vane voltage, B is the transverse focusing strength. Phi is the synchronous phase (phis). Rho/r0 = 0.75. Input current = 140 mA, input energy = 0.100 MeV, input transverse normalized rms emittance = 0.20 mm.mrad.

2.2 CDR Alternative RFQ

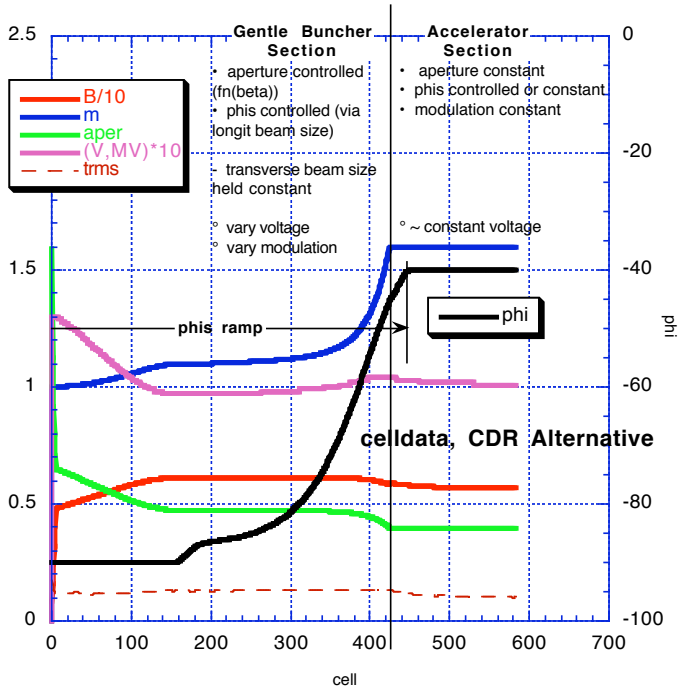

Fig. 2.2-1. Vane parameters for the 130 mA CDR Alternative RFQ. Input current = 130 mA, input energy = 0.095 MeV, input transverse normalized rms emittance = 0.25 mm.mrad.

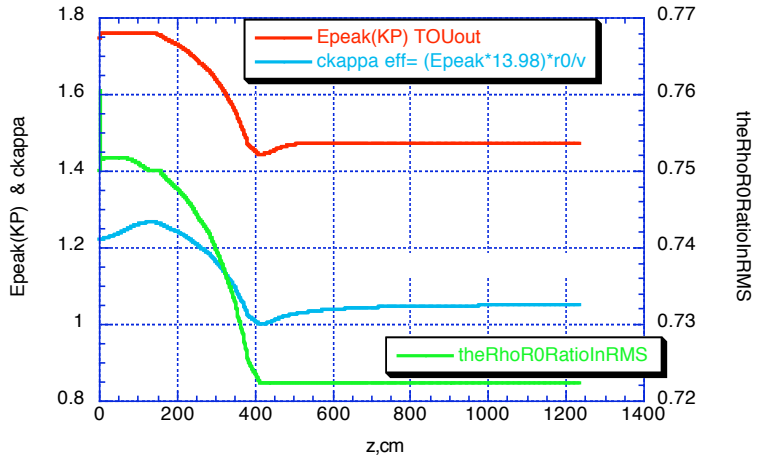

Fig. 2.2-2. The Rho/r0 ratio is varied, to give lower peak surface field (lower KP factor) in the downstream part of the RFQ. Epeak (KP) is the KP factor, ckappa is the ratio between the peak field on the vane surface and the vane-tip field.

2.3 New Post-CDR Equipartitioned RFQ

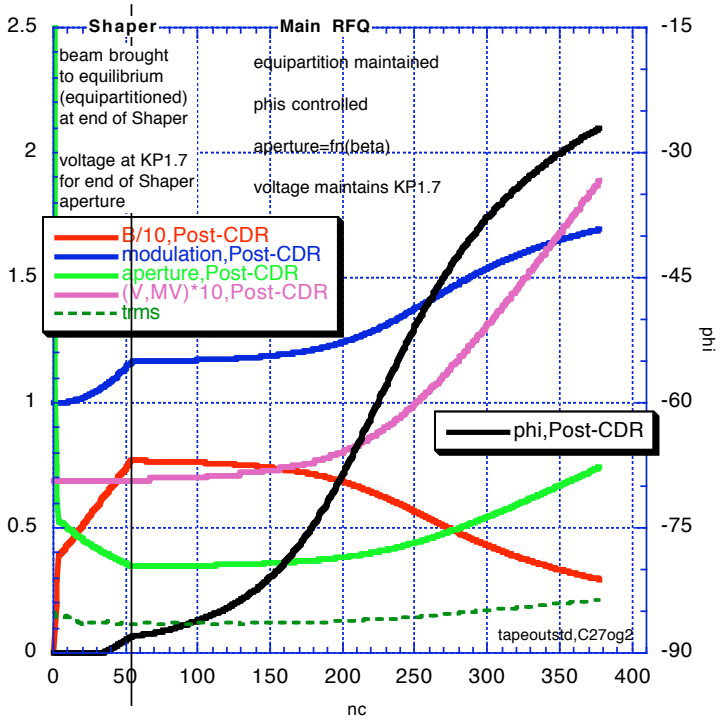

Fig. 2.3-1. Vane parameters for the 130 mA New Post-CDR RFQ. Input current = 130 mA, input energy = 0.095 MeV, input transverse normalized rms emittance = 0.25 mm.mrad.

2.4 Comparisons

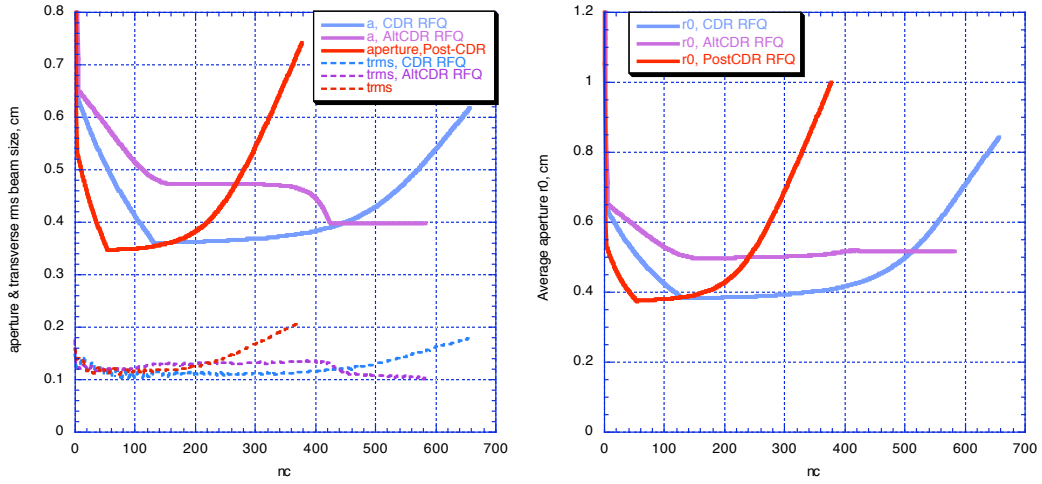

Fig. 2.4-1,2. Comparison of minimum aperture, a (nearly the same for the three RFQs), and average aperture, r0.

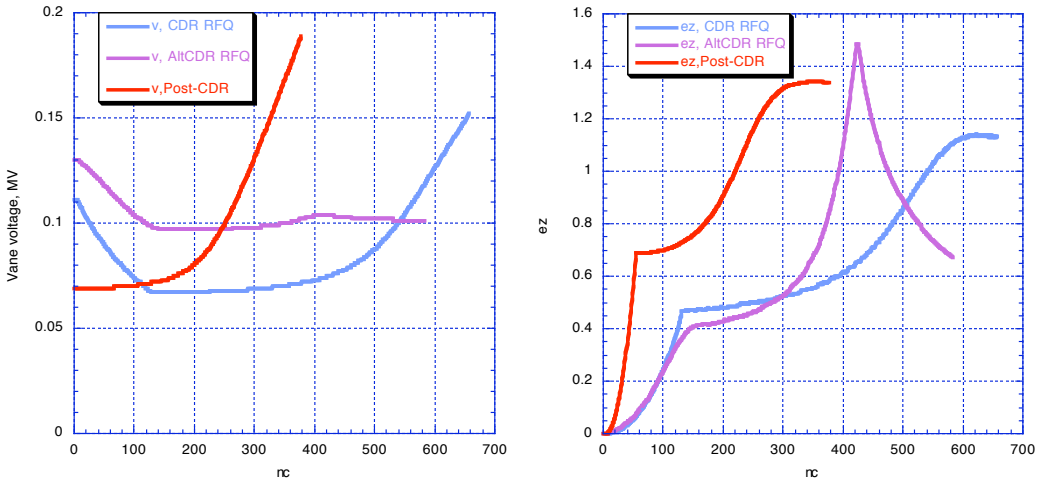

Fig.2.4-3,4. Comparison of vane voltage and accelerating factor ez.

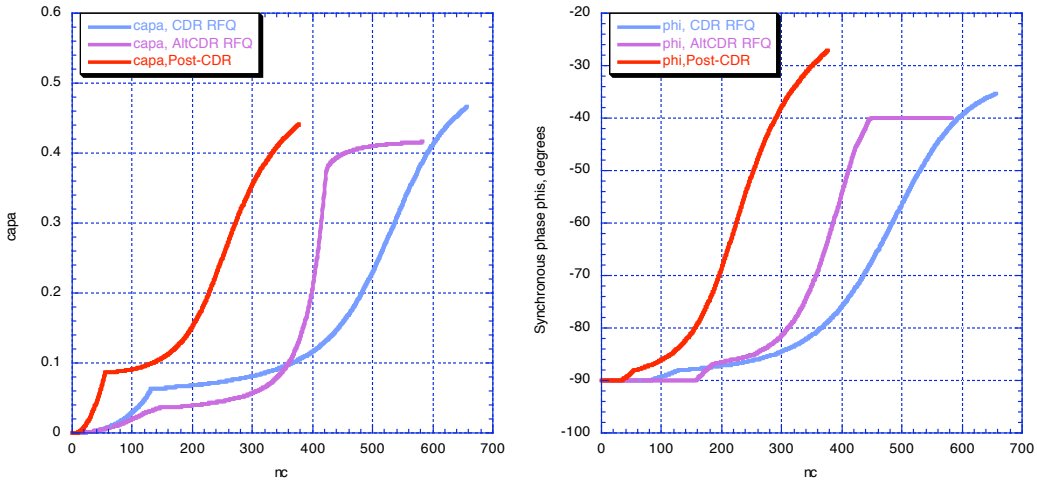

Fig. 2.4-4,5. Comparison of accelerating efficiency A and synchronous phase phis.

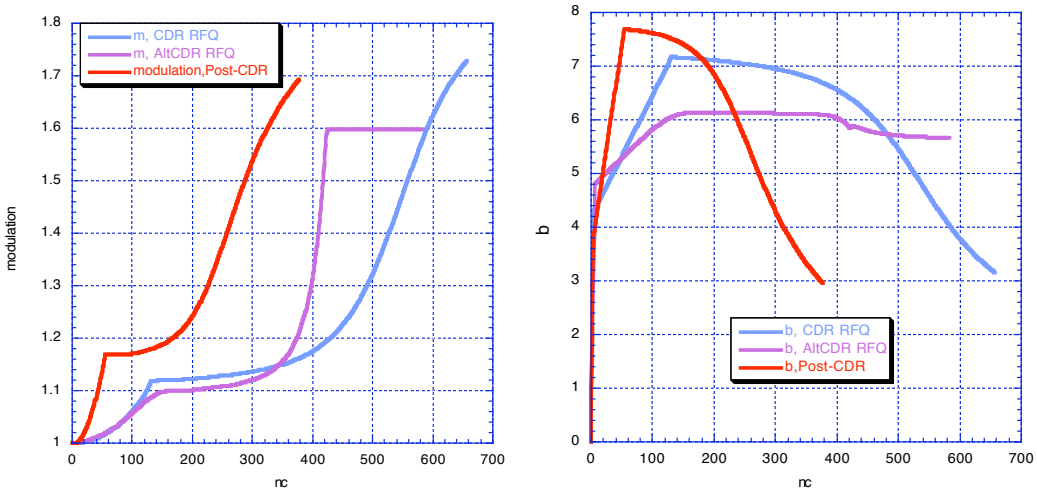

Fig. 2.4-7,8. Comparison of vane modulation m and focusing factor B.

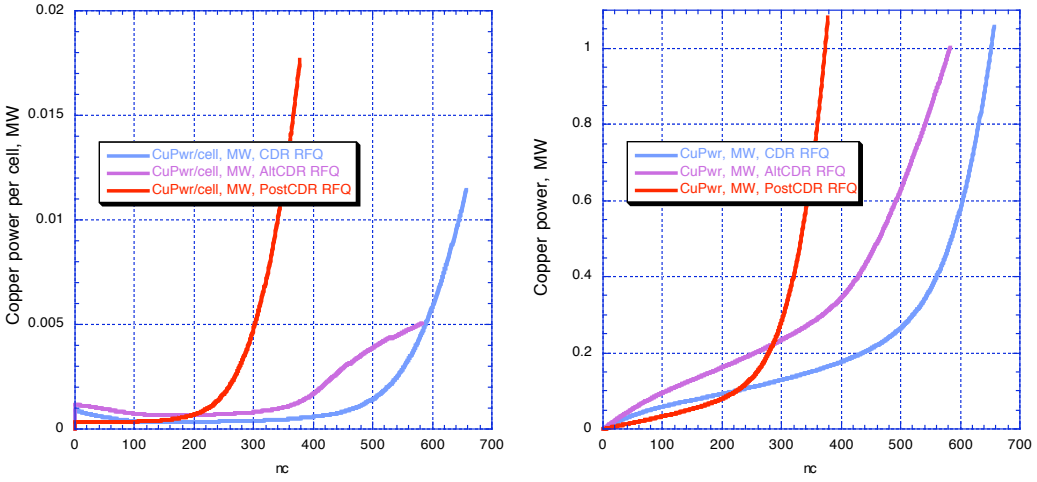

Fig. 2.4-9,10. Comparison of Copper power per cell and integrated copper power.

3. Beam-Loss Distributions and Accelerated Beam Transmission

Some particles are inevitably lost in a particle accelerator; their reactions with the surrounding materials produce radioactive by-products, accumulation of which must be minimized. The location and energy of lost particles is obtained from simulations of the accelerator, and used as input for nuclear physics simulations of radioactivity effects in the IFMIF accelerator hall, to give information for shielding, radiation safety and maintenance design. Conservative safety margins are assigned in each of these areas over the simulated effects.

Simulations were run with up to 1 M particles, including a representative distribution from the ECR ion source. Only the results using this ion source distribution are presented in this Section. It is necessary to build up extensive background in Sections 4 and 5, before discussion of the beam performance can be given in Section 6.

The definitions applied in the accelerator simulation to determine when a particle is assumed lost, and with what energy, are outlined in Section 8.2.2.

3.1 Beam Loss Distribution Comparisons

Confinement of losses to low energy as much as possible helps reduce the induced radioactivity, and this was chosen as the most important of the five main specifications. At the design conditions, the three RFQs are rather similar; for the ion source emittance distribution of ~1M particles rms matched to the RFQ input, the percent of particles lost with energy ≥1 MeV is:

CDR	0.073% loss above 1 MeV
AltCdr	0.123% loss above 1 MeV
Post-CDR	0.081% loss above 1 MeV

Although the totals are similar, Figs. 3.1 and 3.2 show different loss distributions. This will be discussed later in Section 6.

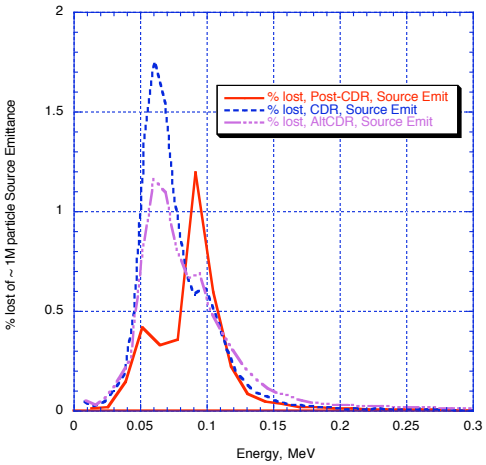

Fig. 3.1-1. % of all lost particles vs. energy where lost, 0.0 - 0.3 MeV.

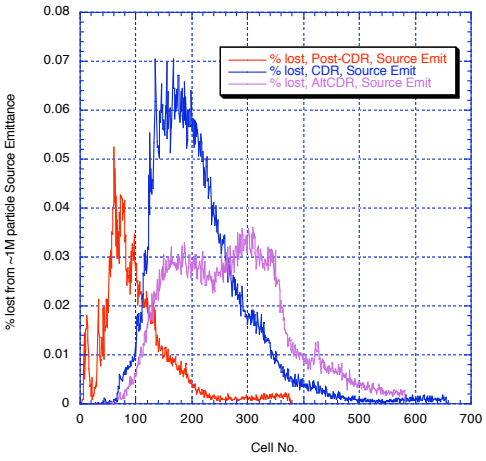

Fig. 3.1-2. % of all lost particles vs. position (z, cm) where lost.

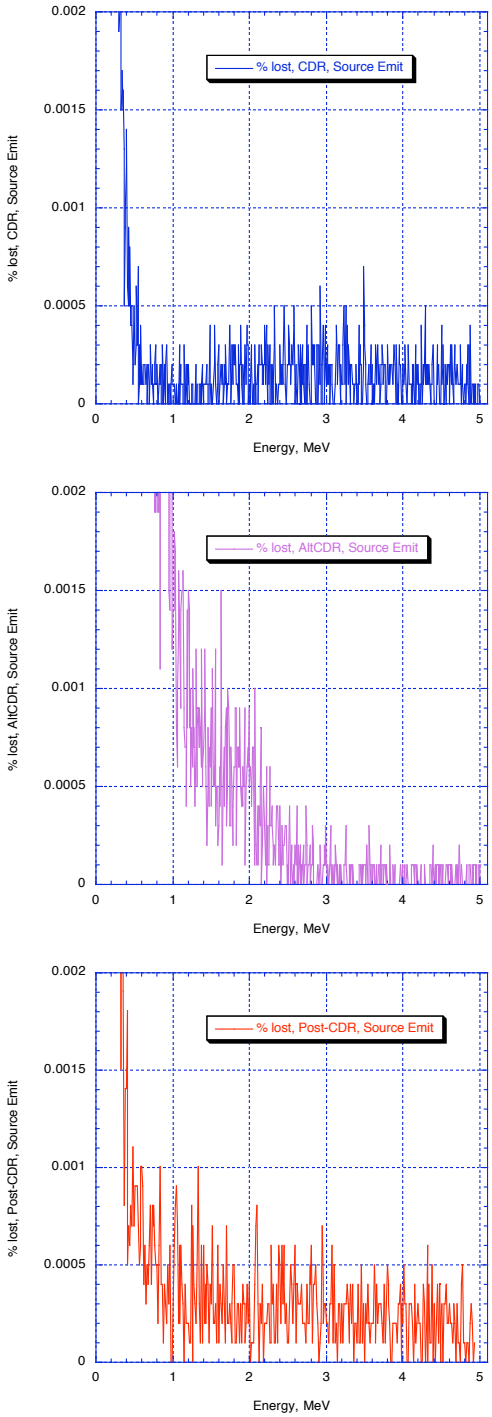

Fig. 3.1-3. % of all lost particles vs. energy where lost, 0.0 - 5.05 MeV, expanded vertical scale.

3.2 Transmission to RFQ output

For the ion source emittance distribution of ~1M particles rms matched to the RFQ input, the percent of *accelerated* beam is:

CDR	89.4%
AltCdr	89.9%
Post-CDR	95.8%

Fig. 3.2-1 shows the percent of accelerated particles through the RFQs. Features will be discussed in Section 6.

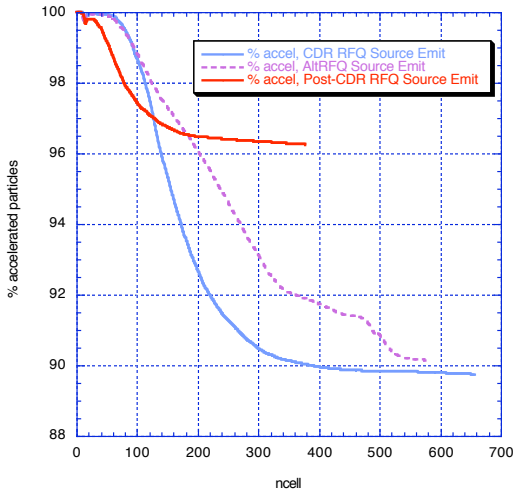

Fig. 3.2-1. % Accelerated particles from Source Emittance initial distribution vs cell number.

The total percentage of transmitted particles, including particles with low energy, is:

CDR	90.0%
AltCdr	92.0%
Post-CDR	97.0%

4. "Conventional" RFQ Design Technique

The job of a linac is to efficiently accelerate a beam of given current from an initial energy to a final energy. If some particles are lost by striking the accelerator structure during this process, they will cause a radioactivity buildup over time - thus minimization of beam loss becomes an overriding concern. It would not be economically feasible to maintain an entire linac by remote manipulators, so the specification requires "hands-on maintenance," meaning there can be local hot spots that may require special tooling, shielding, and limited access, but not remote manipulators.

"Conventional" intense RFQ design, still used almost exclusively today, is exemplified by the design of RFQs as originally laid out by Los Alamos in 1978-1980, in which only a global beam-current-related criterion was invoked for guidance as to the practical maximum current that should be accelerated for given focusing parameters, plus a cell-by-cell recipe for assigning the synchronous phase. The linac is laid out, keeping many parameters constant in the main accelerating section to ease manufacturing and tuning as understood at the time. Then beam acceleration is simulated and the resulting transmission to the output is observed as the measure of successful performance. It has been considered "too difficult" to understand in detail the cell-by-cell performance of the beam as it undergoes the very complicated process of forming a bunch from an initially dc beam and accelerating. This method is thus characterized as design "from the external field to the beam result" - i.e., "from the outside in".

4.1 External Field Quantities as Defined by the RFQ Metal

4.1.1 2-Term Potential Field Description

The RFQ is an accelerating device with time-varying fields. The classical description of the RFQ external fields uses the first two terms of the field solution in the vicinity of the vane tips - called the '2-term potential' - to describe the transverse and longitudinal field. It is emphasized that this representation is only accurate near the beam axis. In practice, this has led to the use of field maps in recent codes (LIDOS, the most recent version of PARMTEQM, and TOUTATIS).

The metal contour of the vane in the 2-term potential description is described by the aperture between opposing vanes and the modulation in the longitudinal direction. A potential, which can vary with the position (z) along the RFQ, is set up between the opposing pairs of vanes by the rf field, to provide the focusing and accelerating fields. Unmodulated vanes produce a purely transverse focusing field. Perturbation of the vanes with a specific, velocity-modulated pattern produces a longitudinal field component that can provide particle acceleration.

Modern practice replaces the 2-term longitudinal profile with a sinusoidal profile, which is easier to machine and gives somewhat more efficient acceleration.

4.1.2 Multipole and Image Fields

In practice, the vanes are not machined to the exact 2-term potential shape; the compromises result in higher order multipole terms that must be included. Older versions of simulation codes handled the higher-order terms analytically with coefficient tables [19,20]; pteqHI incorporates this method.

Duperrier (24) showed, for fields including analytically expressed multipoles, that inaccuracies occur outside the transverse circle drawn at the vane tip minimum. That and removal of paraxial approximation were main reasons why he wrote the simulation code TOUTATIS.

Recent codes (LIDOS, the most recent version of PARMTEQM, and TOUTATIS) incorporate field maps, which represent the exact vane shape used, out to some radius from the axis.

Image-charge effects are important in RFQs with significant beam current. The analytical method of Crandall [20] is implemented in both the design code LINACSrfq (negligible in the envelope design process, but coefficient tables are produced for the simulation code pteqHI), and in pteqHI.

4.2 Minimum Beam-Related Specification

Four variables describe the RFQ vane surface:

- either the minimum aperture a[rfq] or the average aperture r0[rfq]:
- the modulation em[rfq]
- the voltage between opposing vane tips v[rfq]
- the synchronous phase angle phis[rfq] at the location of the synchronous particle in each cell when the rf phase equals zero.

4.2.1 Teplyakov Synchronous Phase Rule

The synchronous phase angle must be specified. This is usually done using the rule invented by Teplyakov [25] which was the key to the success of the RFQ: the charge density of the forming bunch should remain constant; i.e., the ratio between the accelerating bucket length and the beam length should be constant. In “conventional” design procedures, this is the only place where a relationship between the beam and the structure is required at each cell.

The charge density can be allowed to vary to some extent, and specific control is available in the more flexible design procedure available in LINACS. This control of the charge density is especially useful in controlling the length of the RFQ.

4.2.2 Beam-Envelope Matching

Two envelope equations describe the variation of the rms beam radius and length of a bunched ellipsoidal beam in the smooth approximation (rapid variation of the quadrupolar field is smoothed) of a focusing system, as a function of the external fields and the internal space-charge forces within the beam, which work to counteract the external fields:

$$\varepsilon_{tn} = \frac{a^2 \sigma_t \gamma}{\lambda} \quad (1)$$

$$\varepsilon_{\ln} = \frac{(\gamma b)^2 \sigma_l \gamma}{\lambda} \quad (2)$$

where ε is the normalized rms (root mean square) emittance, σ is the phase advance with beam current, t denotes transverse and l longitudinal, a and b are transverse and longitudinal rms beam radii, λ is the rf wavelength.

The emittance terms must be either constant, or with a variation known a-priori.

Expanding the phase advance (or "tune") terms;

$$\sigma^{t\,2} = \sigma_0^{t\,2} - \frac{I\lambda^3(1-ff)}{a^2(\gamma b)\gamma^2}k \quad (3)$$

$$\sigma_l^{\,2} = -\sigma_0^{l\,2} - \frac{2I\lambda^3 ff}{a^2(\gamma b)\gamma^2}k \quad (4)$$

σ_0 is the zero current phase advance:

$$\sigma_0^{t\,2} = \frac{B^2}{8\pi} + \Delta \quad (5)$$

$$\sigma_0^{l\,2} = -2\Delta \quad (6)$$

where B is the RFQ focusing parameter, I is the beam current, ff is the geometry factor ≈ $a/3b$, γ and β are the relativistic gamma and beta, and $k = \frac{3}{8\pi}\frac{z_o q 10^{-6}}{mc^2}$. $\Delta = \frac{\pi^2 q V_0 A \sin\phi_s}{2mc^2\beta^2}$ is the rf defocusing parameter, A, V_0, ϕ_s are accelerating parameter, intervane voltage and synchronous phase respectively.

These equations apply to a periodic focusing system of infinite length, but can be applied locally when the parameter variation is reasonably adiabatic, as indicated by the absence of first and second derivative terms. Careful checks were made from the full Hamiltonian to verify that terms related to acceleration are negligible (always assumed, but a reference has not been found). Equating the second derivatives of the beam sizes to zero means that the beam is "matched" to the focusing system. This condition is essentially satisfied in practical designs; however, there is evidence that in some subtle aspects the derivatives should be taken into account, and this is a subject of ongoing research.

4.2.3 Beam-Envelope Matching at Transitions

Transitions occur often in practical linacs; as energy increases, a different type of accelerator structure must be used, or engineering reasons require parameter changes, etc. The matching equations (1) and (2) immediately indicate how to maintain the matched condition at a transition, across which it would be desired that the emittances and beam sizes remain constant. Maintaining the matched conditions then requires that the phase advances per unit length, σ/λ, also remain constant.

4.2.4 Global Space-charge Rule

If the current is increased until the phase advances equal zero, the "space-charge limit" is reached. At some intermediate current, the matching equations (1) and (2) indicate that the emittances and the current will have equal effect on the beam radii. If the beam bunch is assumed to be spherical, this occurs when the "tune depressions) $\sigma/\sigma 0$ = ~0.4. The original procedure solved Eqs. (1) and (2) independently with $\sigma/\sigma 0 = 0.4$ to find "transverse and longitudinal current limits," which were brought to equality by parameter adjustments. Requiring that the desired operating current be ~half of this "current limit" was then used as a practical guide for RFQ design.

4.3 "Conventional Design"

The design process developed at Los Alamos in 1978-1980 is still the most commonly used. It basically approaches the problem from the point of view of the external fields, and then checking the effect on the beam using a full simulation code. The rule that the "current limit" is twice the desired operating current guides the choice of rf frequency, which in turn governs the maximum allowable intervane voltage according to a "bravery factor" (typically ≤ 2) over a sparkdown criterion such as defined by Kilpatrick.

Parameters (such as the average aperture r0 between vanes, the voltage V between opposing vanes, the transverse focusing parameter B) were held constant along the vanes as much as possible to ease manufacturing complexity. Later it was learned how the parameters could be varied, giving an additional element of flexibility to the design process.

The RFQ is divided into four sections. A "radial matching section" about 4-6 cells long brings the beam into the RFQ by ramping up the fields from zero to a chosen value. The fields are then raised in a "shaper" section to the full transverse focusing ability available from the voltage and aperture chosen (zero modulation and -90° synchronous phase). Then the beam is slowly bunched and accelerated in a "gentle buncher" section, being very careful not to create strong space-charge forces leading to beam blow-up and lost particles, either immediately or later downstream. Typically the gentle buncher accelerates to about ten times the injection energy. Reasonable optimization is achieved by varying the synchronous phase reached at the end of the gentle buncher section.

The average aperture, r0, was held constant, to facilitate tuning the structure, and this also keeps the transverse beam size ~constant as the modulation increases. This has an important consequence, because as the modulation, synchronous phase and beam velocity increase, the required minimum aperture decreases quickly toward zero, as seen from the relation r0= (Minimum Aperture)(1+modulation)/2. Before this can occur, further increase of the modulation must be stopped. This point nominally defines the end of the "gentle buncher" section, and is considered the "choke-point" where the "current-limit" requirement applies.

An improvement for intense beams was to modify the shaper and gentle buncher to have a long initial "porch" section where the synchronous phase remains at -90° with no modulation to allow initial bunching with no acceleration, followed by a section with

increase of phis of a few degrees and small modulation to bring the beam to a satisfactory bunch length, and then using the Teplyakov rule for phis to further bunch and accelerate the beam.

The "acceleration section" then accelerates the beam to the final energy. The modulation is held constant at its end-of-gentle-buncher value. Within the constraint of the focusing available from the vane voltage such that r0 remains constant, the synchronous phase may be raised further, and then is clamped.

It was also found that a lower B at the beginning of the shaper requires less convergence of the injected beam, making the space-charge effects at injection less and making it easier to achieve a good input match. Therefore a lower vane voltage can also be used at the front end, lowering rf losses.

4.3.1 "How to choose the operating point?"

We draw here directly from material in [26] for an equivalent approach to define the end of the gentle buncher, as used in the design of the Alternative CDR RFQ:

"1) We know that the biggest problem should be expected at the end of the Gentle Buncher, when the bunch already exist but it is not really accelerated. At this point we know the energy of the beam, the phase, the emittance and the current.

2) We draw the following figure. There are two sets of curves. The dot curves (o) show the lines of a given Kilpatrick value (1.8 is the desired value in our case, the green curve). So we have to choose a point on that line. The second set is described by lines with (+), representing the modulation value.

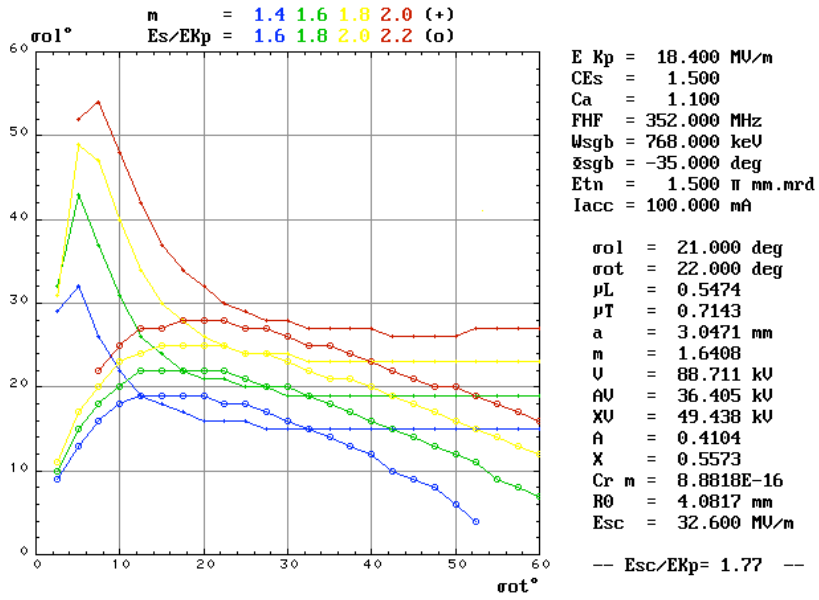

Fig. 4.1 A global design aid - 1. (Caption added.)

So, for a given Kilpatrick we choose the maximum modulation in order to obtain the smallest RFQ. In this particular figure, we have chosen σ_{0t}=22° and σ_{0l}=21°, and this point give the modulation, aperture, vane voltage, depression tune μt and μl.

3) We draw the next figure. It permits to verify that the chosen point is a valid one. We know that a « good » point will be with a depression tune over 0.4. The red curve describes μt as a function of σ_{0t}. We have chosen 22°, so we can verify that this value give us a μt over 0.4. The green curves are a set of curves describing μl as a function of σ_{0t} for different value of σ_{0l}. We verify that the point σ_{0t}=22° and σ_{0l}=21° give us a μl over 0.4."

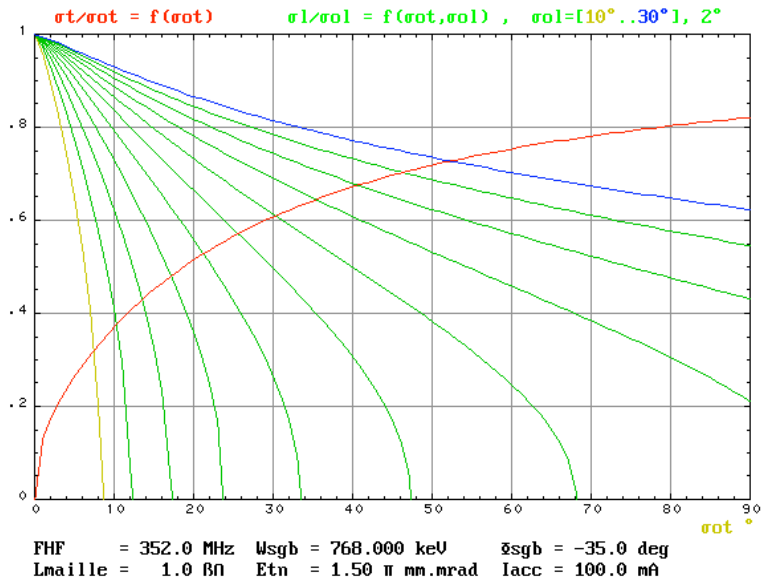

Fig. 4.2 A global design aid - 2. (Caption added.)

(end of direct extraction from [26].)

4) These values were then held constant through the remainder of the RFQ accelerating section.

4.3.2 An Optimization Approach to the "Conventional" Design

The paper [27] compares a "constant r0, constant V" design to a "varying r0 and V" design, to "avoid the 'bottleneck' (of the "constant r0,V" design) in the minimum aperture profile at the end of the gentle buncher, where the minimum aperture has to decrease rapidly in order to accommodate the increasing modulation."

Other parameter choice differences between the two designs caused them to have nearly the same length, copper power and transmission characteristics. This was done to show that a lower peak surface field can be used in the "varying r0, V" design for the same length.

It is stated that the "constant r0,V" design is much easier to machine and tune. In modern design practice, however, the machining and tuning are readily accomplished and would not take any priority over other desirable features.

It was found that beam losses are more localized at the bottleneck in the "constant r0, V" design. In the "varying r0, V" design, the minimum aperture decreases slightly through the RFQ and r0 increases according to the modulation; losses more distributed

along the RFQ, and its transmission is therefore less sensitive to input beam misalignment or increasing transverse input emittance.

Also stated as an important advantage of the "constant r0, V" approach is that it is easier to find an optimized solution in the multi-parameter design space. At this date, the optimization process is still indeed tedious, but advantages of a more encompassing optimization are worth the extra work in the design phase. For example, the beam losses should be confined to occur at the lowest possible energy, in order to minimize buildup of radioactivity. More sophisticated parameter variation methods described below are aimed at including such important aspects in the optimization process.

For an intense, factory-type linac of IFMIF class, all aspects point to design sophistication beyond "constant r0, V."

4.4 The IFMIF Alternative CDR RFQ Design

As seen in Sections 2.2 and 2.4, the IFMIF Alternative CDR design has the "conventional" design, with nearly constant voltage and r0 in the main part of the RFQ. The "bottleneck" in the aperture is apparent (Figs. 2.2-1 and 2.4-1). The voltage is higher at the front end, and falls to the end of the shaper section, from which it remains nearly constant except for a slight adjustment at the bottleneck.

For the Alternative CDR RFQ, changes were made in the IFMIF Specifications used for the CDR RFQ. The normalized rms input emittance was raised from 0.2 pi.mm.mrad to 0.25 pi.mm.mrad, reflecting an estimate of how the ion source and LEBT would perform, easing the space-charge forces in the RFQ. The injection energy was lowered from 0.100 MeV to 0.095 MeV, which would produce a shorter RFQ if all other conditions remained the same. A KP factor (KP) of 1.8 was used, to have the possibility of more focusing and consequently less space-charge effect than the KP = 1.7 CDR design, and reflecting confidence that this field level is practical.

Another parameter variation is introduced in this design. In practice, the vane tip is machined with a transverse radius Rho. Varying the ratio of Rho/r0 changes the ratio of the peak surface field to vanetip field, the capacitance between adjacent vanes, and the size of the multipole potential terms. In the Alternative CDR RFQ, the Rho/r0 ratio is varied, to give lower peak surface field (lower KP factor) at the fixed vane voltage in the downstream part of the RFQ (Fig. 3.2-2). As the higher voltage in the front end is not required to achieve adequate focusing, the strategy there could be modified.

The ability to vary Rho/r0 is an important feature, and could be exploited in the final IFMIF RFQ design.

In Fig. 2.2-1, note that after the bottleneck, in the accelerating section, the modulation and aperture, thus also r0, and synchronous phase are constant. The vane voltage is essentially constant, thus also B. The consequences of this on the beam dynamics, e.g., the longitudinal emittance and beam loss behavior (Fig. 3.2-1) are discussed in Section 6.

5. Beam-Based Linear Accelerator Design Technique

This chapter describes accelerator design techniques that go beyond those commonly used, and which must be understood by project team members, as well as project leaders, reviewers and other interested parties.

Design of an RFQ is the focal point of this discussion, but it applies to linear accelerators of all types.

Repeating from the introduction to Section 4: "Conventional" intense RFQ design, still used almost exclusively today, is exemplified by the design of RFQs as originally laid out by Los Alamos in 1978-1980, in which only a global beam-current-related criterion was invoked for guidance as to the practical maximum current that should be accelerated for given focusing parameters, plus a cell-by-cell recipe for assigning the synchronous phase. The linac is laid out, keeping many parameters constant in the main accelerating section to ease manufacturing and tuning as understood at the time. Then beam acceleration is simulated and the resulting transmission to the output is observed as the measure of successful performance. The detailed pattern of beam loss has rarely been studied. It has been considered "too difficult" to understand in detail the cell-by-cell performance of the beam as it undergoes the very complicated process of forming a bunch from an initially dc beam and accelerating. This method is thus characterized as design "from the external field to the beam result," i.e., "from the outside in."

This method does involve the injected beam in the design, but not the detailed beam behavior inside the RFQ. For intense, factory-type linac facilities like the IFMIF, where continuous operation for a period of ~40 years is expected, and minimized radioactivity buildup is a key objective, a more rigorous design method was sought.

An inverse design procedure is more relevant to the problem of achieving low beam loss: a beam-based design procedure starting from the space-charge physics characteristics of the desired beam, and finding the external fields appropriate to confine it.

Therefore the author has derived a "from the inside out" beam-based approach, in which the desired space-charge physics of the beam is first specified at each cell, and then accelerator fields are derived for the desired conditions.

The beam-based method requires a practical formulation of the space-charge physics, understanding of the effect of accelerator structure resonances and their spreading by space-charge, phase-space transport mechanisms [28], controlled use of a beam internal energy equilibrium and the parameters related to it, and other factors.

A major requirement of the beam-based method is that the desired design performance be very closely verified by the detailed beam simulation. This was not lightly achieved, and required extensive development of the design method to include all of the effects to be simulated, and of the simulation code itself. These tools are discussed in Section 8.

Rules governing the space-charge physics of intense beams in linacs were introduced into the cell-by-cell design procedures starting in 1981 [17]. The evolution of the design methods, and their application to the CDR and Post-CDR RFQ designs presented above, are discussed in the following paragraphs.

5.1 Extension of the "Conventional" Procedure to Achieve Shorter RFQs

Through experience, it was quickly found that RFQs designed by the "conventional" procedure tended to be longer than desired. Other trial-and-error procedures were developed that produced shorter RFQs with nearly as good transmission; these methods remained largely private however.

A thorough investigation of the "traditional" gentle-buncher design procedure and the previously trial-and-error extension to shorter RFQs is given in [29]. Finding a satisfactory synchronous phase at the end of the gentle buncher corresponded to keeping the tune depressions there ≥~0.4. It was found that the conventional approach was allowing the tune depression to be <0.4, and often even to go to zero (the space-charge limit), within the gentle buncher. The conclusion was that for intense beams, the single-point rule at the end of the gentle buncher was inadequate, and that the tune depression in the gentle buncher should be maintained above zero. For moderate to low beam intensities, the original procedure produces adequate results, although the RFQs are often considered long. In addition, the complication of the parameter space was shown, and how shorter RFQs are produced.

Other improvements were found empirically by experienced designers. [30,31,32,33,34] It was realized that lower focusing at injection eased input matching, and as a consequence that a lower vane voltage can be used in this region, saving rf power.

It was found that relaxing the transverse focusing in the accelerating section to keep the transverse phase advance more similar to the longitudinal phase advance gave better transmission. The reason for this was made clear by the author in the following amplification of the space-charge physics relations between the accelerator structure and a beam.

5.2 Space-charge Physics Relations Between the Accelerator Structure and a Beam

For a rigorous and practical beam-based design technique, the central requirement is to *use all available beam physics information in the design process*; the resulting design is then checked by a simulation code *with the same underlying physics*.

5.2.1 The Beam-Envelope Matching Equations

In the "conventional" design, the beam-envelope matching equations 1-6, Section 4.2.2, are used to set a "current limit". For a beam-based design, they are invoked at every cell.

The equations describe the variation of the rms beam radius and length, as a function of the external fields and the internal space-charge forces within the beam, which work to counteract the external fields. They describe a bunched beam of ellipsoidal form, so apply exactly after the beam is bunched enough to be described as an equivalent ellipsoid.

Sacherer [35] showed, in his derivation of these equations, that the actual form of various particle distributions causes only a few percent difference in the solution, if the rms properties of the distributions are the same - a seminal result that enables an "equivalent rms" design method. The remaining difference is, however, important to achievement of the best beam-loss performance. The design strategy incorporated in LINACS can account for the variation in the form factor of the ellipsoid, and this is effective in reducing beam loss[1].

The equations cannot be extended to account for emittance growth - the derivation requires the emittances to be either constant, or to have a functional form known *apriori*. The ability to use an *apriori* form is valuable for certain design problems.

Cylindrical beam envelope equations can also be written. The beam transition in the RFQ from cylindrical to ellipsoidal form is however very complicated and a precise enough (less than ~2% error) analytical expression for the transition has not been found.

The matched beam radius and length should vary smoothly in order to avoid unwanted effects, so that the derivative of the beam size is allowed to vary only slowly - approximately adiabatically in terms of the betatron and synchrotron oscillation wavelengths, so that a' = da/dz is ~zero. When the second derivatives of the beam size are ~0, the beam is "matched" transversely and longitudinally:

Now in addition to the external field variables contained in the zero-current phase advances, four new variables appear - the transverse and longitudinal rms beam sizes and emittances.

Equations (1) and (2) may be solved for any two variables; the others must be prescribed.

5.2.2 Beam Equilibrium - The Equipartitioned Condition

One other space-charge physics relationship that can be employed for design is known, called the equipartitioning relationship [15,17], which requires that the energy content within the beam be equal in the transverse and longitudinal degrees of freedom. When this condition is satisfied, there is no free energy within the beam that is available to drive a resonance condition:

$$\frac{\varepsilon_{tn}\sigma_t}{\varepsilon_{\ln}\sigma_l} = 1 \qquad (7)$$

which also implies $$\frac{\varepsilon_{ln}}{\varepsilon_{tn}} = \frac{\gamma b}{a} = \frac{\sigma^t}{\sigma^l} \qquad (8)$$

[1]The form factor adjustment is a complex subject and beyond the scope of this report.

The availability of an equilibrium, or equipartitioned (EP) condition for the beam is of course a powerful advantage. As explained below, the equilibrium requirement can be invoked at will by the designer; its utility varies according to detailed design requirements.

As the emittances can varied apriori, it is seen that the equipartitioned condition can be applied over a wide range of conditions, and can change within the accelerator.

The equilibrium condition can be required in addition to the matched conditions, and Eqs. (1), (2), and (7) solved simultaneously at each cell.

Now there are three equations, which may be solved for any three variables; the others must be prescribed. Typically, the beam transverse and longitudinal radii must be matched, and the EP condition forces a relationship between the beam radii. Thus two of the equations are effectively used for the beam radii, and the third equation to invoke the EP relationship through the use of one of the available RFQ external parameters, for example, the vane modulation.

5.2.3 Phase Advances - Resonances

Eqs. (1), (2), and (7) represent a typical nonlinear system, with all the complex behavior [28,36,37] that today receives very much attention in the field called nonlinear dynamics, with which the particle accelerator community is in general not familiar. It is interesting that the field of nonlinear dynamics itself changed significantly in the past decade or so. Previously, it was attempted to explain "complex behavior" or "chaos" using theory stemming from a perturbed Hamiltonian. Some relations were found, for example, the Lyapunov Criterion which indicated whether a system was chaotic, which seemed to be useful even though the system was perturbed very far beyond the infinitesimal perturbation over which the theory was valid. More recently, a geometrically based theory of nonlinear behavior has been developed, which can handle large perturbations, and in which it becomes clear that the mechanism for phase-space transport is resonances - with which the accelerator community is very familiar. A combined point of view is useful [38].

With no beam (zero beam current), the structure resonances are defined completely by the local external fields, at all rational number combinations of the tune ratio $\sigma_o{}^l/\sigma_o{}^t$ = sig0l/sig0t. With beam current, these resonances are broadened by the collective effect of space-charge, depending on the rms σ^l/σ^t = sigl/sigt and the internal tune spread of the beam particles.

All satisfactory RFQ designs should avoid the stronger resonances, either purposely or coincidentally to the design procedure used.

When the beam is in the equilibrium, equipartitioned, condition, there is no free energy available to be converted into changes in the particle distribution through resonant actions. In other words, the structure resonance still exists, but although the beam tunes may be in the resonance band, no action occurs because the beam is in equilibrium and there is no free energy.

This is the feature of a very useful tune chart for linear accelerators developed by Hofmann [39]. Fig. 5.2.3-1:

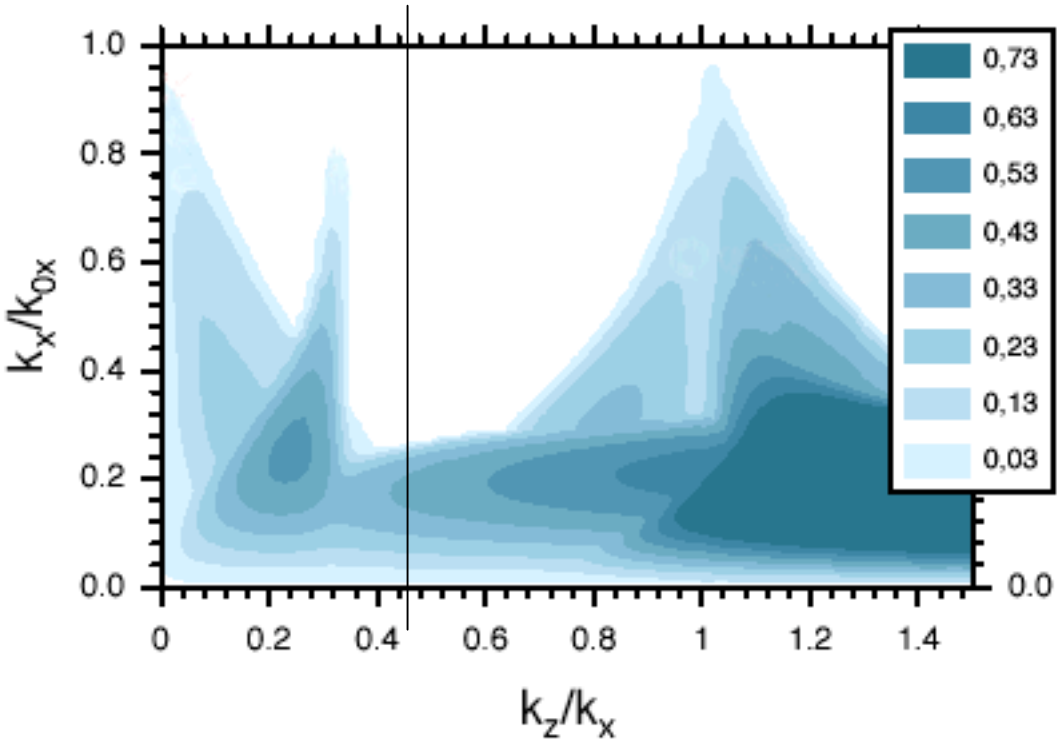

Fig. 5.2.3-1. Hofmann Chart for longitudinal-to-transverse emittance ratio eln/etn = 2.0; thus kz/kx = 0.5 is the equipartitioned condition for this chart.

The abscissa is the ratio of longitudinal tune to transverse tune. The ordinate is the tune depression, here labeled kx/k0x signifying transverse, but in practice, the trajectories of the envelope tunes in the x,y average termed transverse, and z (longitudinal) are both plotted cell-by-cell on the chart. The coloring represents the growth rate of a space-charge broadened tune resonance. Only a few major resonances are shown. On this chart, the growth rates for kz/kx = 1, 1/3, and smaller fractions are seen. If the emittance ratio remains constant, one chart suffices, but the chart is very dependent on emittance ratio, so if it is changing, several charts must be used.

In the early days of the 1980's, it was very tedious to solve the resonance growth rate equations and only some thresholds for growth were available. However, it was found that if either the transverse or longitudinal tune trajectory went below the threshold, emittance growth in that trajectory would occur [40,41]. Later with Mathematica© the charts became practical to generate, and their use is slowly being adopted [42,43,44], albeit mostly to check a design rather than to base a design trajectory on the desired location on the chart, and with some differences; for example, not generally realized are the usefulness of plotting the trajectories in both (or all) degrees of freedom, details about various placements of the trajectory on the chart, or the very detailed evidence of smaller resonances that can be detected.

As indicated above, resonances are present at every rational ratio of the tunes. In the design process, the major resonances should be either be avoided, or if traversed, then quickly so little growth in emittance occurs, or by requiring the beam to be in equilibrium in the vicinity of the resonance - so that even though the resonance is still there, there is no free energy and it is not excited.

Thus the eln/etn = 2/1 = 2 chart of Fig. 5.2.3-1 is equipartitioned at kz/kx = 1/2 = 0.5, and this is why no growth occurs in this region, until the tune depression reaches about 0.3 and less.

It is seen that there are areas in the tune chart where the trajectory can be placed without significant growth, especially around the equipartitioned region. It should be remembered, however, that there are an infinite number of smaller resonances. A (non-equipartitioned) trajectory cutting across a region of kz/kx that is free from the major resonances shown will still exhibit a small, linearly increasing emittance as the beam is excited by these smaller resonances. The linear growth is typical of such a random scattering effect.

Thus, the EP condition need not be satisfied exactly, and good designs are possible without purposely using the equipartitioning relation. However as will be shown, it is practical and effective to satisfy it nearly exactly after the bunch has been formed. The EP ratios eln/etn=b/a=σt/σl can even be varied along the trajectory if desired, always avoiding growth due to the corresponding resonance. That is, one could purposely traverse a major resonance without significant effect if the beam is maintained in equilibrium during the traverse.

The information represented by the Hofmann chart can also be represented in the typical phase-space plots of nonlinear systems, which show resonance islands, and which change depending on the degree of nonlinearity in the system. As the nonlinearity is increased, resonances begin to overlap. Eventually, the last free-standing resonance is overlapped and the system breaks into complete chaos. The degree of nonlinearity at this point is called the stochastic limit, and is seen to occur on the Hofmann Chart when the tune depression reaches ~0.3 and below, where there is a general area of growth.

There is a very significant change in the nature of the phase-space dynamics, phase-space transport, and growth rates or disturbance settling times when the stochastic limit is reached. Beyond the stochastic limit, the system is in chaos, with strong mixing and short settling time. In this region, the term temperature can be invoked. Below the stochastic limit, where a linac usually operates, the growth dynamics is completely different, and use of the terms “temperature” and “thermalization” are not appropriate (although rather widely invoked in the accelerator community). The dynamics is characterized as “meta-stable,” with very long settling times; there are areas of phase-space that are stable and others that are chaotic. Another way of saying this is that “simplification” by using the space-charge limit (tune depression = 0) is inappropriate for practical design work.

The Hofmann Chart will be used below to assist in defining and clarifying the beam dynamics of the three sample RFQs. As a reminder, the designer should remember that if the emittance ratio changes, a different chart is needed.

5.3 Beam-Based Design Procedure

5.3.1 LINACSrfq Design Interface

The ingredients for beam-based design are now in hand - the two matching equations which should always be satisfied, and the third EP equation, which may be invoked if desired and solved simultaneously with the matching equations. Three RFQ parameters, typically the transverse and longitudinal beam sizes, and the modulation if EP is used, are used to satisfy the equations. At this time, the remaining (many) RFQ parameters must be chosen from other perspectives that do not involve beam/structure equations directly. (Design optimization is still an open issue, with many possibilities for more complex expression.)

The LINACSrfq design code incorporates this approach. The designer has cell-by-cell control over all parameters, and over the space-charge physics behavior desired.

It is important to note that now, as the beam itself is specified in terms of its rms emittances as well as current, the design and optimization process are now specific to this beam. This is why certain knowledge of the ion source and LEBT is important. In a factory-type application such as IFMIF, the characteristics of the ion source and LEBT should be reproducible within certain limits (for example, if the ion source is replaced with a spare).

The beam-based design interface for the LINACSrfq code is next outlined to illustrate the design process [7].

(* Set up the general characteristics of the RFQ *)

```
injenergy = 0.095; (* IFMIF EP RFQ, new spec *)
curamp = 0.130;
freq = 175.;
him = 2.0145;
q = 1;
endenergy = 5.; (* final energy of RFQ, MeV *) )
```

(* IFMIF is a 4-vane type RFQ. Rf power factors are specified - see Section 7 *)

```
rfqtype = 4vane;
powcuLEDAscaletoIFMIF = 7.94;
powcuFac = powcuLEDAscaletoIFMIF;
```

(* Initialize V2TERM or VSINE vane geometry functions for 4-vane RFQ. Turn multipoles on (mon) or off (moff), or (mon) with individual control of mpole terms (terms 1 = A01 and 3 = A10 are always 'on'. mpoleterms(A01, A03, A10, A12, A21, A23, A30, A32 *)

```
geom = "VSINE";
```

```
mpoleswitch = "mon";
mpoleterms = {1, 1, 1, 1, 1, 1, 1, 1};
If[mpoleswitch == "moff," mpoleterms = {1,0,1,0,0,0,0,0}];
getvanegeomcoeffs; getimagecoeffs;
```

(* Set RhooverR0 (could also be f(z) *)

```
RhooverR0 = 0.75;
```

(* The "field" is set to the desired Kilpatrick level KPlimit*KPfac. *)

```
KPlimit = limkpfld[freq];
```
(* = 13.98 at 175 MHz *)

```
KPfac = 1.7;
```

(* Enter the desired input normalized rms emittances (pi - cm - rad), *)

```
etnrmsgiven = 0.000025;
elnrmsgiven = 0.000040;
```

(* enter the rms emittances desired in the main RFQ after the shaper: *)

```
etnrmsgivenmain=etnrmsgiven;
elnrmsgivenmain=elnrmsgiven;
```

Here are some examples of apriori varying emittance:

(* etnrmsgivenmain := If[(z - zstart) < 1.0, etnrmsgiven*(1 - 0.2*(z - zstart)/1.0), 0.000016]; *)

(* elnrmsgivenmain := If[z < 1.2, elnrmsgiven, elnrmsgiven + 0.000025*((z - 1.2)/8)]; *)

(*elnrmsgivenmain := -5.3276*10^(-5) + 2.174*10^(-6)*(i/celldiv) - 1.9926*10^(-8)*(i/celldiv)^2 + □ 9.0126*10^(-11)*(i/celldiv)^3 - 1.9926*10^(-13)*(i/celldiv)^4 + 1.7246*10^(-16)*(i/celldiv)^5; *)

(* Set up the engineering choices and rules for the RFQ *)

(* Shaper parameters : *)

The design process starts at the end of the shaper section, where the beam is required to be equipartitioned. The aperture is entered as a fraction of the wavelength, as a comparison to the cell length, which is βλ/2. Transmission can be optimized by varying this aperture.

```
EOSaperfac = 5.1;
apertgt = (100.*betalaminject/EOSaperfac);
```

The synchronous phase phis at the end of the shaper is near -90°, typically -88 to -84°. The RFQ will be shorter if phis is raised higher, but transmission may be lower.

```
phistarget = -84.;
```

Next the reduction in B at the beginning of the shaper is specified:

```
bfraction = 0.55;
```

Continuing to work backwards, specify the number of cells in the radial matching section.

```
rmscells = 4;
```

v[rfq] voltage rule for the shaper

frontendvrule:=(e.g., the voltage found by the KP limit at the end of the shaper)

Finally, the length of the shaper has to be specified. The program uses a rule involving the integrated zero-current longitudinal phase advance (i.e., the phase advance of a particle very near the synchronous particle), but the relation is not rigorous - siglint is only a number that controls the shaper length. The "porch" is the initial fraction of the shaper length where phis remains at -90°; phis is raised to phistarget in the remainder of the shaper. The shaper length and porch fraction are used as optimization variables to minimize the energy of lost particles.

```
siglint = 270.;
porch = 75.;
```

(* Main part of RFQ : *)

In a final design optimization step, the form factor is adjusted to conform to the actual distribution formed in the RFQ.

(* Interpolating function for ffadj : *)

```
ffadjrule :=
```

Rules are now specified for the main RFQ parameters. The general form is:

- *Specify some rules*
- *Select the rule to be used in this design*

(* phis[rfq] law in main rfq. *)

Specification of the Teplyakov-Kapschinsky Rule, here with saturation at -20° if reached. The bucket-beam length ratio can be varied along the RFQ; lfacincr is the change in the ratio, lfacdist is the distance over which the change is made.

```
lfacincr = 0.0;
lfacdist = 10.0;
c2 = lfacincr/lfacdist;
TKphisrule := (If[phisbw ≤ -20., phis[rfq] = phisbw,
                  phis[rfq] = -20.];);
```

Another rule, with cosine-like form:

```
cossec = 0.4;
endphis = -20.;
Cosphisrule := (If[phizz ≤ -20., phis[rfq] = phizz,
                  phis[rfq] = -20.];);
```

A rule linear with position along the RFQ:

```
philinear := -88. + 43.*((z - zstart)/(2.7 - zstart));
```

Choose which rule to use in this run:

```
mainrfqphisrule := TKphisrule;
```

Another example of a rule which could be used:

(* mainrfqphisrule:=If[philinear > phisbw, phis[rfq] = philinear, (philinear = -90.; TKphisrule)]; *)

(* a[rfq] aperture rule for main RFQ : *)

```
mainrfqaperrule := (endbeta = 0.073;
          c3 = 1.2;
          a[rfq] := atarget*(1 +
     c3*((beta-betastart)/(endbeta-betastart))^1.0); );
```

(* v[rfq] voltage rule for the main RFQ *)

(* mainrfq voltage definitions : *)

```
vKP = KPlimit*KPfac*r0[rfq]/ckappa[rfq];
vlinear = vol0*(1.0 + (1.33* (z - zstart)/endz));
endz = 1.63;
```

Choose rule:

```
mainrfqvrule :=vKP;
```

(* em[rfq] modulation law in main rfq. *)

(*1. For EP, em[rfq] is used to solve for the EP condition. Also used for Constant B strategy. *)

```
mfree := (em[rfq] =.;);
```

(* 2. Function for em[rfq] : *)

```
mfunc := (em[rfq] = Min[emtarget*(1. + 1.*((z -
              zstart)/0.85)^1.0),3.0];);
```

(* 3. em[rfq] is driven by a cosine function which starts using the em[rfq] slope at the end of the shaper, has length = cossecem, and ends with zero slope at the specified end value of em[rfq](endmodl). *)

```
cossecem = 1.75;
endmodl = 3.;
mCostype := emzz;
```

(* Set mainrfqemrule to one of the laws *)

```
mainrfqemrule := mfree;
```

(* Choose strategy for main RFQ : *)

(* 1. **matchonly** - will use a rule for em[fq], e.g., mfunc, and the two matching equations.

2. **matchEP** - em[rfq] is a variable (use mainrfqemrule := mfree;), matching and EP equations are satisfied.

3. **matchConstB** - em[rfq] is a variable (use mainrfqemrule := mfree;), matching equations are satisfied and B is kept constant.

4. **matchboaRatio** - em[rfq] is a variable (use mainrfqemrule := mfree;), matching equations are satisfied and rmsl/ rmsr is kept constant **boaratio = 1.2;**

5. matchUser - user written criteria *)

```
matchUser := ……;
```
Select the strategy to be used for this run:
```
mainRFQstrategy := matchEP;
```

Everything has now been specified and the design program is ready to run. Many other variations could be specified; all the parameters are under control.

(* Run the subroutines that generate the shaper *)
The front end is generated from the end of the shaper (EOS) backwards. First the EP and matched condition at the EOS is found, then the conditions at the beginning of the shaper, then at the entrance of the RFQ. Working forward, the radial matching section and shaper are generated. The process is iterated using the energy found at the EOS on the first pass. Two passes suffice.

```
nshprpasses = 2;
For[(j = 1;emtarget = setbeginem;),j <= nshprpasses, j++,
      (dum =x; shprpass=j; shprend;
      If[j==1, (energy = injenergy),
            (energy = energystart)];
      shprtgt; beginshprtgt; enterrms; rfqshramp; pass)];
```

(* Run the subroutines that generate the main RFQ *)
Then the main RFQ is generated from the EOS to the final energy.
```
phisemrules; rfqaemvar; passmain;
```

5.3.2 Design Strategy Discussion

The RFQ has now three sections - radial matching, shaper (to bring the beam to EP), and acceleration.

Bringing the beam to the EP condition at the end of the shaper (EOS) has proven so robust and useful that it is the standard approach. It is easy to change the shaper rules, for example, to the constant r0 conventional method which exhibits the bottleneck, but tests of this method against the EP at EOS method (ref. Comment in [7]) have consistently shown better beam-loss performance for the EP at EOS method.

Complex rules in the main RFQ can be specified; for example:

- The CDR and Post-CDR RFQs , typical of high-intensity cw RFQs, maintain EP from the EOS to the end of the RFQ.
- Bringing the RFQ to EP at the EOS, and then relaxing the EP condition downstream while taking care to not let the tune depressions become too low, and if a major resonance is crossed, then to cross it quickly, has been an effective method for some applications [44].

Rules are specified for all other parameters.

The original goal of this approach was first to bring all of the RFQ parameters and beam physics (the matching and EP envelope equations, plus some detailed extensions, which are all we know at this time) under complete and flexible control. This is now achieved. The original goal was then to investigate optimization.

5.3.3 Design Optimization Discussion

There are so many parameters, and so many different views of what an optimum constitutes, that optimization if still an open and very interesting research topic. As computer power continues to increase, it becomes more feasible, and modern optimization methods, which can handle many variables and strategies, should be applied to the accelerator design problem.

Experience with LINACS has resulted in an effective, but tedious optimization procedure [7]; after each LINACS step, pteqHI has to be run to check transmission, energy at which losses occur, etc.

1. Get a rough design using the desired design strategy and default values that results in a solution.
2. Find a reasonable input beam ellipse alpha and beta.
3. Optimize transmission varying EOSaperfac.
4. Minimize beam loss above ~10 times the input energy (e.g., above 1 MeV) by varying the shaper parameters siglint and porch. The length of the shaper and porch have influence on the transmission and also on the maximum energy of the bulk of the lost particles.
5. Find the input match for best transmission using the transmission matrix option in pteqHI. Using the simulation code pteqHI, the input match must be checked occasionally as the design develops. The most reliable input matching method is to find the transmission over a matrix of input ellipse alphas and betas.

All five of the main RFQ specifications are strongly influenced by the coefficients used in the Teplyakov synchronous phase rule, the voltage and aperture rules, and by the equipartitioning and emittance rules selected.

6. The aperture must open enough as a function of beta to keep radial beam loss low; this raises the voltage and the length.
7. Reduce the RFQ length if possible using a negative lfacincr to allow the beam length to grow relative to the bucket length.
8. Length is also reduced for lower EP ratio. Varying EP strategy may be useful.
9. For lower current designs, abandoning EP after the shaper may be useful.
10. Iterate, iterate. Tedious.

When the design has been optimized, a final optimization step almost always produces another significant improvement in transmission - an adjustment in the design code of the space-charge form factor, sometimes augmented by an apriori adjustment of the transverse and longitudinal rms emittances.

6. Comparisons of the Three RFQs in Terms of Beam-based Design

6.1 The IFMIF CDR RFQ Design

The optimized CDR equipartitioned RFQ design and simulation were prepared for the CDA [7] and CDR. The input current was specified as 140 mA, to be sure of accelerating at least 125 mA. The input transverse normalized emittance was specified as 0.20 mm.mrad, the estimated emittance of the ECR ion source. At that time, multiple and image-charge effects were not included in the design code LINACSrfq or the simulation code pteqHI; simulation using codes available at that time which included multipole and image-charge effects indicated transmission of ~95%.

The design optimization (for minimum beam loss at energies above ~ 1 MeV, short length, low peak field, low rf power, high percentage of accelerated particles) was done using the 2-term potential description. The design maintains an equipartitioned beam from the end of the shaper to the end of the RFQ, with fixed emittance ratio eln/etn = 2.0. Simulation using the corresponding 2-term potential description showed that the beam is very closely equipartitioned from the end of the shaper (EOS) to the end of the RFQ, as indicated in Fig. 6.1-1 and on the Hofmann Chart, Fig. 6.1-2. Fig. 6.1-3 shows small emittance growth after the end of the shaper.

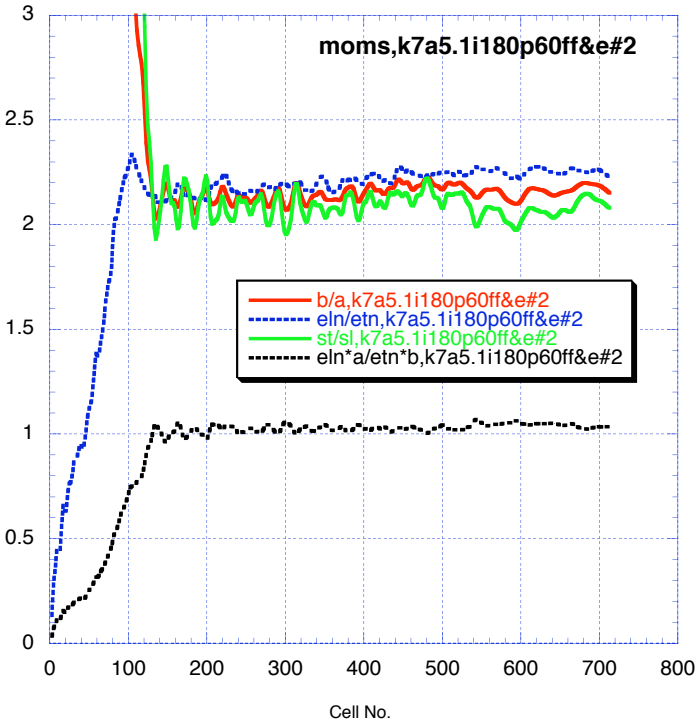

Fig. 6.1-1. Equipartitioning ratio, and corresponding beam size, emittance and tune ratios, Eqs. (7) and (8) for the IFMIF CDR RFQ using the 2-term potential. (Ignore the file ID material after the commas.)

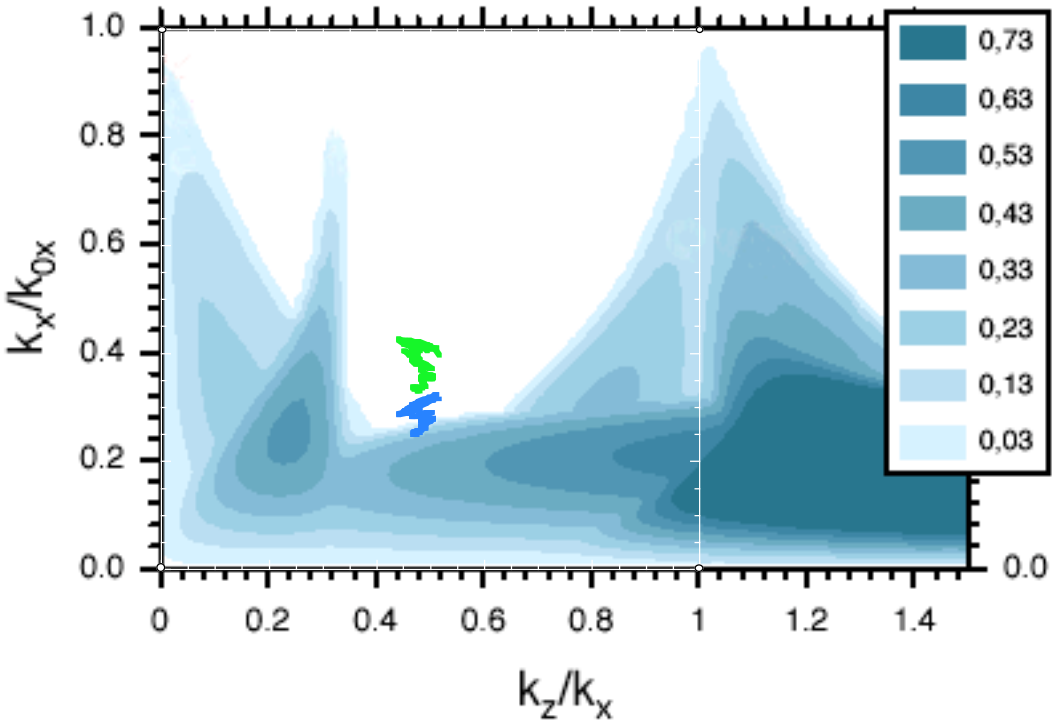

Fig. 6.1-2. Hofmann Chart for eln/etn=2.0, showing the trajectory for the IFMIF CDR RFQ from the EOS to the output, using the 2-term potential.

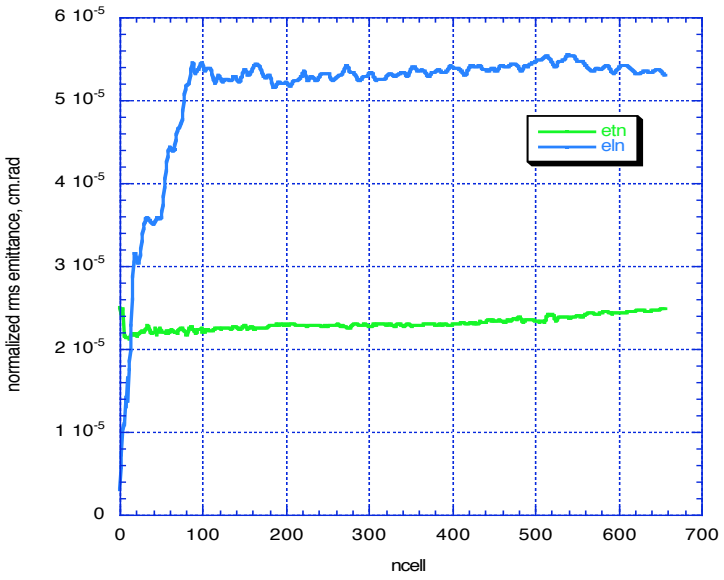

Fig. 6.1-3. Longitudinal and transverse normalized rms emittances through the IFMIF CDR RFQ.

During 2006, multipole and image-charge effects were added to LINACSrfq and pteqHI, and the IFMIF CDR RFQ was resimulated in pteqHI, using the same input beam.

Section 3 shows results; the accelerated beam transmission drops to ~90%, while the percentage of beam loss above 1 MeV remains low at 0.073%. Figs. 6.1-4 and 6.1-5 indicate the effect on the space-charge physics; the beam is no longer equipartitioned, and the trajectory has moved toward the resonance to the left. This simulation with multipoles and image-charges is used below in the comparisons.

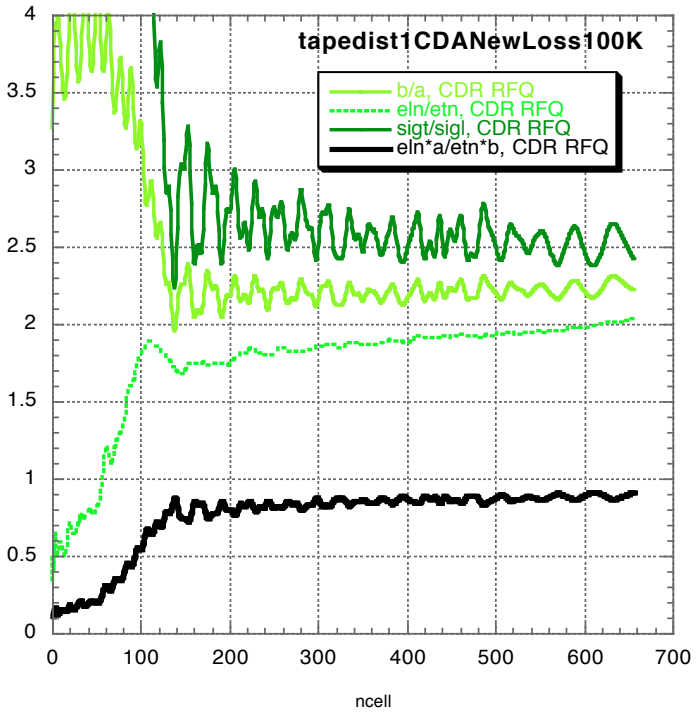

Fig. 6.1-4. Equipartitioning ratio, and corresponding beam size, emittance and tune ratios, Eqs. (7) and (8) for the IFMIF CDR RFQ using pteqHI including multipole and image-charge effects.

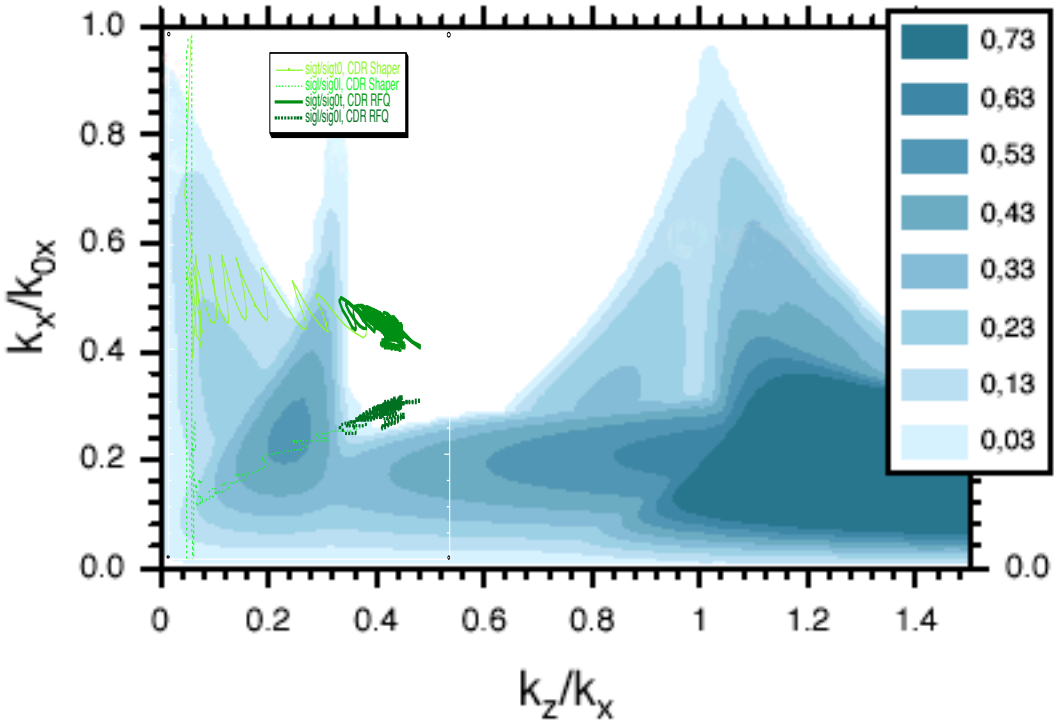

Fig. 6.1-5. Hofmann Chart for eln/etn=2.0, showing the IFMIF CDR RFQ trajectory for the shaper and from the EOS to the output, using pteqHI including multipole and image-charge effects.

The beam size ratio remains nearly constant; the emittance ratio shows growth; Fig. 6.1-6 shows this occurs in the longitudinal rms emittance. The only difference between Figs. 6.1-1,2,3 and 6.1-4,5,6 is the addition of the multipole and image effects in the pteqHI simulation. The linear growth in the longitudinal emittance is characteristic of a scattering effect.

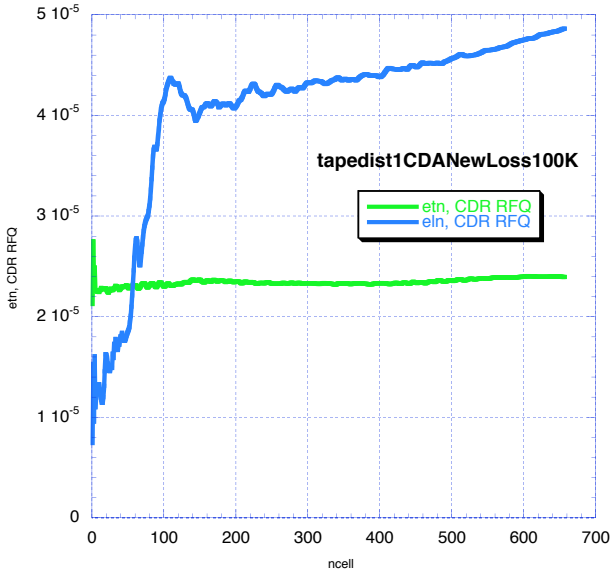

Fig. 6.1-6. Transverse and longitudinal rms normalized emittances for the IFMIF CDR RFQ, using pteqHI including multipole and image-charge effects.

6.2 The IFMIF Post-CDR Equipartitioned RFQ Design

6.2.1 Post-CDR RFQ Design Objectives

The Post-CDR RFQ design effort has several objectives:

- to determine if the design optimization procedure including multipole and image-charge effects would still function in the same way as the procedure outlined in [7] without multipoles and image-charges. The multipole effects are significant in the beam envelope design code LINACSrfq, while the image-effects are not; both are significant in the simulation code pteqHI. The result was that the optimization procedure remains the same, and the design produces a compensation for the multipole effects, resulting in good transmission and low losses at higher energy.
- to use the recommended lower vane voltage at the front end, for easier matching and lower rf power.
- to explore the trade-off between RFQ length and rf copper power requirement, and the effect on performance. It is seen that good beam-loss and transmission performance can be obtained with shorter length than the CDR design, at approximately the same rf power. It is more important to conserve rf power than to have a short RFQ, because of the rf power operating cost. Very roughly from the CDA Cost Estimate:

CDR Design, requiring ~1MW rf copper power for the RFQ:
RFQ structure cost = (the average of Acc#1 and Acc#2)
= ($15.69M + $9.83M) = $12.8M
Accelerator Hall Cost for RFQ = total*(5MeV/40MeV) = $6.7M(1/8) = $0.84M
Total RFQ Cost = $13.64M

RF system cost = (total, the average of Acc#1 and #2)*(1/8)= ($77M)(1/8) = $9.6M
Rf power bay cost = total(1/8) = $5.9M(1/8) = $0.74M
Total RFQ rf power fixed cost = $10.34M

Total fixed cost for RFQ (no spares) = $24M

Electricity cost/ kWhr = $0.10
Total electricity cost/year for Acc#1 = 1.33*10^8 kWhr*0.1 = $13.3M/yr
RFQ electricity cost/year ~ total(1/8) = $1.6625M/yr
RFQ electricity cost for 20 years = $33.2M
RFQ electricity cost for 40 years = $66.4M

Post-CDR Design, requiring ~1.0MW rf copper power for the RFQ:
RFQ structure cost = $12.8M(8m/12m) = $8.5M
Accelerator Hall Cost for RFQ = $0.84M(8m/12m) = $0.56M
Total RFQ Cost = $9.06M

Total RFQ rf power fixed cost = same = $10.34M

Total fixed cost for RFQ (no spares) = $20M

Electricity cost = same

This suggests that the PostCDR RFQ saves the project ~$4M. On the other hand, if the RFQ length remained at 12m and the rf power could be reduced to ~800kW, a savings of nearly $10M would result. Little experience has been obtained so far with optimization; it is possible that a search in the latter direction could be fruitful.

6.2.2 Post-CDR Specification Changes

The Post-CDR specifications were changed in accordance with specification changes adopted for the Alternative CDR RFQ:

- the current was reduced from 140 mA to 130 mA, in expectation that a higher percentage of accelerated current could be obtained from the RFQ to give 125 mA output current.
- the injection energy was lowered from 0.100 MeV to 0.095 MeV. This would result in a shorter RFQ assuming all other conditions were the same.
- the normalized rms input emittance was raised from 0.2 pi.mm.mrad to 0.25 pi.mm.mrad, reflecting a newer estimate of how the ion source and LEBT would perform. This lowers the space-charge effect.

However, the KP factor = 1.8 used for the alternative CDR RFQ was lowered to KP = 1.7, the same as used in the CDR RFQ. It was found that the higher KP factor is not needed to provide adequate focusing, and requires more rf power.

6.2.3 Intermediate Fixed EP Ratio Design

An initial optimization attempt explored a lower EP ratios setting, as this has a strong effect on the RFQ length. Figs. 6.2-1,2,3 show the space-charge physics and emittance behavior of an RFQ designed for a fixed emittance ratio = eln/etn = 1.6, and optimized including the multipole effects.

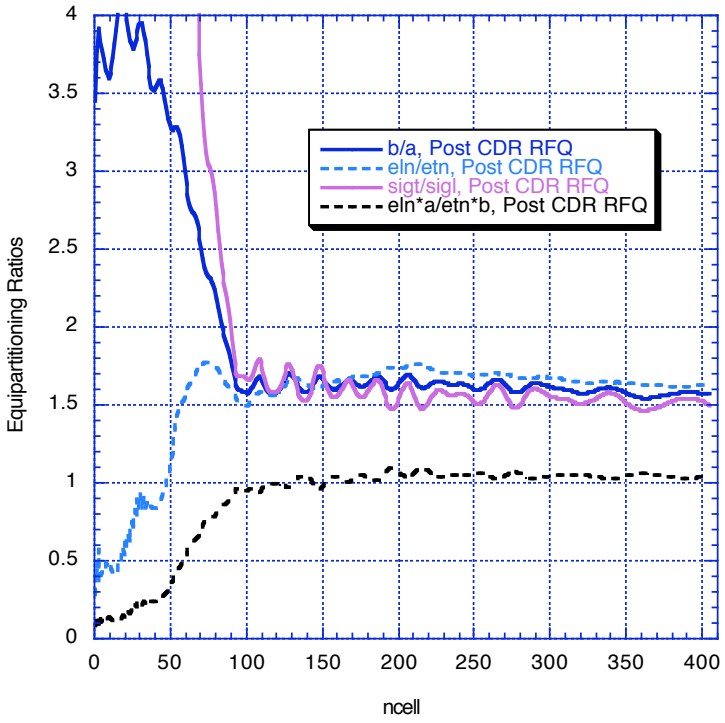

Fig. 6.2-1. Equipartitioning ratio, and corresponding beam size, emittance and tune ratios, Eqs. (7) and (8) for the intermediate RFQ using pteqHI including multipole and image-charge effects.

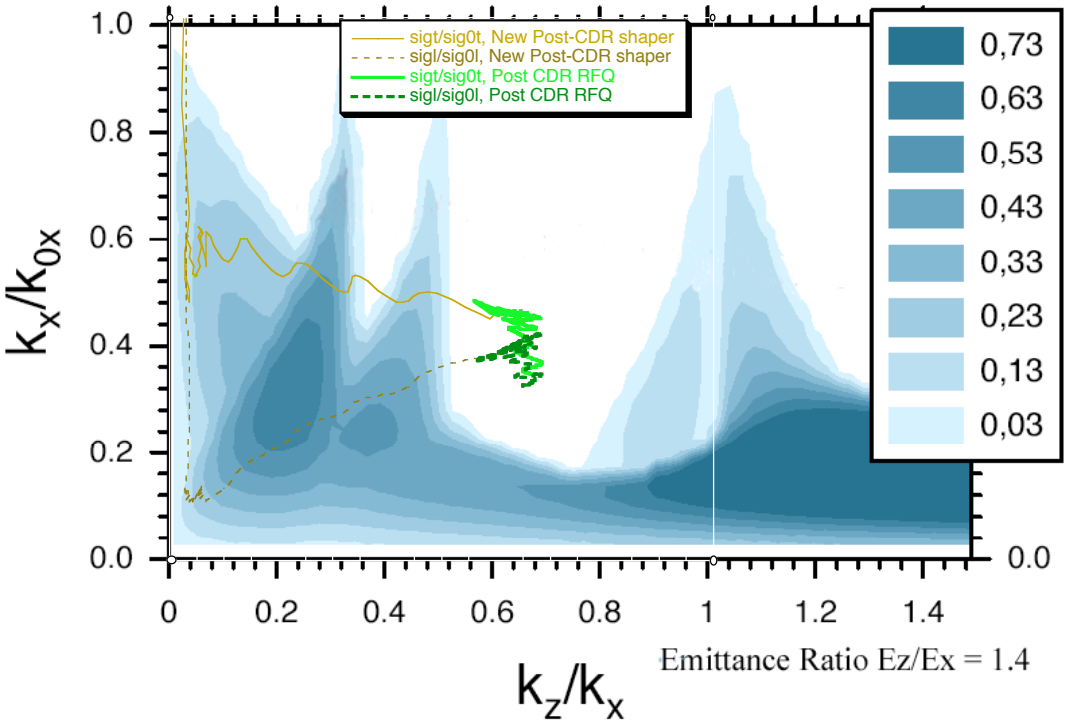

Fig. 6.2-2. Hofmann Chart for eln/etn=1.4, showing the intermediate RFQ trajectory for the shaper and from the EOS to the output, using pteqHI including multipole and image-charge effects.

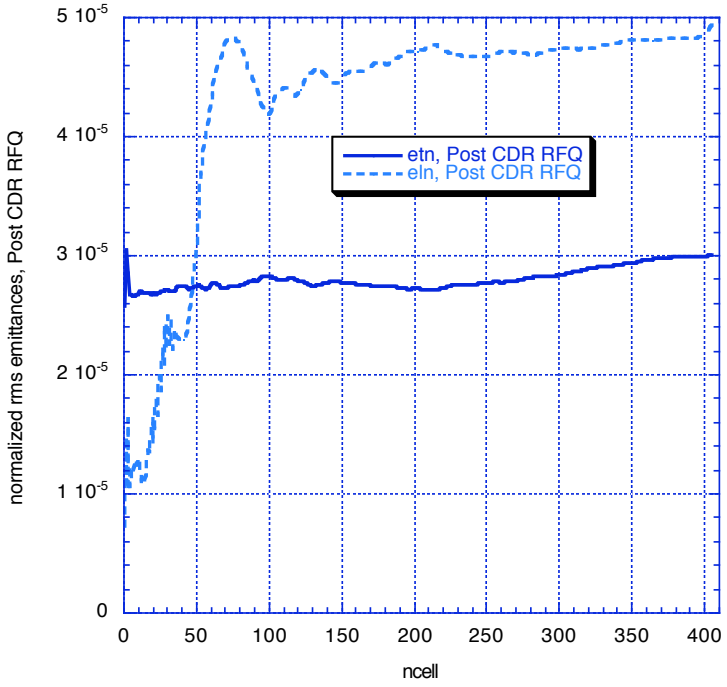

Fig. 6.2-3. Transverse and longitudinal rms normalized emittances for the intermediate RFQ, using pteqHI including multipole and image-charge effects.

The equilbrium, equipartitioned, condition is held closely from the end of the shaper to the end of the RFQ.

This 1.7 KP RFQ requires ~1.0 MW rf power and is ~7.6m long, considerably shorter than the CDR RFQ. However, 0.72% losses above 1 MeV occur for a 1M particle ideal waterbag input distribution, and 1.15% for the ion source distribution - ~10 times the CDR RFQ, and unacceptable. A large fraction of these losses occurs during the synchronous phase rise after the shaper, and is not influenced greatly by the shaper length and porch.

In these RFQs, the Teplyakov synchronous phase rule is relaxed to let the ratio of bucket-to-beam length reduce somewhat through the main RFQ. This provides a significant reduction in the RFQ length.

Figs. 2.4-12, 6.1-5, and 6.2-3 show longitudinal emittance growth approximately linear with cell number after the end of the shaper. The observed emittance growth suggested a strategy for reducing the losses above ~1 MeV.

6.2.4 Post-CDR RFQ Varying EP Ratio Design

In the final Post-CDR design, the longitudinal normalized rms eln is given, on purpose, an apriori growth proportional to beta, while maintaining equipartitioning, with the ratios increasing from 1.6 at the end of the shaper toward 2.0 at the end of the RFQ.

The aperture was allowed to grow (also proportional to beta) more than in the intermediate design, to reduce radial losses. This results in a longer RFQ, but it was

found that the bucket-to-beam length ratio could be reduced more than in the intermediate RFQ, again reducing the length.

With these changes in the main RFQ, the effect of the shaper became more pronounced. Reoptimization resulted in a reduced B at the beginning of the shaper, and a shorter shaper (with the same fraction of porch).

The resulting KP 1.7, Post-CDR RFQ has ~0.081% beam loss above 1 MeV and 95.8% accelerated beam fraction for the source emittance input distribution. It is ~8.0 m long, not including an output Crandall transition cell or output radial matching section. It requires ~1.1 MW rf power, about the same as the CDR RFQ.

Figs. 6.2.-4,5,6 show the space-charge physics and emittance behavior. The ratios rise as a function of beta, and the beam remains closely equipartitioned. A composite Hofmann Chart with eln/etn = 2 overlaid on eln/etn = 1.4 is shown, to convey the required change in the EP ratios from 1.6 at EOS to 2 at the end of the RFQ. There is no resonance growth.

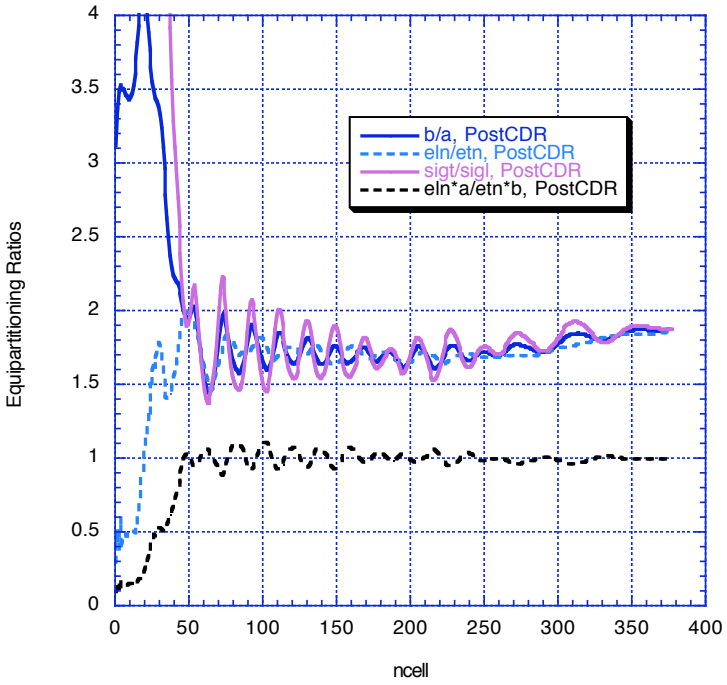

Fig. 6.2-4. Equipartitioning ratio, and corresponding beam size, emittance and tune ratios, Eqs. (7) and (8) for the Post-CDR equipartitioned RFQ using pteqHI including multipole and image-charge effects.

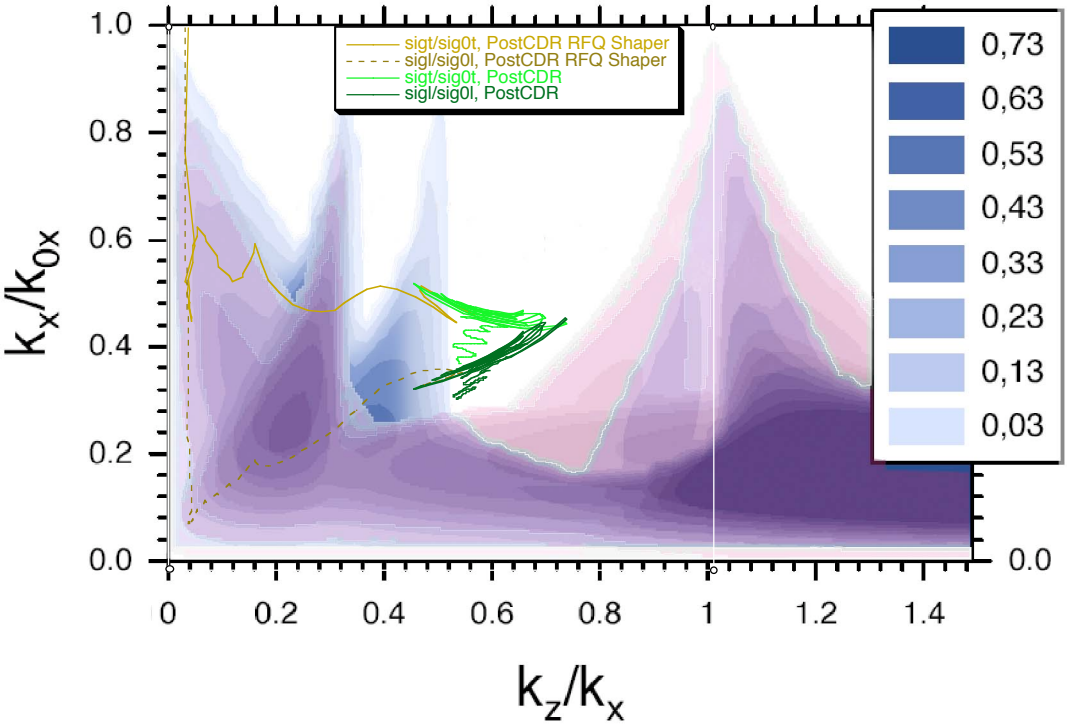

Fig. 6.2-5. Composite Hofmann Chart for eln/etn=1.4 (underlying blue-toned shadows) and eln/etn = 2 (overlying magenta toned shadows). The Post-CDR equipartitioned RFQ trajectories for the shaper and from the EOS to the output are shown, using pteqHI including multipole and image-charge effects.

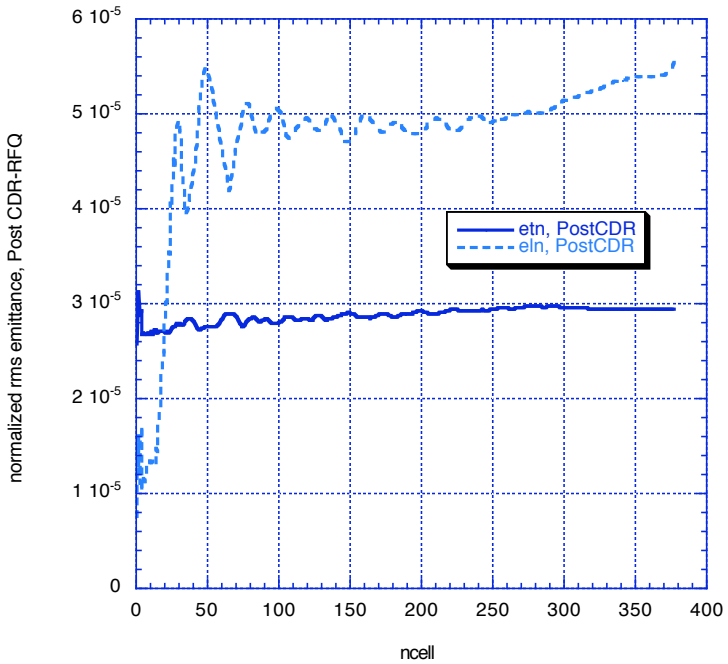

Fig. 6.2-6. Transverse and longitudinal rms normalized emittances for the Post-CDR equipartitioned RFQ, using pteqHI including multipole and image-charge effects.

6.3 The IFMIF Alternative CDR RFQ Design

The space-charge physics of the Alternative CDR RFQ conventional design is more complicated. Figs. 6.3-1,2,3 explain the situation and concerns such as expressed in Section 4.4.

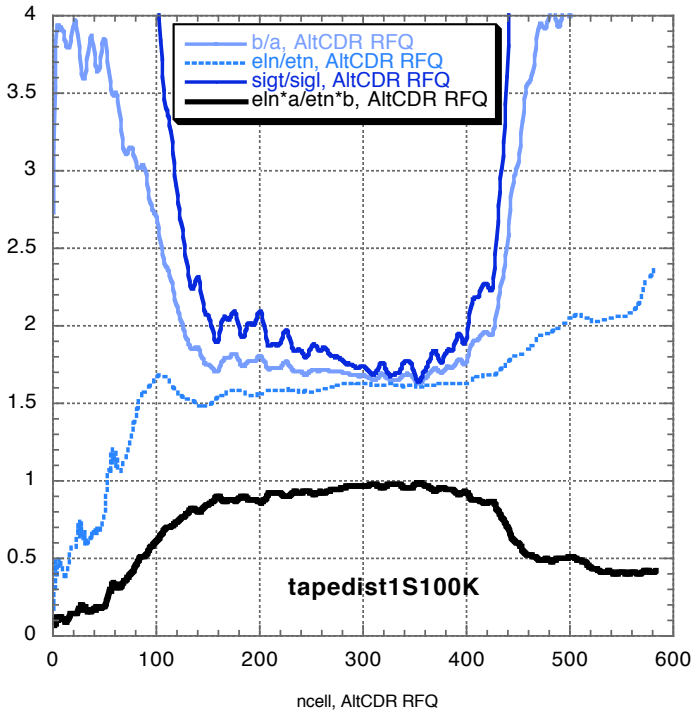

Fig. 6.3-1. Equipartitioning ratio, and corresponding beam size, emittance and tune ratios, Eqs. (7) and (8) for the IFMIF Alternative CDR RFQ using pteqHI including multipole and image-charge effects.

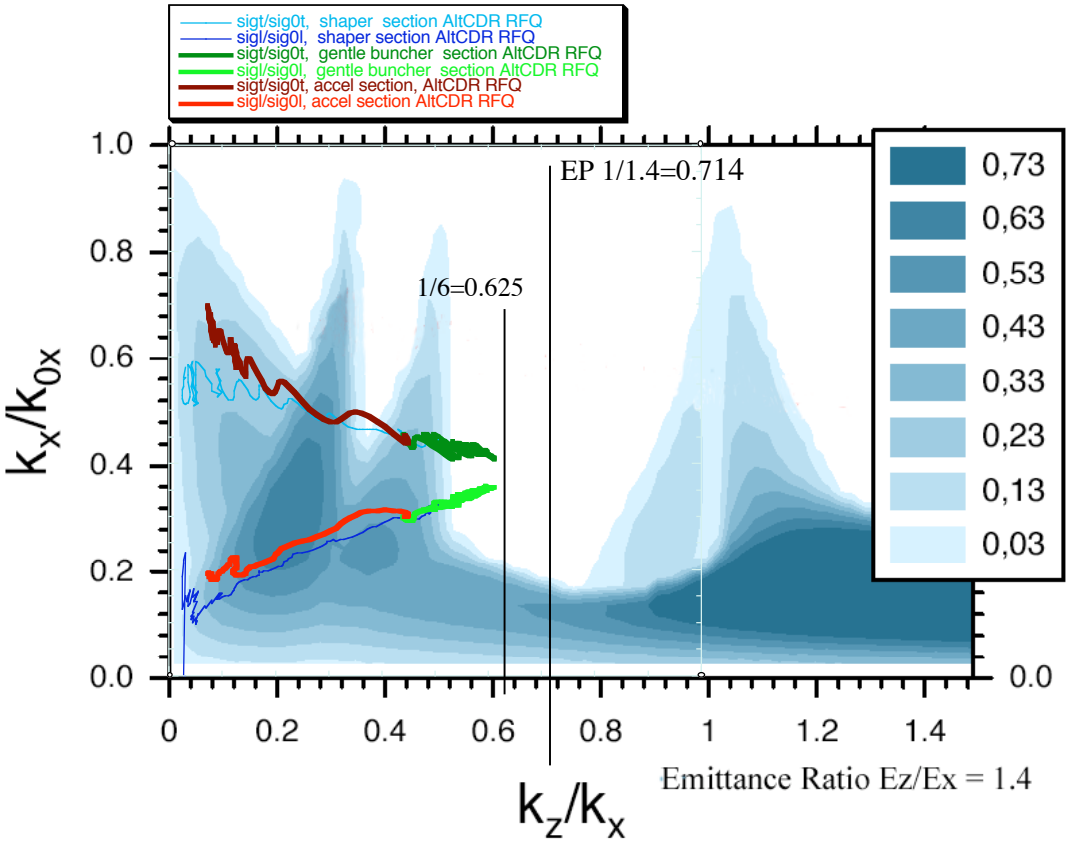

Fig.6.3-2. Hofmann chart for the AltCDR RFQ. Chart is for emittance ratio of 1.4. Beam reached equipartitioned equilibrium briefly at emittance ratio of 1.6 (Fig.6.3-1). (On a chart with 1.6 emittance ratio, the resonance at kz/kx=0.5 would be weakened, and the resonance to the left of kz/kx=1 would be stronger).

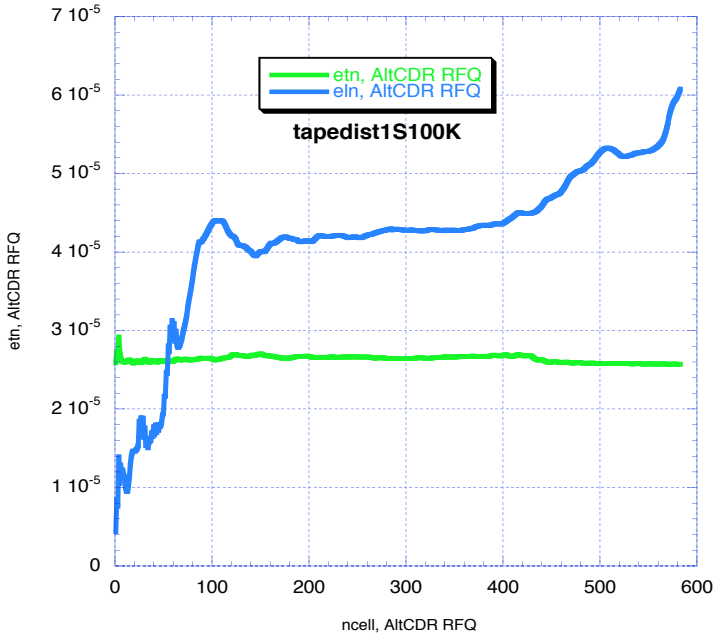

Fig. 6.3-3. Transverse and longitudinal rms normalized emittances for the IFMIF Alternative CDR RFQ, using pteqHI including multipole and image-charge effects.

Near the end of the gentle buncher, the beam coincidentally becomes nearly equipartitioned at emittance ratio eln/etn ~ 1.6. As indicated in Fig.6.3-2, this places the trajectory in a resonance-free region, and the emittances remain essentially constant.

In the acceleration section, the beam departs strongly from EP and there is free energy available to drive resonances. The transverse rms emittance stays essentially constant, with a slight reduction after the end of gentle buncher bottleneck, reflecting the loss of particles in this region. This is a consequence of the conventional design strategy, which maintains strong transverse focusing in the acceleration section. Fig. 6.3-2 shows that the transverse trajectory tune shift rises from ~0.4 to 0.7 in the acceleration section, and although it traverses the 1/2 and 1/3 resonances, the tune depression is not so low (strong transverse focusing), it crosses quickly, and no transverse emittance growth results.

On the other hand, the longitudinal tune shift decreases from 0.3 to 0.2, and traverses a strongly resonant region, with directly correlated strong longitudinal rms emittance growth (Fig. 6.3-3) and beam loss (Fig. 3.2-1 and 6.7-2).

Figs. 6.3-4a,4b show evidence of the longitudinal resonances in the z-z' phase space. The scalloping at the front edge is characteristic of a strong resonance. The tail emerges from the top of the bucket. Fig. 6.3-5 shows the z-z' phase space at Cell 420, before the onset of the resonances.

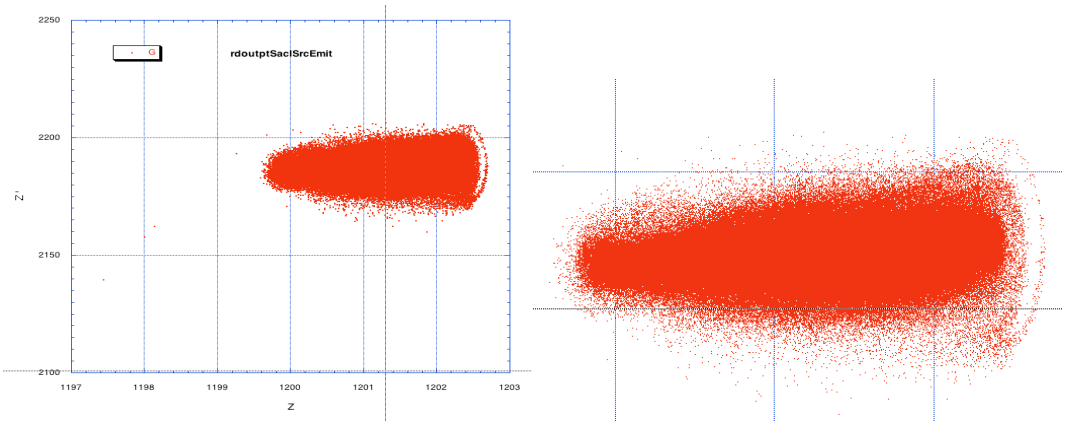

Fig. 6.3-4a. AltCDR RFQ z-z' phase space at the end of the RFQ; 4b - expanded scale

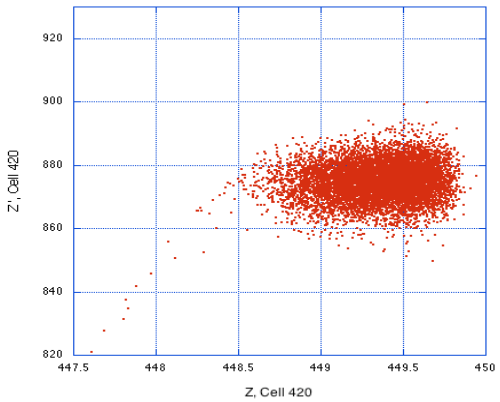

Fig. 6.3-5. AltCDR RFQ z-z' phase space at Cell 420.

6.4 Beam Size and Emittance Comparison

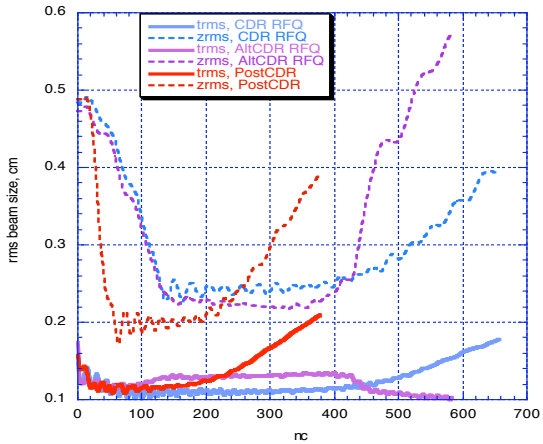

Fig. 6.4-1. Rms beam radius (trms) and length (zrms), cm.

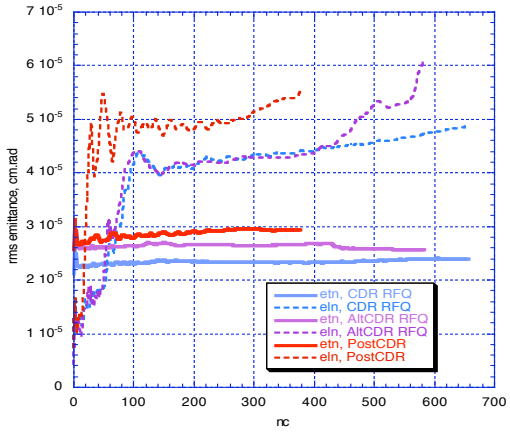

Fig. 6.4-2. Rms normalized transverse (etn) and longitudinal (eln) emittances, cm.rad. The AltCDR and CDR/PostCDR eln are not qualitatively similar, as discussed above. The transverse input distribution is an ideal waterbag, 100K particles, etn = 0.25 mm.mrad for each RFQ; an immediate redistribution in the transverse emittance occurs as the distribution adapts to the RFQ.

6.5 Tune Comparisons

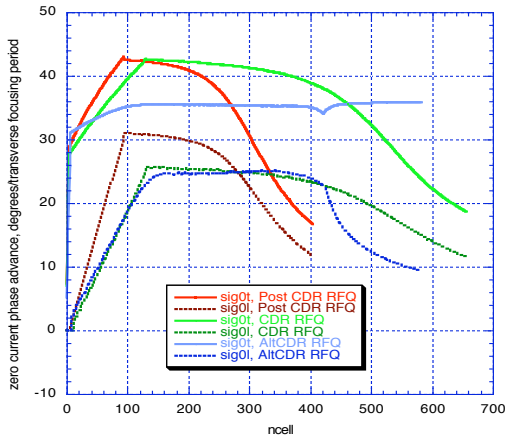

Fig. 6.5-1. Zero-current phase advances/transverse focusing period, degrees.

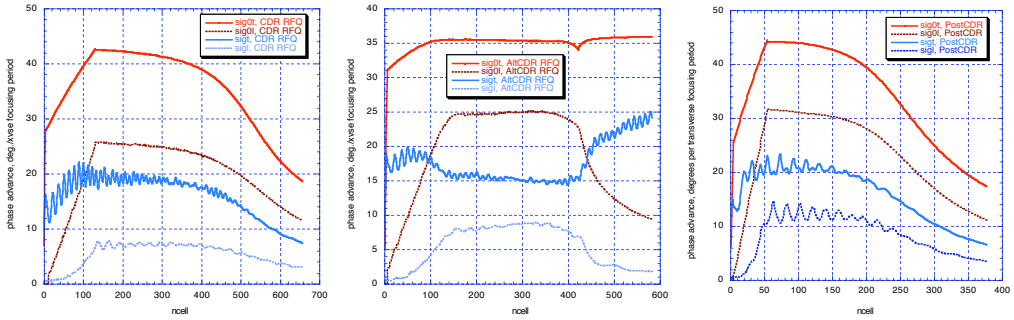

Fig. 6.5-2. Zero-current phase advances σ_0, and depressed tunes σ/σ_0, for the three RFQs.

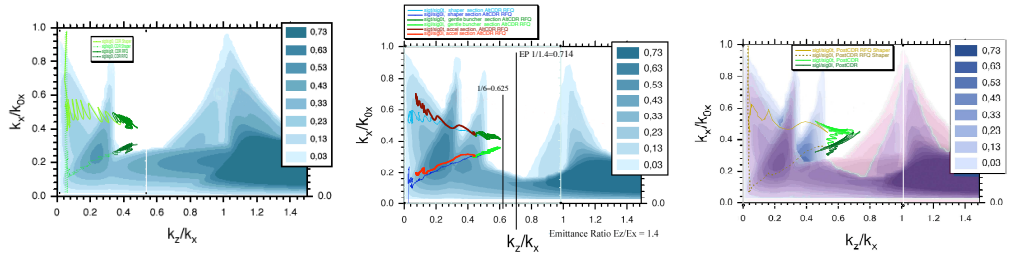

Fig. 6.5-3 Side-by-side comparison of the Hofmann Charts for the three RFQs.

6.6 Beam-Loss Characteristics

6.6.1 Representative Post-CDR and CDR Equipartitioned-Type RFQ Phase-Space Plots and Beam Loss Distribution Characteristics

Plots are at the middle of the last cell. Black: 1M particle ideal waterbag; Red: ~1M particle ion source distribution rms matched to the RFQ.

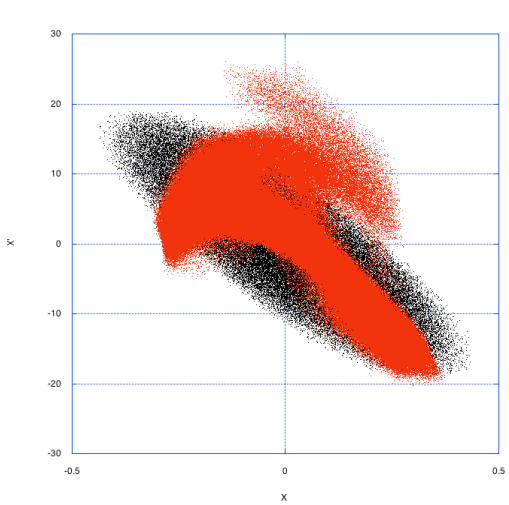

Fig. 6.6-1. RFQ x-x' input distributions.

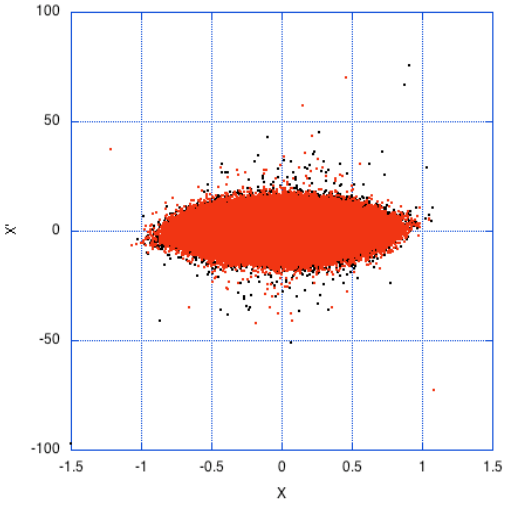

Fig. 6.6-2. RFQ x-x' output distribution.

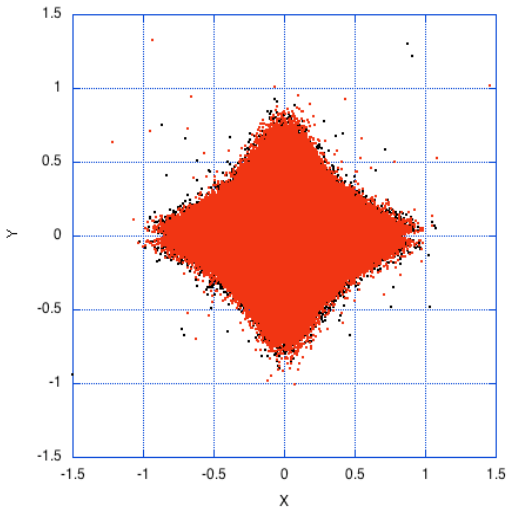

Fig. 6.6-3. RFQ x-y output distribution.

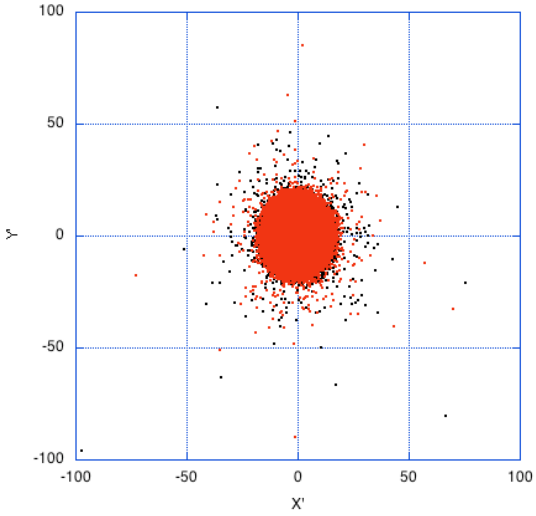

Fig. 6.6-4. RFQ x'-y' output distribution.

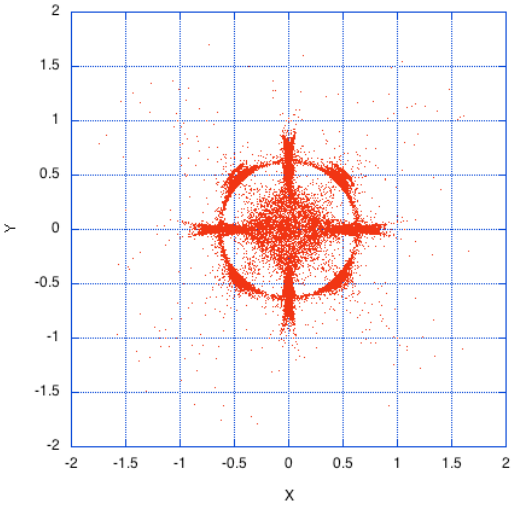

Fig. 6.6-5. x-y distribution of all lost particles.

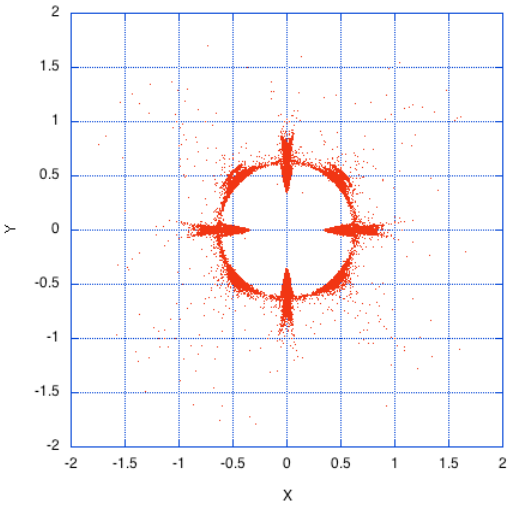

Fig. 6.6-6. x-y distribution of radially lost particles.

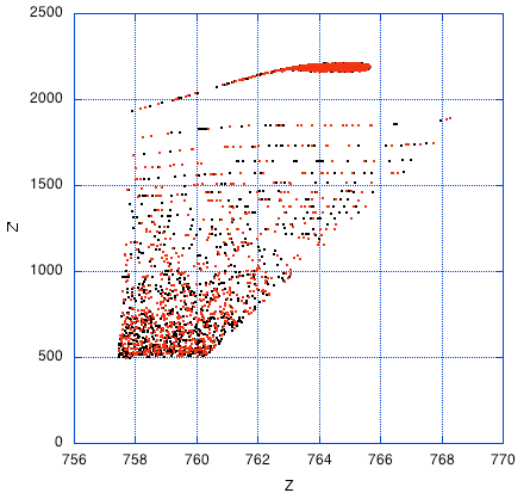

Fig. 6.6-7. RFQ z-z' output distribution.

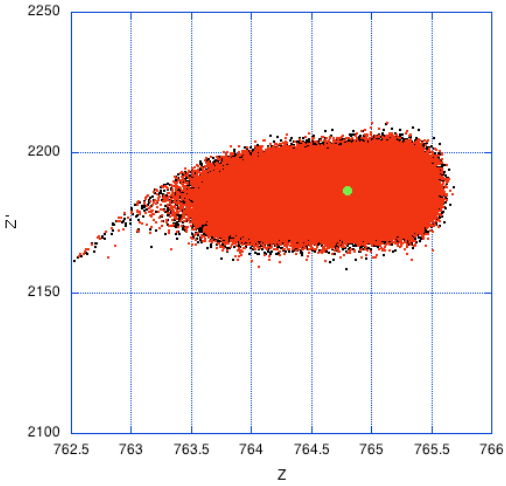

Fig. 6.6-8. RFQ z-z' accelerating bucket output distribution.

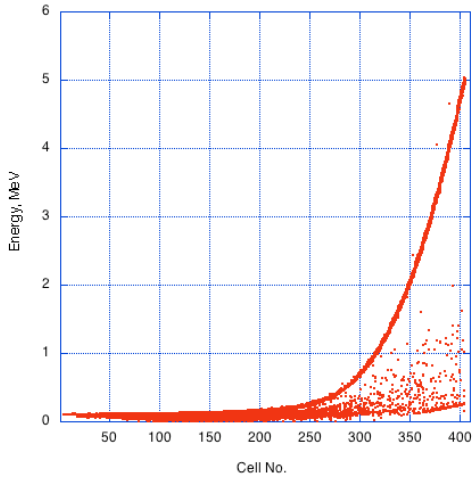

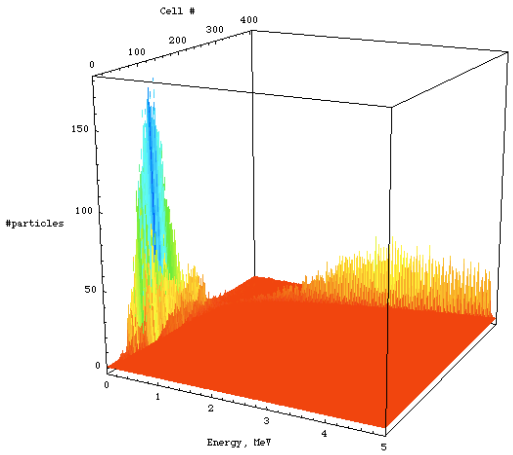

Fig. 6.6-9a,b. RFQ, with ion source input. Particle energy of all losses at each cell. There is a spectrum of lost particle energies at each cell, from ~0.05*(synchronous energy) to ~(synchronous energy).

6.7 Beam-Loss Pattern Comparisons

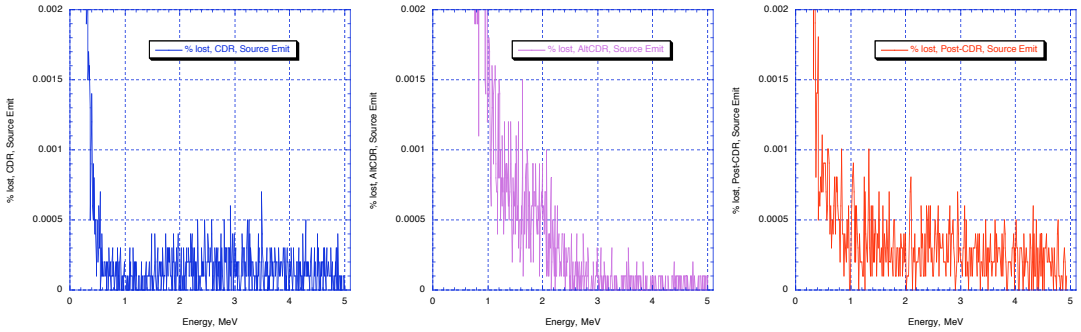

Fig. 6.7-1. Fig. 3.1-3 repeated; beam loss for ~1M particle ion source emittance distribution, expanded scale.

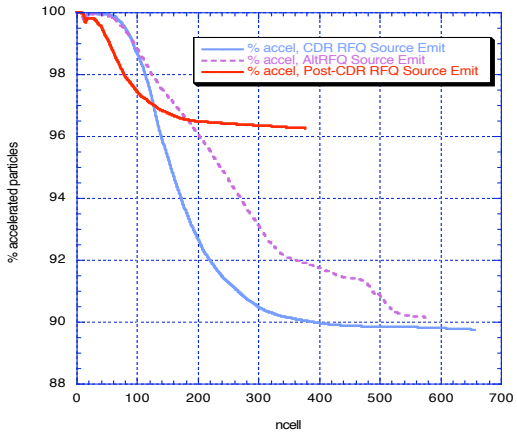

Fig. 6.7-2. % accelerated particles vs. cell number, Source Emittance initial distribution.

As shown in Section 3.1, at the design conditions, the three RFQs are rather similar; for the ion source emittance distribution of ~1M particles rms matched to the RFQ input, the percent of particles lost with energy ≥1 MeV is:

Post-CDR	0.081% loss above 1 MeV
CDR	0.073% loss above 1 MeV
AltCdr	0.123% loss above 1 MeV

The longer CDR RFQ accumulates about the same amount of losses with energies > 1MeV as the shorter Post-CDR RFQ. The AltCDR RFQ has larger losses between 1 MeV and 3 MeV, and less losses with energies above 3 MeV.

6.8 Sensitivity Comparisons

Sensitivities of the percentage of accelerated beam and the percentage of losses above 1 MeV were explored with 100K particle runs for variations of input emittance, input current, and the input emittance alpha and beta parameters. As noted in Section 8, 10K particles is not enough for reliable loss-above-1-MeV statistics, but the running time for 100K particles is long.

The same vertical scales are used for each group of plots to aid the eye in comparing the RFQs. Red - % accelerated beam; blue, % >1MeV losses.

6.8.1 Variation of Input Emittance and Input Current

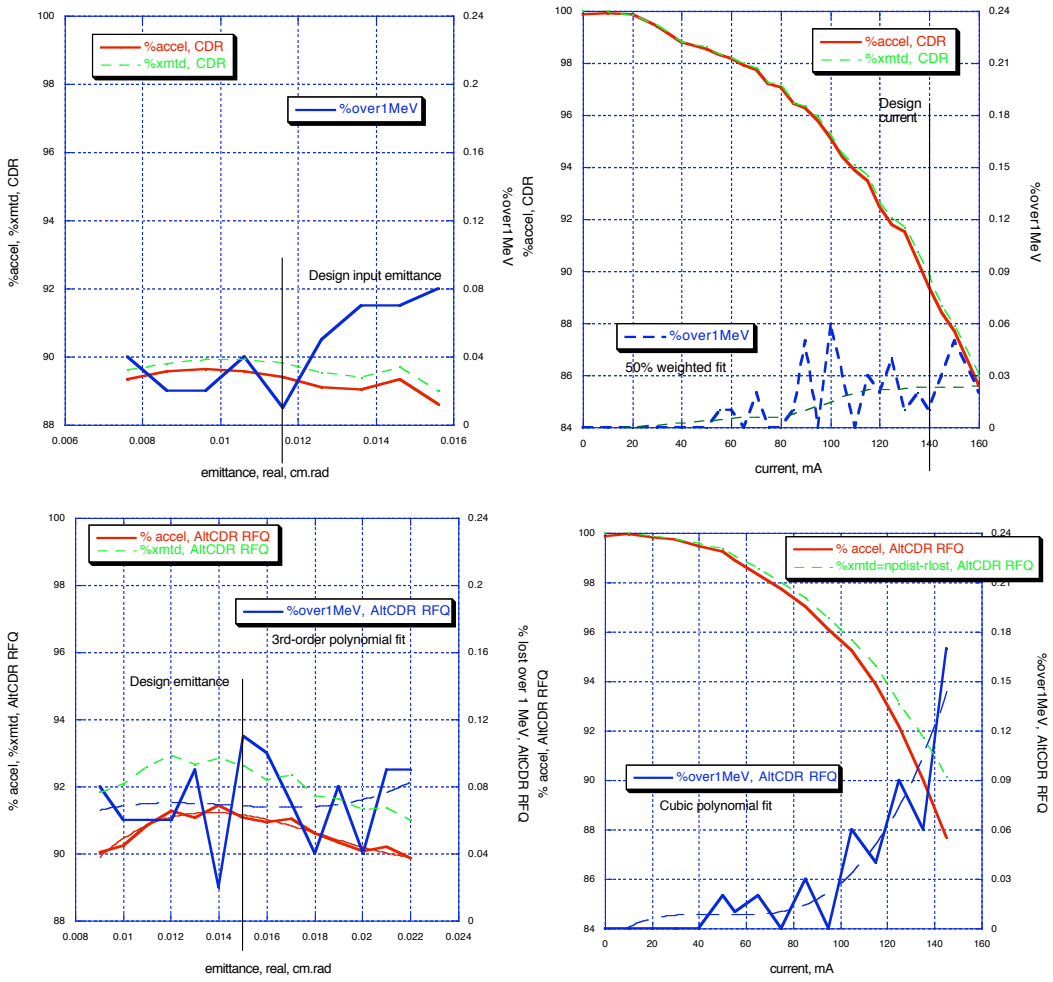

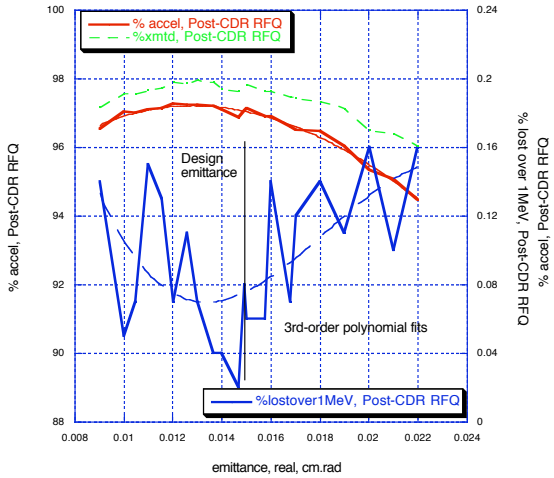

Figs. 6.8-1-a,b,c. Variation with input emittance area.

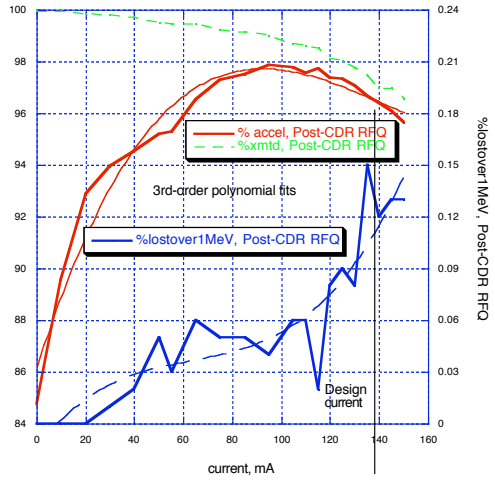

Figs. 6.8-2-a,b,c. Variation with input current.

The >1MeV-losses of the longer CDR RFQ and especially the AltCDR RFQ are quite insensitive to the input emittance area.

The long CDR RFQ has relatively low >1MeV-losses sensitivity to the input current. The AltCDR and Post-CDR RFQs are similar to each other.

The Post-CDR RFQ exhibits a decline in the percentage of *accelerated* beam as the input current is reduced. This is unusual. The behavior is the same for very small input emittance and current - the decline in accelerated beam fraction is a consequence of the quite short shaper, which, however, provided a high %-accelerated beam and acceptable >1MeV-losses at the design current.

6.8.2 Variation of Accelerated Beam with Input Emittance α and β

These figures use the 100K input distribution – see Section 8.2.4.

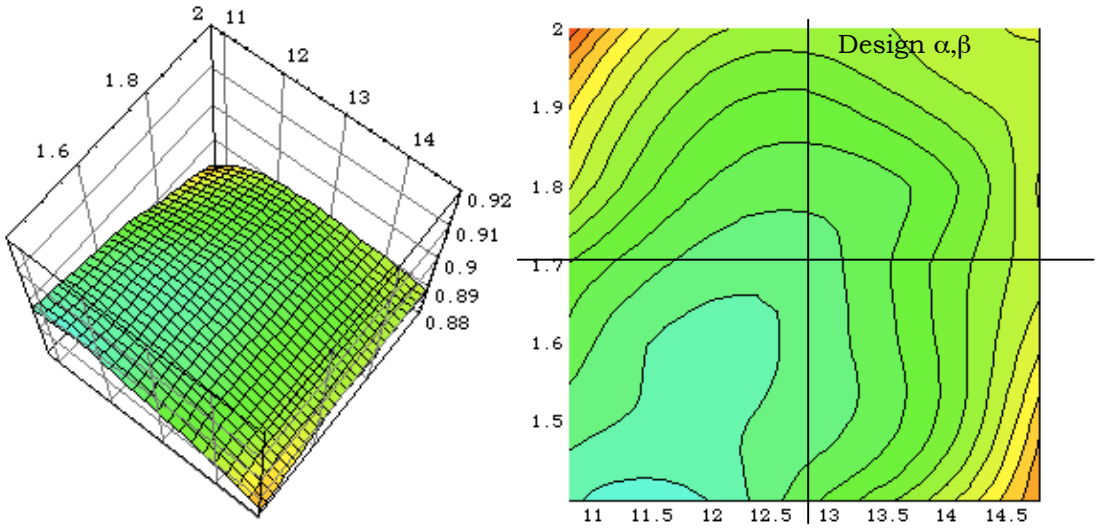

Fig.6.8-3. CDR RFQ - % Accelerated beam sensitivity to input emittance α and β. The design α and β are as found for the original CDR RFQ evaluated without multipole or image fields. At the design α =1.7008, β= 12.7828, {%AccBeam, %Loss>1MeV} is {89.6,0.034}. At α = 1.4, β = 11.5, {89.9,0.030}; at α = 1.4, β = 12.75, {89.6,0.014}; (Fig. 6.8-6).

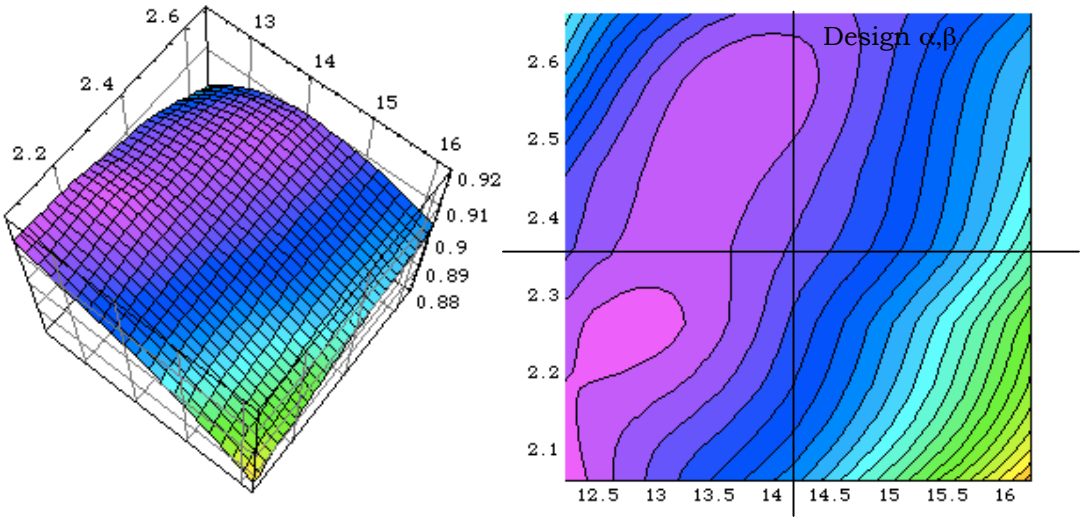

Fig.6.8-4. AltCDR RFQ - Accelerated beam sensitivity to input emittance α and β. At the design α = 2.362, β = 14.2, {%AccBeam, %Loss>1MeV} is {90.0,0.066}. At α= 2.25, β = 12.75, {91.3,0.080}; at α = 2.47, β = 15., {90.7,0.058}; (Fig. 6.8-7).

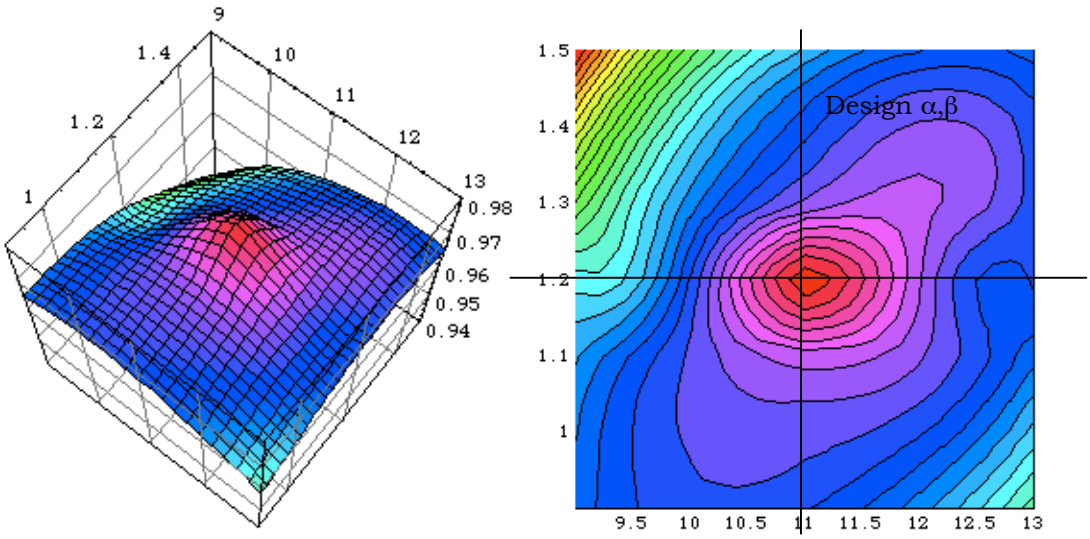

Fig.6.8-5. Post-CDR RFQ - Accelerated beam sensitivity to input emittance α and β. The design α = 1.2, β = 11, as found during the optimization; {%AccBeam, %Loss>1MeV} is {98.0,0.101}. At α = 1.3, β = 10.9, {97.0,0.074}; at α = 1.1, β = 10.1, {96.9,0.076}; (Fig. 6.8-8).

Variation of >1MeV losses with input emittance α and β is shown in the next section. It is seen that the matching for maximum accelerated beam percentage is generally not the same as a match for minimum >1MeV losses.

The CDR and AltCDR RFQs have similar sensitivity of the accelerated beam percentage to the match. The Post CDR RFQ is more sensitive, as expected from pushing the design toward shorter length.

6.8.3 *Variation of >1MeV Losses with Input Emittance α and β*

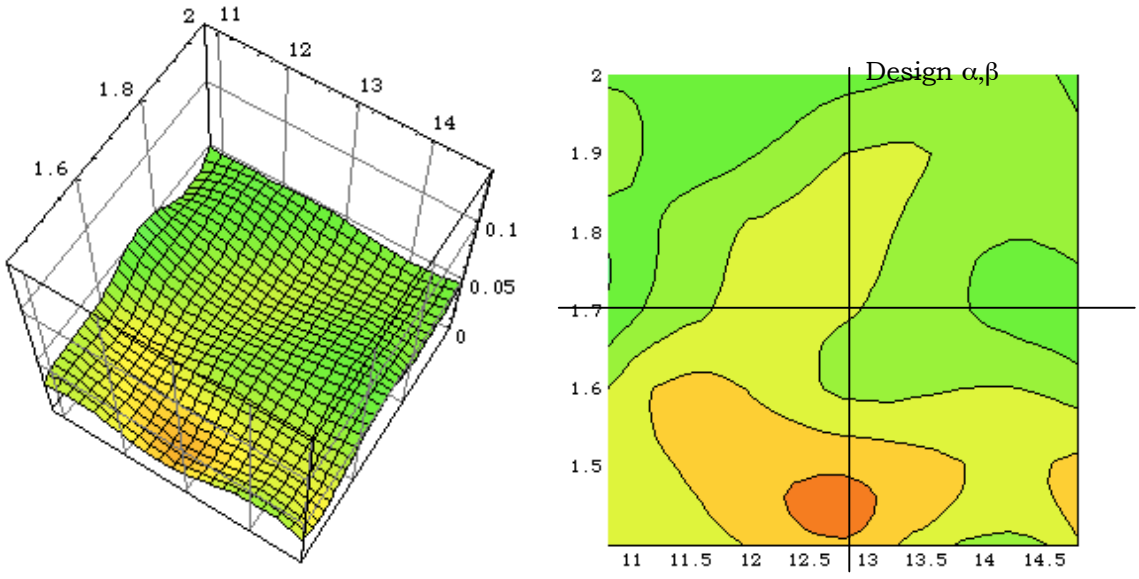

Fig.6.8-6. CDR RFQ - >1MeV-losses sensitivity to input emittance α and β. At the design α =1.7008, β = 12.7828, {%AccBeam, %Loss>1MeV} is {89.6,0.034}. At α = 1.4, b = 11.5, {89.9,0.030}; at α = 1.4, β = 12.75, {89.6,0.014}; (Fig. 6.8-3).

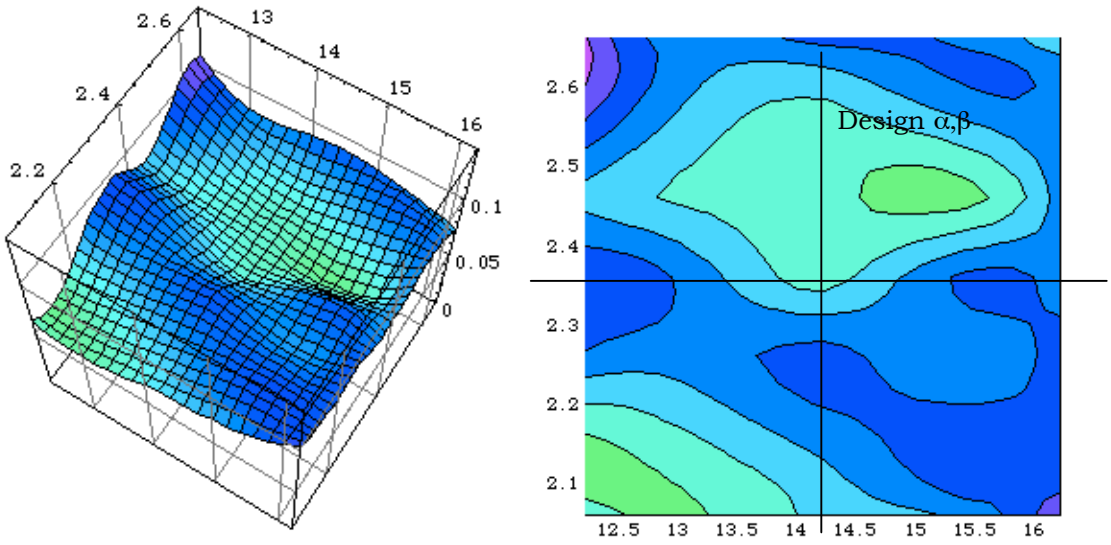

Fig.6.8-7. AltCDR RFQ - >1MeV-losses sensitivity to input emittance α and β. At the design α = 2.362, β = 14.2, {%AccBeam, %Loss>1MeV} is {90.0,0.066}. At α = 2.25, β = 12.75, {91.3,0.080}; at α = 2.47, β = 15., {90.7,0.058}; (Fig. 6.8-4).

The trend of the >1MeV losses to the match is similar for all three RFQs. The exact values are approximate even with 100K particles per point - see the discussion on the number of particles simulated in Section 8.2.4

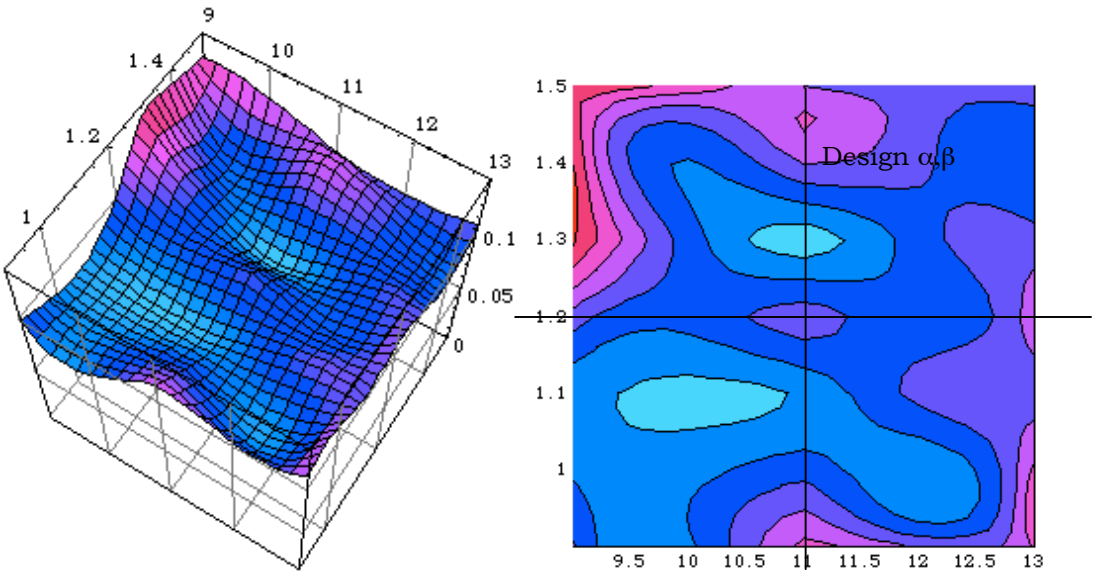

Fig.6.8-8. Post-CDR RFQ - >1MeV-losses sensitivity to input emittance α and β. At the design α = 1.2, β = 11, {%AccBeam, %Loss>1MeV} is {98.0,0.101}. At α = 1.3, β = 10.9, {97.0,0.074}; at α = 1.1, β = 10.1, {96.9,0.076}; (Fig. 6.8-5).

6.9 Comparison Summary

Table 6.9-1 Summary of design conditions, strategy and optimization (a.-e.) and prioritized results (1.-5.) at the design match

	CDR RFQ	AltCDR RFQ	Post-CDR RFQ
a. Input Beam Current, mA	140	130	130
b. Input Beam norm rms emittance, mm.mrad	0.2	0.25	0.25
c. Input energy, MeV	0.100	0.095	0.095
d. Design Strategy	EP	Conventional	EP
e. Optimized	Yes (without multipoles, images)	No	Yes (with multipoles, images)
1. % loss > 1 MeV, Ion Source Input Distribution	0.073	0.123	0.081
2. RF Power, MW	~1.1	~1.0	~1.1
3. Peak Field KP Factor	1.7	1.8	1.7
4. Length, m	~12.3	~12.1	~8
5. % *Accelerated* Beam, Ion Source Input Distribution	89.4	89.9	95.8

6.9.1 Design Conditions, Strategy and Optimization

a. *Input Beam Current* – The 140 mA design current for the CDA/CDR RFQ was lowered to 130 mA for the AltCDR RFQ, and also adopted for the Post=CDR RFQ. This

reflected confidence in obtaining 125 mA accelerated current, requiring ~96.2% accelerated beam fraction.

The Post-CDR meets this goal, depending on how much the ion-source/LEBT injected beam resembles the ideal waterbag distribution.

Re-optimization of the CDR RFQ would probably also reach this performance, as might also an optimization of the AltCDR RFQ

b. *Input beam normalized rms emittance* – The 0.2 mm.mrad CDA/CDR RFQdesign input emittance was raised to 0.25 for the AltCDR RFQ, and also adopted for the Post-CDR RFQ. This reflected a revised estimate of the emittance expected from the ion-source/LEBT. The larger value should ease space-charge somewhat.

c. *Input beam energy* – The 100 keV CDA/CDR RFQ input energy was lowered to 95 keV for the AltCDR RFQ based on the ECR ion source performance, and also adopted for the Post-CDR RFQ. This raises the space-charge at injection, and in general would result in a shorter RFQ.

Design conditions a.-c. result in the CDR RFQ having the hardest specification. However, they appear not to result in much difference between the three designs.

d. *Design strategy* –

CDR RFQ — The CDR RFQ maintains the beam in equilibrium (equipartitioned) from the end of the shaper to the end of the RFQ. There are no interactions with major resonances.

AltCDR RFQ — The conventional design strategy results in a long RFQ and in longitudinal interaction with major resonances.

Post-CDR RFQ — A shorter RFQ that could meet the other specifications with approximately the same rf power requirement as the CDR design was sought. The Post-CDR RFQ maintains the beam in equilibrium (equipartitioned) from the end of the shaper to the end of the RFQ. There are no interactions with major resonances.

e. *Optimization* -

CDR RFQ — The design was optimized using the 2-term potential description, without multipole and image forces. Introduction of these forces lowered the accelerated beam fraction, and therefore a new design was sought.

The simplest re-optimization would have been to keep the rules which result in ~12 m length, and only re-optimize the aperture at the end of the shaper, perhaps accompanied by some adjustment of the shaper length and porch. It is known that slight changes in the aperture and modulation to restore the quadrupole and acceleration potential terms to their 2-term value will result in essentially the 2-term performance – this procedure is implemented in PARMTEQM. Probably this re-

optimization would then result in increased accelerated beam fraction with little change in the other characteristics.

Instead, a new, shorter design was sought, resulting in the Post-CDR design.

AltCDR RFQ — Not optimized. There is little experience with optimization to these or other criteria using the conventional design approach, so it is not clear what could be gained by further work in this direction.

Post-CDR RFQ — The design was optimized using the analytical potential description including multipole and image forces, seeking shorter length with no compromise of the other specifications.

6.9.2 Prioritized Design Results

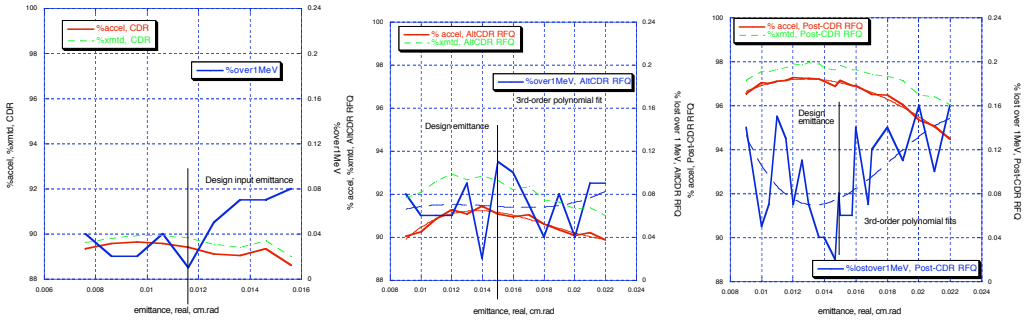

Fig. 6.9-1. Sensitivity of accelerated beam fraction and %>1MeV-losses to input emittance. Repeat of fig. 6.8-1; left-to-right CDR, AltCDR, Post-CDR.

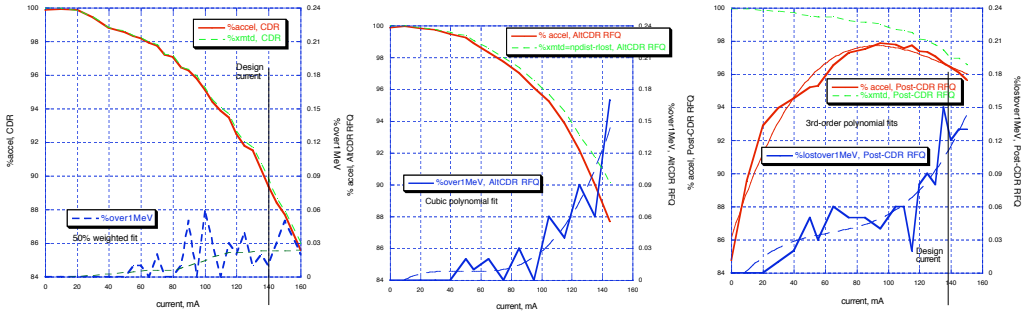

Fig. 6.9-2. Sensitivity of accelerated beam fraction and %>1MeV-losses to input current. Repeat of fig. 6.8-2; left-to-right CDR, AltCDR, Post-CDR.

1. *% loss > 1 MeV*

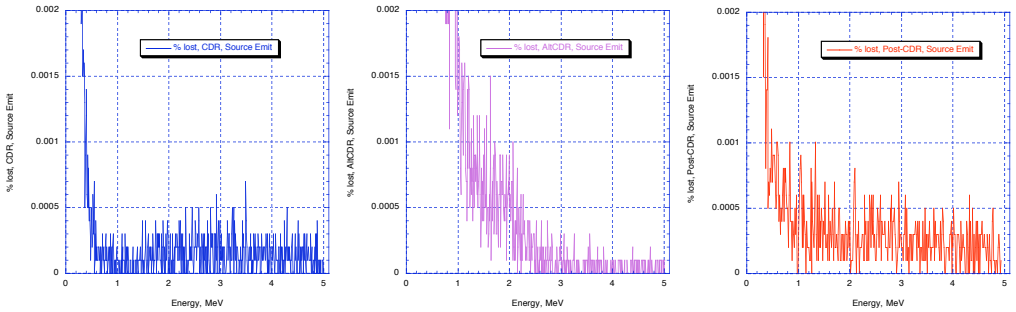

Fig. 6.9-3. Loss patterns for ~ 1M particle Source emittance input distribution, repeat of Fig. 3.1-3. It is necessary to use a simulation code with canonical (time) coordinates for accurate loss patterns. Left-to-right CDR, AltCDR, Post-CDR.

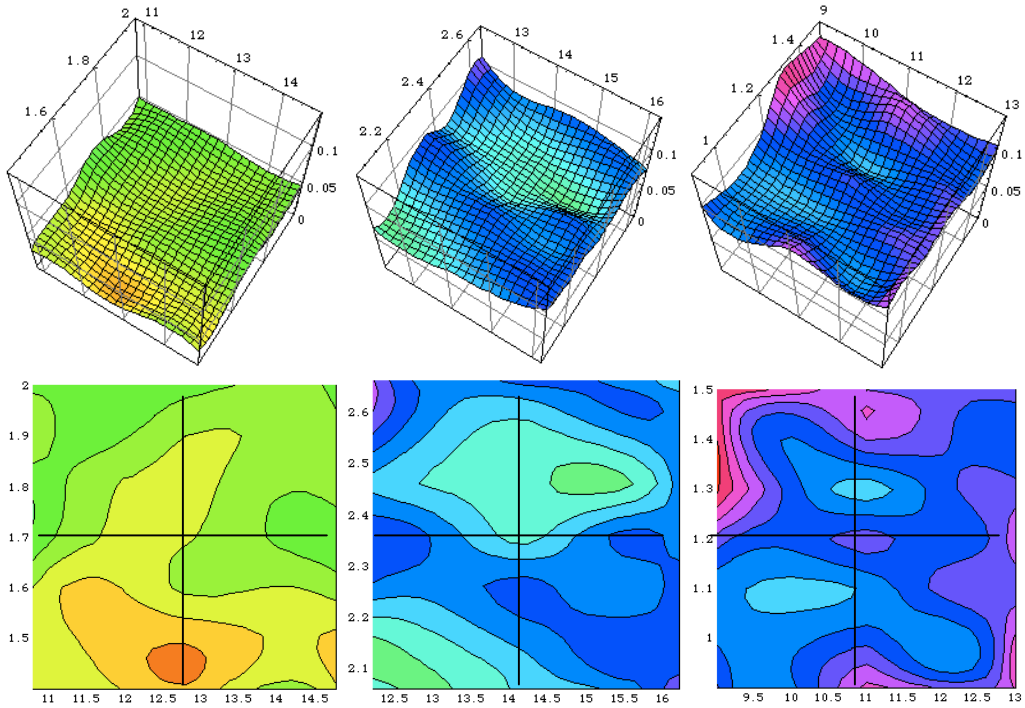

Fig. 6.9-4. % losses >1MeV, repeat of figs. 6.8-6,7,8. Left-to-right CDR, AltCDR, Post-CDR. Produced from 100K particle simulations.

The long, more slowly varying vane profile and resonance-free dynamics of the CDR RFQ appear to result in low and evenly distributed losses with energies >1 MeV. The sensitivities with respect to input emittance, current and matching are also the smallest of the three RFQs.

The conventional AltCDR RFQ has somewhat higher total losses > 1 MeV, concentrated between 1 - 3 MeV and less from 3 - 5 MeV, compared to the other designs. This may be the result of the aperture choke-point discussed in Section 4.3 and 4.4. The lower 3-5 MeV losses result from the strong transverse focusing in the accelerator section.

The Post-CDR RFQ design strategy sought shorter length, and uses a varying EP recipe and shorter shaper. The >1MeV losses at the design point are similar to the other two designs. The sensitivity is greater that for the CDR RFQ, and similar to the AltCDR RFQ but for different reasons.

2. *RF Power, MW*

The rf power of the three design are similar. Note the discussion about the rf power estimate in Section 7.

3. *Peak Field KP Factor*

Contrary to what was thought in the RFQ early days, it is not necessary to use the highest fields feasible without sparking, i.e., the highest KP factor. It is only necessary to provide enough voltage to achieve an optimum performance. It is easier to match the LEBT beam to the RFQ input with weaker initial focusing, so the end-of-shaper (EOS) voltage is a good voltage for the whole shaper. The CDR and AltCDR RFQs rising voltage from the EOS back to the beginning of the RFQ is not necessary, and results in wasted rf power and harder input matching (as evidenced from the design input ellipse matching parameters). The 1.8 KP factor used in the front part of the AltCDR RFQ also appears unnecessary. An optimization following the lines of the Post-CDR with 1.8 KP factor was pursued - similar beam performance and length were obtained, but considerably more rf power was required

As noted, further design optimization work involving the Rho/r0 ratio could be fruitful.

4. *Length*

The Post-CDR design has two-thirds the length of the other two, with better percentage of accelerated beam and about the same percent of losses above 1 MeV. There would be a saving in the initial construction cost of the RFQ. The length is relatively unimportant in terms of construction and tuning technique.

5. *% Accelerated Beam, Ion Source Input Distribution*

The percentage of accelerated beam is highest for the Post-CDR design, and re-optimization of the CDR approach could probably reach this level. As the ion source should produce at least 140 mA, the percent of accelerated beam is not as important as the percentage of lost beam >1 MeV. The CDR and AltCDR RFQs have similar sensitivity of the accelerated beam percentage to the match. The Post CDR RFQ is more sensitive, as expected from pushing the design toward shorter length.

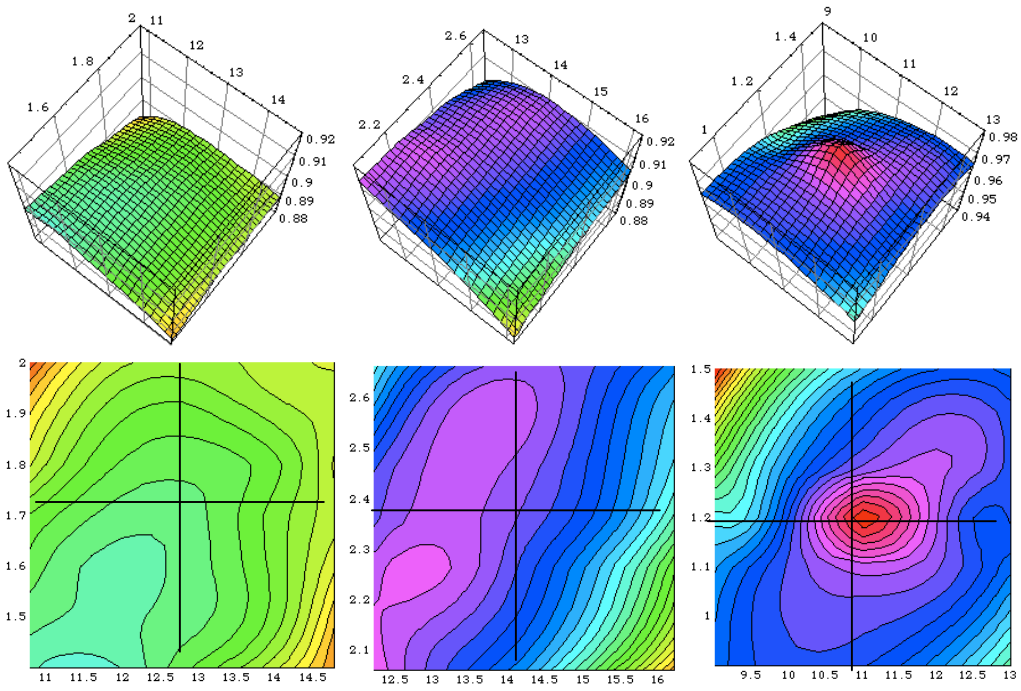

Fig. 6.9-5. Accelerated particles from 100K waterbag input distribution, repeat of Figs. 6.8-6,7,8. Left-to-right CDR, AltCDR, Post-CDR. (Different scale for PostCDR)

6.9.3 Overall Summary and Comment

The Post-CDR design satisfies the beam loss and transmission specifications with shorter length and no sacrifice in rf power. It appears to be somewhat more sensitive to input parameter variations than the CDR design, but this should not be an operational problem in a well-controlled environment. It represents a lower bound on the length while keeping the rf power low.

Overall, the AltRFQ performance is good, but it is long, and more important, the longitudinal dynamics involving interaction with strong resonances is troublesome. The strongly growing longitudinal beam size and emittance do not cause problems in the RFQ, but may in the following 5 - 40 MeV linac or in the HEBT. They also may be sensitive to other errors such as vane manufacturing or alignment errors, not studied here. As the resonance interaction is generic to the conventional approach, it is not clear that better characteristics could be achieved. It is also not apparent that other advantages would be gained by some approach to optimization.

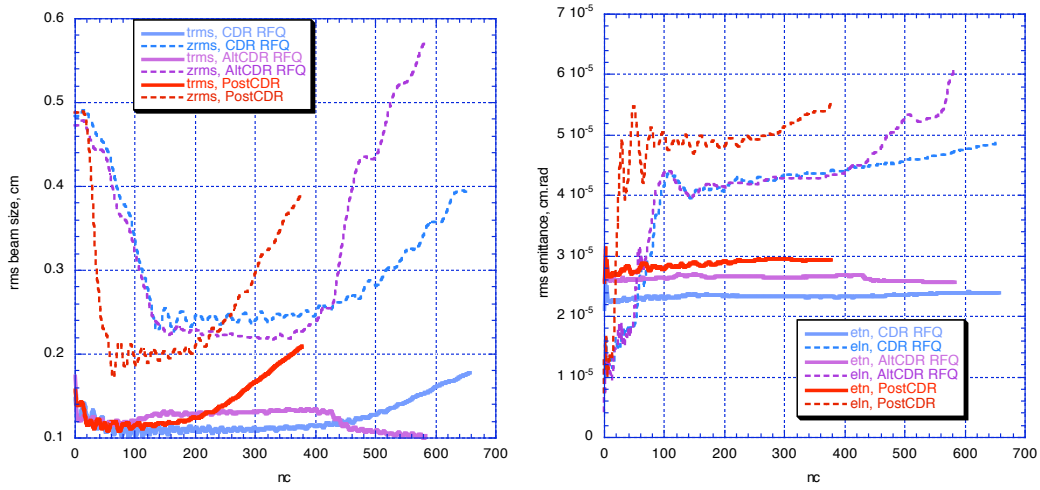

Fig. 6.9.3-1. Repeat of Figs. 6.4-1 and 6.4-2. Rms beam size and emittance comparisons.

The CDR design appears to have lower losses >1 MeV and less sensitivity; higher transmission can be regained by re-optimization. Using the EOS vane voltage for the whole shaper would result in some saving of rf power and make input matching even less sensitive.

Suggestions for further work toward a final design:
1. Pursue the LEBT design to conclusion, and obtain a truly representative input beam distribution.

The EP design strategy is intrinsically robust.

2. Re-optimize the CDR RFQ as suggested in Section 6.8. This is a relatively minor job, and would give a bound on the performance of an IFMIF RFQ ~12 meters long. Some saving in rf power would result.
3. Investigate designs intermediate to the CDR and Post-CDR designs. A somewhat larger increase in aperture might reduce the >1 MeV loss. The best aperture increase, synchronous phase and EP/emittance-control rules might be other than the simple functions used to date - evidence points toward further investigation of very subtle factors such as adiabaticity. The overall transverse focusing that gives optimum >1 MeV loss and acceleration percentage also has subtleties that require further research, which might result in rf power savings. Rf power cost saving could easily override length cost saving. Include investigation of the Rho/r0 factor.

7. RFQ Vane Voltage, RF Power

7.1 Variable Vane Voltage Profile

Freedom to vary the vane voltage is a powerful tool for the designer. Modern construction and tuning techniques afford this option. For example, the LEDA RFQ used tapered vane skirts to vary the voltage. The IFMIF CDR and Post-CDR designs were checked by experts who have successfully built and operated RFQs with a varying vane voltage profile [45]. Their view is that the varying voltage profile can be achieved by the vane design and tuning techniques, and that the power loss per unit length, while possibly challenging, can also be cooled satisfactorily [46].

7.1.1 The Russian IFMIF CDA Preliminary RFQ Proposal

In this regard and as a conceptually different and interesting design approach, the preliminary proposal sketched by the Russian IFMIF partner in the IFMIF CDA, Section 2.6, is important [47]. The parameter table is shown in Fig. 7.1.1-1:

Table 2.6.8-1. Parameters of the RFQ-SPRFQ design for IFMIF

Parameters	RFQ	SPRFQ
Frequency, MHz	175	175
Input energy, MeV	0.1	3.0
Output energy, MeV	3.0	8.0
Intervane voltage, kV	87.	210.
Characteristic bore radius, mm	4.2	4.2
Aperture radius, mm	4.19-3.20	4.0
Length, m	4.97	2.4
Input beam current, mA	130	126.2
Transmission efficiency, %	97.8	100
Input normalized beam emittance, π mm mrad	0.6	0.9
Output normalized beam emittance, π mm mrad	0.8	0.9
Surface field, E_{max}, $kVcm^{-1}$	280	310

Fig. 7.1.1-1. Parameter table for 0.1-3.0 MeV and 3.0-8.0 MeV RFQs for IFMIF proposed by IHEP.

It is stated that "Capacitance is added in a controlled manner through the SPRFQ, allowing a large increase in the vane voltage, up to factors of 3-5 or more, limited by rf power loss considerations. The technique allows the SPRFQ to be considerably shorter, and total rf power losses to be less.

The combined parameters, including the length, are similar to those of the Post-CDR RFQ design. The IHEP approach, outlined further in [48], pp. 65-77 and including the two-tank approach, is worthy of further investigation by the IFMIF project - unfortunately lack of funding prevented this to date.

7.2 RF Copper Power Consumption

The estimates of the rf power required by the RFQ structure given in Fig. 2.4-9,10 are comparatively correct, but the actual values present some questions, and require further attention by the IFMIF design team. These estimates are based on [49], which is essentially repeated here.

7.2.1 RF Shunt Impedance Estimate

RFQUIK Estimate

The RFQ design code RFQUIK has a formula for shunt impedance:

```
(Rs RFQUIK, MΩm) =
      1/(((1.3*10^12*1.25*((frequency,MHz)*48*10^ -
      12*((300/(freq,MHz))/
      ((cell aperture,m)*
      (1+modulation)/(2)))^(1/6))^(3/2)))/0.6)
```

where r0 ≈ aperture(1 + modulation)/2; 0.6 is a "fudge factor" to account for observed differences between theoretical and measured results.

Fig. 7.2.1-1 shows the (Rs RFQUIK) estimate along the IFMIF CDR RFQ

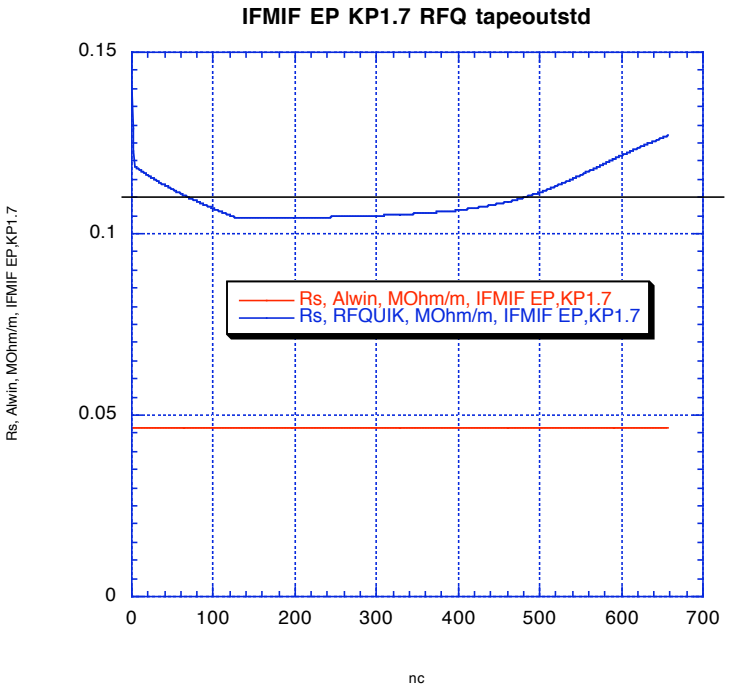

Fig. 7.2.1-1. RFQUIK estimate for rf shunt impedance Rs along the IFMIF CDR RFQ.

```
(CuPwr/cell RFQUIK)=
      (cell length,m)*(vane voltage, MV)^2/(Rs RFQUIK)
```

These equations are integrated along the RFQ to get the total copper power estimate:

Total Copper Power RFQUIK = 1.125 MW

Beam Power
Assume Beam Power = (4.905 MeV)(.132 A)(.95 transmission) = (4.905)(.125) ≈ 620 kW

IAP Estimate
IAP presentation at the EU Monitoring 2/2003 gives total RFQ power = 1.5 MW; minus 620 kW = *880 kW RFQ copper power*.

Saclay Estimate
From Saclay presentations on KEP results,

Main IFMIF RFQ parameters

Parameters	Values	Parameters	Values
Length	12.482 m	Synchronous phase	-90°→ -40°
Frequency	175 MHz	Peak field	1.8 Kp
Voltage	130→ 101.2 kV	Copper power	*683.9 kW*
Mean aperture (R_0)	6.41→ 5.16	Beam power	613.1 kW
Modulation (m)	1. → 1.6	Total power	1297 kW

These IAP and Saclay estimates appear consistent with the RFQUIK estimate without the 0.6 fudge factor.

Experience with Operating RFQs

Various formulas are used to estimate the rf power requirements for an RFQ design. They tend to be more optimistic, that is to give a higher RFQ shunt impedance, Rs, than the values measured on operating RFQs. This is the case even including the "standard" assumption that measured Q will be 0.6-0.7 that of the SUPERFISH calculated Q. These formulas can be summarized as having the form Rs = ~10^5/(frequency, MHz)^(~1.5), but tending to give shunt impedances up to several times higher than Rs=10^5/(f,MHz)^(3/2).

Shunt impedances for operating RFQs have been collected in the literature and from his experience with his own RFQs by Alwin Schempp, and updated by the author from the PAC, EPAC, and LINAC conference proceedings for 2000-2002, as shown in Fig. 6.4.1-2.

The relation Rs=10^5/(f,MHz)^(3/2) is compared to the individual fits for 4-rod type RFQs (Rs=10^4.09496/f^0.98306) and 4-vane-type RFQs (Rs=10^4.45071/f^1.241). It appears that 4-rod and 4-vane RFQs should be fitted separately. It is also clear that the experimental values should be used to help estimate the rf power that will be required in a new design.

There is a fairly large spread in the data, probably due to variations in construction technique that affected the achieved Q value for the structure. For example, the power

required for the VE BERLIN 4-rod structure is almost twice the amount predicted for by the 4-rod-type fitted formula.

```
(rf power per meter, MW) = 1000(vane voltage, MV)^2/(Rs, kΩm)
```

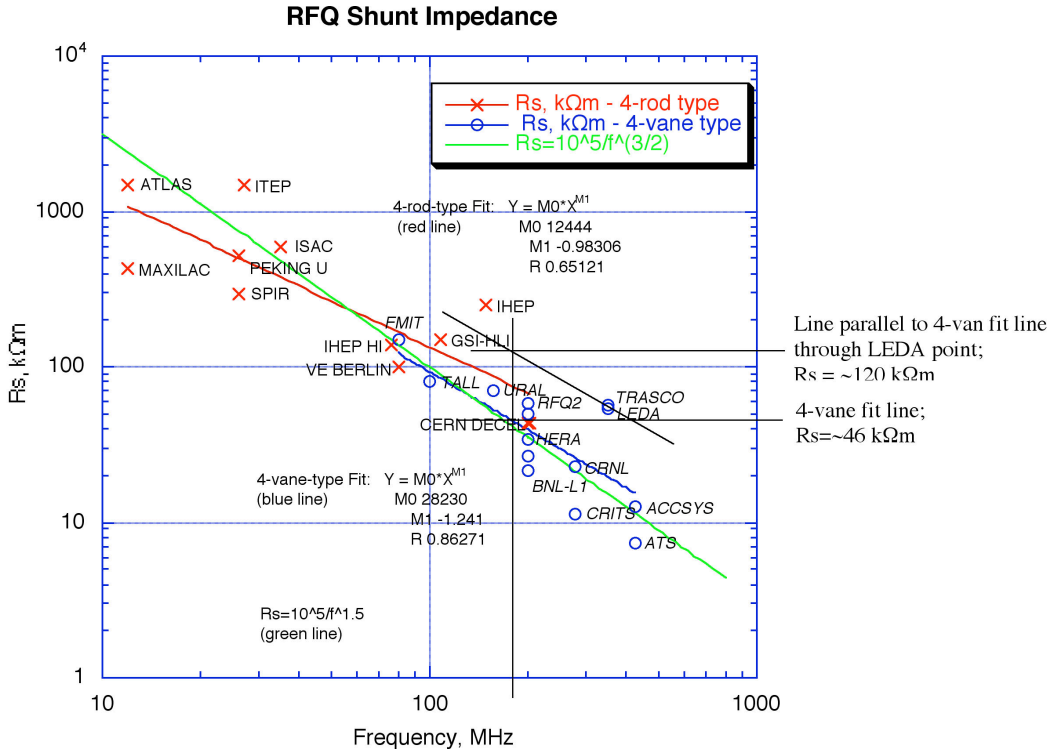

Fig. 7.2.1-2. Rf shunt impedance data from operating RFQs.

At 175 MHZ, the 4-vane fit gives Rs = 0.0460462 MΩm.

Total Copper Power estimate using 4-vane fit = 2.86 MW

The LEDA achieved very good shunt impedance, and represents the RFQ most like IFMIFs. If we have the confidence to extrapolate from the LEDA data point back to 175 MHz using the slope of the 4-vane fit line, we get Rs ≈ 0.120 MΩm. This is close to the average for the Rs RFQUIK curve in Fig. 6.6.1-1.

Total Copper Power estimate using Rs = 0.120 MΩm = 1.1 MW

This is the copper power estimate used in Fig. 2.4-9,10.

Total Power

Total rf power using the above estimates: RFQ copper power ranges from 0.684 - 2.86 MW. Plus beam power, ranges from 1.3 to 3.5 MW. Assume 5% for rf transmission losses; range is 1.37 to 3.68 MW. Assume that the control margin can be absorbed in operational output ceiling of 680 kW (as assumed for the DTL) for the diacrode.

The CDR estimate states 3 MW. This is probably adequate.

Definitions, Questions, Comments
This information was circulated to project participants for comment during preparation of the CDR; no comment was received; funding precluded further pursuit of the question with, for instance, the LEDA group.

The IFMIF Project needs further work on the RFQ power requirement.

7.3 Vary Rho/r0 Ratio?

For a fixed vane voltage profile, Rho/r0 might be varied for lower peak field, as in the Alternative CDR RFQ. The resulting effect of the different multipole components on the beam would then have to be checked.

Similarly, if a Kilpatrick limit is used to set the vane voltage profile, a built-in Rho/r0 profile could be entered in LINACS and the design optimized on that basis.

There is so much flexibility in the parameter options that satisfactory beam performance might be found in combination with some advantage of a varying Rho/r0 profile; the author has not explored this approach.

8. Simulation Codes

Re-emphasizing the statement above: "*A major requirement of the beam-based method is that the desired design performance be very closely verified by the detailed beam simulation*. This was not lightly achieved, and required extensive development of the design method to include all of the effects to be simulated, and of the simulation code itself."

8.1 The RFQ Design Code LINACSrfq

The resulting design code is named "LINACS," of which "LINACSrfq" is a subset. It has also been used to design drift-tube linacs, and coupled-cavity linacs to ~1GeV for radioactive waste transmutation and other purposes. The underlying space-charge physics section is applicable to any linac, requiring only the appropriate cell-by-cell bookkeeping and external field formulation to be applied. As an example of generality, a 2-section linac with frequency jump between sections results in a long beam bunch at the entrance to the second section, which must then be shortened in a controlled way - so there is similarity with the dc-to-bunched beam requirement in an RFQ.

The background is given in Section 5, Section 5.3 - Beam-Based Design Procedure, and accompanying references. The general procedure is apparent in Section 5.3.1 LINACSrfq Design Interface.

The maximum beam radius is determined from Sqrt[5]*(rms beam radius), assuming a uniform distribution. Using the subroutines of PARMTEQM [19,20], the multipole terms are applied at this maximum radius, and the image-charge terms are applied at this maximum radius times the quadrupole flutter factor.

To achieve the required close correspondence to the simulation code results, it was necessary to include the effect of neighboring bunches in the LINACSrfq design code.

Optimization of the design proceeds as outlined in [7] and Section 5.3.3. Globally, the frequency is chosen, for which the global space-charge rule to limit the tune depressions to ~0.4 is useful.

To get started, the following default values should produce a reasonable first design, aided significantly by the use of the matched plus equipartitioned strategy:

```
RhooverR0 = 0.75;
KPfac = 1.7;
etnrmsgiven = 0.000020;
elnrmsgiven = 0.000040;
EOSaperfac = 4.0;
phistarget = -88.;
bfraction = 0.60;
rmscells = 4;
siglint = 180.;
porch = 60.;
```

```
mainrfqphisrule := TKphisrule;
mainrfqaperrule := (endbeta = appropriate;
      c3 = 1.2;
      a[rfq] := atarget*(1 +
      c3*((beta - betastart)/(endbeta -
      betastart))^1.0); );
frontendvrule:=vKP;
mainrfqvrule :=vKP;
mainrfqemrule := mfree;
mainRFQstrategy := matchEP;
```

It is recommended that the strategy of bringing the beam to equipartition at the end of the shaper always be followed, as it always produces a reliable result. Many other strategies have been tested, such as the "conventional" one, but EP at EOS, along with the bunch formation strategy employed in the shaper, always gives good performance. The strategy for the main RFQ is then set as desired. The initial design is simulated in pteqHI, and a reasonable input match must be found.

The power and flexibility of Mathematica© is very useful as a development platform; eventual reprogramming to obtain faster running speed would be useful for the optimization process.

An executable version is available to the project.

8.2 The RFQ Simulation Code pteqHI

8.2.1 Development of pteqHI

For the initial development of the RFQ at Los Alamos in 1978-1980, a simulation code named PARMTEQ was written based on the 2-term potential description of the RFQ fields. The RFQ description from the "conventional" design procedure provided a input table of the transverse focusing strength variable called B, the synchronous phase, the modulation and the voltage as a function of z along the RFQ. The code was based on assumptions appropriate to the design requirements and computer capabilities of the time. For example, it used the position along the RFQ as the independent variable (resulting in non-canonical phase-space variables) and the paraxial approximation in the beam dynamics computation. The longitudinal phase-space is described by the phase and energy differences of each particle from the synchronous particle. Later, the higher-order field terms in the vane potential needed to describe the effects of the vane shape resulting from actual machining procedures were added, as well as many other features necessary to the final detailed design and manufacture of a practical RFQ, resulting in the widely used code PARMTEQM.

In developing a beam-based design procedure based on the envelope equations (and the equipartitioning equation), it became desirable to achieve a closer agreement between the design predictions from these equations and the simulation results given by PARMTEQM. Simply returning to the 2-term description did not suffice. It was also necessary to return to the more physical choice of time as the independent variable, as space-charge forces must be computed when the beam particles are at the same time.

In a procedure where position is the independent variable, it is very difficult to accurately transform the particles from position to the same time, where the space-charge computation is made, and then back again to the position, with the accuracy required to match the design requirement coming from the envelope equations. Also, and even more important for high-intensity machines where avoidance of beam loss is a crucial requirement, the details of beam loss are not handled accurately enough in the bunching and low energy portions of an accelerator (not only an RFQ) when position is used as the independent variable in the simulation code.

Therefore PARMTEQ was changed to a code named "pteqHI," first described in [18], using time as the independent variable for the natural computation of space-charge, eliminating the paraxial and other approximations, extending to enable simulation of multiple ion species and charge states simultaneously, and with many other options. The PARMTEQ r-z mesh PIC method for the space-charge computation and the PARMTEQM analytic method (before the use of field maps) for multipole and image effects are incorporated. In the simple 2-term approximation mode but accurate time-based computation, pteqHI is also designed to be fast and efficient for optimization studies; however the execution time is presently much slower when the multipole and image effects are included. The source code is available.

Of course, all input and output pteqHI data files used for the results in this report are available to the project.

8.2.2 Use of pteqHI

Analysis of the cell-by-cell rms properties of the beam inside the RFQ is nonsense if particles are included that are already lost or in the process of being lost within the RFQ. PteqHI requires two full runs for full analysis. Particles lost within the RFQ are identified in the first run and flagged. In the second run, all the particles are simulated exactly as on the first run, but rms analysis is performed only on the particles that will be successfully transmitted to the RFQ output. This method has made it possible to reliably understand the space-charge physics within the RFQ and to develop the design code in exact correspondence.

Many options are available in pteqHI.

The code is structured to handle simultaneous distributions of ions; each distribution carries its own number of particles, input emittance data, charge, mass, current, and input energy.

The input distributions can be generated as usual from the input parameters in a number of analytical forms; typically a transverse waterbag and dc longitudinal for the RFQ, or input particle distribution tables can be read in.

The RFQ cell parameters can be generated using the 2-term potential description or from multipole coefficient tables provided by LINACSrfq. Image-effect coefficient tables can also be provided by LINACSrfq.

The acceptance of the structure from the input (at any cell) to a downstream point can be measured.

Options are available for the radial and longitudinal loss criteria.

Matrices of runs can be executed in batch mode, varying (for the first distribution listed) the input emittance alpha, beta or emittance, current, injection energy, and the RFQ vane voltage level by a vfac multiplying coefficient; in addition the beam current of two additional distributions can be varied.

Input and output beam transport lines can be added.

Input beam emittance match parameters can be found in a variety of ways.

- PARMTEQM assumes there is a match point just after the radial matching section, and uses an envelope equation method to compute backward to the RFQ input. This method yields an adequate match, but it can be considerably improved. PteqHI can iteratively use the beam itself from the input in to the match point, to minimize the difference between the specified and actual emittance alphas and betas at the match region. Either the same alpha and beta are found for the averaged x- and y- behavior, or separate x- and y- alphas and betas can be found.
- Other match strategies near the beginning of the RFQ have been tested, for example, minimization of the weighted standard deviation of beam size across a match region.
- The most reliable match is still found by a transmission matrix, found by running a batch matrix of input emittance alphas and betas (contamination by other beams can be included in the background). The transmission as a function of input ellipse parameters is often complicated [29] (Section 6.8), thus this matrix method is the most reliable.

At present, no graphics is done inside the code - in the development environment, the graphics requirement changed daily; it is easy to write output files and do the graphics separately.

Availability of the source code makes it easy to change or add other options.

8.2.3 Beam Loss Criteria

Particles in the RFQ are determined radially lost if they hit the vane surface. Some particles also travel between the vane tips out to significant radii. The inaccuracy of the rf fields outside the circle describing the innermost vane tip was discussed above; and assuming other factors (such as the space-charge routine) remain the same, the use of 3-D field maps and a criteria that a lost particle hits the vane surface is best. The accuracy of the 3D maps out to the appropriate particle radii must be established.

PteqHI uses the multipole and image field description of PARMTEQM as described above. A loss radial loss boundary that describes a typical vane-tip contour near the axis is generated using a quadrupolar function, as illustrated in Fig. 8.2-1.

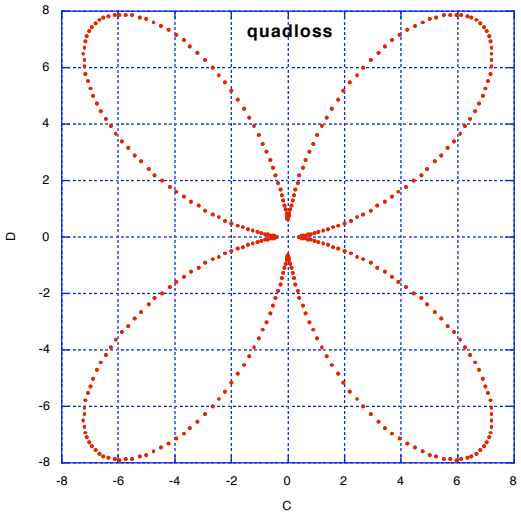

Fig. 8.2-1. Quadrupolar function with +-10° vanetip opening angle, computed at each step for x- and y- location of actual vane tips.

If a particle strays outward into the inter-vane region, the multipole fields rapidly become inaccurate and particles can receive very large energy kicks. A particle is declared radially lost if it hits the quadrupolar function boundary or a radius equal to 1.5 times the location of the outermost vane tip. The particle energy is inspected, and if it is greater than 1.25 times the synchronous energy, the synchronous energy is assigned as the energy of the lost particle.

A few particles can also receive non-realistically large energy kicks, or even have negative energy, although still within the radially accepted region; if this occurs, the particle is dropped from the simulation and its energy is assigned as the synchronous energy at that point. Later, these particles are also considered as radially lost at that position in the RFQ.

Finally, some particles may come nearly to rest and can cause the code to endlessly loop if not removed. Therefore a lower energy bound of 0.05 times the synchronous energy is set and particles are dropped from the simulation if their energy drops below this bound; their energy remains at the bound, and they are later considered as being lost radially at that position with that energy.

The loss criteria are applied at each time step of the simulation.

8.2.4 Variation with Number of Particles simulated

Tables 8.2-1,2,3 indicate the accelerated beam transmission at the output can be found with good accuracy even with 5-10K simulated particles. The statistics for the total loss with energies above 1 MeV are not good for less than 100K simulated particles. The computing time for 100K-1M particles is still large, so such runs would be made only at the final design stage.

Table 8.2-1. CDR RFQ – Variation of transmission with number of particles simulated.

	5K WB	10K WB	100K WB	1M WB	~1M Source Emit
% losses >1MeV	0.0	0.01	0.034	--	0.073
% Accelerated	90.3	89.4	89.6	--	89.4

Table 8.2-2. AltCDR RFQ – Variation of transmission with number of particles simulated.

	5K WB	10K WB	100K WB	1M WB	~1M Source Emit
% losses >1MeV	0.12	0.05	0.068		0.123
% Accelerated	91.2	91.3	90.9		89.8

Table 8.2-3. PostCDR RFQ – Variation of transmission with number of particles simulated.

	5K WB	10K WB	100K WB	1M WB	~1M Source Emit
% losses >1MeV	0.02	0.08	0.077	0.075	0.081
% Accelerated	97.0	97.1	97.1	97.1	95.8

Tables 8.2-1,2,3 Percent of particles accelerated and % losses with energies above 1 MeV, for ideal waterbag input distributions with 5K, 10K, 100K and 1M particles, and for the ion source emittance distribution of ~1M particles rms matched to the RFQ input.

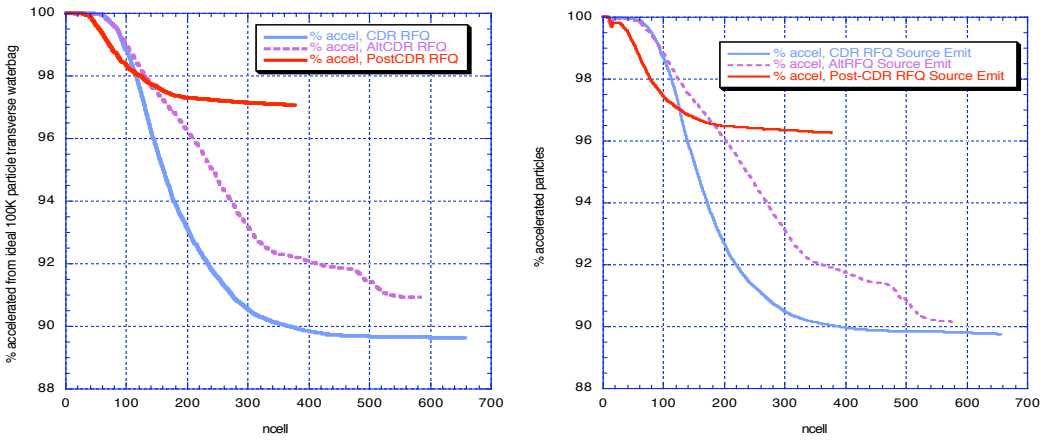

Fig. 8.2.2. Left - % accelerated particles, 100K waterbag initial distribution; Right - % accelerated particles, Source Emittance initial distribution.

Fig. 8.2.2 shows the cell-by-cell transmission of the three RFQs for the 100K waterbag and Source Emittance distributions.

Figs. 8.2.3-5 show, for the Post-CDR RFQ, the variation in the % of all lost particles vs. energy and vs. cell number as a function of the number of particles simulated.

Fig. 6.2.6 shows the matching sensitivity results for all three RFQs for 100K particles (to the left) and 10K particles (to the right). The trends are observable with 10K particles; the statistics are only adequate at 100K particles, but at present the computer runs take a long time even with 100K particles. The figures were generated on a grid of 7 alphas and 5 beta. A Mathematica© interpolation polynomial, which leaves the values unchanged at the given grid points, was used to fill in the mesh by a factor of five in each direction.

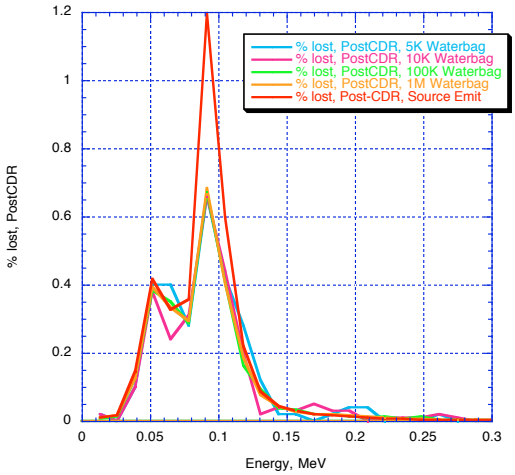

Fig. 8.2-3. Post-CDR RFQ. % of all lost particles vs. energy where lost, 0.0 - 0.3 MeV.

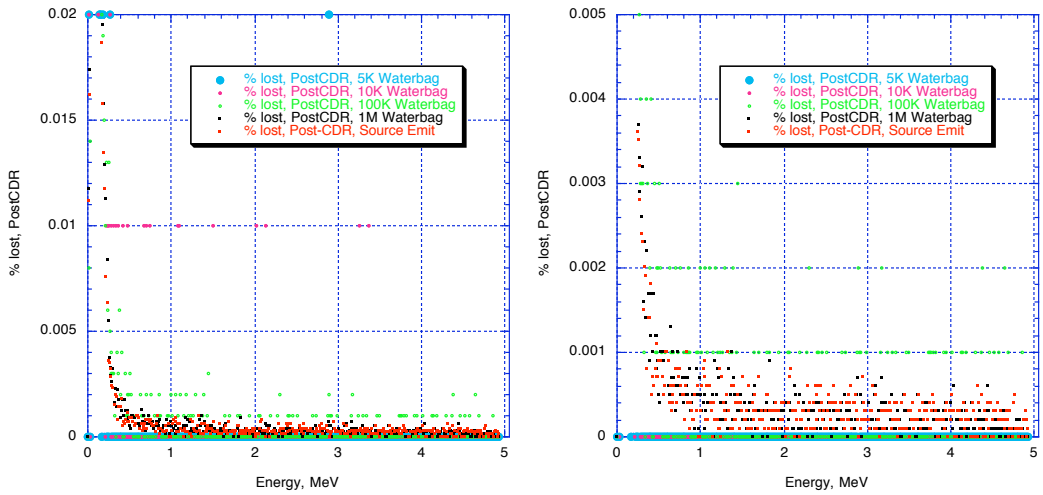

Fig. 8.2-4a,b. Post-CDR RFQ. % of all lost particles vs. energy where lost, expanded vertical scales. For 5K, 10K, 100K, 1M particles, loss of 1 particle is 0.02%, 0.01%, 0.001%, 0.0001%. (400 bins, each 5.05MeV/400 = 0.012625 MeV).

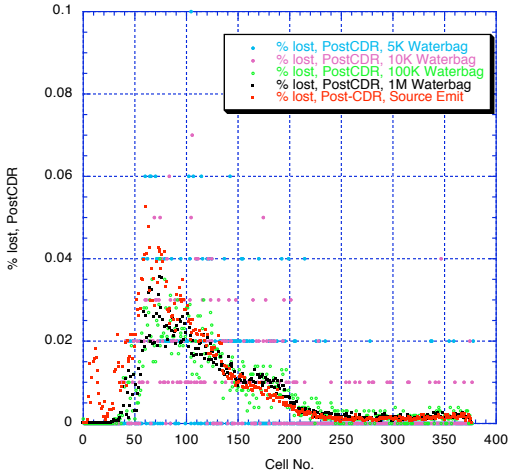

Fig. 8.2-5. Post-CDR RFQ. % of all lost particles vs. position (z, meters) where lost. CDR.

Fig. 8.2.6. Left with 100K particles, right with 10K particles.

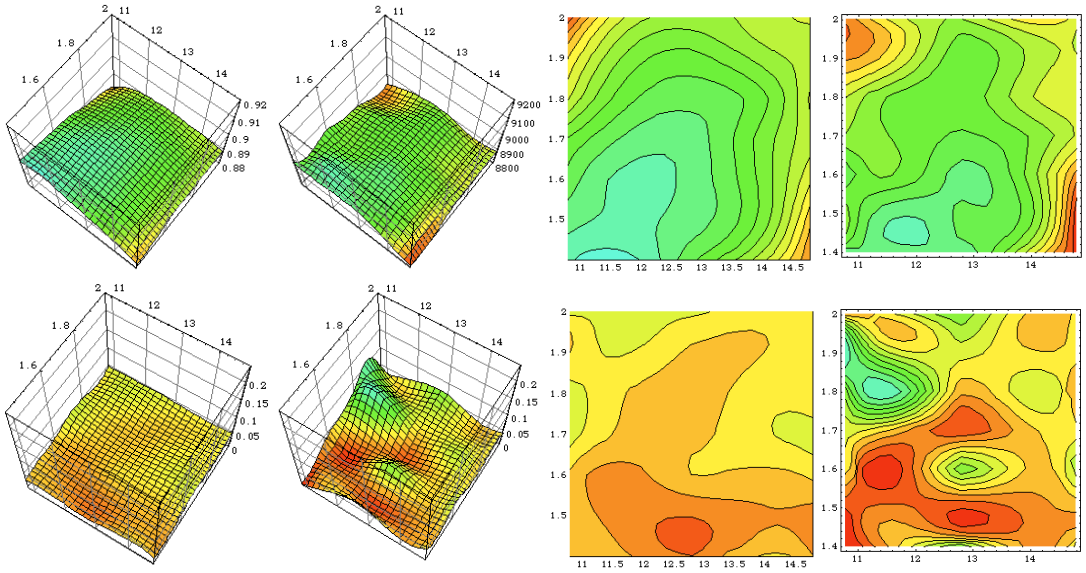

AltCDR

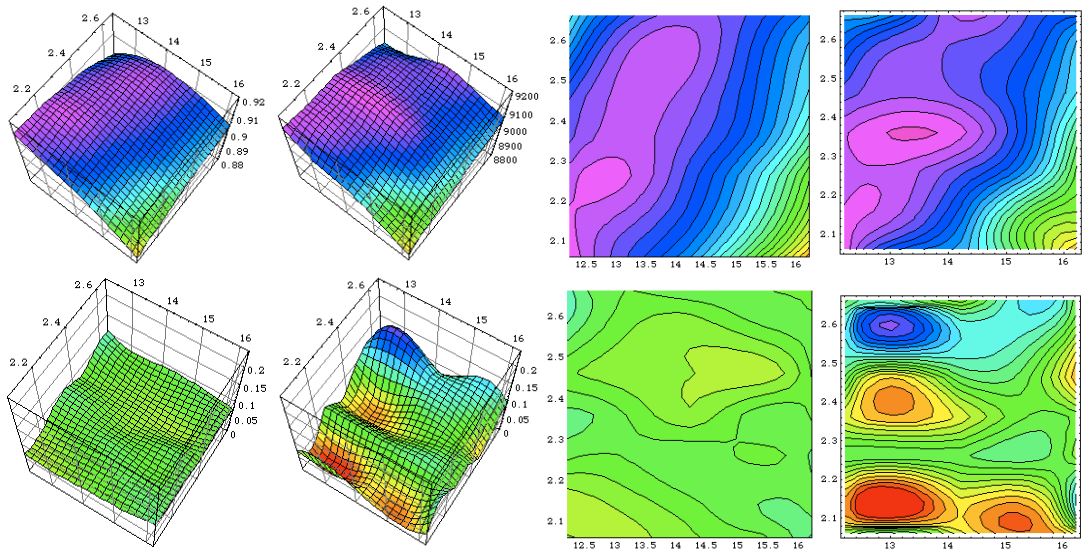

PostCDR

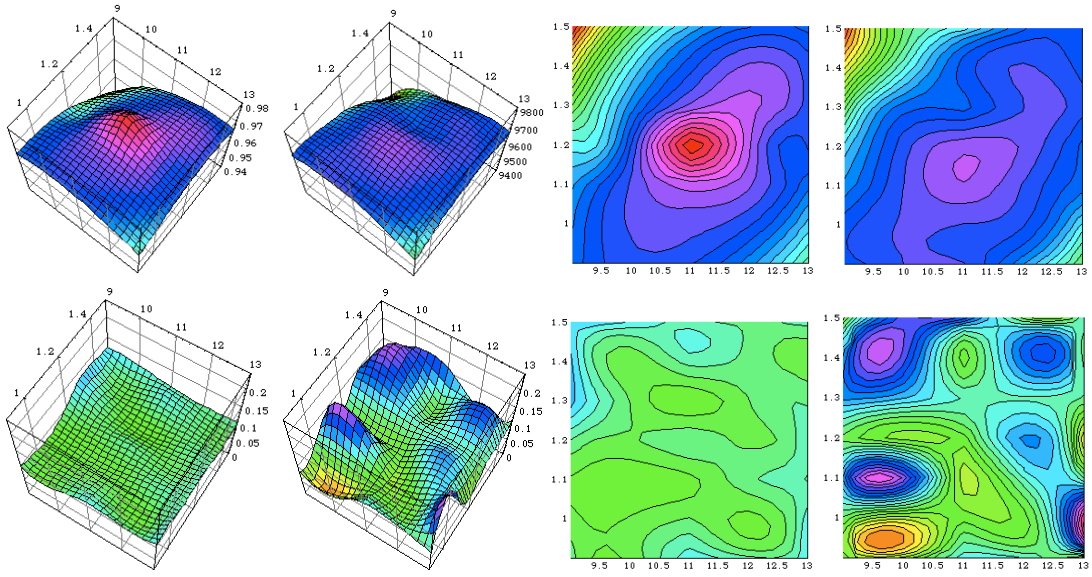

8.3 Other RFQ Simulation Codes

Comparison to PARMTEQM (versions in which the paraxial approximation has been removed) show that the overall transmission may be comparable within a few percent, but that the loss patterns (the distribution and energy of loss particles) differ significantly. This difference has also been observed in the LEDA RFQ, the most powerful and longest cw RFQ to date [12,21]. It has not been possible to compare the LEDA data with a pteqHI simulation; this would be a valuable exercise.

Other groups also made new codes that grew from PARMTEQM but removed many of the assumptions to achieve better accuracy. These codes used time as the independent variable, removed the paraxial approximation, and replace the vane potential description formulas by full 3-D field maps exactly conforming to the metal shape as it would be manufactured. LIDOS, by the Moscow Radiotechnical Institute, is fully developed and available commercially, including the source code. The TOUTATIS [24] code was derived from PARMTEQM with removal of certain approximations, especially the paraxial, and with 3-D field maps; the reference contains an excellent comparison of the fields produced in the vane-tip region by PARMTEQM and by the TOUTATIS 3-D field map method. The PARMTEQM (pteqHI, etc.) analytically expressed fields are really accurate only in the circle describing the innermost vane-tip, and can have large local errors outside this region. (The latest PARMTEQM version has 3D field maps, but unfortunately still has inaccurate space-charge computation by retaining position as the independent variable.) Beam loss results from the analytical method have been compared to LIDOS [50]and TOUTATIS; the overall transmission results are usually within a few percent; detailed comparison and analysis of the beam loss patterns have not been done. A number of other codes are also being developed independently.

The space-charge simulation method itself (assuming that the dynamics correctly assigns the canonical time coordinates to the particles at the space-charge computation point) is central to many details of the beam-loss pattern. PteqHI, PARMTEQM and TOUTATIS all use the same underlying r-z mesh PIC method, which is fundamentally reliable, but which has many details that affect the space-charge computation. Absolute results are subject to error bars, whose magnitude is extremely difficult to determine because of uncertainties in the physical and computational modeling. Relative comparisons between designs might be expected to be trustworthy; however, there is disconcerting evidence when comparing different codes even on this point, and detailed comparison of source code is needed.

Source code availability is essential for a project to be able to make informed decisions about the final modeling for the project. PteqHI and LIDOS source code are available.

The IFMIF project expended a large fraction of the limited resources available in 2004 trying to use the TOUTATIS code to reproduce published results and then work beyond toward improved RFQ designs. An executable version was available and a single input datafile was furnished from which the results had been obtained. Execution did not reproduce the expected transmission. Questions were posed and help requested; finally a petition was made to the code author, who kindly suggested different setting of various options in the input file. Unfortunately, the results were still always less than

the referenced result, and the many other questions were not answered. Therefore official use by the Project was discontinued, until the code is more fully developed, *and most important - until source code would be made available from which independent judgments can be made.*

The exact transmission found by any of these codes should be treated as indicative, as each has various sensitivities in its internal methods. Continued work to compare results between different codes more broadly and deeply than heretofore is highly recommended - this requires comparison at source code level and devising of appropriate tests. It is strongly recommended that the project obtain source code for all important simulation work.

9. Ion-Source/LEBT Input Beam Modeling

A few notes on the ion source/LEBT:

ECR Ion-Source Status

There was substantial concern during the early years of the IFMIF program about the reliability of an IFMIF ion source. IFMIF provided support for a thorough engineering evaluation of the ECR ion source. Several runs accumulating several 1000 hours of cw operation at ~100mA protons showed that the availability of the ECR source should be high.

The 140mA deuteron beam performance within the specified emittance has not been demonstrated, either with deuterons or with ~200mA protons to investigate a scaled result. See Section 1.1.1.

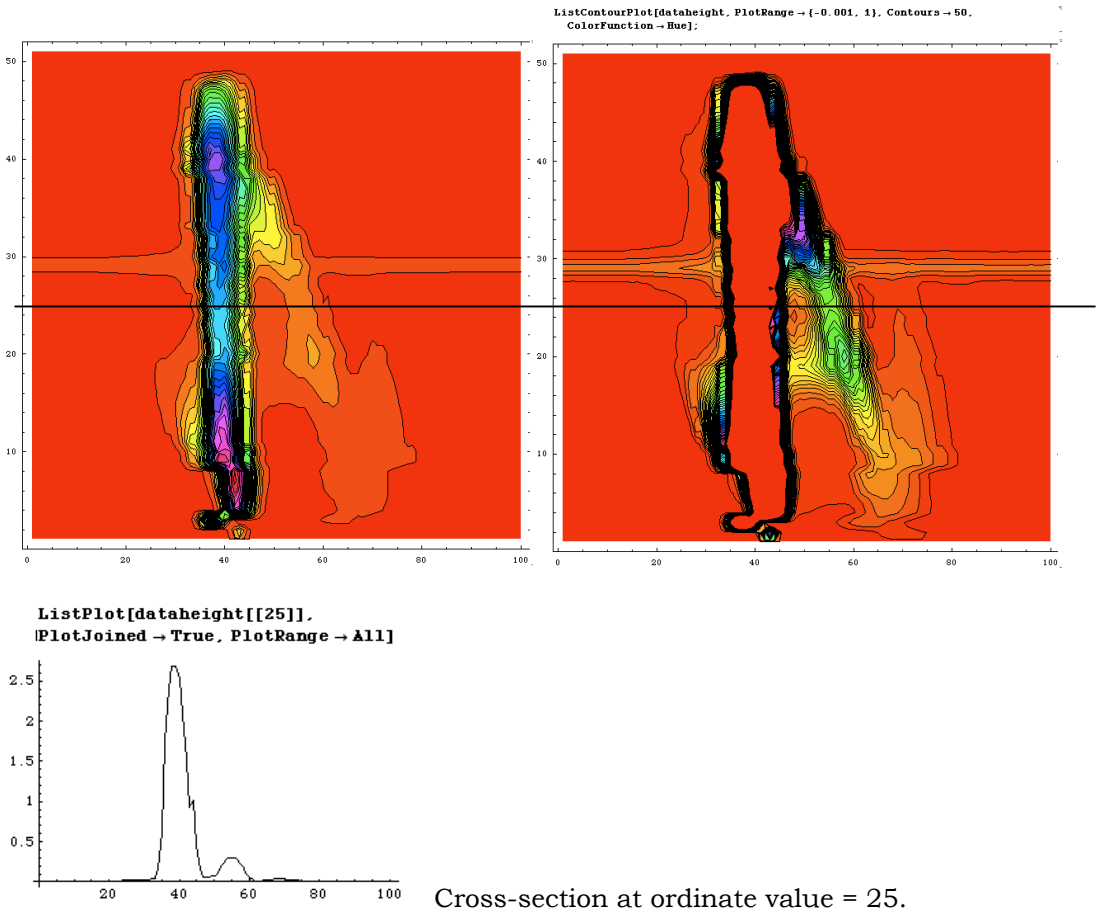

Cross-section at ordinate value = 25.

Fig. 9.1 Raw Data Characteristics of the ECR Ion-Source Emittance Distribution (see figures, Section 6.6) Right figure has expanded vertical scale.

As noted in Section 1.1.1, this result for ~100mA protons is the only emittance data set available to the project. The halo appears to be composed of protons. The data set is

thresholded by an inaccurate (and optimistic) method. The more accurate method developed by M. Stockli at SNS should be used. For this report, the data set has been numerically transformed to the input α and β ellipse matching parameters required by the RFQs. The rms value is also adjusted to equal that of the ideal waterbag distribution.

CDA Section 2.6.2.10.1 Injector beam

The IGUN output is converted to a particle input appropriate for the TOPKARK code, which is used to model beam dynamics in a two-solenoid, space-charge-compensated LEBT. The beam radius is kept to less than half the 6-cm radius of the 15 cm long solenoids, which have a peak on-axis magnetic field of 0.55 T. The fringe fields are modeled using an analytical expression that agrees well with measurements of solenoids encased in an iron shield. Roughly 30 % of the halo (3 % of the beam) is scraped inside the solenoids. The background neutral gas in the LEBT is assumed to provide 98 % space charge neutralization, implying an effective current of 3 mA. Fluctuations in the source current of ± 1 % on a time scale faster than the neutralization time are assumed to vary the effective current from 1.5 mA to 4.5 mA, which leads to a time-varying beam mismatch at the RFQ entrance. Although this process is not fully understood and is difficult to model, the effect is approximated by overlapping the final particle distribution from three separate simulations using the minimum, average and maximum effective current. This results in an effective RMS emittance growth of 33 %. Aberrations due to nonlinear magnetic fields and space charge forces are small compared to this mismatch effect.

LEDA LEBT

An electron ring is needed just before the RFQ input, to compensate for the short unneutralized section between the end of the LEBT and the beginning of the RFQ vanes. (LYoung, LINAC'2000, [33])

CDA LEBT – CDA Section 2.6.2.2, Fig. 2.6.2-3

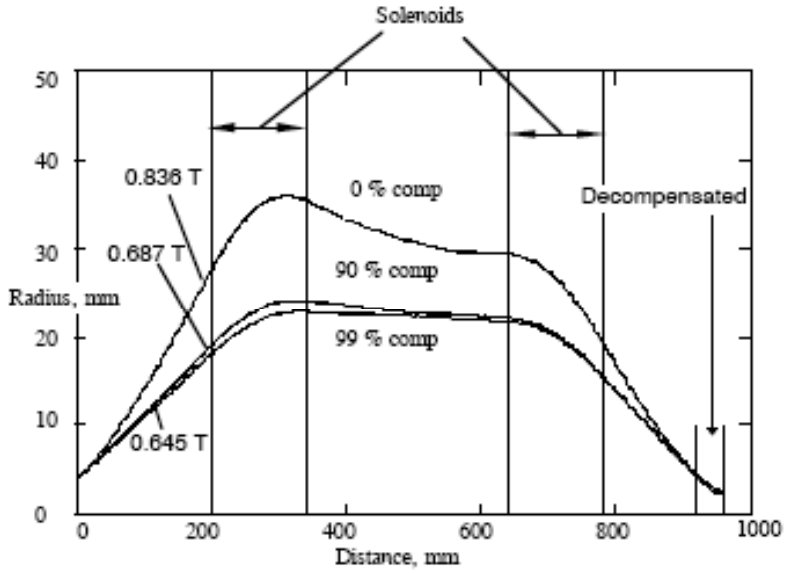

Figure 2.6.2-3. Effect of charge compensation on beam radius in a solenoidal LEBT.

Fig. 9.2 LEBT outlined in the CDA

From an IAP Report.

Extensive new work has been performed by IAP in 2006 under this same EFDA Work Package.

spectrometer.

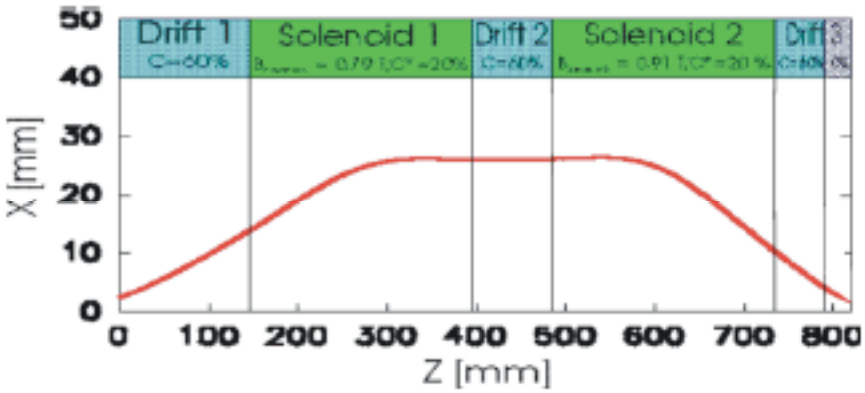

Figure 7: Schematic drawing of the magnetic LEBT for IFMIF including beam envelope for 140 mA.

Fig. 9.3 A representative LEBT outlined by IAP

SILHI LEBT

`/Users/rajameson/Documents/Folders/IFMIF/\ ACC\ IS:LEBT/IFMIF\ BLM/ECR\&LEBT/EmMsmtSaclECRLEBT.bmp`

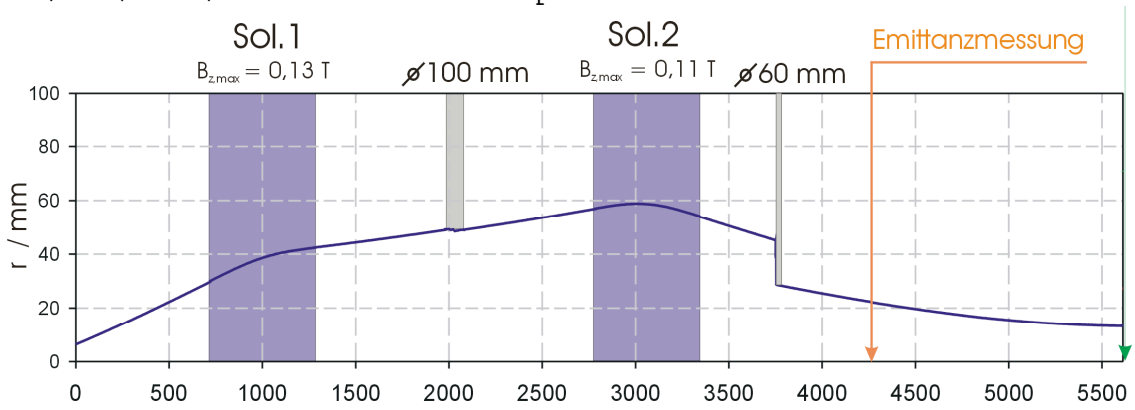

Fig. 9.4 A LEBT considered by Saclay includes a collimator.

A collimator in the LEBT (also used at SNS) may be helpful for scraping halo beam.

10. Concluding Remarks

Summary observations and comments are given in Section 6.9.

The careful reader will have noticed various features, such as some oscillation of the "matched" rms beam profiles. These are the subject of ongoing research, involving basic issues such as adiabaticity, phase-space mixing and so on. There is also subtle evidence concerning the role of adiabaticity in the optimization process. The RFQ remains a very interesting example of general linear accelerator physics.

The simulations reported were performed with a consistent family of codes. Relevant comparison with other codes has not been possible as their source code is not available. Certain differences have been noted but are not consistent over a broad range of designs and parameter range. The exact transmission found by any of these codes should be treated as indicative, as each has various sensitivities in its internal methods. Continued work to compare results between different codes more broadly and deeply than heretofore is highly recommended - this requires comparison at source code level and devising of appropriate tests. It is strongly recommended that the project obtain source code for all important simulation work.

Acknowledgement

"Vielen herzlichen Dank" to Professor Dr. H. Klein for his reading of the manuscript and his useful comments.

References

1 A.L. Trego et al., “Fusion Materials Irradiation Test Facility - A facility for Fusion Materials Qualification”, Nuclear Technology/Fusion 4(2), 695 (1983).

2 K. Noda et al., “Capability of energy selective neutron irradiation test facility (ESNIT) for fusion reactor materials testing and the status of ESNIT program”, Journal of Nuclear Materials 191-194, 1367 (1992).

3 IFMIF Comprehensive Design Report, IFMIF International Team, An Activity of the International Energy Agency (IEA) Implementing Agreement for a Program of Research and Development on Fusion Materials, January 2004.

4 K. R. Crandall et al., “RF Quadrupole Beam Dynamics Design Studies,” Proceedings of the 1979 Linear Accelerator Conference (Brookhaven National Laboratory, Upton, New York, 1980) BNL-51134, p. 205.

5 T. Wangler, “RF Linear Accelerators,” Wiley Series in Beams Physics and Accelerators Technology.

6 L. Young, “25 Years of Technical Advances in RFQ Accelerators,” MOPPB001, PAC 2003.

7 IFMIF Comprehensive Design Report, IFMIF International Team, An Activity of the International Energy Agency (IEA) Implementing Agreement for a Program of Research and Development on Fusion Materials, January 2004. RFQ design based on R. A. Jameson, “Some Characteristics of IFMIF RFQ KP1.7 Designs,” IFMIF Memorandum RAJ-24-May-2000, Revised 6 September 2000. Included as Appendix 1.

8 Email from R. A. Jameson, IFMIF Accelerator Facility Design Team Leader, to Distribution, Subject: “AccFac CDR Draft 3 June 2003," Date: Tuesday, June 3, 2003, 4:01 PM.

9 IFMIF CDA, Section 2.6.2.10, Beam dynamics, beam performance and beam loss simulations; Injector and RFQ modeling by D. Bruhwiler.

10 M. Stockli, file: ‘stockli emit meas.pdf,’ title: ‘Microsoft PowerPoint - stockli_final_for_cd.ppt,’ 9/25/2002, 9:20 pm, detailed presentation to the SNS ASAC, September 2002, “Self-Consistent, Unbiased Exclusion Methods of Emittance Analysis,” PAC 2004.

11 “IFMIF Accelerator Technical Memorandum 3-10-96: LEBT Material, R. A. Jameson, AOT-1:96-078, Los Alamos National Laboratory, 10 March 1996.

12 “Record of discussions about the Accelerator Production of Tritium (APT) Low Energy Demonstration Accelerator (LEDA) Radio Frequency Quadrupole RFQ Discussion at LANL on 1/14/2000 with Lloyd Young and Dave Schneider,” IFMIF Memorandum, R. A. Jameson, 8 February 2000.

13 “Coulomb Scattering of Beam Particles on Residual Gas: A Source of the Halo at Low Energy,” N. Pichoff, G. Haouat, and P.-Y. Beauvais.

14 KEP Report, 3.1.2 AC11B-EU-IAP, Long run test of ion source.

15 R. A. Jameson et al., “Scaling and Optimization in High-Intensity Linear Accelerators,” LA-CP-91-272, Los Alamos National Laboratory, July 1991 (introduction of LINACS design code).

16 R. A. Jameson, “On Scaling and Optimization of High Intensity, Low-Beam-Loss RF Linacs for Neutron Source Drivers,” AIP Conference Proceedings 279 (1992), p. 969.

17 R. A. Jameson, “Beam-Intensity Limitations in Linear Accelerators,” (Invited), Proceedings of the 1981 Particle Accelerator Conference, Washington, D.C., March 11-13, 1981, IEEE Trans. Nucl. Sci. 28, p. 2408, June 1981; Los Alamos National Laboratory Report LA-UR-81-765, 9 March 1981. Correction, Jameson, R. A.; IEEE Trans. Nucl. Sci.; 1981; Vol. 28, No. 4, pp. 3665-3665.

18 R. A. Jameson, “A Discussion of RFQ Linac Simulation,” Los Alamos National Laboratory Report LA-CP-97-54, September 1997.
19 K. R. Crandall, “Effects of Vane-Tip Geometry on the Electric Fields in Radio-Frequency Quadrupole Linacs,” Los Alamos National Laboratory, LA-9695-MS, April 1983.
20 K. R. Crandall, “PARMTEQ with Image Charges,” Los Alamos National Laboratory, AT-1-92-213, October 1991.
21 L. Young, “Simulations of the LEDA RFQ 6.7 MeV Accelerator,” PAC 1997.
22 B. Bondarev et al., “The Lidos RFQ Designer Development,” Proceedings of the 2001 Particle Accelerator Conference, Chicago.
23 R. Duperrier and R. Ferdinand, “TOUTATIS, THE CEA-Saclay RFQ Code,” XX International Linac Conference, Monterey, California.
24 R. Duperrier, “Intense Beam dynamics in RFQs,” Thesis, U. Paris XI Orsay, Orsay Serial No. 6194, 7 July 2000.
25 V. A. Teplyakov, “The First CW Accelerator in USSR and a Birth of Accelerating Field Focusing,” EPAC 2006, Edinburgh, June 2006.
26 R. Ferdinand, “How to Chose the Operating Point,” Pac 1995, Vol. 2, p. 1146.
27 “Optimization of RFQ Design,” R. Ferdinand et al., EPAC 1998, THP23G.
28 R. A. Jameson, “Self-Consistent Beam Halo Studies and Halo Diagnostic Development in a Continuous Linear Focusing Channel,” LA-UR-94-3753, Los Alamos National Laboratory, 9 November 1994. AIP Proceedings of the 1994 Joint US-CERN-Japan International School on Frontiers of Accelerator Technology, Maui, Hawaii, USA, 3-9 November 1994, World Scientific, ISBN 981-02-2537-7, pp. 530-560.
29 “RFQ Optimization Study for ESNIT,” H. Takeda and R. A. Jameson, Los Alamos National Laboratory Report LA-CP-93-5, “Deuteron Linac Design Aspects for ESNIT,” pp. 4-25, January 1993.
30 A. Schempp, Proceedings of EPAC88, 1989, p 464.
31 A. Schempp, Proceedings of PAC89, IEEE89, CH2669-0, 1989, p. 1093.
32 S. Yamada, “Buncher section optimization of heavy ion RFQ linac,” Proceedings of the 1981 Linear Accelerator Conference.
33 L. Young, “High Power Operations of LEDA,” LINAC 2000.
34 L. Young, “Operations of the LEDA Resonantly Coupled RFQ,” WOAA004, PAC 2001, Snowmass.
35 F. Sacherer, “RMS envelope equations with space charge, CERN Internal Report, SI-DL/70-12.
36 R. A. Jameson, 1993 Particle Accelerator Conference, Washington, D.C., 17-20 May 1993, IEEE Conference Proceedings, IEEE Cat. No. 93CH3279-7, 88-647453, ISBN 0-7803-1203-1.
37 R. A. Jameson, “Beam Halo from Collective Core/Single-Particle Interactions, Los Alamos National Laboratory Report LA-UR-93-1209, March 1993.
38 R. A. Jameson, “An Approach to Fundamental Study of Beam Loss Minimization,” AIP Conference Proceedings 480, “Space Charge Dominated Beam Physics for Heavy Ion Fusion,” Saitama, Japan, December 1998, Y. K. Batygin, Editor.
39 I. Hofmann,, "Emittance Growth of Beams Close to the Space Charge Limit,” 1981 PAC, IEEE Trans. Nucl. Sci., Vol. NS-28, No. 3, June 1981, p. 2399, I. Hofmann and I. Bozsik, "Computer Simulation of Longitudinal-Transverse Space Charge Effects in Bunched Beams,” 1981 Linac Conference, October 1981, LA-9234-C, Los Alamos National Laboratory, February 1982, p. 116.
40 R. A. Jameson, “Equipartitioning in Linear Accelerators,” Proceedings of the 1981 Linear Accelerator Conference, Santa Fe, New Mexico, October l9-23, 1981, Los Alamos National

Laboratory Report LA-9234-C, p. 125, February 1982; Los Alamos National Laboratory Report LA-UR-81-3073, 19 October 1981.

41 R. A. Jameson, "On Scaling and Optimization of High Intensity, Low-Beam-Loss RF Linacs for Neutron Source Drivers," AIP Conference Proceedings 279, ISBN 1-56396-191-1, DOE Conf-9206193 (1992) pp. 969-998, Proceedings of the Third Workshop on Advanced Accelerator Concepts, 14-20 June 1992, Port Jefferson, Long Island, New York, LA-UR-92-2474, Los Alamos National Laboratory, 28 July 1992.

42 R. A. Jameson, "An Approach to Fundamental Study of Beam Loss Minimization," AIP Conference Proceedings 480, "Space Charge Dominated Beam Physics for Heavy Ion Fusion," Saitama, Japan, December 1998, Y. K. Batygin, Editor. Workshop on Space Charge Dominated Beam Physics for Heavy Ion , 10-12 December 1998, Institute of Physical and Chemical Research (RIKEN), Wako-shi, Japan. Los Alamos National Laboratory Report LA-UR-99-129, 8 January 1999.

43 "Review of Beam Dynamics and Space Charge Resonances in High Intensity Linacs," I. Hofmann et al., EPAC 2002.

44 C. Zhang, Z. Y. Guo, A. Schempp, R. A. Jameson, J. E. Chen, and J. X. Fang, Low-beam-loss design of a compact, high-current deuteron radio frequency quadrupole accelerator, Phys. Rev. Special topics - Accelerators and Beams, Vol. 7, 100101 (2004).

45 L. Young (1/21/2006), A. Schempp (2006), and V. A. Teplyakov (2006); private communications.

46 J. Rathke, private communication (1/24/2006).

47 "IFMIF Conceptual Design Activity, Final Report", IFMIF-CDA Team (ed. by M. Martone), ENEA Frascati Report, RT/ERG/FUS/96/11, December 1996.

48 Accelerator Team Meeting for the IFMIF Conceptual Design Activity, Santa Fe, New Mexico, USA, 11-13 September 1995, Los Alamos National Laboratory Report LA-UR-95-4416.

49 R. A. Jameson, "RF Power Estimate for IFMIF CDR RFQ," IFMIF Memorandum IFMIF-RAJ-030603-DRAFT.

50 Report "IFMIF RFQ Investigations," International Science and Technology Center Moscow Radiotechnical Institute, Computer Codes For High Power Linacs, Project #2135p, Moscow 2003.

Appendix

Post-CDR RFQ LINACS Summary Table

```
rfqtype= 4 vane    Win= 0.095    Wout= 5.    I= 0.13    him= 2.0145    q= 1    freq= 175.

powcuFac= 7.94  RhooverR0= 0.75

vane geometry= VSINE. mpole= 1  mpoleterms= 1  1  1  1  1  1  1  1   image= 0

ckap := VSINEepk[RhooverR0, localls, localem]

KPlimit= 13.9855  KPfac= 1.7  vKilpatrick := KPlimit KPfac r0[rfq] / ckappa[rfq]

etnrmsgiven= 0.000025  elnrmsgiven= 0.00004

etnrmsgivenmain := etnrmsgiven

elnrmsgivenmain := (endbeta = 0.073; elnrmsgiven (1 + 0.25 ((beta - betaEOS) / (endbeta - betaEOS))^1.))

Shaper parameters: EOSaperfac= 5.    phistgt= -88.    bfrac= 0.5    rmscells= 4

          siglint= 105   porch= 60.  setbeginem= 1.12  celldiv= 10

shapervrule := (v[rfq] = N[field r0[rfq] / ckappa[rfq]];)

ffadjrule := ffadj := wtfit[i / celldiv]

         ffadj0= 1.

phis rule:  lfacincr= -1.    lfacdist= 12.

            lgapfac := c1 + c2 (z - zEOS)

            c1= 3.89408    c2= -0.0833333

            TKphisrule := (If[phisbw ≤ -20., phis[rfq] = phisbw, phis[rfq] = -20.];)

            mainrfqphisrule := TKphisrule

mainrfqaperrule := (endbeta = 0.073; c3 = 1.15; a[rfq] := aEOS (1 + c3 ((beta - betaEOS) / (endbeta - betaEOS))^1.);)

mainrfqvrule := (v[rfq] = vKilpatrick /. {a[rfq] → astart, em[rfq] → mstart};)

mainrfqemrule := mfree

         mfunc = none

mainRFQstrategy := matchEP

matchUser = none

Copperpower= 1.08726  {phase length, rms phase length, Degrees}  11.1596     24.9537
```

Post-CDR RFQ PteqHI tapeinput

```
run 1 0 0 0 2 0 0 0 0 0 0 0 0 0 0 0
title
 IFMIF C27og3
linac 1 0.095 175. 2.0145 1
tank 1 5.  -90 0.1 0 1.0 0 1.0 0 0 1.0  10 1 36 0.0 0.0
zdata -5 -3.44745   0.01   -90.   1.   0.0689503
-2.58559   0.974581   -90.   1.   0.0689503
-1.72372   1.93916   -90.   1.   0.0689503
-0.861862   2.90374   -90.   1.   0.0689503    4
zdata  -5
0.   3.86832   -90.   1.   0.0689503
8.61862   4.62525   -90.   1.00814   0.0689503
17.2372   5.38986   -90.   1.02966   0.0689503
25.8559   6.15447   -90.   1.06247   0.0689503
27.5796   6.3074   -89.8473   1.07032   0.0689503
29.3034   6.46033   -89.6496   1.07861   0.0689503
31.0275   6.61328   -89.4519   1.08735   0.0689503
32.752   6.76627   -89.2542   1.09653   0.0689503
```

```
34.4771   6.91931   -89.0564   1.10618   0.0689503
36.203   7.07243   -88.8585   1.11631   0.0689503
37.9301   7.22564   -88.6604   1.12694   0.0689503
39.6587   7.37899   -88.4622   1.1381   0.0689503
41.3892   7.5325   -88.2638   1.14981   0.0689503
43.122   7.68622   -88.0651   1.16212   0.0689503
51.8282   7.67661   -87.772   1.16786   0.0694543
60.6166   7.66451   -87.4101   1.16834   0.0696384
69.5008   7.64954   -86.9795   1.16906   0.0698553
78.4972   7.63126   -86.4643   1.17003   0.0701113
87.6256   7.60939   -85.8441   1.1713   0.0704176
96.9102   7.58035   -85.1046   1.17347   0.0707951
106.381   7.54343   -84.2168   1.17654   0.0712555
116.074   7.49937   -83.139   1.18023   0.0718093
126.037   7.44623   -81.8325   1.18474   0.0724813
136.325   7.38181   -80.2554   1.19034   0.0733035
147.012   7.30324   -78.3666   1.19741   0.0743186
158.186   7.20755   -76.1296   1.20638   0.0755799
169.959   7.09103   -73.5247   1.21768   0.0771432
182.468   6.95024   -70.5596   1.23163   0.0790632
195.875   6.78048   -67.2858   1.24911   0.0814188
210.377   6.58202   -63.7733   1.27016   0.0842767
226.192   6.35517   -60.1325   1.29514   0.0877114
243.566   6.10302   -56.4872   1.32359   0.0917385
262.757   5.83116   -52.9547   1.35513   0.0963772
284.027   5.54597   -49.63   1.38877   0.101578
307.629   5.25647   -46.5728   1.42307   0.107253
333.798   4.97457   -43.7905   1.45652   0.113364
362.737   4.70355   -41.2937   1.48937   0.119884
394.626   4.44644   -39.0654   1.52072   0.126704
429.616   4.20712   -37.0709   1.54938   0.133716
467.829   3.98738   -35.2765   1.57484   0.140847
509.359   3.78653   -33.6547   1.59777   0.148117
554.284   3.60132   -32.1874   1.61926   0.155538
602.67   3.43084   -30.848   1.63904   0.163053
654.571   3.27422   -29.6138   1.65693   0.170619
710.03   3.13015   -28.468   1.67317   0.178223
769.082   2.99719   -27.3972   1.68818   0.185871     -1
rfqout 1
start 1
stop -1
elimit 0.25 0.25
input -6 -100000 1.2 11. .01491 1.2 11. .01491
   180. 0.0 0.0
 0.0 0.0 0.0 0.0 0.0 0.0 1. 2.0145 130. 0.095
output 2 -1 2 0 1 1 1 2000 1
scheff 130.0 0.029 -0.04425 20 40  20  1  4
optcon  120000   7 0.9 1.5 .1    1  11. 11. 1.    0 0 0 0
0 0 0 0   0 0 0 0    0 0 0 0
begin
end
```

Post-CDR RFQ Cell Table

nc	v	ws	beta	ez	capa	phi	a	m	b	cl	tl
0	0.069	0.0950	0.0101	0.000	0.00000	-90.0	10.384	1.000	0.010	0.000	0.00
1	0.069	0.0950	0.0101	0.000	0.00000	-90.0	1.052	1.000	0.975	0.862	0.86
2	0.069	0.0950	0.0101	0.000	0.00000	-90.0	0.746	1.000	1.939	0.862	1.72
3	0.069	0.0950	0.0101	0.000	0.00000	-90.0	0.609	1.000	2.904	0.862	2.59
4	0.069	0.0950	0.0101	0.000	0.00000	-90.0	0.528	1.000	3.868	0.862	3.45
5	0.069	0.0950	0.0101	0.000	0.00003	-90.0	0.523	1.000	3.937	0.862	4.31
6	0.069	0.0950	0.0101	0.001	0.00013	-90.0	0.518	1.000	4.014	0.862	5.17
7	0.069	0.0950	0.0101	0.002	0.00030	-90.0	0.513	1.001	4.090	0.862	6.03
8	0.069	0.0950	0.0101	0.004	0.00053	-90.0	0.508	1.001	4.167	0.862	6.89
9	0.069	0.0950	0.0101	0.007	0.00083	-90.0	0.504	1.002	4.243	0.862	7.76
10	0.069	0.0950	0.0101	0.010	0.00119	-90.0	0.499	1.003	4.319	0.862	8.62
11	0.069	0.0950	0.0101	0.013	0.00162	-90.0	0.494	1.004	4.396	0.862	9.48
12	0.069	0.0950	0.0101	0.017	0.00211	-90.0	0.490	1.005	4.472	0.862	10.34
13	0.069	0.0950	0.0101	0.021	0.00267	-90.0	0.485	1.007	4.549	0.862	11.20
14	0.069	0.0950	0.0101	0.026	0.00330	-90.0	0.481	1.008	4.625	0.862	12.07

15	0.069	0.0950	0.0101	0.032	0.00399	-90.0	0.477	1.010	4.702	0.862	12.93
16	0.069	0.0950	0.0101	0.038	0.00475	-90.0	0.472	1.011	4.778	0.862	13.79
17	0.069	0.0950	0.0101	0.045	0.00557	-90.0	0.468	1.013	4.855	0.862	14.65
18	0.069	0.0950	0.0101	0.052	0.00646	-90.0	0.464	1.015	4.931	0.862	15.51
19	0.069	0.0950	0.0101	0.059	0.00742	-90.0	0.460	1.017	5.008	0.862	16.38
20	0.069	0.0950	0.0101	0.067	0.00844	-90.0	0.456	1.020	5.084	0.862	17.24
21	0.069	0.0950	0.0101	0.076	0.00952	-90.0	0.452	1.022	5.161	0.862	18.10
22	0.069	0.0950	0.0101	0.085	0.01068	-90.0	0.448	1.024	5.237	0.862	18.96
23	0.069	0.0950	0.0101	0.095	0.01190	-90.0	0.444	1.027	5.313	0.862	19.82
24	0.069	0.0950	0.0101	0.105	0.01318	-90.0	0.441	1.030	5.390	0.862	20.68
25	0.069	0.0950	0.0101	0.116	0.01453	-90.0	0.437	1.032	5.466	0.862	21.55
26	0.069	0.0950	0.0101	0.128	0.01595	-90.0	0.433	1.035	5.543	0.862	22.41
27	0.069	0.0950	0.0101	0.139	0.01743	-90.0	0.430	1.038	5.619	0.862	23.27
28	0.069	0.0950	0.0101	0.152	0.01898	-90.0	0.426	1.041	5.696	0.862	24.13
29	0.069	0.0950	0.0101	0.165	0.02059	-90.0	0.423	1.045	5.772	0.862	24.99
30	0.069	0.0950	0.0101	0.178	0.02227	-90.0	0.419	1.048	5.849	0.862	25.86
31	0.069	0.0950	0.0101	0.192	0.02401	-90.0	0.416	1.051	5.925	0.862	26.72
32	0.069	0.0950	0.0101	0.207	0.02583	-90.0	0.413	1.055	6.002	0.862	27.58
33	0.069	0.0950	0.0101	0.222	0.02770	-90.0	0.409	1.059	6.078	0.862	28.44
34	0.069	0.0950	0.0101	0.237	0.02965	-90.0	0.406	1.062	6.155	0.862	29.30
35	0.069	0.0950	0.0101	0.253	0.03165	-89.9	0.403	1.066	6.231	0.862	30.17
36	0.069	0.0950	0.0101	0.270	0.03373	-89.8	0.399	1.070	6.307	0.862	31.03
37	0.069	0.0950	0.0101	0.287	0.03587	-89.7	0.396	1.074	6.384	0.862	31.89
38	0.069	0.0950	0.0101	0.305	0.03808	-89.6	0.393	1.079	6.460	0.862	32.75
39	0.069	0.0950	0.0101	0.323	0.04036	-89.6	0.390	1.083	6.537	0.862	33.61
40	0.069	0.0951	0.0101	0.342	0.04271	-89.5	0.387	1.087	6.613	0.862	34.48
41	0.069	0.0951	0.0101	0.361	0.04513	-89.4	0.384	1.092	6.690	0.862	35.34
42	0.069	0.0951	0.0101	0.381	0.04762	-89.3	0.381	1.097	6.766	0.862	36.20
43	0.069	0.0951	0.0101	0.401	0.05018	-89.2	0.378	1.101	6.843	0.863	37.06
44	0.069	0.0952	0.0101	0.422	0.05281	-89.1	0.375	1.106	6.919	0.863	37.92
45	0.069	0.0952	0.0101	0.444	0.05552	-89.0	0.372	1.111	6.996	0.863	38.79
46	0.069	0.0953	0.0101	0.466	0.05830	-88.9	0.369	1.116	7.072	0.863	39.65
47	0.069	0.0954	0.0101	0.488	0.06116	-88.8	0.366	1.122	7.149	0.864	40.51
48	0.069	0.0954	0.0101	0.512	0.06409	-88.7	0.363	1.127	7.226	0.864	41.38
49	0.069	0.0955	0.0101	0.535	0.06711	-88.6	0.360	1.132	7.302	0.864	42.24
50	0.069	0.0956	0.0101	0.560	0.07021	-88.5	0.358	1.138	7.379	0.865	43.11
51	0.069	0.0957	0.0101	0.585	0.07339	-88.4	0.355	1.144	7.456	0.865	43.97
52	0.069	0.0959	0.0101	0.610	0.07665	-88.3	0.352	1.150	7.533	0.866	44.84
53	0.069	0.0960	0.0101	0.637	0.08001	-88.2	0.349	1.156	7.609	0.866	45.70
54	0.069	0.0961	0.0101	0.664	0.08345	-88.1	0.346	1.162	7.686	0.867	46.57
55	0.069	0.0963	0.0101	0.687	0.08596	-88.0	0.347	1.168	7.685	0.868	47.44
56	0.069	0.0964	0.0101	0.687	0.08603	-88.0	0.347	1.168	7.684	0.868	48.31
57	0.069	0.0966	0.0101	0.687	0.08609	-88.0	0.347	1.168	7.684	0.869	49.18
58	0.069	0.0968	0.0102	0.687	0.08616	-88.0	0.347	1.168	7.683	0.870	50.05
59	0.069	0.0969	0.0102	0.687	0.08624	-87.9	0.347	1.168	7.682	0.871	50.92
60	0.069	0.0971	0.0102	0.687	0.08631	-87.9	0.347	1.168	7.681	0.871	51.79
61	0.069	0.0973	0.0102	0.687	0.08638	-87.9	0.347	1.168	7.680	0.872	52.66
62	0.069	0.0975	0.0102	0.688	0.08646	-87.8	0.347	1.168	7.679	0.873	53.53
63	0.069	0.0976	0.0102	0.688	0.08653	-87.8	0.347	1.168	7.678	0.874	54.41
64	0.069	0.0978	0.0102	0.688	0.08661	-87.8	0.347	1.168	7.677	0.875	55.28
65	0.069	0.0980	0.0102	0.688	0.08669	-87.7	0.347	1.168	7.676	0.875	56.16
66	0.069	0.0982	0.0102	0.688	0.08678	-87.7	0.347	1.168	7.674	0.876	57.03
67	0.070	0.0984	0.0102	0.688	0.08687	-87.7	0.347	1.168	7.673	0.877	57.91
68	0.070	0.0986	0.0102	0.689	0.08695	-87.6	0.347	1.168	7.672	0.878	58.79
69	0.070	0.0988	0.0103	0.689	0.08704	-87.6	0.347	1.168	7.671	0.879	59.67
70	0.070	0.0990	0.0103	0.689	0.08714	-87.6	0.347	1.168	7.670	0.880	60.55
71	0.070	0.0992	0.0103	0.689	0.08723	-87.5	0.347	1.168	7.668	0.881	61.43
72	0.070	0.0994	0.0103	0.689	0.08732	-87.5	0.348	1.168	7.667	0.882	62.31
73	0.070	0.0996	0.0103	0.690	0.08742	-87.4	0.348	1.168	7.666	0.882	63.19
74	0.070	0.0998	0.0103	0.690	0.08752	-87.4	0.348	1.168	7.665	0.883	64.08
75	0.070	0.1000	0.0103	0.690	0.08762	-87.4	0.348	1.168	7.663	0.884	64.96
76	0.070	0.1003	0.0103	0.690	0.08773	-87.3	0.348	1.168	7.662	0.885	65.85
77	0.070	0.1005	0.0103	0.691	0.08783	-87.3	0.348	1.169	7.660	0.886	66.73
78	0.070	0.1007	0.0104	0.691	0.08794	-87.2	0.348	1.169	7.659	0.887	67.62
79	0.070	0.1009	0.0104	0.691	0.08805	-87.2	0.348	1.169	7.657	0.888	68.51
80	0.070	0.1012	0.0104	0.692	0.08816	-87.2	0.348	1.169	7.656	0.889	69.40
81	0.070	0.1014	0.0104	0.692	0.08828	-87.1	0.348	1.169	7.654	0.891	70.29
82	0.070	0.1017	0.0104	0.692	0.08840	-87.1	0.348	1.169	7.653	0.892	71.18
83	0.070	0.1019	0.0104	0.692	0.08852	-87.0	0.348	1.169	7.651	0.893	72.07
84	0.070	0.1022	0.0104	0.693	0.08864	-87.0	0.348	1.169	7.650	0.894	72.97
85	0.070	0.1024	0.0104	0.693	0.08877	-86.9	0.349	1.169	7.648	0.895	73.86

86	0.070	0.1027	0.0105	0.693	0.08889	-86.9	0.349	1.169	7.646	0.896	74.76
87	0.070	0.1030	0.0105	0.694	0.08902	-86.8	0.349	1.169	7.644	0.897	75.65
88	0.070	0.1032	0.0105	0.694	0.08916	-86.8	0.349	1.169	7.643	0.898	76.55
89	0.070	0.1035	0.0105	0.695	0.08929	-86.7	0.349	1.170	7.641	0.900	77.45
90	0.070	0.1038	0.0105	0.695	0.08943	-86.7	0.349	1.170	7.639	0.901	78.35
91	0.070	0.1041	0.0105	0.695	0.08957	-86.6	0.349	1.170	7.637	0.902	79.25
92	0.070	0.1044	0.0105	0.696	0.08971	-86.6	0.349	1.170	7.635	0.903	80.16
93	0.070	0.1047	0.0106	0.696	0.08985	-86.5	0.349	1.170	7.633	0.905	81.06
94	0.070	0.1050	0.0106	0.697	0.09000	-86.5	0.349	1.170	7.631	0.906	81.97
95	0.070	0.1053	0.0106	0.697	0.09015	-86.4	0.349	1.170	7.629	0.907	82.88
96	0.070	0.1056	0.0106	0.697	0.09030	-86.3	0.350	1.170	7.627	0.909	83.78
97	0.070	0.1059	0.0106	0.698	0.09046	-86.3	0.350	1.170	7.625	0.910	84.69
98	0.070	0.1062	0.0106	0.698	0.09061	-86.2	0.350	1.170	7.623	0.911	85.61
99	0.070	0.1066	0.0107	0.699	0.09077	-86.2	0.350	1.171	7.621	0.913	86.52
100	0.070	0.1069	0.0107	0.699	0.09093	-86.1	0.350	1.171	7.619	0.914	87.43
101	0.070	0.1072	0.0107	0.700	0.09110	-86.0	0.350	1.171	7.617	0.916	88.35
102	0.070	0.1076	0.0107	0.700	0.09127	-86.0	0.350	1.171	7.614	0.917	89.27
103	0.070	0.1080	0.0107	0.701	0.09144	-85.9	0.350	1.171	7.612	0.919	90.18
104	0.070	0.1083	0.0107	0.701	0.09163	-85.8	0.350	1.171	7.609	0.920	91.10
105	0.070	0.1087	0.0108	0.702	0.09183	-85.8	0.351	1.171	7.607	0.922	92.03
106	0.070	0.1091	0.0108	0.702	0.09202	-85.7	0.351	1.172	7.604	0.923	92.95
107	0.071	0.1094	0.0108	0.703	0.09224	-85.6	0.351	1.172	7.601	0.925	93.88
108	0.071	0.1098	0.0108	0.704	0.09245	-85.6	0.351	1.172	7.599	0.927	94.80
109	0.071	0.1102	0.0108	0.705	0.09267	-85.5	0.351	1.172	7.596	0.928	95.73
110	0.071	0.1106	0.0109	0.705	0.09290	-85.4	0.351	1.172	7.593	0.930	96.66
111	0.071	0.1111	0.0109	0.706	0.09312	-85.3	0.351	1.173	7.590	0.932	97.59
112	0.071	0.1115	0.0109	0.707	0.09336	-85.3	0.351	1.173	7.587	0.934	98.53
113	0.071	0.1119	0.0109	0.708	0.09360	-85.2	0.352	1.173	7.584	0.935	99.46
114	0.071	0.1124	0.0109	0.709	0.09386	-85.1	0.352	1.173	7.580	0.937	100.40
115	0.071	0.1128	0.0110	0.710	0.09411	-85.0	0.352	1.174	7.577	0.939	101.34
116	0.071	0.1133	0.0110	0.711	0.09437	-84.9	0.352	1.174	7.574	0.941	102.28
117	0.071	0.1137	0.0110	0.712	0.09464	-84.9	0.352	1.174	7.570	0.943	103.22
118	0.071	0.1142	0.0110	0.713	0.09492	-84.8	0.352	1.175	7.567	0.945	104.17
119	0.071	0.1147	0.0111	0.714	0.09520	-84.7	0.352	1.175	7.563	0.947	105.11
120	0.071	0.1152	0.0111	0.715	0.09550	-84.6	0.353	1.175	7.559	0.949	106.06
121	0.071	0.1157	0.0111	0.716	0.09579	-84.5	0.353	1.176	7.555	0.951	107.01
122	0.071	0.1162	0.0111	0.717	0.09610	-84.4	0.353	1.176	7.551	0.953	107.97
123	0.071	0.1167	0.0112	0.718	0.09640	-84.3	0.353	1.176	7.547	0.955	108.92
124	0.071	0.1173	0.0112	0.720	0.09672	-84.2	0.353	1.177	7.543	0.958	109.88
125	0.071	0.1178	0.0112	0.721	0.09704	-84.1	0.353	1.177	7.539	0.960	110.84
126	0.071	0.1184	0.0112	0.722	0.09736	-84.0	0.354	1.177	7.535	0.962	111.80
127	0.071	0.1190	0.0113	0.723	0.09769	-83.9	0.354	1.178	7.531	0.964	112.77
128	0.071	0.1196	0.0113	0.724	0.09802	-83.8	0.354	1.178	7.527	0.967	113.73
129	0.072	0.1202	0.0113	0.726	0.09835	-83.7	0.354	1.178	7.522	0.969	114.70
130	0.072	0.1208	0.0113	0.727	0.09870	-83.6	0.354	1.179	7.518	0.972	115.67
131	0.072	0.1214	0.0114	0.728	0.09905	-83.5	0.354	1.179	7.513	0.974	116.65
132	0.072	0.1220	0.0114	0.730	0.09940	-83.4	0.355	1.179	7.509	0.977	117.63
133	0.072	0.1227	0.0114	0.731	0.09976	-83.3	0.355	1.180	7.504	0.979	118.61
134	0.072	0.1234	0.0115	0.732	0.10013	-83.1	0.355	1.180	7.499	0.982	119.59
135	0.072	0.1240	0.0115	0.734	0.10051	-83.0	0.355	1.181	7.495	0.985	120.57
136	0.072	0.1247	0.0115	0.735	0.10089	-82.9	0.355	1.181	7.490	0.988	121.56
137	0.072	0.1254	0.0116	0.736	0.10129	-82.8	0.356	1.181	7.484	0.990	122.55
138	0.072	0.1262	0.0116	0.738	0.10169	-82.6	0.356	1.182	7.479	0.993	123.54
139	0.072	0.1269	0.0116	0.739	0.10209	-82.5	0.356	1.182	7.474	0.996	124.54
140	0.072	0.1277	0.0117	0.741	0.10251	-82.4	0.356	1.183	7.469	0.999	125.54
141	0.072	0.1285	0.0117	0.742	0.10293	-82.3	0.356	1.183	7.463	1.002	126.54
142	0.072	0.1292	0.0117	0.744	0.10337	-82.1	0.357	1.184	7.458	1.005	127.55
143	0.072	0.1301	0.0118	0.745	0.10381	-82.0	0.357	1.184	7.452	1.008	128.55
144	0.072	0.1309	0.0118	0.747	0.10426	-81.8	0.357	1.185	7.446	1.012	129.57
145	0.073	0.1317	0.0118	0.749	0.10472	-81.7	0.357	1.185	7.440	1.015	130.58
146	0.073	0.1326	0.0119	0.750	0.10519	-81.5	0.358	1.186	7.434	1.018	131.60
147	0.073	0.1335	0.0119	0.752	0.10567	-81.4	0.358	1.186	7.428	1.022	132.62
148	0.073	0.1344	0.0120	0.754	0.10616	-81.2	0.358	1.187	7.422	1.025	133.65
149	0.073	0.1354	0.0120	0.756	0.10666	-81.1	0.358	1.187	7.416	1.029	134.68
150	0.073	0.1363	0.0121	0.757	0.10716	-80.9	0.359	1.188	7.409	1.032	135.71
151	0.073	0.1373	0.0121	0.759	0.10768	-80.8	0.359	1.189	7.402	1.036	136.74
152	0.073	0.1383	0.0121	0.761	0.10821	-80.6	0.359	1.189	7.396	1.040	137.78
153	0.073	0.1393	0.0122	0.763	0.10874	-80.4	0.360	1.190	7.389	1.044	138.83
154	0.073	0.1404	0.0122	0.765	0.10929	-80.3	0.360	1.190	7.382	1.048	139.87
155	0.073	0.1415	0.0123	0.767	0.10986	-80.1	0.360	1.191	7.375	1.052	140.93
156	0.073	0.1426	0.0123	0.769	0.11043	-79.9	0.360	1.192	7.367	1.056	141.98

157	0.074	0.1437	0.0124	0.771	0.11102	-79.7	0.361	1.192	7.360	1.060	143.04
158	0.074	0.1448	0.0124	0.773	0.11161	-79.5	0.361	1.193	7.352	1.064	144.11
159	0.074	0.1460	0.0125	0.775	0.11223	-79.4	0.361	1.194	7.344	1.069	145.17
160	0.074	0.1472	0.0125	0.777	0.11285	-79.2	0.362	1.194	7.337	1.073	146.25
161	0.074	0.1485	0.0126	0.779	0.11349	-79.0	0.362	1.195	7.329	1.077	147.33
162	0.074	0.1498	0.0126	0.782	0.11415	-78.8	0.362	1.196	7.320	1.082	148.41
163	0.074	0.1511	0.0127	0.784	0.11481	-78.6	0.363	1.197	7.312	1.087	149.49
164	0.074	0.1524	0.0127	0.786	0.11550	-78.4	0.363	1.197	7.303	1.092	150.59
165	0.074	0.1538	0.0128	0.789	0.11619	-78.2	0.363	1.198	7.294	1.097	151.68
166	0.075	0.1552	0.0129	0.791	0.11690	-77.9	0.364	1.199	7.286	1.102	152.78
167	0.075	0.1566	0.0129	0.794	0.11763	-77.7	0.364	1.200	7.276	1.107	153.89
168	0.075	0.1581	0.0130	0.796	0.11837	-77.5	0.365	1.201	7.267	1.112	155.00
169	0.075	0.1596	0.0130	0.799	0.11913	-77.3	0.365	1.202	7.258	1.117	156.12
170	0.075	0.1612	0.0131	0.801	0.11990	-77.1	0.365	1.203	7.248	1.123	157.24
171	0.075	0.1628	0.0132	0.804	0.12069	-76.8	0.366	1.203	7.238	1.128	158.37
172	0.075	0.1644	0.0132	0.807	0.12149	-76.6	0.366	1.204	7.228	1.134	159.50
173	0.075	0.1661	0.0133	0.810	0.12232	-76.4	0.367	1.205	7.218	1.140	160.64
174	0.076	0.1679	0.0134	0.813	0.12316	-76.1	0.367	1.206	7.208	1.146	161.79
175	0.076	0.1696	0.0134	0.815	0.12402	-75.9	0.368	1.207	7.197	1.152	162.94
176	0.076	0.1715	0.0135	0.818	0.12490	-75.6	0.368	1.208	7.186	1.158	164.10
177	0.076	0.1733	0.0136	0.821	0.12579	-75.4	0.368	1.210	7.175	1.164	165.26
178	0.076	0.1752	0.0137	0.824	0.12670	-75.1	0.369	1.211	7.164	1.171	166.43
179	0.076	0.1772	0.0137	0.828	0.12763	-74.9	0.369	1.212	7.152	1.177	167.61
180	0.076	0.1792	0.0138	0.831	0.12859	-74.6	0.370	1.213	7.140	1.184	168.79
181	0.077	0.1813	0.0139	0.834	0.12956	-74.3	0.370	1.214	7.128	1.191	169.99
182	0.077	0.1834	0.0140	0.837	0.13054	-74.1	0.371	1.215	7.116	1.198	171.18
183	0.077	0.1856	0.0141	0.841	0.13155	-73.8	0.371	1.216	7.104	1.205	172.39
184	0.077	0.1879	0.0141	0.844	0.13257	-73.5	0.372	1.218	7.091	1.212	173.60
185	0.077	0.1902	0.0142	0.847	0.13362	-73.2	0.373	1.219	7.078	1.219	174.82
186	0.077	0.1925	0.0143	0.851	0.13468	-73.0	0.373	1.220	7.065	1.227	176.05
187	0.078	0.1950	0.0144	0.854	0.13577	-72.7	0.374	1.222	7.052	1.235	177.28
188	0.078	0.1975	0.0145	0.858	0.13687	-72.4	0.374	1.223	7.038	1.243	178.52
189	0.078	0.2000	0.0146	0.861	0.13800	-72.1	0.375	1.224	7.024	1.251	179.77
190	0.078	0.2027	0.0147	0.865	0.13915	-71.8	0.375	1.226	7.010	1.259	181.03
191	0.078	0.2054	0.0148	0.869	0.14031	-71.5	0.376	1.227	6.995	1.267	182.30
192	0.079	0.2081	0.0149	0.872	0.14151	-71.2	0.377	1.229	6.981	1.276	183.57
193	0.079	0.2110	0.0150	0.876	0.14273	-70.9	0.377	1.230	6.966	1.284	184.86
194	0.079	0.2139	0.0151	0.880	0.14397	-70.6	0.378	1.232	6.950	1.293	186.15
195	0.079	0.2169	0.0152	0.884	0.14524	-70.2	0.379	1.233	6.935	1.302	187.45
196	0.079	0.2200	0.0153	0.888	0.14653	-69.9	0.379	1.235	6.919	1.312	188.77
197	0.080	0.2232	0.0154	0.892	0.14785	-69.6	0.380	1.236	6.902	1.321	190.09
198	0.080	0.2265	0.0155	0.896	0.14920	-69.3	0.381	1.238	6.886	1.331	191.42
199	0.080	0.2298	0.0156	0.901	0.15057	-69.0	0.382	1.240	6.869	1.340	192.76
200	0.080	0.2333	0.0158	0.905	0.15197	-68.6	0.382	1.242	6.852	1.350	194.11
201	0.081	0.2368	0.0159	0.909	0.15339	-68.3	0.383	1.243	6.835	1.361	195.47
202	0.081	0.2405	0.0160	0.914	0.15484	-68.0	0.384	1.245	6.817	1.371	196.84
203	0.081	0.2442	0.0161	0.918	0.15631	-67.6	0.385	1.247	6.799	1.382	198.22
204	0.081	0.2480	0.0163	0.923	0.15781	-67.3	0.385	1.249	6.780	1.393	199.62
205	0.082	0.2520	0.0164	0.927	0.15933	-66.9	0.386	1.251	6.762	1.404	201.02
206	0.082	0.2560	0.0165	0.932	0.16087	-66.6	0.387	1.253	6.743	1.415	202.43
207	0.082	0.2602	0.0167	0.936	0.16243	-66.3	0.388	1.255	6.724	1.426	203.86
208	0.082	0.2645	0.0168	0.941	0.16402	-65.9	0.389	1.257	6.704	1.438	205.30
209	0.083	0.2689	0.0169	0.946	0.16562	-65.6	0.390	1.259	6.685	1.450	206.75
210	0.083	0.2734	0.0171	0.950	0.16727	-65.2	0.390	1.261	6.665	1.462	208.21
211	0.083	0.2780	0.0172	0.955	0.16893	-64.8	0.391	1.263	6.644	1.474	209.68
212	0.084	0.2828	0.0174	0.960	0.17061	-64.5	0.392	1.266	6.624	1.487	211.17
213	0.084	0.2876	0.0175	0.965	0.17232	-64.1	0.393	1.268	6.603	1.500	212.67
214	0.084	0.2927	0.0177	0.970	0.17406	-63.8	0.394	1.270	6.582	1.513	214.18
215	0.085	0.2978	0.0178	0.975	0.17583	-63.4	0.395	1.272	6.561	1.526	215.71
216	0.085	0.3031	0.0180	0.980	0.17762	-63.1	0.396	1.275	6.539	1.539	217.25
217	0.085	0.3085	0.0181	0.985	0.17943	-62.7	0.397	1.277	6.517	1.553	218.80
218	0.086	0.3141	0.0183	0.990	0.18126	-62.3	0.398	1.280	6.495	1.567	220.37
219	0.086	0.3198	0.0185	0.995	0.18313	-62.0	0.399	1.282	6.472	1.581	221.95
220	0.086	0.3257	0.0186	1.000	0.18501	-61.6	0.400	1.285	6.449	1.596	223.54
221	0.087	0.3318	0.0188	1.005	0.18693	-61.2	0.401	1.287	6.426	1.610	225.16
222	0.087	0.3379	0.0190	1.011	0.18886	-60.9	0.403	1.290	6.403	1.625	226.78
223	0.087	0.3443	0.0192	1.016	0.19082	-60.5	0.404	1.292	6.379	1.641	228.42
224	0.088	0.3508	0.0193	1.021	0.19280	-60.1	0.405	1.295	6.355	1.656	230.08
225	0.088	0.3575	0.0195	1.026	0.19480	-59.8	0.406	1.298	6.331	1.672	231.75
226	0.088	0.3644	0.0197	1.032	0.19682	-59.4	0.407	1.301	6.307	1.688	233.44
227	0.089	0.3714	0.0199	1.037	0.19885	-59.0	0.408	1.303	6.282	1.704	235.14

228	0.089	0.3786	0.0201	1.042	0.20091	-58.7	0.410	1.306	6.257	1.720	236.86
229	0.090	0.3860	0.0203	1.048	0.20298	-58.3	0.411	1.309	6.232	1.737	238.60
230	0.090	0.3936	0.0205	1.053	0.20508	-57.9	0.412	1.312	6.207	1.754	240.35
231	0.090	0.4014	0.0207	1.058	0.20718	-57.6	0.413	1.315	6.181	1.771	242.12
232	0.091	0.4094	0.0209	1.063	0.20932	-57.2	0.415	1.318	6.155	1.789	243.91
233	0.091	0.4176	0.0211	1.069	0.21146	-56.8	0.416	1.321	6.129	1.807	245.72
234	0.092	0.4260	0.0213	1.074	0.21362	-56.5	0.417	1.324	6.103	1.825	247.54
235	0.092	0.4346	0.0215	1.079	0.21581	-56.1	0.419	1.327	6.077	1.843	249.39
236	0.093	0.4434	0.0217	1.085	0.21800	-55.8	0.420	1.330	6.050	1.862	251.25
237	0.093	0.4524	0.0220	1.090	0.22022	-55.4	0.421	1.333	6.023	1.880	253.13
238	0.094	0.4616	0.0222	1.095	0.22245	-55.1	0.423	1.336	5.996	1.900	255.03
239	0.094	0.4711	0.0224	1.100	0.22469	-54.7	0.424	1.339	5.969	1.919	256.95
240	0.094	0.4808	0.0226	1.106	0.22696	-54.3	0.426	1.342	5.942	1.939	258.89
241	0.095	0.4907	0.0229	1.111	0.22925	-54.0	0.427	1.345	5.914	1.958	260.85
242	0.095	0.5008	0.0231	1.116	0.23153	-53.6	0.429	1.349	5.887	1.979	262.82
243	0.096	0.5112	0.0233	1.122	0.23383	-53.3	0.430	1.352	5.859	1.999	264.82
244	0.096	0.5219	0.0236	1.127	0.23616	-53.0	0.432	1.355	5.831	2.020	266.84
245	0.097	0.5328	0.0238	1.132	0.23848	-52.6	0.433	1.358	5.803	2.041	268.88
246	0.097	0.5439	0.0241	1.137	0.24082	-52.3	0.435	1.362	5.775	2.062	270.95
247	0.098	0.5553	0.0243	1.142	0.24316	-51.9	0.436	1.365	5.747	2.083	273.03
248	0.098	0.5669	0.0246	1.148	0.24551	-51.6	0.438	1.368	5.718	2.105	275.13
249	0.099	0.5788	0.0248	1.153	0.24787	-51.3	0.440	1.372	5.690	2.127	277.26
250	0.099	0.5910	0.0251	1.158	0.25024	-50.9	0.441	1.375	5.662	2.149	279.41
251	0.100	0.6034	0.0254	1.163	0.25259	-50.6	0.443	1.379	5.633	2.172	281.58
252	0.101	0.6161	0.0256	1.168	0.25495	-50.3	0.445	1.382	5.604	2.194	283.78
253	0.101	0.6291	0.0259	1.172	0.25729	-50.0	0.446	1.385	5.575	2.217	285.99
254	0.102	0.6424	0.0262	1.177	0.25964	-49.6	0.448	1.389	5.546	2.241	288.23
255	0.102	0.6559	0.0264	1.182	0.26199	-49.3	0.450	1.392	5.517	2.264	290.50
256	0.103	0.6698	0.0267	1.186	0.26433	-49.0	0.452	1.396	5.488	2.288	292.79
257	0.103	0.6839	0.0270	1.191	0.26666	-48.7	0.453	1.399	5.459	2.312	295.10
258	0.104	0.6983	0.0273	1.195	0.26900	-48.4	0.455	1.403	5.430	2.336	297.43
259	0.104	0.7130	0.0276	1.200	0.27132	-48.1	0.457	1.406	5.401	2.361	299.79
260	0.105	0.7280	0.0278	1.204	0.27364	-47.8	0.459	1.409	5.372	2.385	302.18
261	0.106	0.7433	0.0281	1.208	0.27594	-47.5	0.461	1.413	5.343	2.410	304.59
262	0.106	0.7589	0.0284	1.212	0.27824	-47.2	0.462	1.416	5.314	2.435	307.02
263	0.107	0.7748	0.0287	1.216	0.28051	-46.9	0.464	1.420	5.285	2.461	309.49
264	0.107	0.7910	0.0290	1.220	0.28278	-46.6	0.466	1.423	5.256	2.486	311.97
265	0.108	0.8075	0.0293	1.224	0.28503	-46.3	0.468	1.426	5.228	2.512	314.48
266	0.108	0.8243	0.0296	1.227	0.28727	-46.0	0.470	1.430	5.199	2.538	317.02
267	0.109	0.8414	0.0299	1.231	0.28950	-45.7	0.472	1.433	5.171	2.564	319.59
268	0.110	0.8589	0.0302	1.235	0.29171	-45.4	0.474	1.437	5.142	2.591	322.18
269	0.110	0.8767	0.0306	1.238	0.29390	-45.1	0.476	1.440	5.114	2.617	324.79
270	0.111	0.8948	0.0309	1.241	0.29608	-44.9	0.478	1.443	5.086	2.644	327.44
271	0.111	0.9132	0.0312	1.245	0.29825	-44.6	0.480	1.447	5.058	2.671	330.11
272	0.112	0.9319	0.0315	1.248	0.30041	-44.3	0.482	1.450	5.030	2.698	332.81
273	0.113	0.9510	0.0318	1.251	0.30256	-44.1	0.484	1.453	5.002	2.726	335.53
274	0.113	0.9704	0.0321	1.254	0.30469	-43.8	0.486	1.457	4.975	2.754	338.29
275	0.114	0.9901	0.0325	1.258	0.30682	-43.5	0.488	1.460	4.947	2.781	341.07
276	0.115	1.0102	0.0328	1.261	0.30894	-43.3	0.490	1.463	4.919	2.809	343.88
277	0.115	1.0306	0.0331	1.264	0.31104	-43.0	0.492	1.466	4.892	2.838	346.72
278	0.116	1.0514	0.0335	1.267	0.31313	-42.8	0.494	1.470	4.865	2.866	349.58
279	0.117	1.0724	0.0338	1.269	0.31521	-42.5	0.496	1.473	4.838	2.895	352.48
280	0.117	1.0939	0.0341	1.272	0.31728	-42.3	0.499	1.476	4.811	2.923	355.40
281	0.118	1.1157	0.0345	1.275	0.31934	-42.0	0.501	1.480	4.784	2.952	358.35
282	0.119	1.1378	0.0348	1.278	0.32138	-41.8	0.503	1.483	4.757	2.981	361.33
283	0.119	1.1603	0.0351	1.281	0.32340	-41.5	0.505	1.486	4.730	3.011	364.34
284	0.120	1.1831	0.0355	1.283	0.32542	-41.3	0.507	1.489	4.704	3.040	367.38
285	0.121	1.2063	0.0358	1.286	0.32741	-41.1	0.509	1.493	4.677	3.070	370.45
286	0.121	1.2298	0.0362	1.288	0.32940	-40.8	0.512	1.496	4.651	3.100	373.55
287	0.122	1.2537	0.0365	1.291	0.33136	-40.6	0.514	1.499	4.625	3.129	376.68
288	0.123	1.2779	0.0369	1.293	0.33329	-40.4	0.516	1.502	4.599	3.160	379.84
289	0.123	1.3025	0.0372	1.295	0.33523	-40.1	0.518	1.505	4.573	3.190	383.03
290	0.124	1.3275	0.0376	1.298	0.33713	-39.9	0.521	1.508	4.547	3.220	386.25
291	0.125	1.3528	0.0380	1.300	0.33901	-39.7	0.523	1.512	4.522	3.251	389.50
292	0.125	1.3785	0.0383	1.302	0.34088	-39.5	0.525	1.515	4.496	3.281	392.79
293	0.126	1.4046	0.0387	1.304	0.34271	-39.3	0.527	1.518	4.471	3.312	396.10
294	0.127	1.4310	0.0390	1.306	0.34453	-39.1	0.530	1.521	4.446	3.343	399.44
295	0.127	1.4578	0.0394	1.308	0.34633	-38.9	0.532	1.524	4.422	3.374	402.81
296	0.128	1.4849	0.0398	1.309	0.34810	-38.6	0.534	1.527	4.397	3.406	406.22
297	0.129	1.5125	0.0401	1.311	0.34987	-38.4	0.537	1.530	4.373	3.437	409.66
298	0.129	1.5403	0.0405	1.313	0.35160	-38.2	0.539	1.533	4.348	3.468	413.13

299	0.130	1.5686	0.0409	1.314	0.35331	-38.0	0.541	1.535	4.324	3.500	416.63
300	0.131	1.5972	0.0412	1.316	0.35500	-37.8	0.544	1.538	4.301	3.532	420.16
301	0.132	1.6262	0.0416	1.317	0.35666	-37.6	0.546	1.541	4.277	3.564	423.72
302	0.132	1.6556	0.0420	1.318	0.35830	-37.5	0.548	1.544	4.253	3.596	427.32
303	0.133	1.6853	0.0424	1.320	0.35993	-37.3	0.551	1.547	4.230	3.628	430.94
304	0.134	1.7154	0.0427	1.321	0.36153	-37.1	0.553	1.549	4.207	3.660	434.60
305	0.134	1.7458	0.0431	1.322	0.36310	-36.9	0.555	1.552	4.184	3.692	438.30
306	0.135	1.7767	0.0435	1.323	0.36466	-36.7	0.558	1.555	4.162	3.725	442.02
307	0.136	1.8079	0.0439	1.324	0.36618	-36.5	0.560	1.557	4.139	3.757	445.78
308	0.137	1.8394	0.0442	1.325	0.36769	-36.3	0.563	1.560	4.117	3.790	449.57
309	0.137	1.8714	0.0446	1.326	0.36918	-36.2	0.565	1.563	4.095	3.822	453.39
310	0.138	1.9037	0.0450	1.327	0.37064	-36.0	0.568	1.565	4.073	3.855	457.25
311	0.139	1.9363	0.0454	1.327	0.37209	-35.8	0.570	1.568	4.051	3.888	461.13
312	0.139	1.9694	0.0458	1.328	0.37351	-35.6	0.572	1.570	4.030	3.921	465.06
313	0.140	2.0028	0.0462	1.329	0.37492	-35.4	0.575	1.572	4.008	3.954	469.01
314	0.141	2.0366	0.0466	1.329	0.37630	-35.3	0.577	1.575	3.987	3.987	473.00
315	0.142	2.0707	0.0469	1.330	0.37768	-35.1	0.580	1.577	3.966	4.021	477.02
316	0.142	2.1052	0.0473	1.330	0.37903	-34.9	0.582	1.580	3.946	4.054	481.07
317	0.143	2.1401	0.0477	1.331	0.38038	-34.8	0.585	1.582	3.925	4.087	485.16
318	0.144	2.1754	0.0481	1.331	0.38173	-34.6	0.587	1.584	3.905	4.121	489.28
319	0.144	2.2110	0.0485	1.332	0.38304	-34.4	0.590	1.587	3.885	4.154	493.43
320	0.145	2.2470	0.0489	1.333	0.38438	-34.3	0.592	1.589	3.865	4.188	497.62
321	0.146	2.2834	0.0493	1.333	0.38568	-34.1	0.595	1.591	3.845	4.222	501.84
322	0.147	2.3202	0.0497	1.333	0.38696	-34.0	0.597	1.593	3.825	4.255	506.10
323	0.147	2.3573	0.0501	1.334	0.38826	-33.8	0.600	1.596	3.806	4.289	510.39
324	0.148	2.3948	0.0505	1.335	0.38952	-33.7	0.602	1.598	3.787	4.323	514.71
325	0.149	2.4327	0.0509	1.335	0.39077	-33.5	0.605	1.600	3.767	4.357	519.07
326	0.150	2.4710	0.0513	1.335	0.39204	-33.3	0.607	1.602	3.748	4.391	523.46
327	0.150	2.5096	0.0517	1.336	0.39327	-33.2	0.610	1.604	3.729	4.425	527.89
328	0.151	2.5486	0.0521	1.336	0.39449	-33.1	0.612	1.607	3.711	4.460	532.35
329	0.152	2.5880	0.0525	1.337	0.39572	-32.9	0.615	1.609	3.692	4.494	536.84
330	0.153	2.6278	0.0529	1.337	0.39693	-32.8	0.617	1.611	3.674	4.528	541.37
331	0.153	2.6680	0.0533	1.338	0.39812	-32.6	0.620	1.613	3.655	4.563	545.93
332	0.154	2.7085	0.0537	1.338	0.39931	-32.5	0.622	1.615	3.637	4.597	550.53
333	0.155	2.7495	0.0541	1.338	0.40047	-32.3	0.625	1.617	3.619	4.632	555.16
334	0.156	2.7908	0.0545	1.339	0.40163	-32.2	0.628	1.619	3.601	4.666	559.83
335	0.156	2.8325	0.0549	1.339	0.40278	-32.0	0.630	1.621	3.584	4.701	564.53
336	0.157	2.8746	0.0553	1.339	0.40391	-31.9	0.633	1.623	3.566	4.736	569.26
337	0.158	2.9170	0.0557	1.340	0.40503	-31.8	0.635	1.625	3.549	4.770	574.03
338	0.159	2.9599	0.0561	1.340	0.40614	-31.6	0.638	1.627	3.531	4.805	578.84
339	0.159	3.0031	0.0565	1.340	0.40722	-31.5	0.640	1.629	3.514	4.840	583.68
340	0.160	3.0467	0.0569	1.340	0.40830	-31.4	0.643	1.631	3.497	4.875	588.55
341	0.161	3.0907	0.0573	1.341	0.40938	-31.2	0.646	1.633	3.480	4.910	593.46
342	0.162	3.1351	0.0577	1.341	0.41043	-31.1	0.648	1.635	3.464	4.945	598.41
343	0.162	3.1798	0.0581	1.341	0.41149	-31.0	0.651	1.637	3.447	4.980	603.39
344	0.163	3.2250	0.0586	1.341	0.41252	-30.8	0.653	1.639	3.431	5.015	608.40
345	0.164	3.2705	0.0590	1.341	0.41354	-30.7	0.656	1.641	3.415	5.050	613.45
346	0.165	3.3164	0.0594	1.341	0.41456	-30.6	0.659	1.643	3.398	5.086	618.54
347	0.165	3.3627	0.0598	1.342	0.41555	-30.5	0.661	1.645	3.382	5.121	623.66
348	0.166	3.4094	0.0602	1.342	0.41653	-30.3	0.664	1.646	3.367	5.156	628.82
349	0.167	3.4564	0.0606	1.342	0.41751	-30.2	0.666	1.648	3.351	5.192	634.01
350	0.168	3.5039	0.0610	1.342	0.41847	-30.1	0.669	1.650	3.335	5.227	639.24
351	0.168	3.5517	0.0614	1.342	0.41942	-30.0	0.672	1.652	3.320	5.263	644.50
352	0.169	3.5999	0.0619	1.342	0.42036	-29.9	0.674	1.654	3.304	5.298	649.80
353	0.170	3.6485	0.0623	1.342	0.42128	-29.7	0.677	1.655	3.289	5.334	655.13
354	0.171	3.6975	0.0627	1.342	0.42219	-29.6	0.680	1.657	3.274	5.369	660.50
355	0.171	3.7469	0.0631	1.342	0.42311	-29.5	0.682	1.659	3.259	5.405	665.90
356	0.172	3.7966	0.0635	1.342	0.42401	-29.4	0.685	1.660	3.244	5.440	671.34
357	0.173	3.8467	0.0639	1.342	0.42489	-29.3	0.687	1.662	3.230	5.476	676.82
358	0.174	3.8972	0.0643	1.341	0.42576	-29.1	0.690	1.664	3.215	5.512	682.33
359	0.174	3.9481	0.0648	1.341	0.42664	-29.0	0.693	1.665	3.201	5.548	687.88
360	0.175	3.9994	0.0652	1.341	0.42749	-28.9	0.695	1.667	3.186	5.583	693.46
361	0.176	4.0510	0.0656	1.341	0.42834	-28.8	0.698	1.668	3.172	5.619	699.08
362	0.177	4.1031	0.0660	1.341	0.42919	-28.7	0.701	1.670	3.158	5.655	704.74
363	0.177	4.1555	0.0664	1.341	0.43001	-28.6	0.703	1.672	3.144	5.691	710.43
364	0.178	4.2083	0.0669	1.341	0.43083	-28.5	0.706	1.673	3.130	5.727	716.16
365	0.179	4.2615	0.0673	1.341	0.43165	-28.4	0.709	1.675	3.116	5.763	721.92
366	0.180	4.3151	0.0677	1.341	0.43246	-28.2	0.711	1.676	3.103	5.799	727.72
367	0.181	4.3690	0.0681	1.340	0.43325	-28.1	0.714	1.678	3.089	5.835	733.55
368	0.181	4.4234	0.0685	1.340	0.43405	-28.0	0.717	1.679	3.076	5.871	739.42
369	0.182	4.4781	0.0690	1.340	0.43482	-27.9	0.719	1.681	3.062	5.907	745.33

```
 370 0.183  4.5332 0.0694 1.340 0.43560 -27.8  0.722 1.682  3.049  5.943  751.27
 371 0.184  4.5887 0.0698 1.340 0.43638 -27.7  0.725 1.684  3.036  5.979  757.25
 372 0.184  4.6445 0.0702 1.340 0.43714 -27.6  0.727 1.685  3.023  6.015  763.27
 373 0.185  4.7008 0.0706 1.339 0.43790 -27.5  0.730 1.687  3.010  6.052  769.32
 374 0.186  4.7574 0.0711 1.339 0.43865 -27.4  0.733 1.688  2.997  6.088  775.41
 375 0.187  4.8145 0.0715 1.339 0.43939 -27.3  0.735 1.690  2.984  6.124  781.53
 376 0.187  4.8719 0.0719 1.339 0.44013 -27.2  0.738 1.691  2.972  6.160  787.69
 377 0.188  4.9297 0.0723 1.339 0.44086 -27.1  0.741 1.692  2.959  6.197  793.89
 378 0.189  4.9878 0.0728 1.339 0.44158 -27.0  0.743 1.694  2.947  6.233  800.12
```

CDR RFQ PteqHI tapeinput

```
run 1 0 0 0 2 0 657 0 0 0 0 657 0 0 0 0
title
IFMIF KP1.7 CDA Design
linac 1 0.1 175. 2.01 1
tank 1 8.  -90 0.1 0 1.0 0 1.0 0 0 1.0  10 1 36 0.0 0.0
zdata -5 -3.53691   0.01   -90.   1.   0.111022
         -2.65268   1.08371   -90.   1.   0.111022
         -1.76846   2.15743   -90.   1.   0.111022
         -0.884228   3.23114   -90.   1.   0.111022
         -0.00001   4.30486   -90.   1.   0.111022    4
zdata  -5
0.   4.30486   -90.   1.   0.111022
8.84228   4.5083   -90.   1.00062   0.106012
17.6846   4.73437   -90.   1.00255   0.100949
26.5268   4.96044   -90.   1.00574   0.0963487
35.3691   5.18651   -90.   1.01019   0.0921491
44.2114   5.41259   -90.   1.0159   0.0883002
53.0537   5.63866   -90.   1.02293   0.08476
61.8959   5.86473   -90.   1.03133   0.0814927
70.7382   6.0908   -89.8884   1.04119   0.0784679
79.5822   6.31691   -89.4945   1.05262   0.0756593
88.4334   6.54318   -89.1003   1.0658   0.0730429
97.3004   6.76983   -88.7054   1.08098   0.0705974
106.195   6.99715   -88.3094   1.09847   0.0683039
111.623   7.15824   -88.0287   1.11275   0.0667667
111.802   7.16284   -88.0207   1.1141   0.0667239
111.983   7.16746   -88.0127   1.11549   0.0666808
112.165   7.17212   -88.0045   1.11691   0.0666376
112.239   7.17399   -88.0013   1.11749   0.0666202
112.257   7.17445   -88.0005   1.11764   0.0666158
116.02   7.17026   -87.9514   1.118   0.0666544
125.242   7.16205   -87.8626   1.11865   0.0667309
134.527   7.15344   -87.7654   1.11933   0.0668111
143.878   7.1444   -87.6588   1.12005   0.0668956
153.299   7.1349   -87.5416   1.12081   0.0669847
162.793   7.12487   -87.4125   1.12162   0.0670789
172.364   7.11428   -87.2702   1.12248   0.0671788
182.018   7.10304   -87.1128   1.1234   0.067285
191.758   7.0911   -86.9385   1.12438   0.0673983
201.592   7.07838   -86.745   1.12543   0.0675194
211.525   7.06478   -86.5298   1.12657   0.0676493
221.564   7.05019   -86.29   1.12779   0.0677892
231.718   7.03451   -86.0222   1.12912   0.0679402
241.995   7.0176   -85.7228   1.13056   0.0681039
252.406   6.99929   -85.3872   1.13214   0.0682819
262.962   6.97941   -85.0106   1.13387   0.0684763
273.675   6.95776   -84.5875   1.13578   0.0686893
284.562   6.93408   -84.1114   1.13789   0.0689237
295.638   6.90813   -83.5754   1.14024   0.0691825
306.922   6.87957   -82.9718   1.14286   0.0694695
318.437   6.84806   -82.2922   1.1458   0.069789
330.207   6.81317   -81.5274   1.1491   0.070146
342.261   6.77446   -80.6682   1.15285   0.0705465
354.631   6.73139   -79.7051   1.1571   0.0709975
367.355   6.68339   -78.6287   1.16194   0.0715071
380.476   6.62979   -77.4307   1.16748   0.0720847
394.041   6.5699   -76.104   1.17384   0.0727412
408.108   6.50296   -74.644   1.18116   0.0734892
```

```
422.738   6.42819   -73.0488   1.18959   0.0743432
438.003   6.3448   -71.3204   1.1993   0.0753193
453.984   6.25203   -69.4652   1.21048   0.0764358
470.769   6.1492   -67.4943   1.22335   0.0777127
488.457   6.03578   -65.4236   1.2381   0.0791717
507.16   5.91143   -63.2736   1.25494   0.0808355
526.994   5.77613   -61.0688   1.27403   0.0827273
548.091   5.6302   -58.8366   1.2955   0.0848696
570.586   5.47443   -56.6061   1.31941   0.0872826
594.623   5.31008   -54.4066   1.34572   0.0899823
620.352   5.13888   -52.2666   1.37424   0.0929783
647.923   4.96303   -50.2122   1.40466   0.0962715
677.488   4.78504   -48.266   1.43651   0.0998516
709.193   4.60759   -46.4462   1.46917   0.103697
743.176   4.43332   -44.766   1.50193   0.107774
779.565   4.2646   -43.2331   1.53405   0.112039
818.475   4.10337   -41.85   1.56482   0.116443
860.004   3.95101   -40.6142   1.59366   0.120936
904.235   3.80829   -39.5189   1.62017   0.125471
951.232   3.67543   -38.5539   1.64413   0.130009
1001.05   3.55215   -37.7071   1.66555   0.134524
1053.71   3.43784   -36.9649   1.68461   0.139
1109.25   3.33172   -36.3135   1.70158   0.14343
1167.69   3.23289   -35.7397   1.71682   0.147816
1229.03   3.14053   -35.2316   1.73064   0.152165
1293.27   3.05393   -34.7792   1.74331   0.156482
1360.41   2.97259   -34.3743   1.75494   0.160765
1430.45   2.89626   -34.0116   1.7655   0.165004
1503.39   2.82495   -33.6885   1.77472   0.169171
1579.22   2.75902   -33.4056   1.78206   0.173217
1621.36   2.72586   -33.2708   1.78497   0.175326
1622.15   2.72527   -33.2684   1.78502   0.175364   -1
start 1
stop -1
rfqout 1
elimit 0.25 0.25
input -6 -100000 1.7008 12.7828 .011622 1.7008 12.7828 .011622
   180.0 0.0  0.0
 0.0 0.0 0.0 0.0 0.0 0.0 1. 2.01 140. 0.100
output 2 -1 2 0 1 1 1 2000 1
scheff 140.0 0.029 -0.04425 20 40  20  1  4
optcon  120000   4 1.1 1.4 .1    3  8. 10. 1.    0 0 0 0
0 0 0 0   0 0 0 0    0 0 0 0
begin
end
```

CDR RFQ Cell Table

nc	v	ws	beta	ez	capa	phi	a	m	b	cl	tl
0	0.111	0.1000	0.0103	0.000	0.00000	-90.0	13.192	1.000	0.010	0.000	0.00
1	0.111	0.1000	0.0103	0.000	0.00000	-90.0	1.266	1.000	1.085	0.885	0.89
2	0.111	0.1000	0.0103	0.000	0.00000	-90.0	0.898	1.000	2.160	0.885	1.77
3	0.111	0.1000	0.0103	0.000	0.00000	-90.0	0.733	1.000	3.235	0.885	2.66
4	0.111	0.1000	0.0103	0.000	0.00000	-90.0	0.635	1.000	4.310	0.885	3.54
5	0.111	0.1000	0.0103	0.000	0.00000	-90.0	0.633	1.000	4.325	0.885	4.43
6	0.110	0.1000	0.0103	0.000	0.00000	-90.0	0.630	1.000	4.346	0.885	5.31
7	0.110	0.1000	0.0103	0.000	0.00000	-90.0	0.627	1.000	4.366	0.885	6.20
8	0.109	0.1000	0.0103	0.000	0.00000	-90.0	0.624	1.000	4.386	0.885	7.08
9	0.109	0.1000	0.0103	0.000	0.00000	-90.0	0.621	1.000	4.407	0.885	7.97
10	0.108	0.1000	0.0103	0.000	0.00000	-90.0	0.618	1.000	4.427	0.885	8.85
11	0.108	0.1000	0.0103	0.000	0.00000	-90.0	0.615	1.000	4.448	0.885	9.74
12	0.107	0.1000	0.0103	0.000	0.00000	-90.0	0.613	1.000	4.468	0.885	10.62
13	0.107	0.1000	0.0103	0.003	0.00029	-90.0	0.610	1.001	4.488	0.885	11.51
14	0.106	0.1000	0.0103	0.003	0.00029	-90.0	0.607	1.001	4.509	0.885	12.39
15	0.105	0.1000	0.0103	0.003	0.00029	-90.0	0.604	1.001	4.531	0.885	13.28
16	0.105	0.1000	0.0103	0.004	0.00030	-90.0	0.601	1.001	4.554	0.885	14.16
17	0.104	0.1000	0.0103	0.004	0.00030	-90.0	0.598	1.001	4.577	0.885	15.05
18	0.104	0.1000	0.0103	0.004	0.00030	-90.0	0.595	1.001	4.599	0.885	15.93
19	0.103	0.1000	0.0103	0.007	0.00061	-90.0	0.592	1.002	4.622	0.885	16.82
20	0.103	0.1000	0.0103	0.007	0.00062	-90.0	0.589	1.002	4.644	0.885	17.70

21	0.102	0.1000	0.0103	0.007	0.00062	-90.0	0.586	1.002	4.667	0.885	18.59
22	0.102	0.1000	0.0103	0.007	0.00063	-90.0	0.583	1.002	4.690	0.885	19.48
23	0.101	0.1000	0.0103	0.007	0.00063	-90.0	0.580	1.002	4.712	0.885	20.36
24	0.101	0.1000	0.0103	0.011	0.00096	-90.0	0.577	1.003	4.735	0.885	21.25
25	0.100	0.1000	0.0103	0.011	0.00096	-90.0	0.575	1.003	4.758	0.885	22.13
26	0.100	0.1000	0.0103	0.011	0.00097	-90.0	0.572	1.003	4.780	0.885	23.02
27	0.100	0.1000	0.0103	0.015	0.00131	-90.0	0.569	1.004	4.803	0.885	23.90
28	0.099	0.1000	0.0103	0.015	0.00132	-90.0	0.566	1.004	4.826	0.885	24.79
29	0.099	0.1000	0.0103	0.015	0.00133	-90.0	0.564	1.004	4.848	0.885	25.67
30	0.098	0.1000	0.0103	0.015	0.00134	-90.0	0.561	1.004	4.871	0.885	26.56
31	0.098	0.1000	0.0103	0.019	0.00169	-90.0	0.558	1.005	4.893	0.885	27.44
32	0.097	0.1000	0.0103	0.019	0.00170	-90.0	0.555	1.005	4.916	0.885	28.33
33	0.097	0.1000	0.0103	0.019	0.00172	-90.0	0.553	1.005	4.939	0.885	29.21
34	0.096	0.1000	0.0103	0.023	0.00207	-90.0	0.550	1.006	4.961	0.885	30.10
35	0.096	0.1000	0.0103	0.023	0.00209	-90.0	0.548	1.006	4.984	0.885	30.98
36	0.095	0.1000	0.0103	0.026	0.00245	-90.0	0.545	1.007	5.007	0.885	31.87
37	0.095	0.1000	0.0103	0.027	0.00248	-90.0	0.542	1.007	5.029	0.885	32.75
38	0.095	0.1000	0.0103	0.031	0.00284	-90.0	0.540	1.008	5.052	0.885	33.64
39	0.094	0.1000	0.0103	0.031	0.00287	-90.0	0.537	1.008	5.074	0.885	34.52
40	0.094	0.1000	0.0103	0.031	0.00289	-90.0	0.535	1.008	5.097	0.885	35.41
41	0.093	0.1000	0.0103	0.034	0.00327	-90.0	0.532	1.009	5.120	0.885	36.29
42	0.093	0.1001	0.0103	0.035	0.00329	-90.0	0.530	1.009	5.142	0.886	37.18
43	0.093	0.1001	0.0103	0.039	0.00369	-90.0	0.527	1.010	5.165	0.886	38.07
44	0.092	0.1001	0.0103	0.039	0.00371	-90.0	0.525	1.010	5.188	0.886	38.95
45	0.092	0.1001	0.0103	0.043	0.00410	-90.0	0.523	1.011	5.210	0.886	39.84
46	0.091	0.1001	0.0103	0.043	0.00413	-90.0	0.520	1.011	5.233	0.886	40.72
47	0.091	0.1001	0.0103	0.047	0.00453	-90.0	0.518	1.012	5.256	0.886	41.61
48	0.091	0.1001	0.0103	0.051	0.00494	-90.0	0.515	1.013	5.278	0.886	42.49
49	0.090	0.1001	0.0103	0.051	0.00497	-90.0	0.513	1.013	5.301	0.886	43.38
50	0.090	0.1001	0.0103	0.055	0.00538	-90.0	0.511	1.014	5.323	0.886	44.26
51	0.089	0.1001	0.0103	0.055	0.00543	-90.0	0.508	1.014	5.346	0.886	45.15
52	0.089	0.1001	0.0103	0.059	0.00584	-90.0	0.506	1.015	5.369	0.886	46.03
53	0.089	0.1001	0.0103	0.059	0.00587	-90.0	0.504	1.015	5.391	0.886	46.92
54	0.088	0.1001	0.0103	0.063	0.00629	-90.0	0.502	1.016	5.414	0.886	47.80
55	0.088	0.1001	0.0103	0.067	0.00673	-90.0	0.499	1.017	5.437	0.886	48.69
56	0.088	0.1001	0.0103	0.068	0.00677	-90.0	0.497	1.017	5.459	0.886	49.57
57	0.087	0.1001	0.0103	0.071	0.00720	-90.0	0.495	1.018	5.482	0.886	50.46
58	0.087	0.1001	0.0103	0.075	0.00763	-90.0	0.493	1.019	5.505	0.886	51.34
59	0.087	0.1001	0.0103	0.076	0.00767	-90.0	0.491	1.019	5.527	0.886	52.23
60	0.086	0.1001	0.0103	0.079	0.00813	-90.0	0.488	1.020	5.550	0.886	53.11
61	0.086	0.1001	0.0103	0.084	0.00858	-90.0	0.486	1.021	5.572	0.886	54.00
62	0.085	0.1001	0.0103	0.087	0.00903	-90.0	0.484	1.022	5.595	0.886	54.88
63	0.085	0.1001	0.0103	0.087	0.00908	-90.0	0.482	1.022	5.618	0.886	55.77
64	0.085	0.1001	0.0103	0.092	0.00954	-90.0	0.480	1.023	5.640	0.886	56.66
65	0.084	0.1001	0.0103	0.095	0.01000	-90.0	0.478	1.024	5.663	0.886	57.54
66	0.084	0.1001	0.0103	0.100	0.01046	-90.0	0.476	1.025	5.686	0.886	58.43
67	0.084	0.1001	0.0103	0.104	0.01093	-90.0	0.474	1.026	5.708	0.886	59.31
68	0.083	0.1001	0.0103	0.103	0.01099	-90.0	0.472	1.026	5.731	0.886	60.20
69	0.083	0.1002	0.0103	0.108	0.01150	-90.0	0.469	1.027	5.753	0.886	61.08
70	0.083	0.1002	0.0103	0.113	0.01198	-90.0	0.467	1.028	5.776	0.886	61.97
71	0.082	0.1002	0.0103	0.116	0.01246	-90.0	0.465	1.029	5.799	0.886	62.85
72	0.082	0.1002	0.0103	0.120	0.01295	-90.0	0.463	1.030	5.821	0.886	63.74
73	0.082	0.1002	0.0103	0.125	0.01345	-90.0	0.461	1.031	5.844	0.886	64.62
74	0.081	0.1002	0.0103	0.124	0.01352	-90.0	0.459	1.031	5.867	0.886	65.51
75	0.081	0.1002	0.0103	0.129	0.01402	-90.0	0.457	1.032	5.889	0.886	66.39
76	0.081	0.1002	0.0103	0.133	0.01453	-90.0	0.455	1.033	5.912	0.886	67.28
77	0.081	0.1002	0.0103	0.138	0.01499	-90.0	0.454	1.034	5.935	0.886	68.16
78	0.080	0.1002	0.0103	0.141	0.01550	-90.0	0.452	1.035	5.957	0.886	69.05
79	0.080	0.1002	0.0103	0.145	0.01602	-89.9	0.450	1.036	5.980	0.886	69.93
80	0.080	0.1002	0.0103	0.150	0.01654	-89.9	0.448	1.037	6.002	0.886	70.82
81	0.079	0.1002	0.0103	0.153	0.01707	-89.9	0.446	1.038	6.025	0.886	71.70
82	0.079	0.1002	0.0103	0.158	0.01759	-89.9	0.444	1.039	6.048	0.886	72.59
83	0.079	0.1002	0.0103	0.162	0.01813	-89.9	0.442	1.040	6.070	0.886	73.48
84	0.078	0.1002	0.0103	0.165	0.01867	-89.9	0.440	1.041	6.093	0.886	74.36
85	0.078	0.1003	0.0103	0.170	0.01921	-89.8	0.438	1.042	6.116	0.887	75.25
86	0.078	0.1003	0.0103	0.178	0.02016	-89.8	0.437	1.044	6.138	0.887	76.13
87	0.078	0.1003	0.0103	0.183	0.02072	-89.8	0.435	1.045	6.161	0.887	77.02
88	0.077	0.1003	0.0103	0.186	0.02127	-89.7	0.433	1.046	6.184	0.887	77.90
89	0.077	0.1003	0.0104	0.189	0.02184	-89.7	0.431	1.047	6.206	0.887	78.79
90	0.077	0.1003	0.0104	0.194	0.02240	-89.6	0.429	1.048	6.229	0.887	79.67
91	0.076	0.1003	0.0104	0.196	0.02297	-89.6	0.427	1.049	6.251	0.887	80.56

92	0.076	0.1004	0.0104	0.200	0.02348	-89.6	0.426	1.050	6.274	0.887	81.45
93	0.076	0.1004	0.0104	0.209	0.02451	-89.5	0.424	1.052	6.297	0.887	82.33
94	0.076	0.1004	0.0104	0.214	0.02509	-89.5	0.422	1.053	6.319	0.887	83.22
95	0.075	0.1004	0.0104	0.216	0.02568	-89.5	0.420	1.054	6.342	0.887	84.10
96	0.075	0.1004	0.0104	0.221	0.02620	-89.4	0.419	1.055	6.365	0.887	84.99
97	0.075	0.1005	0.0104	0.229	0.02725	-89.4	0.417	1.057	6.387	0.887	85.88
98	0.075	0.1005	0.0104	0.235	0.02786	-89.3	0.415	1.058	6.410	0.887	86.76
99	0.074	0.1005	0.0104	0.236	0.02846	-89.3	0.413	1.059	6.433	0.887	87.65
100	0.074	0.1006	0.0104	0.245	0.02945	-89.3	0.412	1.061	6.455	0.888	88.53
101	0.074	0.1006	0.0104	0.250	0.03011	-89.2	0.410	1.062	6.478	0.888	89.42
102	0.074	0.1006	0.0104	0.255	0.03073	-89.2	0.408	1.063	6.501	0.888	90.31
103	0.073	0.1007	0.0104	0.260	0.03173	-89.1	0.407	1.065	6.523	0.888	91.19
104	0.073	0.1007	0.0104	0.265	0.03237	-89.1	0.405	1.066	6.546	0.888	92.08
105	0.073	0.1008	0.0104	0.274	0.03347	-89.1	0.403	1.068	6.569	0.889	92.97
106	0.073	0.1008	0.0104	0.279	0.03402	-89.0	0.402	1.069	6.591	0.889	93.86
107	0.072	0.1009	0.0104	0.284	0.03513	-89.0	0.400	1.071	6.614	0.889	94.74
108	0.072	0.1009	0.0104	0.290	0.03583	-88.9	0.398	1.072	6.637	0.889	95.63
109	0.072	0.1010	0.0104	0.298	0.03685	-88.9	0.397	1.074	6.659	0.890	96.52
110	0.072	0.1010	0.0104	0.303	0.03752	-88.9	0.395	1.075	6.682	0.890	97.41
111	0.071	0.1011	0.0104	0.308	0.03866	-88.8	0.393	1.077	6.705	0.890	98.29
112	0.071	0.1012	0.0104	0.313	0.03928	-88.8	0.392	1.078	6.728	0.891	99.18
113	0.071	0.1012	0.0104	0.322	0.04043	-88.7	0.390	1.080	6.750	0.891	100.07
114	0.071	0.1013	0.0104	0.327	0.04101	-88.7	0.389	1.081	6.773	0.891	100.96
115	0.070	0.1014	0.0104	0.331	0.04217	-88.7	0.387	1.083	6.796	0.891	101.85
116	0.070	0.1014	0.0104	0.341	0.04339	-88.6	0.385	1.085	6.818	0.891	102.74
117	0.070	0.1015	0.0104	0.346	0.04398	-88.6	0.384	1.086	6.841	0.892	103.63
118	0.070	0.1016	0.0104	0.355	0.04516	-88.5	0.382	1.088	6.864	0.892	104.52
119	0.069	0.1017	0.0104	0.358	0.04628	-88.5	0.381	1.090	6.887	0.893	105.41
120	0.069	0.1018	0.0104	0.368	0.04747	-88.5	0.379	1.092	6.909	0.893	106.30
121	0.069	0.1019	0.0104	0.373	0.04821	-88.4	0.377	1.093	6.932	0.894	107.19
122	0.069	0.1020	0.0104	0.382	0.04934	-88.4	0.376	1.095	6.955	0.894	108.08
123	0.068	0.1021	0.0104	0.386	0.05056	-88.3	0.374	1.097	6.978	0.894	108.98
124	0.068	0.1022	0.0104	0.394	0.05165	-88.3	0.373	1.099	7.001	0.895	109.87
125	0.068	0.1023	0.0105	0.400	0.05294	-88.3	0.371	1.101	7.028	0.895	110.76
126	0.068	0.1024	0.0105	0.413	0.05465	-88.2	0.369	1.104	7.054	0.896	111.66
127	0.068	0.1025	0.0105	0.423	0.05596	-88.2	0.367	1.106	7.081	0.896	112.55
128	0.067	0.1027	0.0105	0.425	0.05707	-88.1	0.366	1.108	7.107	0.897	113.44
129	0.067	0.1028	0.0105	0.439	0.05887	-88.1	0.364	1.111	7.134	0.898	114.34
130	0.067	0.1029	0.0105	0.448	0.06014	-88.0	0.362	1.113	7.160	0.898	115.23
131	0.067	0.1031	0.0105	0.467	0.06275	-88.0	0.361	1.118	7.174	0.899	116.13
132	0.067	0.1032	0.0105	0.467	0.06275	-88.0	0.361	1.118	7.173	0.899	117.03
133	0.067	0.1034	0.0105	0.468	0.06282	-88.0	0.361	1.118	7.172	0.900	117.92
134	0.067	0.1035	0.0105	0.469	0.06289	-88.0	0.361	1.118	7.171	0.901	118.82
135	0.067	0.1036	0.0105	0.469	0.06289	-87.9	0.361	1.118	7.170	0.901	119.72
136	0.067	0.1038	0.0105	0.469	0.06296	-87.9	0.361	1.118	7.169	0.902	120.62
137	0.067	0.1039	0.0105	0.469	0.06296	-87.9	0.361	1.118	7.169	0.902	121.52
138	0.067	0.1041	0.0105	0.470	0.06303	-87.9	0.361	1.118	7.168	0.903	122.42
139	0.067	0.1042	0.0106	0.466	0.06309	-87.9	0.361	1.118	7.167	0.904	123.32
140	0.067	0.1044	0.0106	0.466	0.06309	-87.9	0.361	1.118	7.166	0.905	124.22
141	0.067	0.1045	0.0106	0.466	0.06316	-87.9	0.361	1.118	7.165	0.905	125.12
142	0.067	0.1047	0.0106	0.467	0.06323	-87.9	0.361	1.118	7.165	0.906	126.02
143	0.067	0.1048	0.0106	0.470	0.06371	-87.9	0.361	1.119	7.164	0.906	126.93
144	0.067	0.1050	0.0106	0.471	0.06377	-87.9	0.361	1.119	7.163	0.907	127.83
145	0.067	0.1051	0.0106	0.471	0.06377	-87.9	0.361	1.119	7.162	0.908	128.74
146	0.067	0.1052	0.0106	0.471	0.06384	-87.9	0.361	1.119	7.161	0.908	129.64
147	0.067	0.1054	0.0106	0.472	0.06391	-87.8	0.361	1.119	7.160	0.909	130.55
148	0.067	0.1055	0.0106	0.472	0.06391	-87.8	0.361	1.119	7.160	0.909	131.45
149	0.067	0.1057	0.0106	0.472	0.06398	-87.8	0.361	1.119	7.159	0.910	132.36
150	0.067	0.1059	0.0106	0.473	0.06404	-87.8	0.361	1.119	7.158	0.911	133.27
151	0.067	0.1060	0.0106	0.473	0.06404	-87.8	0.361	1.119	7.157	0.911	134.18
152	0.067	0.1062	0.0106	0.473	0.06411	-87.8	0.361	1.119	7.156	0.912	135.09
153	0.067	0.1063	0.0107	0.469	0.06418	-87.8	0.361	1.119	7.155	0.913	135.99
154	0.067	0.1065	0.0107	0.469	0.06418	-87.8	0.361	1.119	7.155	0.914	136.91
155	0.067	0.1066	0.0107	0.470	0.06424	-87.8	0.361	1.119	7.154	0.914	137.82
156	0.067	0.1068	0.0107	0.470	0.06431	-87.8	0.361	1.119	7.153	0.915	138.73
157	0.067	0.1069	0.0107	0.470	0.06431	-87.7	0.361	1.119	7.152	0.915	139.64
158	0.067	0.1071	0.0107	0.474	0.06486	-87.7	0.361	1.120	7.151	0.916	140.55
159	0.067	0.1073	0.0107	0.475	0.06493	-87.7	0.361	1.120	7.150	0.917	141.47
160	0.067	0.1074	0.0107	0.475	0.06493	-87.7	0.361	1.120	7.149	0.917	142.38
161	0.067	0.1076	0.0107	0.474	0.06482	-87.7	0.362	1.120	7.148	0.918	143.30
162	0.067	0.1078	0.0107	0.474	0.06489	-87.7	0.362	1.120	7.148	0.919	144.21

163	0.067	0.1079	0.0107	0.475	0.06496	-87.7	0.362	1.120	7.147	0.920	145.13
164	0.067	0.1081	0.0107	0.475	0.06496	-87.7	0.362	1.120	7.146	0.920	146.05
165	0.067	0.1082	0.0108	0.471	0.06503	-87.7	0.362	1.120	7.145	0.921	146.96
166	0.067	0.1084	0.0108	0.471	0.06509	-87.7	0.362	1.120	7.144	0.922	147.88
167	0.067	0.1086	0.0108	0.471	0.06509	-87.6	0.362	1.120	7.143	0.923	148.80
168	0.067	0.1088	0.0108	0.472	0.06516	-87.6	0.362	1.120	7.142	0.923	149.72
169	0.067	0.1089	0.0108	0.472	0.06522	-87.6	0.362	1.120	7.141	0.924	150.64
170	0.067	0.1091	0.0108	0.473	0.06529	-87.6	0.362	1.120	7.140	0.925	151.56
171	0.067	0.1093	0.0108	0.473	0.06529	-87.6	0.362	1.120	7.139	0.925	152.49
172	0.067	0.1094	0.0108	0.477	0.06584	-87.6	0.362	1.121	7.138	0.926	153.41
173	0.067	0.1096	0.0108	0.477	0.06591	-87.6	0.362	1.121	7.137	0.927	154.33
174	0.067	0.1098	0.0108	0.477	0.06591	-87.6	0.362	1.121	7.136	0.928	155.26
175	0.067	0.1100	0.0108	0.478	0.06597	-87.5	0.362	1.121	7.136	0.928	156.18
176	0.067	0.1101	0.0108	0.478	0.06604	-87.5	0.362	1.121	7.135	0.929	157.11
177	0.067	0.1103	0.0109	0.474	0.06610	-87.5	0.362	1.121	7.134	0.930	158.04
178	0.067	0.1105	0.0109	0.474	0.06610	-87.5	0.362	1.121	7.133	0.931	158.96
179	0.067	0.1107	0.0109	0.475	0.06617	-87.5	0.362	1.121	7.132	0.931	159.89
180	0.067	0.1109	0.0109	0.475	0.06623	-87.5	0.362	1.121	7.131	0.932	160.82
181	0.067	0.1110	0.0109	0.476	0.06630	-87.5	0.362	1.121	7.130	0.933	161.75
182	0.067	0.1112	0.0109	0.476	0.06630	-87.5	0.362	1.121	7.129	0.933	162.68
183	0.067	0.1114	0.0109	0.476	0.06636	-87.4	0.362	1.121	7.128	0.934	163.61
184	0.067	0.1116	0.0109	0.477	0.06643	-87.4	0.362	1.121	7.127	0.935	164.54
185	0.067	0.1118	0.0109	0.481	0.06698	-87.4	0.362	1.122	7.126	0.936	165.48
186	0.067	0.1120	0.0109	0.481	0.06705	-87.4	0.362	1.122	7.125	0.937	166.41
187	0.067	0.1122	0.0109	0.481	0.06705	-87.4	0.362	1.122	7.124	0.938	167.34
188	0.067	0.1124	0.0110	0.477	0.06711	-87.4	0.362	1.122	7.123	0.939	168.28
189	0.067	0.1125	0.0110	0.478	0.06718	-87.4	0.362	1.122	7.122	0.939	169.22
190	0.067	0.1127	0.0110	0.477	0.06707	-87.4	0.363	1.122	7.121	0.940	170.15
191	0.067	0.1129	0.0110	0.477	0.06714	-87.3	0.363	1.122	7.120	0.941	171.09
192	0.067	0.1131	0.0110	0.477	0.06714	-87.3	0.363	1.122	7.119	0.941	172.03
193	0.067	0.1133	0.0110	0.478	0.06720	-87.3	0.363	1.122	7.118	0.942	172.97
194	0.067	0.1135	0.0110	0.478	0.06727	-87.3	0.363	1.122	7.116	0.943	173.91
195	0.067	0.1137	0.0110	0.479	0.06733	-87.3	0.363	1.122	7.115	0.944	174.85
196	0.067	0.1139	0.0110	0.479	0.06740	-87.3	0.363	1.122	7.114	0.945	175.79
197	0.067	0.1141	0.0110	0.483	0.06795	-87.3	0.363	1.123	7.113	0.946	176.73
198	0.067	0.1143	0.0111	0.479	0.06795	-87.2	0.363	1.123	7.112	0.946	177.68
199	0.067	0.1145	0.0111	0.479	0.06802	-87.2	0.363	1.123	7.111	0.947	178.62
200	0.067	0.1147	0.0111	0.480	0.06808	-87.2	0.363	1.123	7.110	0.948	179.57
201	0.067	0.1150	0.0111	0.480	0.06815	-87.2	0.363	1.123	7.109	0.949	180.51
202	0.067	0.1152	0.0111	0.481	0.06821	-87.2	0.363	1.123	7.108	0.950	181.46
203	0.067	0.1154	0.0111	0.481	0.06827	-87.2	0.363	1.123	7.107	0.951	182.41
204	0.067	0.1156	0.0111	0.482	0.06834	-87.1	0.363	1.123	7.106	0.952	183.35
205	0.067	0.1158	0.0111	0.482	0.06834	-87.1	0.363	1.123	7.105	0.953	184.30
206	0.067	0.1160	0.0111	0.482	0.06840	-87.1	0.363	1.123	7.103	0.953	185.25
207	0.067	0.1162	0.0111	0.482	0.06846	-87.1	0.363	1.123	7.102	0.954	186.21
208	0.067	0.1164	0.0112	0.482	0.06903	-87.1	0.363	1.124	7.101	0.955	187.16
209	0.067	0.1167	0.0112	0.483	0.06909	-87.1	0.363	1.124	7.100	0.956	188.11
210	0.067	0.1169	0.0112	0.483	0.06915	-87.1	0.363	1.124	7.099	0.957	189.06
211	0.067	0.1171	0.0112	0.483	0.06922	-87.0	0.363	1.124	7.098	0.958	190.02
212	0.067	0.1173	0.0112	0.484	0.06928	-87.0	0.363	1.124	7.096	0.959	190.97
213	0.067	0.1176	0.0112	0.484	0.06934	-87.0	0.363	1.124	7.095	0.960	191.93
214	0.067	0.1178	0.0112	0.485	0.06941	-87.0	0.363	1.124	7.094	0.961	192.89
215	0.067	0.1180	0.0112	0.484	0.06924	-87.0	0.364	1.124	7.093	0.962	193.85
216	0.067	0.1183	0.0112	0.484	0.06930	-86.9	0.364	1.124	7.092	0.963	194.81
217	0.067	0.1185	0.0112	0.484	0.06937	-86.9	0.364	1.124	7.090	0.964	195.77
218	0.067	0.1187	0.0113	0.484	0.06993	-86.9	0.364	1.125	7.089	0.964	196.73
219	0.067	0.1190	0.0113	0.484	0.06999	-86.9	0.364	1.125	7.088	0.966	197.69
220	0.067	0.1192	0.0113	0.485	0.07006	-86.9	0.364	1.125	7.087	0.966	198.65
221	0.067	0.1194	0.0113	0.485	0.07012	-86.9	0.364	1.125	7.086	0.967	199.62
222	0.067	0.1197	0.0113	0.486	0.07018	-86.8	0.364	1.125	7.084	0.969	200.58
223	0.067	0.1199	0.0113	0.486	0.07024	-86.8	0.364	1.125	7.083	0.969	201.55
224	0.067	0.1202	0.0113	0.487	0.07031	-86.8	0.364	1.125	7.082	0.971	202.52
225	0.067	0.1204	0.0113	0.487	0.07037	-86.8	0.364	1.125	7.081	0.971	203.48
226	0.068	0.1207	0.0114	0.490	0.07043	-86.8	0.364	1.125	7.079	0.973	204.45
227	0.068	0.1209	0.0114	0.491	0.07050	-86.7	0.364	1.125	7.078	0.973	205.42
228	0.068	0.1212	0.0114	0.495	0.07106	-86.7	0.364	1.126	7.077	0.975	206.40
229	0.068	0.1214	0.0114	0.495	0.07112	-86.7	0.364	1.126	7.075	0.975	207.37
230	0.068	0.1217	0.0114	0.496	0.07119	-86.7	0.364	1.126	7.074	0.977	208.34
231	0.068	0.1219	0.0114	0.496	0.07125	-86.7	0.364	1.126	7.073	0.977	209.31
232	0.068	0.1222	0.0114	0.497	0.07131	-86.6	0.364	1.126	7.071	0.979	210.29
233	0.068	0.1225	0.0114	0.497	0.07137	-86.6	0.364	1.126	7.070	0.980	211.27

234	0.068	0.1227	0.0114	0.497	0.07144	-86.6	0.364	1.126	7.069	0.981	212.24
235	0.068	0.1230	0.0115	0.494	0.07150	-86.6	0.364	1.126	7.067	0.982	213.22
236	0.068	0.1233	0.0115	0.493	0.07146	-86.5	0.365	1.126	7.066	0.983	214.20
237	0.068	0.1235	0.0115	0.497	0.07202	-86.5	0.365	1.127	7.065	0.984	215.18
238	0.068	0.1238	0.0115	0.498	0.07209	-86.5	0.365	1.127	7.063	0.985	216.16
239	0.068	0.1241	0.0115	0.498	0.07215	-86.5	0.365	1.127	7.062	0.986	217.15
240	0.068	0.1244	0.0115	0.498	0.07221	-86.5	0.365	1.127	7.060	0.987	218.13
241	0.068	0.1246	0.0115	0.499	0.07227	-86.4	0.365	1.127	7.059	0.988	219.12
242	0.068	0.1249	0.0116	0.495	0.07233	-86.4	0.365	1.127	7.057	0.989	220.10
243	0.068	0.1252	0.0116	0.495	0.07240	-86.4	0.365	1.127	7.056	0.991	221.09
244	0.068	0.1255	0.0116	0.496	0.07246	-86.4	0.365	1.127	7.055	0.992	222.08
245	0.068	0.1258	0.0116	0.500	0.07309	-86.3	0.365	1.128	7.053	0.993	223.07
246	0.068	0.1261	0.0116	0.501	0.07315	-86.3	0.365	1.128	7.052	0.994	224.06
247	0.068	0.1264	0.0116	0.501	0.07321	-86.3	0.365	1.128	7.050	0.995	225.05
248	0.068	0.1267	0.0116	0.501	0.07327	-86.3	0.365	1.128	7.049	0.996	226.04
249	0.068	0.1270	0.0116	0.502	0.07334	-86.2	0.365	1.128	7.047	0.998	227.04
250	0.068	0.1273	0.0117	0.498	0.07340	-86.2	0.365	1.128	7.046	0.999	228.03
251	0.068	0.1276	0.0117	0.499	0.07352	-86.2	0.365	1.128	7.044	1.000	229.03
252	0.068	0.1279	0.0117	0.499	0.07358	-86.2	0.365	1.128	7.043	1.001	230.03
253	0.068	0.1282	0.0117	0.503	0.07415	-86.1	0.365	1.129	7.041	1.002	231.03
254	0.068	0.1285	0.0117	0.504	0.07421	-86.1	0.365	1.129	7.040	1.003	232.03
255	0.068	0.1288	0.0117	0.503	0.07411	-86.1	0.366	1.129	7.038	1.005	233.03
256	0.068	0.1292	0.0117	0.504	0.07423	-86.1	0.366	1.129	7.036	1.006	234.03
257	0.068	0.1295	0.0118	0.500	0.07429	-86.0	0.366	1.129	7.035	1.007	235.03
258	0.068	0.1298	0.0118	0.500	0.07435	-86.0	0.366	1.129	7.033	1.009	236.04
259	0.068	0.1301	0.0118	0.501	0.07441	-86.0	0.366	1.129	7.032	1.010	237.05
260	0.068	0.1305	0.0118	0.505	0.07505	-85.9	0.366	1.130	7.030	1.011	238.05
261	0.068	0.1308	0.0118	0.505	0.07511	-85.9	0.366	1.130	7.028	1.012	239.06
262	0.068	0.1311	0.0118	0.506	0.07517	-85.9	0.366	1.130	7.027	1.014	240.07
263	0.068	0.1315	0.0118	0.507	0.07529	-85.9	0.366	1.130	7.025	1.015	241.08
264	0.068	0.1318	0.0119	0.503	0.07535	-85.8	0.366	1.130	7.023	1.016	242.10
265	0.068	0.1322	0.0119	0.503	0.07541	-85.8	0.366	1.130	7.022	1.018	243.11
266	0.068	0.1325	0.0119	0.504	0.07553	-85.8	0.366	1.130	7.020	1.019	244.13
267	0.068	0.1329	0.0119	0.508	0.07611	-85.7	0.366	1.131	7.018	1.021	245.14
268	0.068	0.1332	0.0119	0.508	0.07617	-85.7	0.366	1.131	7.016	1.022	246.16
269	0.068	0.1336	0.0119	0.509	0.07629	-85.7	0.366	1.131	7.015	1.023	247.18
270	0.068	0.1339	0.0120	0.505	0.07635	-85.6	0.366	1.131	7.013	1.024	248.20
271	0.068	0.1343	0.0120	0.504	0.07624	-85.6	0.367	1.131	7.011	1.026	249.22
272	0.068	0.1347	0.0120	0.505	0.07636	-85.6	0.367	1.131	7.009	1.027	250.25
273	0.068	0.1350	0.0120	0.506	0.07642	-85.5	0.367	1.131	7.008	1.029	251.27
274	0.068	0.1354	0.0120	0.510	0.07706	-85.5	0.367	1.132	7.006	1.030	252.30
275	0.068	0.1358	0.0120	0.510	0.07712	-85.5	0.367	1.132	7.004	1.032	253.33
276	0.068	0.1362	0.0121	0.507	0.07724	-85.4	0.367	1.132	7.002	1.033	254.36
277	0.068	0.1366	0.0121	0.507	0.07730	-85.4	0.367	1.132	7.000	1.035	255.39
278	0.068	0.1370	0.0121	0.508	0.07736	-85.4	0.367	1.132	6.998	1.036	256.42
279	0.068	0.1373	0.0121	0.508	0.07748	-85.3	0.367	1.132	6.996	1.037	257.46
280	0.068	0.1377	0.0121	0.512	0.07806	-85.3	0.367	1.133	6.994	1.039	258.49
281	0.068	0.1381	0.0121	0.513	0.07818	-85.3	0.367	1.133	6.993	1.040	259.53
282	0.068	0.1386	0.0122	0.509	0.07824	-85.2	0.367	1.133	6.991	1.042	260.57
283	0.068	0.1390	0.0122	0.510	0.07836	-85.2	0.367	1.133	6.989	1.044	261.61
284	0.068	0.1394	0.0122	0.511	0.07847	-85.1	0.367	1.133	6.987	1.045	262.65
285	0.068	0.1398	0.0122	0.511	0.07853	-85.1	0.367	1.133	6.985	1.047	263.69
286	0.068	0.1402	0.0122	0.514	0.07901	-85.1	0.368	1.134	6.983	1.048	264.74
287	0.068	0.1406	0.0123	0.510	0.07907	-85.0	0.368	1.134	6.981	1.050	265.78
288	0.068	0.1411	0.0123	0.511	0.07918	-85.0	0.368	1.134	6.979	1.052	266.83
289	0.069	0.1415	0.0123	0.519	0.07930	-85.0	0.368	1.134	6.977	1.053	267.88
290	0.069	0.1420	0.0123	0.520	0.07936	-84.9	0.368	1.134	6.975	1.055	268.93
291	0.069	0.1424	0.0123	0.521	0.07947	-84.9	0.368	1.134	6.972	1.056	269.98
292	0.069	0.1428	0.0124	0.520	0.08006	-84.8	0.368	1.135	6.970	1.058	271.04
293	0.069	0.1433	0.0124	0.521	0.08018	-84.8	0.368	1.135	6.968	1.060	272.09
294	0.069	0.1438	0.0124	0.522	0.08029	-84.7	0.368	1.135	6.966	1.062	273.15
295	0.069	0.1442	0.0124	0.522	0.08035	-84.7	0.368	1.135	6.964	1.063	274.21
296	0.069	0.1447	0.0124	0.523	0.08047	-84.7	0.368	1.135	6.962	1.065	275.27
297	0.069	0.1452	0.0125	0.523	0.08111	-84.6	0.368	1.136	6.960	1.067	276.34
298	0.069	0.1456	0.0125	0.523	0.08123	-84.6	0.368	1.136	6.957	1.068	277.40
299	0.069	0.1461	0.0125	0.523	0.08112	-84.5	0.369	1.136	6.955	1.070	278.47
300	0.069	0.1466	0.0125	0.524	0.08123	-84.5	0.369	1.136	6.953	1.072	279.53
301	0.069	0.1471	0.0125	0.524	0.08135	-84.4	0.369	1.136	6.950	1.074	280.60
302	0.069	0.1476	0.0126	0.524	0.08200	-84.4	0.369	1.137	6.948	1.075	281.68
303	0.069	0.1481	0.0126	0.525	0.08211	-84.3	0.369	1.137	6.946	1.077	282.75
304	0.069	0.1486	0.0126	0.526	0.08222	-84.3	0.369	1.137	6.943	1.079	283.83

305	0.069	0.1491	0.0126	0.526	0.08228	-84.3	0.369	1.137	6.941	1.081	284.90
306	0.069	0.1497	0.0126	0.527	0.08240	-84.2	0.369	1.137	6.939	1.083	285.98
307	0.069	0.1502	0.0127	0.527	0.08304	-84.2	0.369	1.138	6.936	1.085	287.06
308	0.069	0.1507	0.0127	0.527	0.08316	-84.1	0.369	1.138	6.934	1.087	288.15
309	0.069	0.1513	0.0127	0.528	0.08327	-84.1	0.369	1.138	6.931	1.089	289.23
310	0.069	0.1518	0.0127	0.528	0.08322	-84.0	0.370	1.138	6.929	1.091	290.32
311	0.069	0.1523	0.0128	0.528	0.08387	-84.0	0.370	1.139	6.926	1.092	291.41
312	0.069	0.1529	0.0128	0.529	0.08398	-83.9	0.370	1.139	6.924	1.095	292.50
313	0.069	0.1535	0.0128	0.529	0.08409	-83.8	0.370	1.139	6.921	1.097	293.59
314	0.069	0.1540	0.0128	0.530	0.08420	-83.8	0.370	1.139	6.919	1.099	294.69
315	0.069	0.1546	0.0129	0.530	0.08485	-83.7	0.370	1.140	6.916	1.101	295.78
316	0.069	0.1552	0.0129	0.531	0.08497	-83.7	0.370	1.140	6.914	1.103	296.88
317	0.069	0.1558	0.0129	0.531	0.08508	-83.6	0.370	1.140	6.911	1.105	297.98
318	0.069	0.1564	0.0129	0.532	0.08519	-83.6	0.370	1.140	6.908	1.107	299.09
319	0.069	0.1570	0.0129	0.533	0.08530	-83.5	0.370	1.140	6.906	1.109	300.19
320	0.069	0.1576	0.0130	0.532	0.08584	-83.5	0.371	1.141	6.903	1.111	301.30
321	0.069	0.1582	0.0130	0.533	0.08595	-83.4	0.371	1.141	6.900	1.113	302.41
322	0.069	0.1588	0.0130	0.533	0.08607	-83.3	0.371	1.141	6.897	1.116	303.52
323	0.069	0.1595	0.0131	0.533	0.08672	-83.3	0.371	1.142	6.894	1.118	304.64
324	0.069	0.1601	0.0131	0.534	0.08683	-83.2	0.371	1.142	6.891	1.120	305.75
325	0.069	0.1608	0.0131	0.535	0.08699	-83.2	0.371	1.142	6.889	1.123	306.87
326	0.069	0.1614	0.0131	0.536	0.08710	-83.1	0.371	1.142	6.886	1.125	307.99
327	0.069	0.1621	0.0132	0.536	0.08776	-83.0	0.371	1.143	6.883	1.127	309.11
328	0.069	0.1627	0.0132	0.536	0.08787	-83.0	0.371	1.143	6.880	1.129	310.24
329	0.069	0.1634	0.0132	0.537	0.08803	-82.9	0.371	1.143	6.877	1.132	311.37
330	0.070	0.1641	0.0132	0.545	0.08797	-82.9	0.372	1.143	6.874	1.134	312.50
331	0.070	0.1648	0.0133	0.545	0.08868	-82.8	0.372	1.144	6.871	1.136	313.63
332	0.070	0.1655	0.0133	0.546	0.08879	-82.7	0.372	1.144	6.868	1.139	314.76
333	0.070	0.1662	0.0133	0.546	0.08890	-82.7	0.372	1.144	6.865	1.141	315.90
334	0.070	0.1669	0.0134	0.547	0.08961	-82.6	0.372	1.145	6.862	1.144	317.04
335	0.070	0.1677	0.0134	0.547	0.08972	-82.5	0.372	1.145	6.858	1.146	318.18
336	0.070	0.1684	0.0134	0.548	0.08988	-82.4	0.372	1.145	6.855	1.149	319.33
337	0.070	0.1692	0.0134	0.549	0.08999	-82.4	0.372	1.145	6.852	1.151	320.48
338	0.070	0.1699	0.0135	0.548	0.09053	-82.3	0.373	1.146	6.849	1.154	321.63
339	0.070	0.1707	0.0135	0.549	0.09069	-82.2	0.373	1.146	6.846	1.157	322.78
340	0.070	0.1715	0.0135	0.550	0.09080	-82.2	0.373	1.146	6.842	1.159	323.93
341	0.070	0.1722	0.0136	0.550	0.09151	-82.1	0.373	1.147	6.839	1.162	325.09
342	0.070	0.1730	0.0136	0.551	0.09167	-82.0	0.373	1.147	6.835	1.164	326.25
343	0.070	0.1739	0.0136	0.551	0.09178	-81.9	0.373	1.147	6.832	1.167	327.42
344	0.070	0.1747	0.0137	0.552	0.09249	-81.9	0.373	1.148	6.828	1.170	328.58
345	0.070	0.1755	0.0137	0.553	0.09265	-81.8	0.373	1.148	6.825	1.173	329.75
346	0.070	0.1763	0.0137	0.552	0.09259	-81.7	0.374	1.148	6.822	1.175	330.92
347	0.070	0.1772	0.0138	0.553	0.09330	-81.6	0.374	1.149	6.818	1.178	332.10
348	0.070	0.1781	0.0138	0.553	0.09346	-81.6	0.374	1.149	6.815	1.181	333.27
349	0.070	0.1789	0.0138	0.554	0.09361	-81.5	0.374	1.149	6.811	1.184	334.45
350	0.070	0.1798	0.0139	0.555	0.09432	-81.4	0.374	1.150	6.807	1.187	335.64
351	0.070	0.1807	0.0139	0.555	0.09448	-81.3	0.374	1.150	6.803	1.190	336.82
352	0.070	0.1816	0.0139	0.556	0.09464	-81.2	0.374	1.150	6.799	1.193	338.01
353	0.070	0.1825	0.0140	0.556	0.09518	-81.1	0.375	1.151	6.796	1.196	339.20
354	0.070	0.1835	0.0140	0.557	0.09534	-81.1	0.375	1.151	6.792	1.199	340.40
355	0.070	0.1844	0.0140	0.561	0.09605	-81.0	0.375	1.152	6.788	1.202	341.60
356	0.070	0.1854	0.0141	0.558	0.09621	-80.9	0.375	1.152	6.784	1.205	342.80
357	0.070	0.1863	0.0141	0.558	0.09636	-80.8	0.375	1.152	6.780	1.208	344.00
358	0.071	0.1873	0.0141	0.571	0.09707	-80.7	0.375	1.153	6.776	1.211	345.21
359	0.071	0.1883	0.0142	0.568	0.09728	-80.6	0.375	1.153	6.772	1.215	346.42
360	0.071	0.1893	0.0142	0.568	0.09727	-80.5	0.376	1.153	6.768	1.218	347.63
361	0.071	0.1903	0.0143	0.568	0.09798	-80.4	0.376	1.154	6.764	1.221	348.85
362	0.071	0.1914	0.0143	0.569	0.09813	-80.3	0.376	1.154	6.760	1.225	350.07
363	0.071	0.1924	0.0143	0.573	0.09889	-80.2	0.376	1.155	6.755	1.228	351.29
364	0.071	0.1935	0.0144	0.570	0.09905	-80.1	0.376	1.155	6.751	1.231	352.52
365	0.071	0.1946	0.0144	0.575	0.09981	-80.0	0.376	1.156	6.747	1.235	353.75
366	0.071	0.1957	0.0145	0.571	0.09996	-80.0	0.376	1.156	6.742	1.238	354.99
367	0.071	0.1968	0.0145	0.572	0.10000	-79.9	0.377	1.156	6.738	1.242	356.22
368	0.071	0.1979	0.0145	0.576	0.10071	-79.8	0.377	1.157	6.734	1.245	357.47
369	0.071	0.1991	0.0146	0.573	0.10091	-79.7	0.377	1.157	6.729	1.249	358.71
370	0.071	0.2002	0.0146	0.577	0.10162	-79.6	0.377	1.158	6.725	1.252	359.96
371	0.071	0.2014	0.0147	0.574	0.10182	-79.4	0.377	1.158	6.720	1.256	361.21
372	0.071	0.2026	0.0147	0.578	0.10242	-79.3	0.378	1.159	6.715	1.260	362.47
373	0.071	0.2038	0.0148	0.574	0.10257	-79.2	0.378	1.159	6.710	1.264	363.73
374	0.071	0.2050	0.0148	0.579	0.10333	-79.1	0.378	1.160	6.706	1.267	364.99
375	0.071	0.2063	0.0148	0.580	0.10353	-79.0	0.378	1.160	6.701	1.271	366.26

376	0.071	0.2075	0.0149	0.580	0.10429	-78.9	0.378	1.161	6.696	1.275	367.53
377	0.071	0.2088	0.0149	0.581	0.10448	-78.8	0.378	1.161	6.691	1.279	368.80
378	0.071	0.2101	0.0150	0.581	0.10508	-78.7	0.379	1.162	6.686	1.283	370.08
379	0.072	0.2114	0.0150	0.590	0.10528	-78.6	0.379	1.162	6.681	1.287	371.36
380	0.072	0.2128	0.0151	0.590	0.10604	-78.5	0.379	1.163	6.676	1.291	372.65
381	0.072	0.2141	0.0151	0.591	0.10623	-78.4	0.379	1.163	6.671	1.295	373.94
382	0.072	0.2155	0.0152	0.592	0.10699	-78.2	0.379	1.164	6.666	1.299	375.24
383	0.072	0.2169	0.0152	0.592	0.10702	-78.1	0.380	1.164	6.660	1.304	376.53
384	0.072	0.2183	0.0153	0.592	0.10778	-78.0	0.380	1.165	6.655	1.308	377.84
385	0.072	0.2198	0.0153	0.593	0.10802	-77.9	0.380	1.165	6.650	1.312	379.15
386	0.072	0.2212	0.0154	0.594	0.10878	-77.8	0.380	1.166	6.644	1.317	380.46
387	0.072	0.2227	0.0154	0.598	0.10955	-77.6	0.380	1.167	6.639	1.321	381.77
388	0.072	0.2242	0.0155	0.594	0.10962	-77.5	0.381	1.167	6.634	1.325	383.10
389	0.072	0.2258	0.0155	0.599	0.11038	-77.4	0.381	1.168	6.628	1.330	384.42
390	0.072	0.2273	0.0156	0.596	0.11061	-77.3	0.381	1.168	6.622	1.335	385.75
391	0.072	0.2289	0.0156	0.600	0.11142	-77.1	0.381	1.169	6.616	1.339	387.09
392	0.072	0.2305	0.0157	0.600	0.11202	-77.0	0.382	1.170	6.610	1.344	388.42
393	0.072	0.2321	0.0157	0.601	0.11225	-76.9	0.382	1.170	6.604	1.349	389.77
394	0.072	0.2338	0.0158	0.601	0.11306	-76.7	0.382	1.171	6.598	1.354	391.12
395	0.072	0.2354	0.0159	0.599	0.11324	-76.6	0.382	1.171	6.592	1.358	392.47
396	0.073	0.2371	0.0159	0.611	0.11405	-76.5	0.382	1.172	6.586	1.363	393.83
397	0.073	0.2388	0.0160	0.611	0.11469	-76.3	0.383	1.173	6.580	1.368	395.19
398	0.073	0.2406	0.0160	0.612	0.11492	-76.2	0.383	1.173	6.574	1.373	396.56
399	0.073	0.2424	0.0161	0.613	0.11572	-76.1	0.383	1.174	6.568	1.378	397.93
400	0.073	0.2442	0.0161	0.617	0.11653	-75.9	0.383	1.175	6.562	1.383	399.31
401	0.073	0.2460	0.0162	0.614	0.11663	-75.8	0.384	1.175	6.555	1.388	400.70
402	0.073	0.2479	0.0163	0.614	0.11744	-75.6	0.384	1.176	6.548	1.394	402.08
403	0.073	0.2498	0.0163	0.618	0.11824	-75.5	0.384	1.177	6.542	1.399	403.48
404	0.073	0.2517	0.0164	0.619	0.11905	-75.3	0.384	1.178	6.535	1.404	404.88
405	0.073	0.2536	0.0165	0.615	0.11915	-75.2	0.385	1.178	6.528	1.410	406.28
406	0.073	0.2556	0.0165	0.620	0.11995	-75.1	0.385	1.179	6.522	1.415	407.69
407	0.073	0.2576	0.0166	0.620	0.12080	-74.9	0.385	1.180	6.515	1.421	409.11
408	0.073	0.2597	0.0167	0.621	0.12160	-74.8	0.385	1.181	6.508	1.426	410.53
409	0.074	0.2618	0.0167	0.630	0.12170	-74.6	0.386	1.181	6.501	1.432	411.96
410	0.074	0.2639	0.0168	0.630	0.12254	-74.5	0.386	1.182	6.494	1.438	413.39
411	0.074	0.2660	0.0169	0.631	0.12339	-74.3	0.386	1.183	6.487	1.444	414.83
412	0.074	0.2682	0.0169	0.634	0.12407	-74.1	0.387	1.184	6.479	1.450	416.27
413	0.074	0.2704	0.0170	0.635	0.12492	-74.0	0.387	1.185	6.472	1.456	417.72
414	0.074	0.2727	0.0171	0.635	0.12576	-73.8	0.387	1.186	6.464	1.462	419.18
415	0.074	0.2750	0.0171	0.637	0.12601	-73.7	0.387	1.186	6.457	1.468	420.64
416	0.074	0.2773	0.0172	0.636	0.12669	-73.5	0.388	1.187	6.449	1.474	422.11
417	0.074	0.2796	0.0173	0.637	0.12753	-73.3	0.388	1.188	6.442	1.480	423.59
418	0.074	0.2820	0.0174	0.637	0.12837	-73.2	0.388	1.189	6.434	1.486	425.07
419	0.074	0.2845	0.0174	0.641	0.12909	-73.0	0.389	1.190	6.427	1.493	426.56
420	0.074	0.2869	0.0175	0.641	0.12993	-72.8	0.389	1.191	6.418	1.499	428.05
421	0.075	0.2895	0.0176	0.651	0.13081	-72.7	0.389	1.192	6.410	1.506	429.55
422	0.075	0.2920	0.0177	0.650	0.13149	-72.5	0.390	1.193	6.402	1.513	431.06
423	0.075	0.2946	0.0177	0.655	0.13237	-72.3	0.390	1.194	6.394	1.519	432.57
424	0.075	0.2973	0.0178	0.655	0.13324	-72.2	0.390	1.195	6.385	1.526	434.09
425	0.075	0.3000	0.0179	0.655	0.13396	-72.0	0.391	1.196	6.377	1.533	435.62
426	0.075	0.3027	0.0180	0.656	0.13484	-71.8	0.391	1.197	6.369	1.540	437.16
427	0.075	0.3055	0.0181	0.654	0.13512	-71.6	0.391	1.197	6.360	1.547	438.70
428	0.075	0.3083	0.0181	0.658	0.13599	-71.5	0.391	1.198	6.352	1.554	440.25
429	0.075	0.3111	0.0182	0.658	0.13671	-71.3	0.392	1.199	6.343	1.561	441.80
430	0.075	0.3141	0.0183	0.661	0.13817	-71.1	0.392	1.201	6.334	1.569	443.37
431	0.076	0.3170	0.0184	0.670	0.13888	-70.9	0.393	1.202	6.325	1.576	444.94
432	0.076	0.3200	0.0185	0.670	0.13979	-70.7	0.393	1.203	6.316	1.583	446.51
433	0.076	0.3231	0.0186	0.671	0.14066	-70.6	0.393	1.204	6.307	1.591	448.10
434	0.076	0.3262	0.0187	0.671	0.14141	-70.4	0.394	1.205	6.297	1.599	449.69
435	0.076	0.3294	0.0188	0.672	0.14232	-70.2	0.394	1.206	6.288	1.607	451.29
436	0.076	0.3326	0.0188	0.676	0.14323	-70.0	0.394	1.207	6.279	1.614	452.90
437	0.076	0.3359	0.0189	0.676	0.14394	-69.8	0.395	1.208	6.269	1.622	454.52
438	0.076	0.3392	0.0190	0.679	0.14544	-69.6	0.395	1.210	6.260	1.630	456.14
439	0.076	0.3426	0.0191	0.679	0.14618	-69.4	0.396	1.211	6.250	1.638	457.77
440	0.077	0.3460	0.0192	0.689	0.14712	-69.2	0.396	1.212	6.240	1.646	459.42
441	0.077	0.3495	0.0193	0.689	0.14802	-69.0	0.396	1.213	6.230	1.655	461.06
442	0.077	0.3531	0.0194	0.689	0.14877	-68.9	0.397	1.214	6.220	1.663	462.72
443	0.077	0.3567	0.0195	0.693	0.15030	-68.7	0.397	1.216	6.210	1.672	464.39
444	0.077	0.3604	0.0196	0.693	0.15104	-68.5	0.398	1.217	6.200	1.680	466.06
445	0.077	0.3641	0.0197	0.694	0.15198	-68.3	0.398	1.218	6.189	1.689	467.74
446	0.077	0.3679	0.0198	0.697	0.15351	-68.1	0.398	1.220	6.179	1.698	469.44

447	0.077	0.3718	0.0199	0.697	0.15429	-67.9	0.399	1.221	6.169	1.707	471.14
448	0.078	0.3757	0.0200	0.707	0.15522	-67.7	0.399	1.222	6.158	1.716	472.85
449	0.078	0.3797	0.0201	0.709	0.15659	-67.5	0.400	1.224	6.148	1.725	474.56
450	0.078	0.3838	0.0202	0.710	0.15752	-67.3	0.400	1.225	6.136	1.734	476.29
451	0.078	0.3879	0.0204	0.707	0.15829	-67.1	0.401	1.226	6.125	1.743	478.03
452	0.078	0.3921	0.0205	0.710	0.15982	-66.9	0.401	1.228	6.114	1.753	479.78
453	0.078	0.3964	0.0206	0.711	0.16079	-66.6	0.401	1.229	6.103	1.762	481.53
454	0.078	0.4007	0.0207	0.713	0.16215	-66.4	0.402	1.231	6.092	1.772	483.30
455	0.079	0.4051	0.0208	0.723	0.16312	-66.2	0.402	1.232	6.080	1.782	485.07
456	0.079	0.4096	0.0209	0.726	0.16452	-66.0	0.403	1.234	6.069	1.791	486.86
457	0.079	0.4142	0.0210	0.727	0.16548	-65.8	0.403	1.235	6.057	1.801	488.65
458	0.079	0.4189	0.0211	0.729	0.16688	-65.6	0.404	1.237	6.046	1.812	490.46
459	0.079	0.4236	0.0213	0.727	0.16784	-65.4	0.404	1.238	6.034	1.822	492.27
460	0.079	0.4284	0.0214	0.729	0.16923	-65.2	0.405	1.240	6.022	1.832	494.10
461	0.080	0.4333	0.0215	0.742	0.17083	-65.0	0.405	1.242	6.010	1.842	495.93
462	0.080	0.4383	0.0216	0.742	0.17162	-64.8	0.406	1.243	5.997	1.853	497.78
463	0.080	0.4433	0.0218	0.742	0.17322	-64.5	0.406	1.245	5.985	1.864	499.64
464	0.080	0.4485	0.0219	0.745	0.17464	-64.3	0.407	1.247	5.973	1.874	501.50
465	0.080	0.4537	0.0220	0.745	0.17560	-64.1	0.407	1.248	5.960	1.885	503.38
466	0.080	0.4590	0.0221	0.748	0.17701	-63.9	0.408	1.250	5.947	1.896	505.27
467	0.081	0.4644	0.0223	0.757	0.17862	-63.7	0.408	1.252	5.935	1.907	507.17
468	0.081	0.4699	0.0224	0.757	0.17943	-63.5	0.409	1.253	5.922	1.919	509.08
469	0.081	0.4755	0.0225	0.761	0.18100	-63.2	0.409	1.255	5.909	1.930	511.01
470	0.081	0.4812	0.0227	0.760	0.18243	-63.0	0.410	1.257	5.896	1.942	512.94
471	0.081	0.4870	0.0228	0.762	0.18383	-62.8	0.411	1.259	5.883	1.953	514.89
472	0.081	0.4929	0.0229	0.766	0.18542	-62.6	0.411	1.261	5.869	1.965	516.85
473	0.082	0.4989	0.0231	0.774	0.18685	-62.4	0.412	1.263	5.856	1.977	518.82
474	0.082	0.5050	0.0232	0.778	0.18844	-62.2	0.412	1.265	5.843	1.989	520.80
475	0.082	0.5112	0.0234	0.777	0.18986	-61.9	0.413	1.267	5.829	2.001	522.79
476	0.082	0.5175	0.0235	0.780	0.19144	-61.7	0.413	1.269	5.815	2.013	524.80
477	0.082	0.5239	0.0237	0.777	0.19226	-61.5	0.414	1.270	5.801	2.026	526.82
478	0.083	0.5304	0.0238	0.789	0.19371	-61.3	0.415	1.272	5.788	2.038	528.85
479	0.083	0.5370	0.0239	0.792	0.19531	-61.0	0.415	1.274	5.774	2.051	530.89
480	0.083	0.5437	0.0241	0.791	0.19671	-60.8	0.416	1.276	5.759	2.064	532.95
481	0.083	0.5506	0.0242	0.796	0.19874	-60.6	0.417	1.279	5.745	2.077	535.02
482	0.083	0.5575	0.0244	0.796	0.20033	-60.4	0.417	1.281	5.731	2.090	537.10
483	0.084	0.5646	0.0246	0.804	0.20175	-60.2	0.418	1.283	5.716	2.103	539.19
484	0.084	0.5718	0.0247	0.807	0.20337	-59.9	0.418	1.285	5.702	2.116	541.30
485	0.084	0.5791	0.0249	0.807	0.20479	-59.7	0.419	1.287	5.687	2.130	543.42
486	0.084	0.5866	0.0250	0.809	0.20623	-59.5	0.420	1.289	5.672	2.144	545.56
487	0.084	0.5941	0.0252	0.811	0.20839	-59.3	0.420	1.292	5.657	2.157	547.71
488	0.085	0.6018	0.0253	0.823	0.20983	-59.0	0.421	1.294	5.642	2.171	549.87
489	0.085	0.6096	0.0255	0.822	0.21127	-58.8	0.422	1.296	5.627	2.185	552.05
490	0.085	0.6176	0.0257	0.822	0.21285	-58.6	0.422	1.298	5.612	2.200	554.24
491	0.085	0.6257	0.0258	0.827	0.21489	-58.4	0.423	1.301	5.597	2.214	556.45
492	0.086	0.6339	0.0260	0.835	0.21632	-58.1	0.424	1.303	5.581	2.228	558.67
493	0.086	0.6422	0.0262	0.835	0.21777	-57.9	0.425	1.305	5.566	2.243	560.90
494	0.086	0.6507	0.0264	0.836	0.21992	-57.7	0.425	1.308	5.550	2.258	563.15
495	0.086	0.6594	0.0265	0.839	0.22135	-57.5	0.426	1.310	5.535	2.273	565.41
496	0.087	0.6681	0.0267	0.850	0.22337	-57.2	0.427	1.313	5.519	2.288	567.69
497	0.087	0.6770	0.0269	0.849	0.22495	-57.0	0.427	1.315	5.503	2.303	569.99
498	0.087	0.6861	0.0271	0.849	0.22641	-56.8	0.428	1.317	5.487	2.318	572.30
499	0.087	0.6953	0.0272	0.853	0.22841	-56.6	0.429	1.320	5.471	2.334	574.62
500	0.088	0.7047	0.0274	0.864	0.23040	-56.3	0.430	1.323	5.455	2.349	576.96
501	0.088	0.7142	0.0276	0.864	0.23199	-56.1	0.430	1.325	5.439	2.365	579.32
502	0.088	0.7238	0.0278	0.865	0.23400	-55.9	0.431	1.328	5.423	2.381	581.69
503	0.088	0.7337	0.0280	0.864	0.23543	-55.7	0.432	1.330	5.406	2.397	584.08
504	0.089	0.7436	0.0282	0.875	0.23743	-55.5	0.433	1.333	5.390	2.413	586.48
505	0.089	0.7538	0.0284	0.876	0.23945	-55.3	0.434	1.336	5.373	2.430	588.90
506	0.089	0.7641	0.0286	0.876	0.24101	-55.0	0.434	1.338	5.357	2.446	591.34
507	0.089	0.7745	0.0288	0.877	0.24301	-54.8	0.435	1.341	5.340	2.463	593.80
508	0.090	0.7852	0.0290	0.888	0.24501	-54.6	0.436	1.344	5.323	2.480	596.27
509	0.090	0.7960	0.0292	0.887	0.24644	-54.4	0.437	1.346	5.306	2.497	598.75
510	0.090	0.8070	0.0294	0.888	0.24840	-54.1	0.438	1.349	5.289	2.514	601.26
511	0.091	0.8181	0.0296	0.899	0.25055	-53.9	0.438	1.352	5.273	2.531	603.78
512	0.091	0.8294	0.0298	0.900	0.25253	-53.7	0.439	1.355	5.256	2.549	606.32
513	0.091	0.8409	0.0300	0.901	0.25452	-53.5	0.440	1.358	5.239	2.566	608.88
514	0.092	0.8526	0.0302	0.910	0.25592	-53.3	0.441	1.360	5.222	2.584	611.45
515	0.092	0.8645	0.0304	0.911	0.25790	-53.1	0.442	1.363	5.204	2.602	614.04
516	0.092	0.8765	0.0306	0.912	0.25987	-52.9	0.443	1.366	5.187	2.620	616.65
517	0.092	0.8887	0.0308	0.913	0.26184	-52.6	0.444	1.369	5.170	2.638	619.28

518	0.093	0.9012	0.0310	0.924	0.26396	-52.4	0.444	1.372	5.152	2.657	621.93
519	0.093	0.9138	0.0312	0.925	0.26591	-52.2	0.445	1.375	5.134	2.675	624.59
520	0.093	0.9266	0.0314	0.926	0.26785	-52.0	0.446	1.378	5.117	2.694	627.28
521	0.094	0.9396	0.0317	0.934	0.26981	-51.8	0.447	1.381	5.100	2.713	629.98
522	0.094	0.9528	0.0319	0.935	0.27177	-51.6	0.448	1.384	5.083	2.732	632.70
523	0.094	0.9661	0.0321	0.936	0.27371	-51.4	0.449	1.387	5.065	2.751	635.44
524	0.095	0.9797	0.0323	0.947	0.27565	-51.2	0.450	1.390	5.048	2.770	638.20
525	0.095	0.9935	0.0326	0.944	0.27760	-51.0	0.451	1.393	5.030	2.789	640.98
526	0.095	1.0075	0.0328	0.945	0.27953	-50.8	0.452	1.396	5.012	2.809	643.78
527	0.096	1.0217	0.0330	0.956	0.28147	-50.6	0.453	1.399	4.994	2.829	646.60
528	0.096	1.0361	0.0333	0.954	0.28340	-50.4	0.454	1.402	4.976	2.848	649.43
529	0.096	1.0508	0.0335	0.956	0.28587	-50.2	0.455	1.406	4.958	2.869	652.29
530	0.097	1.0656	0.0337	0.967	0.28778	-50.0	0.456	1.409	4.941	2.889	655.17
531	0.097	1.0807	0.0340	0.965	0.28969	-49.8	0.457	1.412	4.923	2.909	658.07
532	0.097	1.0959	0.0342	0.966	0.29159	-49.6	0.458	1.415	4.906	2.929	660.98
533	0.098	1.1114	0.0344	0.976	0.29351	-49.4	0.459	1.418	4.888	2.950	663.92
534	0.098	1.1271	0.0347	0.974	0.29541	-49.2	0.460	1.421	4.870	2.971	666.88
535	0.099	1.1430	0.0349	0.985	0.29731	-49.0	0.461	1.424	4.852	2.992	669.86
536	0.099	1.1592	0.0352	0.984	0.29974	-48.8	0.462	1.428	4.834	3.013	672.87
537	0.099	1.1756	0.0354	0.985	0.30162	-48.6	0.463	1.431	4.816	3.034	675.89
538	0.100	1.1922	0.0357	0.993	0.30350	-48.4	0.464	1.434	4.798	3.055	678.93
539	0.100	1.2090	0.0359	0.995	0.30591	-48.2	0.465	1.438	4.780	3.077	682.00
540	0.100	1.2261	0.0362	0.993	0.30782	-48.0	0.466	1.441	4.762	3.098	685.08
541	0.101	1.2434	0.0364	1.003	0.30970	-47.9	0.467	1.444	4.745	3.120	688.19
542	0.101	1.2610	0.0367	1.001	0.31159	-47.7	0.468	1.447	4.727	3.142	691.32
543	0.101	1.2787	0.0369	1.002	0.31348	-47.5	0.469	1.450	4.710	3.164	694.48
544	0.102	1.2968	0.0372	1.011	0.31588	-47.3	0.470	1.454	4.692	3.186	697.65
545	0.102	1.3150	0.0375	1.009	0.31777	-47.1	0.471	1.457	4.674	3.209	700.85
546	0.103	1.3335	0.0377	1.020	0.31963	-46.9	0.472	1.460	4.656	3.231	704.07
547	0.103	1.3522	0.0380	1.019	0.32202	-46.8	0.473	1.464	4.638	3.254	707.31
548	0.103	1.3712	0.0383	1.017	0.32389	-46.6	0.474	1.467	4.620	3.276	710.57
549	0.104	1.3905	0.0385	1.027	0.32573	-46.4	0.475	1.470	4.602	3.299	713.86
550	0.104	1.4100	0.0388	1.025	0.32745	-46.2	0.477	1.473	4.585	3.322	717.17
551	0.105	1.4297	0.0391	1.034	0.32981	-46.1	0.478	1.477	4.568	3.345	720.50
552	0.105	1.4497	0.0393	1.034	0.33164	-45.9	0.479	1.480	4.551	3.369	723.86
553	0.105	1.4699	0.0396	1.032	0.33349	-45.7	0.480	1.483	4.533	3.392	727.24
554	0.106	1.4904	0.0399	1.040	0.33531	-45.6	0.481	1.486	4.516	3.416	730.64
555	0.106	1.5111	0.0402	1.039	0.33765	-45.4	0.482	1.490	4.498	3.439	734.07
556	0.107	1.5321	0.0404	1.050	0.33948	-45.2	0.483	1.493	4.480	3.463	737.52
557	0.107	1.5534	0.0407	1.047	0.34115	-45.0	0.485	1.496	4.463	3.487	740.99
558	0.108	1.5749	0.0410	1.056	0.34346	-44.9	0.486	1.500	4.445	3.511	744.49
559	0.108	1.5967	0.0413	1.054	0.34526	-44.7	0.487	1.503	4.427	3.535	748.01
560	0.108	1.6187	0.0416	1.052	0.34706	-44.6	0.488	1.506	4.411	3.559	751.56
561	0.109	1.6410	0.0418	1.062	0.34886	-44.4	0.489	1.509	4.394	3.584	755.13
562	0.109	1.6636	0.0421	1.061	0.35114	-44.3	0.490	1.513	4.378	3.608	758.73
563	0.110	1.6864	0.0424	1.069	0.35280	-44.1	0.492	1.516	4.361	3.633	762.35
564	0.110	1.7095	0.0427	1.066	0.35458	-44.0	0.493	1.519	4.344	3.658	765.99
565	0.110	1.7328	0.0430	1.064	0.35634	-43.8	0.494	1.522	4.327	3.683	769.66
566	0.111	1.7564	0.0433	1.072	0.35811	-43.6	0.495	1.525	4.310	3.708	773.35
567	0.111	1.7803	0.0436	1.071	0.36036	-43.5	0.496	1.529	4.293	3.733	777.07
568	0.112	1.8044	0.0439	1.078	0.36200	-43.3	0.498	1.532	4.275	3.758	780.82
569	0.112	1.8289	0.0442	1.076	0.36375	-43.2	0.499	1.535	4.258	3.783	784.59
570	0.113	1.8535	0.0445	1.084	0.36548	-43.0	0.500	1.538	4.243	3.808	788.38
571	0.113	1.8785	0.0448	1.081	0.36721	-42.9	0.501	1.541	4.227	3.834	792.20
572	0.114	1.9037	0.0451	1.088	0.36883	-42.8	0.503	1.544	4.211	3.860	796.05
573	0.114	1.9292	0.0454	1.086	0.37056	-42.6	0.504	1.547	4.195	3.885	799.92
574	0.114	1.9549	0.0457	1.084	0.37227	-42.5	0.505	1.550	4.179	3.911	803.82
575	0.115	1.9810	0.0460	1.093	0.37447	-42.4	0.506	1.554	4.162	3.937	807.74
576	0.115	2.0072	0.0463	1.090	0.37606	-42.2	0.508	1.557	4.146	3.963	811.69
577	0.116	2.0338	0.0466	1.098	0.37776	-42.1	0.509	1.560	4.130	3.989	815.67
578	0.116	2.0607	0.0469	1.096	0.37947	-41.9	0.510	1.563	4.113	4.015	819.67
579	0.117	2.0878	0.0472	1.103	0.38116	-41.8	0.511	1.566	4.097	4.042	823.70
580	0.117	2.1152	0.0475	1.101	0.38272	-41.7	0.513	1.569	4.082	4.068	827.75
581	0.118	2.1428	0.0478	1.108	0.38440	-41.6	0.514	1.572	4.067	4.094	831.83
582	0.118	2.1707	0.0481	1.104	0.38561	-41.4	0.515	1.574	4.052	4.121	835.94
583	0.118	2.1989	0.0484	1.102	0.38727	-41.3	0.516	1.577	4.037	4.148	840.07
584	0.119	2.2274	0.0487	1.109	0.38883	-41.2	0.518	1.580	4.022	4.174	844.23
585	0.119	2.2561	0.0490	1.107	0.39049	-41.1	0.519	1.583	4.006	4.201	848.42
586	0.120	2.2851	0.0494	1.112	0.39214	-40.9	0.520	1.586	3.991	4.228	852.63
587	0.120	2.3144	0.0497	1.110	0.39368	-40.8	0.522	1.589	3.975	4.255	856.87
588	0.121	2.3440	0.0500	1.117	0.39532	-40.7	0.523	1.592	3.960	4.282	861.14

589	0.121	2.3738	0.0503	1.115	0.39695	-40.6	0.524	1.595	3.945	4.309	865.43
590	0.122	2.4039	0.0506	1.120	0.39800	-40.5	0.526	1.597	3.931	4.336	869.75
591	0.122	2.4343	0.0509	1.118	0.39964	-40.4	0.527	1.600	3.917	4.364	874.10
592	0.122	2.4649	0.0513	1.114	0.40125	-40.2	0.528	1.603	3.903	4.391	878.48
593	0.123	2.4958	0.0516	1.120	0.40230	-40.1	0.530	1.605	3.889	4.418	882.88
594	0.123	2.5269	0.0519	1.118	0.40392	-40.0	0.531	1.608	3.874	4.446	887.31
595	0.124	2.5584	0.0522	1.125	0.40551	-39.9	0.532	1.611	3.860	4.473	891.77
596	0.124	2.5900	0.0525	1.121	0.40656	-39.8	0.534	1.613	3.845	4.501	896.26
597	0.125	2.6220	0.0529	1.126	0.40816	-39.7	0.535	1.616	3.831	4.528	900.77
598	0.125	2.6543	0.0532	1.124	0.40974	-39.6	0.536	1.619	3.816	4.556	905.31
599	0.126	2.6868	0.0535	1.129	0.41077	-39.5	0.538	1.621	3.802	4.584	909.88
600	0.126	2.7196	0.0538	1.127	0.41234	-39.4	0.539	1.624	3.789	4.612	914.48
601	0.127	2.7526	0.0542	1.131	0.41346	-39.3	0.540	1.626	3.776	4.639	919.10
602	0.127	2.7859	0.0545	1.128	0.41449	-39.2	0.542	1.628	3.763	4.667	923.75
603	0.127	2.8195	0.0548	1.126	0.41605	-39.1	0.543	1.631	3.750	4.695	928.43
604	0.128	2.8533	0.0551	1.131	0.41716	-39.0	0.544	1.633	3.737	4.723	933.14
605	0.128	2.8874	0.0555	1.127	0.41862	-38.9	0.546	1.636	3.723	4.751	937.88
606	0.129	2.9217	0.0558	1.133	0.41972	-38.8	0.547	1.638	3.710	4.780	942.64
607	0.129	2.9563	0.0561	1.130	0.42082	-38.7	0.548	1.640	3.696	4.808	947.44
608	0.130	2.9912	0.0565	1.134	0.42227	-38.6	0.550	1.643	3.683	4.836	952.26
609	0.130	3.0263	0.0568	1.131	0.42336	-38.5	0.551	1.645	3.670	4.864	957.11
610	0.131	3.0617	0.0571	1.137	0.42435	-38.4	0.553	1.647	3.658	4.892	961.98
611	0.131	3.0974	0.0574	1.134	0.42543	-38.3	0.554	1.649	3.645	4.921	966.89
612	0.132	3.1333	0.0578	1.137	0.42651	-38.3	0.555	1.651	3.633	4.949	971.82
613	0.132	3.1694	0.0581	1.135	0.42794	-38.2	0.557	1.654	3.621	4.978	976.78
614	0.132	3.2059	0.0584	1.132	0.42901	-38.1	0.558	1.656	3.609	5.006	981.77
615	0.133	3.2425	0.0588	1.136	0.43008	-38.0	0.559	1.658	3.596	5.034	986.79
616	0.133	3.2794	0.0591	1.133	0.43106	-37.9	0.561	1.660	3.584	5.063	991.84
617	0.134	3.3166	0.0594	1.138	0.43212	-37.8	0.562	1.662	3.571	5.092	996.92
618	0.134	3.3541	0.0598	1.133	0.43309	-37.8	0.564	1.664	3.558	5.120	1002.02
619	0.135	3.3918	0.0601	1.139	0.43414	-37.7	0.565	1.666	3.547	5.149	1007.15
620	0.135	3.4297	0.0604	1.136	0.43519	-37.6	0.566	1.668	3.535	5.177	1012.32
621	0.136	3.4679	0.0608	1.139	0.43615	-37.5	0.568	1.670	3.524	5.206	1017.51
622	0.136	3.5063	0.0611	1.136	0.43720	-37.5	0.569	1.672	3.513	5.235	1022.73
623	0.137	3.5450	0.0614	1.142	0.43824	-37.4	0.570	1.674	3.501	5.263	1027.97
624	0.137	3.5839	0.0618	1.137	0.43919	-37.3	0.572	1.676	3.490	5.292	1033.25
625	0.137	3.6231	0.0621	1.134	0.44024	-37.2	0.573	1.678	3.478	5.321	1038.55
626	0.138	3.6625	0.0625	1.137	0.44120	-37.2	0.575	1.680	3.467	5.350	1043.89
627	0.138	3.7022	0.0628	1.135	0.44225	-37.1	0.576	1.682	3.455	5.379	1049.25
628	0.139	3.7421	0.0631	1.140	0.44329	-37.0	0.577	1.684	3.443	5.407	1054.64
629	0.139	3.7822	0.0635	1.134	0.44381	-36.9	0.579	1.685	3.432	5.436	1060.06
630	0.140	3.8227	0.0638	1.140	0.44485	-36.9	0.580	1.687	3.422	5.465	1065.51
631	0.140	3.8633	0.0641	1.137	0.44580	-36.8	0.582	1.689	3.412	5.494	1070.99
632	0.141	3.9042	0.0645	1.139	0.44640	-36.7	0.583	1.690	3.401	5.523	1076.50
633	0.141	3.9453	0.0648	1.137	0.44743	-36.7	0.584	1.692	3.390	5.552	1082.03
634	0.141	3.9866	0.0652	1.132	0.44837	-36.6	0.586	1.694	3.380	5.581	1087.60
635	0.142	4.0282	0.0655	1.137	0.44940	-36.5	0.587	1.696	3.369	5.610	1093.19
636	0.142	4.0700	0.0658	1.134	0.44991	-36.5	0.589	1.697	3.358	5.639	1098.81
637	0.143	4.1121	0.0662	1.137	0.45093	-36.4	0.590	1.699	3.348	5.668	1104.47
638	0.143	4.1544	0.0665	1.135	0.45194	-36.3	0.591	1.701	3.337	5.697	1110.15
639	0.144	4.1970	0.0668	1.139	0.45245	-36.3	0.593	1.702	3.327	5.726	1115.86
640	0.144	4.2398	0.0672	1.134	0.45345	-36.2	0.594	1.704	3.317	5.755	1121.59
641	0.145	4.2828	0.0675	1.138	0.45395	-36.2	0.596	1.705	3.307	5.784	1127.36
642	0.145	4.3260	0.0679	1.134	0.45495	-36.1	0.597	1.707	3.297	5.813	1133.16
643	0.145	4.3695	0.0682	1.131	0.45554	-36.1	0.598	1.708	3.287	5.842	1138.98
644	0.146	4.4132	0.0685	1.136	0.45646	-36.0	0.600	1.710	3.278	5.871	1144.84
645	0.146	4.4571	0.0689	1.131	0.45704	-35.9	0.601	1.711	3.268	5.900	1150.72
646	0.147	4.5013	0.0692	1.136	0.45795	-35.9	0.603	1.713	3.258	5.929	1156.64
647	0.147	4.5457	0.0696	1.132	0.45894	-35.8	0.604	1.715	3.248	5.958	1162.58
648	0.148	4.5903	0.0699	1.136	0.45943	-35.8	0.606	1.716	3.237	5.987	1168.55
649	0.148	4.6352	0.0702	1.133	0.46041	-35.7	0.607	1.718	3.228	6.016	1174.55
650	0.148	4.6803	0.0706	1.128	0.46098	-35.7	0.608	1.719	3.219	6.045	1180.58
651	0.149	4.7256	0.0709	1.132	0.46147	-35.6	0.610	1.720	3.210	6.074	1186.63
652	0.149	4.7712	0.0713	1.128	0.46244	-35.6	0.611	1.722	3.201	6.103	1192.72
653	0.150	4.8169	0.0716	1.132	0.46301	-35.5	0.612	1.723	3.191	6.132	1198.84
654	0.150	4.8629	0.0719	1.129	0.46349	-35.5	0.614	1.724	3.182	6.161	1204.98
655	0.151	4.9091	0.0723	1.132	0.46446	-35.4	0.615	1.726	3.173	6.191	1211.16
656	0.151	4.9556	0.0726	1.129	0.46494	-35.4	0.617	1.727	3.163	6.220	1217.36
657	0.152	5.0022	0.0730	1.133	0.46591	-35.3	0.618	1.729	3.154	6.249	1223.59

AltCDR RFQ PteqHI tapeinput

```
run 1 0 0 0 2 0 583 0 0 0 0 583 0 0 0 0
title
linac 1  0.095  175.  2.0145  1.0
tank 1  5.00 -90 0.1 0 1.0 0 1.0 0 0 1.0  10 1 36 0.0 0.0
zdata -5
  -5.1712  0.001  -90.000  1.0000  0.13000
  -4.3093  0.80202  -90.000  1.0000  0.13000
  -3.4474  1.6040  -90.000  1.0000  0.13000
  -2.5856  2.4060  -90.000  1.0000  0.13000
  -1.7237  3.2081  -90.000  1.0000  0.13000
  -0.86186  4.0101  -90.000  1.0000  0.13000
  -1.0000e-05  4.8121  -90.000  1.0000  0.13000  6
zdata  -5
  0.  4.81206  -90.  1.  0.13
  20.685  5.07536  -90.  1.0064  0.12416
  40.508  5.31758  -90.  1.0174  0.11715
  60.331  5.57232  -90.  1.0339  0.11025
  80.153  5.8138  -90.  1.0559  0.10407
  100.84  6.01424  -90.  1.0808  0.099212
  120.66  6.11768  -90.  1.0969  0.096779
  130.14  6.12881  -90.  1.0987  0.096525
  154.36  6.12872  -86.867  1.0996  0.096525
  205.94  6.12687  -85.479  1.1065  0.097179
  220.23  6.12646  -84.836  1.1089  0.097386
  240.91  6.12537  -83.532  1.1134  0.097757
  260.46  6.12354  -81.78  1.119  0.098209
  281.06  6.12166  -79.257  1.1271  0.098592
  300.69  6.11933  -76.128  1.1381  0.099175
  320.57  6.11385  -72.261  1.154  0.099827
  340.91  6.10588  -67.76  1.1771  0.10064
  360.31  6.09597  -63.229  1.2083  0.10169
  380.15  6.0749  -58.656  1.2524  0.10286
  400.44  6.03649  -54.313  1.3138  0.10368
  421.09  5.97769  -50.431  1.398  0.10405
  441.87  5.89192  -47.136  1.5113  0.10401
  451.87  5.82667  -45.763  1.5792  0.10381
  457.07  5.89002  -45.101  1.5983  0.10374
  519.54  5.815  -40.315  1.5983  0.10307
  539.87  5.79564  -40.006  1.5983  0.10284
  591.17  5.75761  -40.006  1.5983  0.10236
  639.1  5.7369  -40.006  1.5983  0.10211
  690.39  5.71948  -40.006  1.5983  0.10189
  740.17  5.7085  -40.006  1.5983  0.10176
  792.47  5.69931  -40.006  1.5983  0.10165
  842.08  5.6925  -40.006  1.5983  0.10157
  893.6  5.68658  -40.006  1.5983  0.1015
  941.52  5.68165  -40.006  1.5983  0.10144
  990.88  5.67689  -40.006  1.5983  0.10138
  1041.6  5.67285  -40.006  1.5983  0.10133
  1093.7  5.66948  -40.006  1.5983  0.10129
  1141.2  5.6669  -40.006  1.5983  0.10126
  1189.6  5.66438  -40.006  1.5983  0.10123        -1
start 1
stop -1
rfqout 1
elimit 0.25 0.25
input -6 -100000 2.362 14.218 .01491 2.362 14.218 .01491
  180.0  0.000  0.0
  0.0 0.0 0.0 0.0 0.0 0.0 1. 2.0145 130.0  0.095
output 2 -1 2 0 1 1 1 2000 1
scheff 130.0 0.029 -0.04425 20 40  20  1  6
optcon  120000   4 1.1 1.4 .1    3  8. 10. 1.    0 0 0 0
0 0 0 0   0 0 0 0    0 0 0 0
begin
end
```

AltCDR RFQ Cell Table

nc	v	ws	beta	ez	capa	phi	a	m	b	cl	tl
0	0.130	0.0950	0.0101	0.000	0.00000	-90.0	45.090	1.000	0.001	0.000	0.00
1	0.130	0.0950	0.0101	0.000	0.00000	-90.0	1.592	1.000	0.802	0.862	0.86
2	0.130	0.0950	0.0101	0.000	0.00000	-90.0	1.126	1.000	1.604	0.862	1.72
3	0.130	0.0950	0.0101	0.000	0.00000	-90.0	0.919	1.000	2.406	0.862	2.59
4	0.130	0.0950	0.0101	0.000	0.00000	-90.0	0.796	1.000	3.208	0.862	3.45
5	0.130	0.0950	0.0101	0.000	0.00000	-90.0	0.712	1.000	4.010	0.862	4.31
6	0.130	0.0950	0.0101	0.000	0.00000	-90.0	0.650	1.000	4.812	0.862	5.17
7	0.130	0.0950	0.0101	0.000	0.00000	-90.0	0.649	1.000	4.823	0.862	6.03
8	0.130	0.0950	0.0101	0.004	0.00024	-90.0	0.647	1.001	4.834	0.862	6.89
9	0.129	0.0950	0.0101	0.004	0.00024	-90.0	0.646	1.001	4.845	0.862	7.76
10	0.129	0.0950	0.0101	0.004	0.00024	-90.0	0.644	1.001	4.856	0.862	8.62
11	0.129	0.0950	0.0101	0.004	0.00024	-90.0	0.643	1.001	4.867	0.862	9.48
12	0.129	0.0950	0.0101	0.007	0.00049	-90.0	0.641	1.002	4.878	0.862	10.34
13	0.128	0.0950	0.0101	0.007	0.00049	-90.0	0.640	1.002	4.889	0.862	11.20
14	0.128	0.0950	0.0101	0.007	0.00050	-90.0	0.639	1.002	4.900	0.862	12.07
15	0.128	0.0950	0.0101	0.007	0.00050	-90.0	0.637	1.002	4.911	0.862	12.93
16	0.128	0.0950	0.0101	0.011	0.00075	-90.0	0.636	1.003	4.922	0.862	13.79
17	0.127	0.0950	0.0101	0.011	0.00075	-90.0	0.634	1.003	4.933	0.862	14.65
18	0.127	0.0950	0.0101	0.011	0.00076	-90.0	0.633	1.003	4.944	0.862	15.51
19	0.127	0.0950	0.0101	0.011	0.00076	-90.0	0.632	1.003	4.955	0.862	16.38
20	0.127	0.0950	0.0101	0.015	0.00102	-90.0	0.630	1.004	4.966	0.862	17.24
21	0.126	0.0950	0.0101	0.015	0.00102	-90.0	0.629	1.004	4.977	0.862	18.10
22	0.126	0.0950	0.0101	0.015	0.00103	-90.0	0.627	1.004	4.988	0.862	18.96
23	0.126	0.0950	0.0101	0.019	0.00129	-90.0	0.626	1.005	4.999	0.862	19.82
24	0.126	0.0950	0.0101	0.019	0.00129	-90.0	0.625	1.005	5.010	0.862	20.68
25	0.125	0.0950	0.0101	0.019	0.00130	-90.0	0.623	1.005	5.021	0.862	21.55
26	0.125	0.0950	0.0101	0.019	0.00131	-90.0	0.622	1.005	5.031	0.862	22.41
27	0.125	0.0950	0.0101	0.023	0.00157	-90.0	0.621	1.006	5.042	0.862	23.27
28	0.125	0.0950	0.0101	0.023	0.00158	-90.0	0.619	1.006	5.053	0.862	24.13
29	0.124	0.0950	0.0101	0.023	0.00159	-90.0	0.618	1.006	5.064	0.862	24.99
30	0.124	0.0950	0.0101	0.023	0.00159	-90.0	0.617	1.006	5.075	0.862	25.86
31	0.124	0.0950	0.0101	0.027	0.00187	-90.0	0.615	1.007	5.086	0.862	26.72
32	0.124	0.0950	0.0101	0.027	0.00188	-90.0	0.613	1.007	5.096	0.862	27.58
33	0.123	0.0950	0.0101	0.031	0.00215	-90.0	0.612	1.008	5.107	0.862	28.44
34	0.123	0.0950	0.0101	0.031	0.00216	-90.0	0.610	1.008	5.117	0.862	29.30
35	0.123	0.0951	0.0101	0.035	0.00244	-90.0	0.609	1.009	5.128	0.862	30.17
36	0.122	0.0951	0.0101	0.035	0.00246	-90.0	0.607	1.009	5.139	0.862	31.03
37	0.122	0.0951	0.0101	0.039	0.00273	-90.0	0.606	1.010	5.149	0.862	31.89
38	0.122	0.0951	0.0101	0.039	0.00275	-90.0	0.604	1.010	5.160	0.862	32.75
39	0.121	0.0951	0.0101	0.042	0.00303	-90.0	0.603	1.011	5.170	0.862	33.61
40	0.121	0.0951	0.0101	0.043	0.00305	-90.0	0.601	1.011	5.181	0.862	34.47
41	0.121	0.0951	0.0101	0.047	0.00334	-90.0	0.600	1.012	5.191	0.862	35.34
42	0.121	0.0951	0.0101	0.047	0.00336	-90.0	0.598	1.012	5.202	0.862	36.20
43	0.120	0.0951	0.0101	0.051	0.00365	-90.0	0.597	1.013	5.212	0.862	37.06
44	0.120	0.0951	0.0101	0.051	0.00367	-90.0	0.595	1.013	5.223	0.862	37.92
45	0.120	0.0951	0.0101	0.055	0.00396	-90.0	0.594	1.014	5.233	0.862	38.78
46	0.119	0.0951	0.0101	0.055	0.00399	-90.0	0.592	1.014	5.244	0.862	39.65
47	0.119	0.0951	0.0101	0.059	0.00428	-90.0	0.591	1.015	5.254	0.862	40.51
48	0.119	0.0951	0.0101	0.059	0.00431	-90.0	0.589	1.015	5.265	0.862	41.37
49	0.118	0.0951	0.0101	0.059	0.00432	-90.0	0.588	1.015	5.275	0.862	42.23
50	0.118	0.0951	0.0101	0.063	0.00464	-90.0	0.586	1.016	5.286	0.862	43.09
51	0.118	0.0951	0.0101	0.063	0.00465	-90.0	0.585	1.016	5.297	0.862	43.95
52	0.117	0.0951	0.0101	0.067	0.00497	-90.0	0.583	1.017	5.307	0.862	44.82
53	0.117	0.0951	0.0101	0.067	0.00498	-90.0	0.582	1.017	5.318	0.862	45.68
54	0.117	0.0951	0.0101	0.072	0.00530	-90.0	0.580	1.018	5.329	0.862	46.54
55	0.117	0.0951	0.0101	0.076	0.00561	-90.0	0.579	1.019	5.340	0.862	47.40
56	0.116	0.0951	0.0101	0.080	0.00594	-90.0	0.577	1.020	5.351	0.862	48.26
57	0.116	0.0951	0.0101	0.080	0.00596	-90.0	0.576	1.020	5.362	0.862	49.13
58	0.116	0.0951	0.0101	0.084	0.00629	-90.0	0.574	1.021	5.373	0.862	49.99
59	0.115	0.0951	0.0101	0.088	0.00660	-90.0	0.573	1.022	5.384	0.862	50.85
60	0.115	0.0951	0.0101	0.088	0.00664	-90.0	0.571	1.022	5.395	0.862	51.71
61	0.115	0.0951	0.0101	0.092	0.00696	-90.0	0.570	1.023	5.406	0.862	52.57
62	0.114	0.0951	0.0101	0.096	0.00730	-90.0	0.568	1.024	5.417	0.862	53.44
63	0.114	0.0951	0.0101	0.100	0.00762	-90.0	0.567	1.025	5.428	0.862	54.30
64	0.114	0.0951	0.0101	0.101	0.00767	-90.0	0.565	1.025	5.439	0.862	55.16
65	0.114	0.0952	0.0101	0.105	0.00799	-90.0	0.564	1.026	5.450	0.863	56.02
66	0.113	0.0952	0.0101	0.109	0.00834	-90.0	0.562	1.027	5.462	0.863	56.88
67	0.113	0.0952	0.0101	0.109	0.00837	-90.0	0.561	1.027	5.473	0.863	57.74
68	0.113	0.0952	0.0101	0.114	0.00872	-90.0	0.559	1.028	5.484	0.863	58.61
69	0.112	0.0952	0.0101	0.117	0.00905	-90.0	0.558	1.029	5.495	0.863	59.47

70	0.112	0.0952	0.0101	0.122	0.00941	-90.0	0.556	1.030	5.506	0.863	60.33
71	0.112	0.0952	0.0101	0.122	0.00944	-90.0	0.555	1.030	5.517	0.863	61.19
72	0.111	0.0952	0.0101	0.126	0.00981	-90.0	0.553	1.031	5.528	0.863	62.05
73	0.111	0.0952	0.0101	0.130	0.01014	-90.0	0.552	1.032	5.539	0.863	62.92
74	0.111	0.0952	0.0101	0.131	0.01021	-90.0	0.550	1.032	5.550	0.863	63.78
75	0.111	0.0952	0.0101	0.135	0.01055	-90.0	0.549	1.033	5.561	0.863	64.64
76	0.110	0.0952	0.0101	0.139	0.01092	-90.0	0.547	1.034	5.572	0.863	65.50
77	0.110	0.0952	0.0101	0.143	0.01127	-90.0	0.546	1.035	5.583	0.863	66.36
78	0.110	0.0952	0.0101	0.148	0.01165	-90.0	0.544	1.036	5.593	0.863	67.23
79	0.109	0.0952	0.0101	0.151	0.01199	-90.0	0.543	1.037	5.604	0.863	68.09
80	0.109	0.0952	0.0101	0.156	0.01238	-90.0	0.541	1.038	5.614	0.863	68.95
81	0.109	0.0952	0.0101	0.160	0.01273	-90.0	0.540	1.039	5.625	0.863	69.81
82	0.109	0.0952	0.0101	0.165	0.01308	-90.0	0.539	1.040	5.635	0.863	70.67
83	0.108	0.0952	0.0101	0.168	0.01348	-90.0	0.537	1.041	5.646	0.863	71.53
84	0.108	0.0952	0.0101	0.173	0.01384	-90.0	0.536	1.042	5.656	0.863	72.40
85	0.108	0.0953	0.0101	0.178	0.01424	-90.0	0.534	1.043	5.667	0.863	73.26
86	0.108	0.0953	0.0101	0.178	0.01428	-90.0	0.533	1.043	5.677	0.863	74.12
87	0.107	0.0953	0.0101	0.181	0.01464	-90.0	0.532	1.044	5.688	0.863	74.98
88	0.107	0.0953	0.0101	0.186	0.01505	-90.0	0.530	1.045	5.698	0.863	75.84
89	0.107	0.0953	0.0101	0.191	0.01542	-90.0	0.529	1.046	5.709	0.863	76.71
90	0.106	0.0953	0.0101	0.194	0.01583	-90.0	0.527	1.047	5.719	0.863	77.57
91	0.106	0.0953	0.0101	0.199	0.01620	-90.0	0.526	1.048	5.730	0.863	78.43
92	0.106	0.0953	0.0101	0.203	0.01657	-90.0	0.525	1.049	5.740	0.863	79.29
93	0.106	0.0953	0.0101	0.208	0.01700	-90.0	0.523	1.050	5.751	0.863	80.15
94	0.105	0.0953	0.0101	0.211	0.01737	-90.0	0.522	1.051	5.761	0.863	81.01
95	0.105	0.0953	0.0101	0.216	0.01780	-90.0	0.520	1.052	5.772	0.863	81.88
96	0.105	0.0953	0.0101	0.221	0.01818	-90.0	0.519	1.053	5.782	0.863	82.74
97	0.105	0.0953	0.0101	0.225	0.01856	-90.0	0.518	1.054	5.793	0.863	83.60
98	0.104	0.0953	0.0101	0.228	0.01900	-90.0	0.516	1.055	5.803	0.863	84.46
99	0.104	0.0953	0.0101	0.233	0.01938	-90.0	0.515	1.056	5.814	0.863	85.32
100	0.104	0.0953	0.0101	0.238	0.01976	-90.0	0.514	1.057	5.822	0.863	86.19
101	0.104	0.0953	0.0101	0.242	0.02015	-90.0	0.513	1.058	5.831	0.863	87.05
102	0.103	0.0954	0.0101	0.244	0.02053	-90.0	0.512	1.059	5.839	0.864	87.91
103	0.103	0.0954	0.0101	0.249	0.02092	-90.0	0.511	1.060	5.847	0.864	88.77
104	0.103	0.0954	0.0101	0.255	0.02138	-90.0	0.509	1.061	5.856	0.864	89.63
105	0.103	0.0954	0.0101	0.259	0.02177	-90.0	0.508	1.062	5.864	0.864	90.50
106	0.103	0.0954	0.0101	0.264	0.02216	-90.0	0.507	1.063	5.872	0.864	91.36
107	0.102	0.0954	0.0101	0.266	0.02256	-90.0	0.506	1.064	5.881	0.864	92.22
108	0.102	0.0954	0.0101	0.271	0.02296	-90.0	0.505	1.065	5.889	0.864	93.08
109	0.102	0.0954	0.0101	0.275	0.02335	-90.0	0.504	1.066	5.897	0.864	93.94
110	0.102	0.0954	0.0101	0.280	0.02375	-90.0	0.503	1.067	5.906	0.864	94.80
111	0.102	0.0954	0.0101	0.285	0.02415	-90.0	0.502	1.068	5.914	0.864	95.67
112	0.101	0.0954	0.0101	0.287	0.02456	-90.0	0.501	1.069	5.922	0.864	96.53
113	0.101	0.0954	0.0101	0.291	0.02496	-90.0	0.500	1.070	5.931	0.864	97.39
114	0.101	0.0954	0.0101	0.297	0.02544	-90.0	0.498	1.071	5.939	0.864	98.25
115	0.101	0.0954	0.0101	0.302	0.02585	-90.0	0.497	1.072	5.947	0.864	99.11
116	0.101	0.0954	0.0101	0.310	0.02659	-90.0	0.496	1.074	5.956	0.864	99.98
117	0.100	0.0954	0.0101	0.312	0.02700	-90.0	0.495	1.075	5.964	0.864	100.84
118	0.100	0.0954	0.0101	0.317	0.02741	-90.0	0.494	1.076	5.972	0.864	101.70
119	0.100	0.0955	0.0101	0.322	0.02782	-90.0	0.493	1.077	5.981	0.864	102.56
120	0.100	0.0955	0.0101	0.326	0.02824	-90.0	0.492	1.078	5.989	0.864	103.42
121	0.100	0.0955	0.0101	0.331	0.02866	-90.0	0.491	1.079	5.998	0.864	104.29
122	0.099	0.0955	0.0101	0.333	0.02907	-90.0	0.490	1.080	6.006	0.864	105.15
123	0.099	0.0955	0.0101	0.338	0.02949	-90.0	0.489	1.081	6.014	0.864	106.01
124	0.099	0.0955	0.0101	0.339	0.02958	-90.0	0.488	1.081	6.019	0.864	106.87
125	0.099	0.0955	0.0101	0.342	0.02991	-90.0	0.488	1.082	6.023	0.864	107.73
126	0.099	0.0955	0.0101	0.347	0.03034	-90.0	0.487	1.083	6.028	0.864	108.59
127	0.099	0.0955	0.0101	0.352	0.03076	-90.0	0.486	1.084	6.032	0.864	109.46
128	0.099	0.0955	0.0101	0.352	0.03076	-90.0	0.486	1.084	6.037	0.864	110.32
129	0.099	0.0955	0.0101	0.357	0.03119	-90.0	0.485	1.085	6.041	0.864	111.18
130	0.098	0.0955	0.0101	0.357	0.03152	-90.0	0.485	1.086	6.046	0.864	112.04
131	0.098	0.0955	0.0101	0.358	0.03161	-90.0	0.484	1.086	6.050	0.864	112.90
132	0.098	0.0955	0.0101	0.363	0.03204	-90.0	0.483	1.087	6.055	0.864	113.77
133	0.098	0.0955	0.0101	0.367	0.03237	-90.0	0.483	1.088	6.059	0.864	114.63
134	0.098	0.0955	0.0101	0.368	0.03247	-90.0	0.482	1.088	6.064	0.864	115.49
135	0.098	0.0955	0.0101	0.372	0.03280	-90.0	0.482	1.089	6.068	0.864	116.35
136	0.098	0.0955	0.0101	0.376	0.03323	-90.0	0.481	1.090	6.073	0.864	117.21
137	0.098	0.0955	0.0101	0.381	0.03367	-90.0	0.480	1.091	6.077	0.864	118.08
138	0.098	0.0955	0.0101	0.381	0.03367	-90.0	0.480	1.091	6.082	0.864	118.94
139	0.098	0.0955	0.0101	0.386	0.03410	-90.0	0.479	1.092	6.086	0.864	119.80
140	0.097	0.0955	0.0101	0.386	0.03443	-90.0	0.479	1.093	6.091	0.864	120.66

141	0.097	0.0955	0.0101	0.387	0.03454	-90.0	0.478	1.093	6.095	0.864	121.52
142	0.097	0.0956	0.0101	0.392	0.03497	-90.0	0.477	1.094	6.100	0.865	122.38
143	0.097	0.0956	0.0101	0.396	0.03531	-90.0	0.477	1.095	6.104	0.865	123.25
144	0.097	0.0956	0.0101	0.401	0.03574	-90.0	0.476	1.096	6.109	0.865	124.11
145	0.097	0.0956	0.0101	0.401	0.03574	-90.0	0.476	1.096	6.113	0.865	124.97
146	0.097	0.0956	0.0101	0.406	0.03619	-90.0	0.475	1.097	6.118	0.865	125.83
147	0.097	0.0956	0.0101	0.406	0.03619	-90.0	0.475	1.097	6.119	0.865	126.69
148	0.097	0.0956	0.0101	0.406	0.03619	-90.0	0.475	1.097	6.120	0.865	127.56
149	0.097	0.0956	0.0101	0.406	0.03619	-90.0	0.475	1.097	6.121	0.865	128.42
150	0.097	0.0956	0.0101	0.409	0.03652	-90.0	0.475	1.098	6.122	0.865	129.28
151	0.097	0.0956	0.0101	0.411	0.03663	-90.0	0.474	1.098	6.123	0.865	130.14
152	0.097	0.0956	0.0101	0.411	0.03663	-90.0	0.474	1.098	6.124	0.865	131.00
153	0.097	0.0956	0.0101	0.411	0.03663	-90.0	0.474	1.098	6.125	0.865	131.86
154	0.097	0.0956	0.0101	0.411	0.03663	-90.0	0.474	1.098	6.126	0.865	132.73
155	0.097	0.0956	0.0101	0.411	0.03663	-90.0	0.474	1.098	6.127	0.865	133.59
156	0.097	0.0956	0.0101	0.414	0.03696	-90.0	0.474	1.099	6.128	0.865	134.45
157	0.097	0.0956	0.0101	0.414	0.03696	-90.0	0.474	1.099	6.129	0.865	135.31
158	0.097	0.0956	0.0101	0.414	0.03696	-89.9	0.474	1.099	6.129	0.865	136.17
159	0.097	0.0956	0.0101	0.414	0.03696	-89.8	0.474	1.099	6.129	0.865	137.04
160	0.097	0.0956	0.0101	0.414	0.03696	-89.7	0.474	1.099	6.129	0.865	137.90
161	0.097	0.0956	0.0101	0.415	0.03702	-89.6	0.474	1.099	6.129	0.865	138.76
162	0.097	0.0957	0.0101	0.415	0.03702	-89.4	0.474	1.099	6.129	0.865	139.62
163	0.097	0.0957	0.0101	0.415	0.03702	-89.3	0.474	1.099	6.129	0.865	140.49
164	0.097	0.0958	0.0101	0.415	0.03702	-89.2	0.474	1.099	6.129	0.865	141.35
165	0.097	0.0958	0.0101	0.415	0.03702	-89.1	0.474	1.099	6.129	0.865	142.21
166	0.097	0.0959	0.0101	0.416	0.03708	-89.0	0.474	1.099	6.129	0.866	143.08
167	0.097	0.0959	0.0101	0.416	0.03708	-88.9	0.474	1.099	6.129	0.866	143.94
168	0.097	0.0960	0.0101	0.416	0.03708	-88.8	0.474	1.099	6.129	0.866	144.81
169	0.097	0.0961	0.0101	0.416	0.03714	-88.7	0.474	1.099	6.129	0.867	145.67
170	0.097	0.0962	0.0101	0.416	0.03714	-88.5	0.474	1.099	6.129	0.867	146.54
171	0.097	0.0963	0.0101	0.416	0.03714	-88.4	0.474	1.099	6.129	0.868	147.40
172	0.097	0.0964	0.0101	0.417	0.03720	-88.3	0.474	1.099	6.129	0.868	148.27
173	0.097	0.0965	0.0101	0.417	0.03720	-88.2	0.474	1.099	6.129	0.869	149.13
174	0.097	0.0966	0.0101	0.418	0.03726	-88.1	0.474	1.099	6.129	0.869	150.00
175	0.097	0.0967	0.0102	0.414	0.03726	-88.0	0.474	1.099	6.129	0.870	150.87
176	0.097	0.0969	0.0102	0.414	0.03732	-87.9	0.474	1.099	6.129	0.870	151.73
177	0.097	0.0970	0.0102	0.414	0.03732	-87.8	0.474	1.099	6.129	0.871	152.60
178	0.097	0.0972	0.0102	0.415	0.03738	-87.7	0.474	1.099	6.129	0.872	153.47
179	0.097	0.0973	0.0102	0.416	0.03744	-87.5	0.474	1.099	6.129	0.872	154.34
180	0.097	0.0975	0.0102	0.416	0.03750	-87.4	0.474	1.099	6.129	0.873	155.21
181	0.097	0.0976	0.0102	0.416	0.03750	-87.3	0.474	1.099	6.129	0.874	156.08
182	0.097	0.0978	0.0102	0.422	0.03801	-87.2	0.473	1.100	6.129	0.874	156.96
183	0.097	0.0980	0.0102	0.423	0.03807	-87.1	0.473	1.100	6.129	0.875	157.83
184	0.097	0.0982	0.0102	0.423	0.03813	-87.0	0.473	1.100	6.129	0.876	158.70
185	0.097	0.0984	0.0102	0.424	0.03819	-86.9	0.473	1.100	6.129	0.877	159.58
186	0.097	0.0986	0.0103	0.420	0.03819	-86.8	0.473	1.100	6.129	0.878	160.45
187	0.097	0.0988	0.0103	0.421	0.03825	-86.8	0.473	1.100	6.129	0.879	161.33
188	0.097	0.0990	0.0103	0.421	0.03831	-86.8	0.473	1.100	6.129	0.880	162.20
189	0.097	0.0992	0.0103	0.422	0.03836	-86.8	0.473	1.100	6.129	0.881	163.08
190	0.097	0.0994	0.0103	0.422	0.03842	-86.7	0.473	1.100	6.129	0.882	163.96
191	0.097	0.0996	0.0103	0.423	0.03848	-86.7	0.473	1.100	6.129	0.882	164.84
192	0.097	0.0999	0.0103	0.424	0.03854	-86.7	0.473	1.100	6.129	0.884	165.72
193	0.097	0.1001	0.0103	0.428	0.03894	-86.7	0.473	1.101	6.128	0.885	166.60
194	0.097	0.1003	0.0103	0.429	0.03900	-86.7	0.473	1.101	6.128	0.886	167.49
195	0.097	0.1005	0.0104	0.425	0.03906	-86.6	0.473	1.101	6.128	0.886	168.37
196	0.097	0.1007	0.0104	0.425	0.03906	-86.6	0.473	1.101	6.128	0.887	169.25
197	0.097	0.1010	0.0104	0.426	0.03911	-86.6	0.473	1.101	6.128	0.889	170.14
198	0.097	0.1012	0.0104	0.427	0.03917	-86.6	0.473	1.101	6.128	0.890	171.03
199	0.097	0.1014	0.0104	0.427	0.03923	-86.5	0.473	1.101	6.128	0.890	171.91
200	0.097	0.1017	0.0104	0.428	0.03934	-86.5	0.473	1.101	6.128	0.892	172.80
201	0.097	0.1019	0.0104	0.429	0.03940	-86.5	0.473	1.101	6.128	0.893	173.69
202	0.097	0.1021	0.0104	0.433	0.03981	-86.5	0.473	1.102	6.128	0.893	174.58
203	0.097	0.1024	0.0104	0.434	0.03987	-86.4	0.473	1.102	6.128	0.895	175.47
204	0.097	0.1026	0.0105	0.431	0.03992	-86.4	0.473	1.102	6.128	0.896	176.37
205	0.097	0.1029	0.0105	0.430	0.03987	-86.4	0.474	1.102	6.128	0.897	177.26
206	0.097	0.1031	0.0105	0.431	0.03993	-86.4	0.474	1.102	6.128	0.898	178.15
207	0.097	0.1034	0.0105	0.431	0.03999	-86.3	0.474	1.102	6.128	0.899	179.05
208	0.097	0.1036	0.0105	0.432	0.04004	-86.3	0.474	1.102	6.128	0.900	179.95
209	0.097	0.1039	0.0105	0.433	0.04011	-86.3	0.474	1.102	6.128	0.901	180.84
210	0.097	0.1041	0.0105	0.437	0.04052	-86.3	0.474	1.103	6.128	0.902	181.74
211	0.097	0.1044	0.0105	0.438	0.04058	-86.2	0.474	1.103	6.128	0.903	182.64

212	0.097	0.1046	0.0106	0.434	0.04064	-86.2	0.474	1.103	6.128	0.904	183.55
213	0.097	0.1049	0.0106	0.436	0.04077	-86.2	0.474	1.103	6.128	0.906	184.45
214	0.097	0.1052	0.0106	0.436	0.04083	-86.2	0.474	1.103	6.128	0.907	185.35
215	0.097	0.1054	0.0106	0.437	0.04089	-86.1	0.474	1.103	6.128	0.908	186.26
216	0.097	0.1057	0.0106	0.438	0.04095	-86.1	0.474	1.103	6.128	0.909	187.16
217	0.097	0.1060	0.0106	0.438	0.04101	-86.1	0.474	1.103	6.128	0.910	188.07
218	0.097	0.1063	0.0106	0.443	0.04143	-86.1	0.474	1.104	6.128	0.912	188.98
219	0.097	0.1065	0.0107	0.439	0.04149	-86.1	0.474	1.104	6.128	0.913	189.89
220	0.097	0.1068	0.0107	0.440	0.04162	-86.0	0.474	1.104	6.128	0.914	190.80
221	0.097	0.1071	0.0107	0.441	0.04168	-86.0	0.474	1.104	6.128	0.915	191.71
222	0.097	0.1074	0.0107	0.442	0.04174	-86.0	0.474	1.104	6.128	0.916	192.62
223	0.097	0.1077	0.0107	0.442	0.04180	-86.0	0.474	1.104	6.128	0.918	193.54
224	0.097	0.1080	0.0107	0.444	0.04193	-85.9	0.474	1.104	6.127	0.919	194.45
225	0.097	0.1083	0.0107	0.444	0.04199	-85.9	0.474	1.104	6.127	0.920	195.37
226	0.097	0.1086	0.0108	0.445	0.04241	-85.9	0.474	1.105	6.127	0.921	196.29
227	0.097	0.1089	0.0108	0.445	0.04247	-85.9	0.474	1.105	6.127	0.923	197.21
228	0.097	0.1092	0.0108	0.447	0.04260	-85.8	0.474	1.105	6.127	0.924	198.13
229	0.097	0.1095	0.0108	0.447	0.04266	-85.8	0.474	1.105	6.127	0.925	199.05
230	0.097	0.1098	0.0108	0.448	0.04272	-85.8	0.474	1.105	6.127	0.927	199.97
231	0.097	0.1101	0.0108	0.449	0.04278	-85.8	0.474	1.105	6.127	0.928	200.90
232	0.097	0.1104	0.0108	0.450	0.04291	-85.7	0.474	1.105	6.127	0.929	201.82
233	0.097	0.1107	0.0109	0.446	0.04297	-85.7	0.474	1.105	6.127	0.930	202.75
234	0.097	0.1110	0.0109	0.451	0.04339	-85.7	0.474	1.106	6.127	0.932	203.68
235	0.097	0.1113	0.0109	0.452	0.04352	-85.7	0.474	1.106	6.127	0.933	204.61
236	0.097	0.1116	0.0109	0.453	0.04358	-85.6	0.474	1.106	6.127	0.934	205.54
237	0.097	0.1120	0.0109	0.453	0.04364	-85.6	0.474	1.106	6.127	0.936	206.47
238	0.097	0.1123	0.0109	0.455	0.04376	-85.6	0.474	1.106	6.127	0.937	207.40
239	0.097	0.1126	0.0110	0.451	0.04383	-85.6	0.474	1.106	6.127	0.938	208.34
240	0.097	0.1130	0.0110	0.452	0.04389	-85.5	0.474	1.106	6.127	0.940	209.28
241	0.097	0.1133	0.0110	0.453	0.04401	-85.5	0.474	1.106	6.127	0.941	210.21
242	0.097	0.1136	0.0110	0.458	0.04444	-85.5	0.474	1.107	6.127	0.942	211.15
243	0.097	0.1140	0.0110	0.459	0.04457	-85.4	0.474	1.107	6.127	0.944	212.09
244	0.097	0.1143	0.0110	0.459	0.04463	-85.4	0.474	1.107	6.127	0.945	213.04
245	0.097	0.1147	0.0111	0.457	0.04475	-85.3	0.474	1.107	6.127	0.947	213.98
246	0.097	0.1150	0.0111	0.457	0.04481	-85.3	0.474	1.107	6.127	0.948	214.92
247	0.097	0.1154	0.0111	0.458	0.04487	-85.3	0.474	1.107	6.127	0.950	215.87
248	0.097	0.1157	0.0111	0.459	0.04500	-85.2	0.474	1.107	6.127	0.951	216.82
249	0.097	0.1161	0.0111	0.463	0.04543	-85.2	0.474	1.108	6.127	0.953	217.77
250	0.097	0.1165	0.0111	0.465	0.04555	-85.1	0.474	1.108	6.127	0.954	218.72
251	0.097	0.1169	0.0112	0.461	0.04562	-85.1	0.474	1.108	6.127	0.956	219.67
252	0.097	0.1172	0.0112	0.462	0.04574	-85.1	0.474	1.108	6.127	0.957	220.62
253	0.097	0.1176	0.0112	0.464	0.04586	-85.0	0.474	1.108	6.127	0.959	221.58
254	0.097	0.1180	0.0112	0.464	0.04592	-85.0	0.474	1.108	6.127	0.961	222.54
255	0.097	0.1184	0.0112	0.469	0.04642	-84.9	0.474	1.109	6.127	0.962	223.50
256	0.097	0.1188	0.0113	0.466	0.04648	-84.9	0.474	1.109	6.126	0.964	224.46
257	0.097	0.1192	0.0113	0.467	0.04661	-84.8	0.474	1.109	6.126	0.965	225.42
258	0.097	0.1196	0.0113	0.470	0.04686	-84.8	0.473	1.109	6.126	0.967	226.38
259	0.097	0.1200	0.0113	0.470	0.04692	-84.7	0.473	1.109	6.126	0.969	227.35
260	0.097	0.1205	0.0113	0.475	0.04742	-84.7	0.473	1.110	6.126	0.971	228.31
261	0.097	0.1209	0.0114	0.472	0.04754	-84.6	0.473	1.110	6.126	0.972	229.28
262	0.097	0.1213	0.0114	0.473	0.04761	-84.5	0.473	1.110	6.126	0.974	230.25
263	0.097	0.1218	0.0114	0.474	0.04773	-84.5	0.473	1.110	6.126	0.976	231.23
264	0.098	0.1222	0.0114	0.480	0.04785	-84.4	0.473	1.110	6.126	0.977	232.20
265	0.098	0.1227	0.0114	0.485	0.04836	-84.3	0.473	1.111	6.126	0.979	233.18
266	0.098	0.1231	0.0115	0.482	0.04848	-84.3	0.473	1.111	6.126	0.981	234.15
267	0.098	0.1236	0.0115	0.483	0.04854	-84.2	0.473	1.111	6.126	0.983	235.13
268	0.098	0.1241	0.0115	0.484	0.04867	-84.2	0.473	1.111	6.126	0.985	236.11
269	0.098	0.1245	0.0115	0.485	0.04879	-84.1	0.473	1.111	6.126	0.987	237.10
270	0.098	0.1250	0.0115	0.490	0.04930	-84.0	0.473	1.112	6.126	0.989	238.08
271	0.098	0.1255	0.0116	0.487	0.04942	-84.0	0.473	1.112	6.126	0.991	239.07
272	0.098	0.1260	0.0116	0.489	0.04954	-83.9	0.473	1.112	6.126	0.993	240.06
273	0.098	0.1265	0.0116	0.490	0.04967	-83.8	0.473	1.112	6.126	0.995	241.05
274	0.098	0.1271	0.0116	0.495	0.05018	-83.8	0.473	1.113	6.126	0.997	242.04
275	0.098	0.1276	0.0117	0.492	0.05030	-83.7	0.473	1.113	6.126	0.999	243.04
276	0.098	0.1281	0.0117	0.493	0.05043	-83.7	0.473	1.113	6.125	1.001	244.03
277	0.098	0.1287	0.0117	0.494	0.05055	-83.6	0.473	1.113	6.125	1.003	245.03
278	0.098	0.1292	0.0117	0.495	0.05067	-83.5	0.473	1.113	6.125	1.005	246.04
279	0.098	0.1298	0.0118	0.497	0.05125	-83.4	0.473	1.114	6.125	1.007	247.04
280	0.098	0.1303	0.0118	0.498	0.05137	-83.4	0.473	1.114	6.125	1.009	248.04
281	0.098	0.1309	0.0118	0.499	0.05149	-83.3	0.473	1.114	6.125	1.012	249.05
282	0.098	0.1315	0.0118	0.504	0.05201	-83.2	0.473	1.115	6.125	1.014	250.06

283	0.098	0.1321	0.0119	0.502	0.05220	-83.1	0.473	1.115	6.125	1.016	251.08
284	0.098	0.1327	0.0119	0.503	0.05232	-83.0	0.473	1.115	6.125	1.019	252.09
285	0.098	0.1333	0.0119	0.504	0.05244	-82.9	0.473	1.115	6.125	1.021	253.11
286	0.098	0.1339	0.0119	0.510	0.05303	-82.8	0.473	1.116	6.125	1.023	254.13
287	0.098	0.1346	0.0120	0.507	0.05315	-82.7	0.473	1.116	6.125	1.026	255.15
288	0.098	0.1352	0.0120	0.508	0.05327	-82.6	0.473	1.116	6.124	1.028	256.17
289	0.098	0.1359	0.0120	0.513	0.05386	-82.5	0.473	1.117	6.124	1.031	257.20
290	0.098	0.1366	0.0121	0.510	0.05398	-82.4	0.473	1.117	6.124	1.033	258.23
291	0.098	0.1372	0.0121	0.512	0.05416	-82.4	0.473	1.117	6.124	1.036	259.26
292	0.098	0.1379	0.0121	0.514	0.05434	-82.3	0.473	1.117	6.124	1.038	260.30
293	0.098	0.1386	0.0122	0.515	0.05487	-82.2	0.473	1.118	6.124	1.041	261.33
294	0.098	0.1394	0.0122	0.516	0.05506	-82.1	0.473	1.118	6.124	1.044	262.37
295	0.098	0.1401	0.0122	0.518	0.05524	-82.0	0.473	1.118	6.124	1.047	263.42
296	0.098	0.1408	0.0123	0.519	0.05577	-81.9	0.473	1.119	6.124	1.049	264.46
297	0.098	0.1416	0.0123	0.520	0.05596	-81.8	0.473	1.119	6.124	1.052	265.51
298	0.098	0.1424	0.0123	0.522	0.05614	-81.7	0.473	1.119	6.123	1.055	266.56
299	0.098	0.1432	0.0124	0.523	0.05674	-81.5	0.473	1.120	6.123	1.058	267.62
300	0.098	0.1440	0.0124	0.525	0.05692	-81.4	0.473	1.120	6.123	1.061	268.67
301	0.098	0.1448	0.0124	0.531	0.05752	-81.3	0.473	1.121	6.123	1.064	269.73
302	0.098	0.1456	0.0125	0.528	0.05770	-81.1	0.473	1.121	6.123	1.067	270.80
303	0.098	0.1465	0.0125	0.530	0.05788	-81.0	0.473	1.121	6.123	1.070	271.86
304	0.098	0.1473	0.0125	0.535	0.05848	-80.9	0.473	1.122	6.123	1.073	272.93
305	0.098	0.1482	0.0126	0.533	0.05873	-80.8	0.473	1.122	6.123	1.076	274.00
306	0.098	0.1491	0.0126	0.539	0.05933	-80.6	0.473	1.123	6.123	1.080	275.08
307	0.098	0.1501	0.0126	0.540	0.05951	-80.5	0.473	1.123	6.123	1.083	276.16
308	0.098	0.1510	0.0127	0.542	0.06012	-80.4	0.473	1.124	6.122	1.087	277.24
309	0.098	0.1520	0.0127	0.544	0.06036	-80.2	0.473	1.124	6.122	1.090	278.33
310	0.098	0.1530	0.0128	0.541	0.06054	-80.1	0.473	1.124	6.122	1.094	279.42
311	0.098	0.1540	0.0128	0.547	0.06121	-80.0	0.473	1.125	6.122	1.097	280.51
312	0.099	0.1550	0.0129	0.551	0.06145	-79.8	0.473	1.125	6.122	1.101	281.61
313	0.099	0.1560	0.0129	0.556	0.06206	-79.7	0.473	1.126	6.122	1.104	282.71
314	0.099	0.1571	0.0129	0.558	0.06230	-79.6	0.473	1.126	6.122	1.108	283.81
315	0.099	0.1582	0.0130	0.561	0.06312	-79.4	0.472	1.127	6.122	1.112	284.92
316	0.099	0.1593	0.0130	0.563	0.06336	-79.3	0.472	1.127	6.122	1.116	286.03
317	0.099	0.1604	0.0131	0.565	0.06403	-79.1	0.472	1.128	6.122	1.120	287.14
318	0.099	0.1616	0.0131	0.567	0.06427	-78.9	0.472	1.128	6.121	1.124	288.26
319	0.099	0.1627	0.0132	0.569	0.06495	-78.8	0.472	1.129	6.121	1.128	289.39
320	0.099	0.1639	0.0132	0.575	0.06563	-78.6	0.472	1.130	6.121	1.132	290.52
321	0.099	0.1652	0.0133	0.572	0.06587	-78.4	0.472	1.130	6.121	1.136	291.65
322	0.099	0.1664	0.0133	0.578	0.06655	-78.2	0.472	1.131	6.121	1.141	292.78
323	0.099	0.1677	0.0134	0.577	0.06685	-78.0	0.472	1.131	6.121	1.145	293.92
324	0.099	0.1691	0.0134	0.583	0.06753	-77.8	0.472	1.132	6.121	1.150	295.07
325	0.099	0.1704	0.0135	0.585	0.06828	-77.7	0.472	1.133	6.120	1.154	296.22
326	0.099	0.1718	0.0135	0.587	0.06851	-77.5	0.472	1.133	6.120	1.159	297.37
327	0.099	0.1732	0.0136	0.589	0.06926	-77.3	0.472	1.134	6.120	1.164	298.53
328	0.099	0.1747	0.0136	0.595	0.07001	-77.1	0.472	1.135	6.120	1.169	299.70
329	0.099	0.1761	0.0137	0.593	0.07030	-76.9	0.472	1.135	6.120	1.173	300.87
330	0.099	0.1777	0.0138	0.595	0.07105	-76.7	0.472	1.136	6.120	1.179	302.04
331	0.099	0.1792	0.0138	0.601	0.07181	-76.5	0.472	1.137	6.120	1.184	303.22
332	0.099	0.1808	0.0139	0.601	0.07225	-76.4	0.471	1.137	6.120	1.189	304.40
333	0.099	0.1824	0.0139	0.607	0.07300	-76.2	0.471	1.138	6.119	1.194	305.59
334	0.099	0.1841	0.0140	0.609	0.07381	-75.9	0.471	1.139	6.119	1.200	306.79
335	0.099	0.1858	0.0141	0.611	0.07457	-75.7	0.471	1.140	6.119	1.205	307.99
336	0.099	0.1875	0.0141	0.618	0.07539	-75.5	0.471	1.141	6.118	1.211	309.19
337	0.099	0.1893	0.0142	0.620	0.07620	-75.2	0.471	1.142	6.118	1.217	310.41
338	0.099	0.1911	0.0143	0.622	0.07696	-75.0	0.471	1.143	6.118	1.222	311.62
339	0.099	0.1930	0.0143	0.629	0.07777	-74.8	0.471	1.144	6.117	1.228	312.85
340	0.099	0.1949	0.0144	0.631	0.07859	-74.5	0.471	1.145	6.117	1.234	314.08
341	0.099	0.1969	0.0145	0.633	0.07946	-74.3	0.471	1.146	6.117	1.241	315.31
342	0.100	0.1989	0.0146	0.643	0.08043	-74.0	0.470	1.147	6.116	1.247	316.55
343	0.100	0.2010	0.0146	0.650	0.08124	-73.8	0.470	1.148	6.116	1.254	317.80
344	0.100	0.2031	0.0147	0.652	0.08212	-73.6	0.470	1.149	6.116	1.260	319.06
345	0.100	0.2053	0.0148	0.655	0.08300	-73.3	0.470	1.150	6.115	1.267	320.32
346	0.100	0.2076	0.0149	0.657	0.08387	-73.1	0.470	1.151	6.115	1.274	321.59
347	0.100	0.2099	0.0150	0.659	0.08469	-72.8	0.470	1.152	6.115	1.281	322.86
348	0.100	0.2122	0.0150	0.666	0.08562	-72.6	0.470	1.153	6.114	1.288	324.14
349	0.100	0.2146	0.0151	0.669	0.08650	-72.3	0.470	1.154	6.114	1.295	325.43
350	0.100	0.2171	0.0152	0.672	0.08753	-72.0	0.469	1.155	6.113	1.303	326.73
351	0.100	0.2196	0.0153	0.679	0.08895	-71.8	0.469	1.157	6.113	1.310	328.04
352	0.100	0.2222	0.0154	0.681	0.08988	-71.5	0.469	1.158	6.112	1.318	329.35
353	0.100	0.2249	0.0155	0.687	0.09126	-71.2	0.469	1.160	6.112	1.326	330.67

354	0.100	0.2277	0.0156	0.690	0.09219	-70.9	0.469	1.161	6.111	1.334	332.00
355	0.100	0.2305	0.0157	0.698	0.09384	-70.6	0.468	1.163	6.111	1.342	333.33
356	0.100	0.2334	0.0158	0.700	0.09477	-70.3	0.468	1.164	6.110	1.351	334.68
357	0.100	0.2364	0.0159	0.707	0.09626	-70.0	0.468	1.166	6.110	1.359	336.03
358	0.100	0.2395	0.0160	0.709	0.09720	-69.7	0.468	1.167	6.109	1.368	337.40
359	0.100	0.2426	0.0161	0.716	0.09869	-69.4	0.468	1.169	6.109	1.377	338.77
360	0.100	0.2459	0.0162	0.720	0.09984	-69.1	0.467	1.170	6.108	1.387	340.15
361	0.100	0.2492	0.0163	0.726	0.10139	-68.8	0.467	1.172	6.108	1.396	341.54
362	0.101	0.2526	0.0164	0.740	0.10288	-68.5	0.467	1.174	6.107	1.405	342.94
363	0.101	0.2562	0.0165	0.743	0.10392	-68.1	0.467	1.175	6.107	1.415	344.34
364	0.101	0.2598	0.0166	0.749	0.10547	-67.8	0.467	1.177	6.106	1.425	345.76
365	0.101	0.2635	0.0168	0.752	0.10718	-67.5	0.466	1.179	6.105	1.435	347.19
366	0.101	0.2673	0.0169	0.759	0.10873	-67.2	0.466	1.181	6.105	1.446	348.63
367	0.101	0.2712	0.0170	0.769	0.11085	-66.8	0.466	1.184	6.104	1.456	350.08
368	0.101	0.2753	0.0171	0.776	0.11257	-66.5	0.465	1.186	6.103	1.467	351.54
369	0.101	0.2795	0.0173	0.778	0.11417	-66.1	0.465	1.188	6.102	1.478	353.01
370	0.101	0.2838	0.0174	0.788	0.11634	-65.8	0.465	1.191	6.102	1.490	354.50
371	0.101	0.2882	0.0175	0.796	0.11811	-65.4	0.464	1.193	6.101	1.501	355.99
372	0.101	0.2928	0.0177	0.798	0.11976	-65.1	0.464	1.195	6.100	1.513	357.49
373	0.101	0.2975	0.0178	0.808	0.12194	-64.7	0.464	1.198	6.099	1.525	359.01
374	0.101	0.3023	0.0179	0.815	0.12376	-64.4	0.463	1.200	6.098	1.537	360.54
375	0.102	0.3073	0.0181	0.829	0.12594	-64.0	0.463	1.203	6.098	1.550	362.09
376	0.102	0.3124	0.0182	0.835	0.12763	-63.7	0.463	1.205	6.097	1.563	363.64
377	0.102	0.3177	0.0184	0.842	0.13003	-63.3	0.462	1.208	6.096	1.576	365.21
378	0.102	0.3231	0.0186	0.847	0.13225	-62.9	0.462	1.211	6.095	1.589	366.79
379	0.102	0.3287	0.0187	0.860	0.13505	-62.6	0.462	1.215	6.093	1.603	368.39
380	0.102	0.3345	0.0189	0.866	0.13749	-62.2	0.461	1.218	6.091	1.617	369.99
381	0.102	0.3404	0.0190	0.879	0.14029	-61.8	0.461	1.222	6.089	1.631	371.62
382	0.102	0.3466	0.0192	0.889	0.14331	-61.4	0.460	1.226	6.088	1.646	373.25
383	0.102	0.3529	0.0194	0.895	0.14579	-61.1	0.459	1.229	6.086	1.661	374.91
384	0.102	0.3595	0.0196	0.903	0.14862	-60.7	0.459	1.233	6.084	1.676	376.58
385	0.102	0.3662	0.0198	0.912	0.15163	-60.3	0.458	1.237	6.082	1.692	378.26
386	0.103	0.3732	0.0199	0.930	0.15398	-59.9	0.458	1.240	6.081	1.708	379.96
387	0.103	0.3803	0.0201	0.939	0.15704	-59.5	0.457	1.244	6.079	1.724	381.67
388	0.103	0.3877	0.0203	0.948	0.15997	-59.1	0.457	1.248	6.077	1.741	383.41
389	0.103	0.3953	0.0205	0.957	0.16307	-58.7	0.456	1.252	6.075	1.758	385.15
390	0.103	0.4032	0.0207	0.968	0.16670	-58.3	0.455	1.257	6.072	1.775	386.92
391	0.103	0.4113	0.0209	0.982	0.17068	-57.9	0.455	1.263	6.068	1.793	388.70
392	0.103	0.4197	0.0211	0.994	0.17435	-57.5	0.454	1.268	6.065	1.811	390.50
393	0.103	0.4284	0.0214	1.004	0.17859	-57.2	0.453	1.274	6.062	1.830	392.32
394	0.103	0.4373	0.0216	1.015	0.18229	-56.8	0.452	1.279	6.058	1.849	394.16
395	0.103	0.4466	0.0218	1.029	0.18651	-56.4	0.451	1.285	6.055	1.868	396.02
396	0.103	0.4561	0.0220	1.040	0.19024	-56.0	0.450	1.290	6.051	1.888	397.90
397	0.103	0.4659	0.0223	1.049	0.19449	-55.6	0.449	1.296	6.047	1.908	399.80
398	0.104	0.4761	0.0225	1.072	0.19874	-55.1	0.448	1.302	6.044	1.929	401.71
399	0.104	0.4865	0.0228	1.081	0.20301	-54.7	0.447	1.308	6.040	1.950	403.65
400	0.104	0.4973	0.0230	1.094	0.20732	-54.3	0.446	1.314	6.036	1.972	405.61
401	0.104	0.5085	0.0233	1.108	0.21264	-53.9	0.445	1.322	6.031	1.994	407.60
402	0.104	0.5200	0.0235	1.126	0.21799	-53.6	0.444	1.330	6.025	2.016	409.60
403	0.104	0.5319	0.0238	1.141	0.22357	-53.2	0.442	1.338	6.019	2.039	411.63
404	0.104	0.5442	0.0241	1.156	0.22946	-52.8	0.441	1.347	6.014	2.062	413.68
405	0.104	0.5570	0.0244	1.170	0.23507	-52.4	0.439	1.355	6.008	2.087	415.75
406	0.104	0.5701	0.0246	1.189	0.24097	-52.0	0.438	1.364	6.002	2.111	417.85
407	0.104	0.5836	0.0249	1.202	0.24660	-51.6	0.436	1.372	5.996	2.136	419.97
408	0.104	0.5976	0.0252	1.216	0.25245	-51.2	0.435	1.381	5.989	2.161	422.12
409	0.104	0.6120	0.0255	1.230	0.25832	-50.8	0.434	1.390	5.983	2.187	424.29
410	0.104	0.6269	0.0258	1.244	0.26435	-50.4	0.432	1.399	5.977	2.214	426.49
411	0.104	0.6422	0.0262	1.260	0.27185	-50.0	0.430	1.411	5.968	2.240	428.72
412	0.104	0.6581	0.0265	1.282	0.27983	-49.7	0.428	1.424	5.958	2.268	430.97
413	0.104	0.6745	0.0268	1.302	0.28728	-49.3	0.426	1.436	5.949	2.296	433.26
414	0.104	0.6915	0.0271	1.323	0.29520	-49.0	0.424	1.449	5.939	2.325	435.56
415	0.104	0.7090	0.0275	1.336	0.30255	-48.6	0.422	1.461	5.930	2.354	437.90
416	0.104	0.7271	0.0278	1.356	0.31053	-48.2	0.419	1.474	5.920	2.384	440.27
417	0.104	0.7457	0.0282	1.370	0.31825	-47.8	0.417	1.487	5.910	2.414	442.67
418	0.104	0.7649	0.0285	1.391	0.32640	-47.4	0.415	1.501	5.900	2.445	445.10
419	0.104	0.7847	0.0289	1.405	0.33445	-47.1	0.413	1.515	5.889	2.476	447.56
420	0.104	0.8051	0.0293	1.425	0.34399	-46.7	0.410	1.532	5.872	2.508	450.05
421	0.104	0.8262	0.0297	1.444	0.35326	-46.4	0.408	1.549	5.856	2.541	452.57
422	0.104	0.8479	0.0301	1.463	0.36261	-46.0	0.405	1.566	5.839	2.574	455.13
423	0.104	0.8703	0.0304	1.483	0.37138	-45.7	0.402	1.582	5.835	2.608	457.72
424	0.104	0.8932	0.0308	1.486	0.37699	-45.3	0.399	1.591	5.867	2.642	460.35

425	0.104	0.9164	0.0312	1.485	0.38147	-45.0	0.397	1.598	5.889	2.676	463.00
426	0.104	0.9399	0.0316	1.469	0.38241	-44.8	0.397	1.598	5.886	2.710	465.69
427	0.104	0.9635	0.0320	1.454	0.38333	-44.6	0.397	1.598	5.883	2.744	468.42
428	0.104	0.9872	0.0324	1.440	0.38420	-44.4	0.397	1.598	5.879	2.777	471.18
429	0.104	1.0111	0.0328	1.425	0.38508	-44.2	0.397	1.598	5.876	2.811	473.97
430	0.104	1.0350	0.0332	1.412	0.38599	-44.0	0.397	1.598	5.873	2.844	476.79
431	0.104	1.0591	0.0336	1.398	0.38689	-43.8	0.397	1.598	5.869	2.877	479.65
432	0.104	1.0833	0.0340	1.385	0.38772	-43.5	0.397	1.598	5.866	2.909	482.54
433	0.103	1.1076	0.0343	1.362	0.38854	-43.3	0.397	1.598	5.862	2.942	485.47
434	0.103	1.1320	0.0347	1.349	0.38933	-43.1	0.397	1.598	5.859	2.974	488.43
435	0.103	1.1565	0.0351	1.336	0.39007	-42.9	0.397	1.598	5.855	3.006	491.41
436	0.103	1.1812	0.0355	1.324	0.39079	-42.6	0.397	1.598	5.851	3.038	494.44
437	0.103	1.2059	0.0358	1.315	0.39148	-42.4	0.397	1.598	5.848	3.069	497.49
438	0.103	1.2308	0.0362	1.303	0.39213	-42.2	0.397	1.598	5.844	3.101	500.57
439	0.103	1.2558	0.0366	1.290	0.39278	-41.9	0.397	1.598	5.840	3.132	503.69
440	0.103	1.2809	0.0369	1.282	0.39339	-41.7	0.397	1.598	5.836	3.163	506.84
441	0.103	1.3061	0.0373	1.270	0.39398	-41.4	0.397	1.598	5.833	3.194	510.01
442	0.103	1.3314	0.0376	1.262	0.39454	-41.2	0.397	1.598	5.829	3.225	513.22
443	0.103	1.3568	0.0380	1.250	0.39509	-40.9	0.397	1.598	5.825	3.255	516.46
444	0.103	1.3823	0.0384	1.239	0.39562	-40.7	0.397	1.598	5.821	3.286	519.73
445	0.103	1.4079	0.0387	1.231	0.39612	-40.4	0.397	1.598	5.817	3.316	523.04
446	0.103	1.4337	0.0391	1.220	0.39658	-40.3	0.397	1.598	5.813	3.346	526.37
447	0.103	1.4595	0.0394	1.212	0.39702	-40.2	0.397	1.598	5.810	3.376	529.72
448	0.103	1.4853	0.0398	1.201	0.39747	-40.2	0.397	1.598	5.807	3.406	533.11
449	0.103	1.5111	0.0401	1.193	0.39790	-40.1	0.397	1.598	5.804	3.435	536.53
450	0.103	1.5370	0.0404	1.186	0.39831	-40.1	0.397	1.598	5.800	3.465	539.98
451	0.103	1.5629	0.0408	1.175	0.39871	-40.0	0.397	1.598	5.797	3.494	543.45
452	0.103	1.5889	0.0411	1.168	0.39909	-40.0	0.397	1.598	5.794	3.523	546.96
453	0.103	1.6148	0.0415	1.157	0.39945	-40.0	0.397	1.598	5.792	3.551	550.49
454	0.103	1.6408	0.0418	1.150	0.39982	-40.0	0.397	1.598	5.789	3.580	554.05
455	0.103	1.6668	0.0421	1.143	0.40021	-40.0	0.397	1.598	5.786	3.608	557.64
456	0.103	1.6927	0.0424	1.136	0.40059	-40.0	0.397	1.598	5.784	3.636	561.26
457	0.103	1.7187	0.0428	1.127	0.40096	-40.0	0.397	1.598	5.781	3.663	564.91
458	0.103	1.7447	0.0431	1.120	0.40132	-40.0	0.397	1.598	5.778	3.691	568.58
459	0.103	1.7707	0.0434	1.113	0.40166	-40.0	0.397	1.598	5.775	3.718	572.28
460	0.103	1.7967	0.0437	1.106	0.40199	-40.0	0.397	1.598	5.773	3.746	576.01
461	0.103	1.8227	0.0440	1.100	0.40232	-40.0	0.397	1.598	5.770	3.773	579.76
462	0.102	1.8487	0.0444	1.080	0.40264	-40.0	0.397	1.598	5.767	3.799	583.55
463	0.102	1.8747	0.0447	1.073	0.40295	-40.0	0.397	1.598	5.764	3.826	587.36
464	0.102	1.9007	0.0450	1.067	0.40325	-40.0	0.397	1.598	5.761	3.852	591.19
465	0.102	1.9267	0.0453	1.061	0.40353	-40.0	0.397	1.598	5.759	3.879	595.05
466	0.102	1.9528	0.0456	1.055	0.40381	-40.0	0.397	1.598	5.756	3.905	598.94
467	0.102	1.9788	0.0459	1.048	0.40408	-40.0	0.397	1.598	5.755	3.931	602.86
468	0.102	2.0048	0.0462	1.042	0.40435	-40.0	0.397	1.598	5.753	3.956	606.80
469	0.102	2.0309	0.0465	1.036	0.40461	-40.0	0.397	1.598	5.751	3.982	610.76
470	0.102	2.0569	0.0468	1.030	0.40485	-40.0	0.397	1.598	5.750	4.007	614.75
471	0.102	2.0830	0.0471	1.024	0.40509	-40.0	0.397	1.598	5.748	4.033	618.77
472	0.102	2.1090	0.0474	1.018	0.40533	-40.0	0.397	1.598	5.746	4.058	622.81
473	0.102	2.1351	0.0477	1.012	0.40556	-40.0	0.397	1.598	5.744	4.083	626.88
474	0.102	2.1612	0.0480	1.007	0.40579	-40.0	0.397	1.598	5.743	4.107	630.97
475	0.102	2.1872	0.0482	1.003	0.40599	-40.0	0.397	1.598	5.741	4.132	635.08
476	0.102	2.2133	0.0485	0.997	0.40621	-40.0	0.397	1.598	5.739	4.157	639.23
477	0.102	2.2394	0.0488	0.992	0.40641	-40.0	0.397	1.598	5.737	4.181	643.39
478	0.102	2.2655	0.0491	0.986	0.40661	-40.0	0.397	1.598	5.736	4.205	647.58
479	0.102	2.2916	0.0494	0.981	0.40680	-40.0	0.397	1.598	5.734	4.229	651.79
480	0.102	2.3176	0.0497	0.975	0.40699	-40.0	0.397	1.598	5.733	4.253	656.03
481	0.102	2.3437	0.0499	0.972	0.40718	-40.0	0.397	1.598	5.731	4.277	660.29
482	0.102	2.3698	0.0502	0.966	0.40736	-40.0	0.397	1.598	5.730	4.301	664.58
483	0.102	2.3959	0.0505	0.961	0.40752	-40.0	0.397	1.598	5.729	4.324	668.89
484	0.102	2.4220	0.0508	0.956	0.40770	-40.0	0.397	1.598	5.727	4.348	673.22
485	0.102	2.4481	0.0510	0.952	0.40786	-40.0	0.397	1.598	5.726	4.371	677.58
486	0.102	2.4743	0.0513	0.947	0.40802	-40.0	0.397	1.598	5.724	4.394	681.96
487	0.102	2.5004	0.0516	0.942	0.40818	-40.0	0.397	1.598	5.723	4.417	686.36
488	0.102	2.5265	0.0518	0.939	0.40833	-40.0	0.397	1.598	5.721	4.440	690.79
489	0.102	2.5526	0.0521	0.934	0.40848	-40.0	0.397	1.598	5.720	4.463	695.23
490	0.102	2.5787	0.0524	0.929	0.40862	-40.0	0.397	1.598	5.719	4.486	699.71
491	0.102	2.6048	0.0526	0.925	0.40877	-40.0	0.397	1.598	5.718	4.508	704.20
492	0.102	2.6310	0.0529	0.921	0.40893	-40.0	0.397	1.598	5.717	4.531	708.72
493	0.102	2.6571	0.0532	0.916	0.40908	-40.0	0.397	1.598	5.716	4.553	713.26
494	0.102	2.6832	0.0534	0.913	0.40924	-40.0	0.397	1.598	5.715	4.576	717.82
495	0.102	2.7094	0.0537	0.908	0.40938	-40.0	0.397	1.598	5.714	4.598	722.40

496	0.102	2.7355	0.0539	0.905	0.40953	-40.0	0.397	1.598	5.713	4.620	727.01
497	0.102	2.7616	0.0542	0.900	0.40967	-40.0	0.397	1.598	5.712	4.642	731.63
498	0.102	2.7878	0.0544	0.897	0.40981	-40.0	0.397	1.598	5.710	4.664	736.28
499	0.102	2.8139	0.0547	0.892	0.40994	-40.0	0.397	1.598	5.709	4.686	740.96
500	0.102	2.8401	0.0550	0.888	0.41007	-40.0	0.397	1.598	5.708	4.707	745.65
501	0.102	2.8662	0.0552	0.885	0.41021	-40.0	0.397	1.598	5.708	4.729	750.37
502	0.102	2.8924	0.0555	0.880	0.41034	-40.0	0.397	1.598	5.707	4.750	755.10
503	0.102	2.9186	0.0557	0.878	0.41046	-40.0	0.397	1.598	5.706	4.772	759.86
504	0.102	2.9447	0.0560	0.873	0.41058	-40.0	0.397	1.598	5.705	4.793	764.64
505	0.102	2.9709	0.0562	0.870	0.41071	-40.0	0.397	1.598	5.704	4.814	769.44
506	0.102	2.9970	0.0565	0.866	0.41082	-40.0	0.397	1.598	5.703	4.835	774.26
507	0.102	3.0232	0.0567	0.863	0.41094	-40.0	0.397	1.598	5.703	4.856	779.10
508	0.102	3.0494	0.0569	0.860	0.41105	-40.0	0.397	1.598	5.702	4.877	783.97
509	0.102	3.0756	0.0572	0.856	0.41116	-40.0	0.397	1.598	5.701	4.898	788.85
510	0.102	3.1017	0.0574	0.853	0.41128	-40.0	0.397	1.598	5.700	4.919	793.76
511	0.102	3.1279	0.0577	0.849	0.41138	-40.0	0.397	1.598	5.699	4.939	798.69
512	0.102	3.1541	0.0579	0.846	0.41149	-40.0	0.397	1.598	5.698	4.960	803.63
513	0.102	3.1803	0.0581	0.844	0.41159	-40.0	0.397	1.598	5.698	4.981	808.60
514	0.102	3.2065	0.0584	0.839	0.41169	-40.0	0.397	1.598	5.697	5.001	813.59
515	0.102	3.2327	0.0586	0.837	0.41179	-40.0	0.397	1.598	5.696	5.021	818.60
516	0.102	3.2588	0.0589	0.833	0.41189	-40.0	0.397	1.598	5.696	5.041	823.62
517	0.102	3.2850	0.0591	0.830	0.41198	-40.0	0.397	1.598	5.695	5.062	828.67
518	0.102	3.3112	0.0593	0.828	0.41208	-40.0	0.397	1.598	5.694	5.082	833.74
519	0.102	3.3374	0.0596	0.824	0.41217	-40.0	0.397	1.598	5.694	5.102	838.83
520	0.102	3.3636	0.0598	0.821	0.41226	-40.0	0.397	1.598	5.693	5.122	843.94
521	0.102	3.3898	0.0600	0.818	0.41235	-40.0	0.397	1.598	5.692	5.142	849.07
522	0.102	3.4160	0.0603	0.814	0.41244	-40.0	0.397	1.598	5.692	5.161	854.22
523	0.102	3.4422	0.0605	0.812	0.41252	-40.0	0.397	1.598	5.691	5.181	859.39
524	0.102	3.4684	0.0607	0.809	0.41260	-40.0	0.397	1.598	5.691	5.201	864.57
525	0.102	3.4947	0.0609	0.807	0.41269	-40.0	0.397	1.598	5.690	5.220	869.78
526	0.102	3.5209	0.0612	0.803	0.41276	-40.0	0.397	1.598	5.689	5.240	875.01
527	0.102	3.5471	0.0614	0.801	0.41285	-40.0	0.397	1.598	5.689	5.259	880.26
528	0.102	3.5733	0.0616	0.798	0.41292	-40.0	0.397	1.598	5.688	5.278	885.52
529	0.102	3.5995	0.0618	0.796	0.41300	-40.0	0.397	1.598	5.687	5.298	890.81
530	0.102	3.6257	0.0621	0.792	0.41308	-40.0	0.397	1.598	5.687	5.317	896.11
531	0.101	3.6519	0.0623	0.782	0.41315	-40.0	0.397	1.598	5.686	5.336	901.44
532	0.101	3.6782	0.0625	0.780	0.41322	-40.0	0.397	1.598	5.686	5.355	906.78
533	0.101	3.7044	0.0627	0.777	0.41329	-40.0	0.397	1.598	5.685	5.374	912.14
534	0.101	3.7306	0.0630	0.774	0.41336	-40.0	0.397	1.598	5.685	5.393	917.52
535	0.101	3.7568	0.0632	0.771	0.41343	-40.0	0.397	1.598	5.684	5.412	922.92
536	0.101	3.7831	0.0634	0.769	0.41350	-40.0	0.397	1.598	5.684	5.431	928.34
537	0.101	3.8093	0.0636	0.767	0.41356	-40.0	0.397	1.598	5.683	5.449	933.78
538	0.101	3.8355	0.0638	0.764	0.41363	-40.0	0.397	1.598	5.682	5.468	939.24
539	0.101	3.8617	0.0641	0.761	0.41369	-40.0	0.397	1.598	5.682	5.487	944.71
540	0.101	3.8880	0.0643	0.759	0.41375	-40.0	0.397	1.598	5.681	5.505	950.20
541	0.101	3.9142	0.0645	0.757	0.41382	-40.0	0.397	1.598	5.681	5.524	955.72
542	0.101	3.9405	0.0647	0.754	0.41388	-40.0	0.397	1.598	5.680	5.542	961.25
543	0.101	3.9667	0.0649	0.752	0.41394	-40.0	0.397	1.598	5.680	5.561	966.79
544	0.101	3.9929	0.0651	0.750	0.41400	-40.0	0.397	1.598	5.679	5.579	972.36
545	0.101	4.0192	0.0653	0.748	0.41406	-40.0	0.397	1.598	5.679	5.597	977.95
546	0.101	4.0454	0.0656	0.744	0.41411	-40.0	0.397	1.598	5.678	5.615	983.55
547	0.101	4.0716	0.0658	0.742	0.41417	-40.0	0.397	1.598	5.678	5.633	989.17
548	0.101	4.0979	0.0660	0.740	0.41423	-40.0	0.397	1.598	5.677	5.651	994.81
549	0.101	4.1241	0.0662	0.738	0.41429	-40.0	0.397	1.598	5.677	5.669	1000.47
550	0.101	4.1504	0.0664	0.736	0.41435	-40.0	0.397	1.598	5.676	5.687	1006.15
551	0.101	4.1766	0.0666	0.734	0.41441	-40.0	0.397	1.598	5.676	5.705	1011.84
552	0.101	4.2029	0.0668	0.732	0.41447	-40.0	0.397	1.598	5.675	5.723	1017.55
553	0.101	4.2291	0.0670	0.730	0.41453	-40.0	0.397	1.598	5.675	5.741	1023.28
554	0.101	4.2554	0.0672	0.727	0.41459	-40.0	0.397	1.598	5.674	5.759	1029.03
555	0.101	4.2816	0.0674	0.725	0.41464	-40.0	0.397	1.598	5.674	5.776	1034.80
556	0.101	4.3079	0.0676	0.723	0.41470	-40.0	0.397	1.598	5.673	5.794	1040.58
557	0.101	4.3341	0.0678	0.721	0.41475	-40.0	0.397	1.598	5.673	5.812	1046.38
558	0.101	4.3604	0.0681	0.718	0.41481	-40.0	0.397	1.598	5.672	5.829	1052.20
559	0.101	4.3866	0.0683	0.716	0.41486	-40.0	0.397	1.598	5.672	5.846	1058.03
560	0.101	4.4129	0.0685	0.714	0.41491	-40.0	0.397	1.598	5.672	5.864	1063.88
561	0.101	4.4391	0.0687	0.712	0.41497	-40.0	0.397	1.598	5.671	5.881	1069.75
562	0.101	4.4654	0.0689	0.710	0.41502	-40.0	0.397	1.598	5.671	5.899	1075.64
563	0.101	4.4916	0.0691	0.708	0.41507	-40.0	0.397	1.598	5.671	5.916	1081.55
564	0.101	4.5179	0.0693	0.706	0.41512	-40.0	0.397	1.598	5.670	5.933	1087.47
565	0.101	4.5442	0.0695	0.704	0.41517	-40.0	0.397	1.598	5.670	5.950	1093.41
566	0.101	4.5704	0.0697	0.702	0.41522	-40.0	0.397	1.598	5.669	5.967	1099.37

567	0.101	4.5967	0.0699	0.701	0.41527	-40.0	0.397	1.598	5.669	5.984	1105.34
568	0.101	4.6230	0.0701	0.699	0.41531	-40.0	0.397	1.598	5.669	6.001	1111.33
569	0.101	4.6492	0.0703	0.697	0.41536	-40.0	0.397	1.598	5.668	6.018	1117.34
570	0.101	4.6755	0.0705	0.695	0.41540	-40.0	0.397	1.598	5.668	6.035	1123.36
571	0.101	4.7018	0.0707	0.693	0.41545	-40.0	0.397	1.598	5.668	6.052	1129.40
572	0.101	4.7280	0.0709	0.691	0.41549	-40.0	0.397	1.598	5.667	6.069	1135.46
573	0.101	4.7543	0.0710	0.690	0.41554	-40.0	0.397	1.598	5.667	6.086	1141.54
574	0.101	4.7806	0.0712	0.688	0.41558	-40.0	0.397	1.598	5.667	6.102	1147.63
575	0.101	4.8068	0.0714	0.686	0.41563	-40.0	0.397	1.598	5.667	6.119	1153.74
576	0.101	4.8331	0.0716	0.685	0.41567	-40.0	0.397	1.598	5.666	6.136	1159.86
577	0.101	4.8594	0.0718	0.683	0.41571	-40.0	0.397	1.598	5.666	6.152	1166.00
578	0.101	4.8857	0.0720	0.681	0.41575	-40.0	0.397	1.598	5.666	6.169	1172.16
579	0.101	4.9119	0.0722	0.679	0.41579	-40.0	0.397	1.598	5.665	6.185	1178.34
580	0.101	4.9382	0.0724	0.677	0.41583	-40.0	0.397	1.598	5.665	6.202	1184.53
581	0.101	4.9645	0.0726	0.675	0.41587	-40.0	0.397	1.598	5.665	6.218	1190.74
582	0.101	4.9908	0.0728	0.674	0.41591	-40.0	0.397	1.598	5.664	6.235	1196.96
583	0.101	5.0170	0.0730	0.672	0.41595	-40.0	0.397	1.598	5.664	6.251	1203.20